Developing methodologies for exploring myosin-5 elasticity under strain

Anna Lopata

Submitted in accordance with the requirements for the degree of Doctor of Philosophy

The University of Leeds
Faculty of Biological Sciences
School of Molecular and Cellular Biology

September 2016

The candidate confirms that the work submitted is her own and that appropriate credit has been given where reference has been made to the work of others.

Acknowledgement

First, I would like to thank my supervisors, Michelle Peckham, Peter Knight and Jim Sellers for giving me the opportunity to conduct my PhD studies in their laboratories and for their invaluable scientific advice and guidance.

This work was made possible by the prestigious NIH-Wellcome Trust fellowship that gave me the unique opportunity to undertake a joint PhD program between the University of Leeds and National Institutes of Health, Bethesda, MD. I would like to thank the financial support for both the Wellcome Trust and the NIH.

I would like to thank the past and present members of the Molecular Contractility and Microscopy Research Group at Leeds. I am indebted to Matt Walker for teaching me how to use the electron microscope and for his scientific advice. I am thankful for Kieran Lee for teaching me how to run Western blots and for being a fun colleague. I am thankful for Adriana Klyszejko for helping me out with everything. I am grateful that I had Mara Rusu, Marta Kurzawa, Charlie Scarff and Marcin Wolny both as colleagues and friends.

I would also like to thank the past and present members of the Laboratory of Molecular Physiology at the NIH. I am very grateful to Attila Nagy for his invaluable scientific and personal support throughout my entire PhD student time. His help on the myosin purification techniques and biophysical assays were essential to the success of my PhD project. I want to thank Jonathan Bird for helping me with the *Sf9* cell culture techniques and for his advice on using the chaperones. I am also very thankful to Sarah Heissler, Neil Billington and Harry Takagi for helping me with scientific and personal advice, for supporting me and for being friends, not just colleagues.

I would like to thank the help and support of the members of my former lab in Hungary, the Genome Metabolism and Biostruct Laboratory. I am especially thankful for Beáta Vértessy, Judit Tóth, Judit Szabó, Rita Hirmondó, Gergely Róna, Gergely Nagy, András Benedek and András Horváth.

I am thankful for my friends from all over the world for supporting me. Most importantly, I would like to thank my parents, Ilona Szabó and Antal Lopata for always supporting me and believing in me.

Abstract

Motor proteins drive the movement of organelles and other types of cargo inside every eukaryotic cell type. These motors include myosins, kinesins and dyneins. Myosin-5a, a ubiquitous motor protein, has been intensively studied and its enzymatic properties and cellular functions have been described in great detail. This dimeric molecule walks processively along actin filaments, enabling it to transport a variety of cargos including mRNA, pigment granules, organelles such as the endoplasmic reticulum and endocytic vesicles. Cargos bind to the C-terminal globular tail domain of the molecule, while the N-terminal motor domain hydrolyses ATP to take regular steps on the actin filament.

The structure and enzymatic properties of myosin-5 moving processively along actin under unloaded conditions have already been well characterised. However, while pulling a cargo through the viscoelastic cytoplasm, the molecule will experience variable forces. Therefore it is important to study how these forces alter the structure and kinetic behaviour of myosin-5.

The purpose of this study was to design myosin-5 constructs that could be tethered, in a controlled manner, to actin via sequences introduced into the tail region of the molecule. The tethered motor protein is expected to ’stall’ while moving along the actin filament. In this way, the effects of strain on the myosin-5 structure and kinetics could then be investigated. This would simulate a case where inside the cell myosin-5 stalls due to strain, for example, whilst trying to move its cargo through spatially restricted areas of the actin cytoskeleton.

To find a new way to attach the tail of myosin-5 to actin, small, artificial actin-binding proteins named Adhirons were raised with phage display assay and their properties were explored. They bind to actin with high affinity and they are also useful for staining actin in cells or for attaching actin to coverslips in various motility assays. Multiple myosin-5 constructs were explored, that had either an Avi-tag or an actin-binding Adhiron at their C-terminal ends. A construct that contained the full predicted coiled-coil motif of myosin-5, could not be attached to the same actin filament via its tail as the motors were bound to. Two further constructs that have an artificial long coiled-coil tail, were cloned and expression trials are currently in progress.

Table of Contents

List of Figures

List of Tables

List of Abbreviations

2YT	yeast extract tryptone
ADP	adenosine-5'-diphosphate
ATP	adenosine-5'-triphosphate
a.u.	arbitrary unit
Bis-Tris	2,2-bis(hydroxymethyl)-2,2',2''-nitrilotriethanol
BSA	bovine serum albumin
CaM	calmodulin
DAPI	4',6-diamidino-2-phenylindole, dihydrochloride
deac-aminoATP	3'-(7-diethylaminocoumarin-3-carbonylamino)-ATP
DMEM	Dulbecco's modified eagle medium
DMSO	dimethyl sulfoxide
DTT	dithiothreitol
ECL	enhanced chemiluminescence
EDTA	ethylene diamine tetraacetic acid
eGFP	enhanced green fluorescent protein
EGTA	ethylene glycol-bis(2-aminoethylether)-N,N,N',N'-tetraacetic acid
ELISA	enzyme-linked immunosorbent assay
EM	electron microscope
FBS	fetal bovine serum
GTD	globular tail domain
HMM	heavy meromyosin
HRP	horseradish peroxidase
IPTG	isopropyl β-D-1-thiogalactopyranoside
kb	kilobase
LAC	lactate
LB	lysogeny broth
MCS	multi cloning site
MES	2-(*N*-morpholino)ethanesulfonic acid
MOPS	3-(N-morpholino)propanesulfonic acid
NAD^+	nicotinamide adenine dinucleotide
NADH	reduced form of nicotinamide adenine dinucleotide
NEM	N-ethyl-maleimide
P1	passage 1
PBS	phosphate buffered saline
PCR	polymerase chain reaction
PEG	polyethylene glycol
PEI	polyethyleneimine
PEP	phospho(enol)pyruvate
P_i	inorganic phosphate
PMSF	phenylmethylsulfonyl fluoride

PYR	pyruvate
rpm	revolution per minute
SDS-PAGE	sodium dodecyl sulphate polyacrylamide gel electrophoresis
SFM	serum free medium
SOC	super optimal broth with catabolite repression
TCEP	tris(2-carboxyethyl)phosphine
TIRF	total internal reflection fluorescence
TMB	3,3’,5,5’-tetramethylbenzidine
Tris	tris(hydroxymethyl)aminomethane
Triton	4-(1,1,3,3-tetramethylbutyl)phenyl-polyethylene glycol
UV	ultraviolet
v/v	volume/volume
w/v	weight/volume

1. Introduction

1.1 Myosins

Every eukaryotic cell utilises motor proteins in order to move and position their organelles and other types of cargo. Molecular motors, which include myosins, kinesins and dyneins, use the energy of ATP hydrolysis for cargo transport. In eukaryotes the cytoskeleton is comprised of the interconnected network of actin filaments and microtubules. Molecular motors in the cell use these filaments as tracks for transporting and anchoring cargos. Kinesins and dyneins move along microtubules, while myosins move along actin filaments, reviewed by (Hartman and Spudich, 2012). The superfamily of myosins consists of at least 35 classes and members of the superfamily participate in numerous cellular processes reviewed by (Odronitz and Kollmar, 2007; Bloemink and Geeves, 2011).

Muscle myosin-2, responsible for muscle contraction, was the first myosin discovered in 1864 by Willy Kühne. The first non-muscle myosin was discovered in 1973 (Pollard and Korn, 1973) and later on other non-muscle myosins were also found with various functions (Figure 1.1). Initially these other myosins were called unconventional in order to distinguish them from the muscle myosin that had been the sole myosin studied up to that point. Nowadays, these other myosins are the subject of many studies, so the term unconventional is rarely used.

1.1.1 Basic structure of myosins

Members of the myosin superfamily contain a conserved motor domain that includes the actin and ATP binding sites (Figure 1.2). This is typically followed by a lever that binds calmodulin or calmodulin-like light chains to its IQ motifs. IQ motifs are ~24 residues long motifs usually starting with an isoleucine, invariably followed by a glutamine. In some myosins the lever also contains a stable single-alpha helical domain (SAH) which allows extension of the lever without the need for binding light chains (Yang et al., 2009; Knight et al., 2005; Spink et al., 2008). Rotation of this lever about a pivot point near the base of the motor domain is the major conformational change which underlies myosin based motility. The lever is followed by a tail that has widely varying functions across the myosin superfamily. These functions include oligomerisation, regulation of enzymatic activity, subcellular targeting and cargo binding.

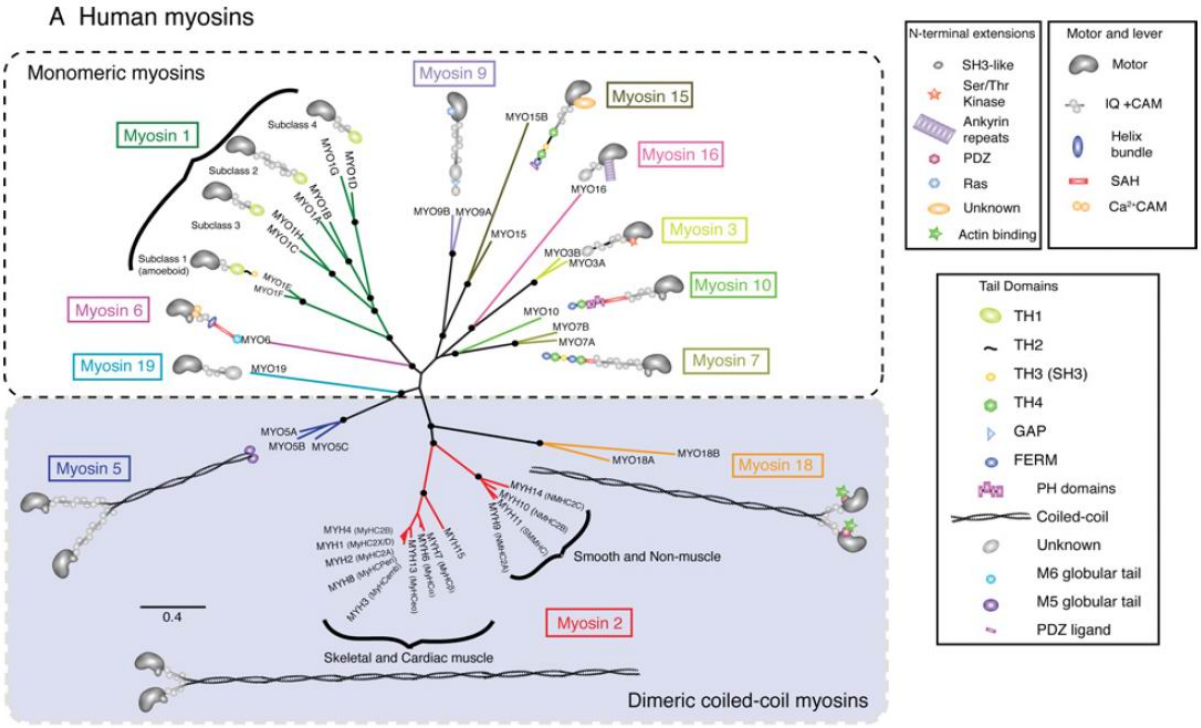

Figure 1.1. *Family tree of 12 classes of human myosin heavy chains, according to Uniprot. Labels such as MYO5A are the names of the human genes. Differential splicing of these genes produces more different myosins. The heavy chains can also bind various light chains that leads to even more diversity. Right panel legend describes additional bound molecules, domains and structural parts present in various human myosins. Figure is taken from (Peckham, 2011).*

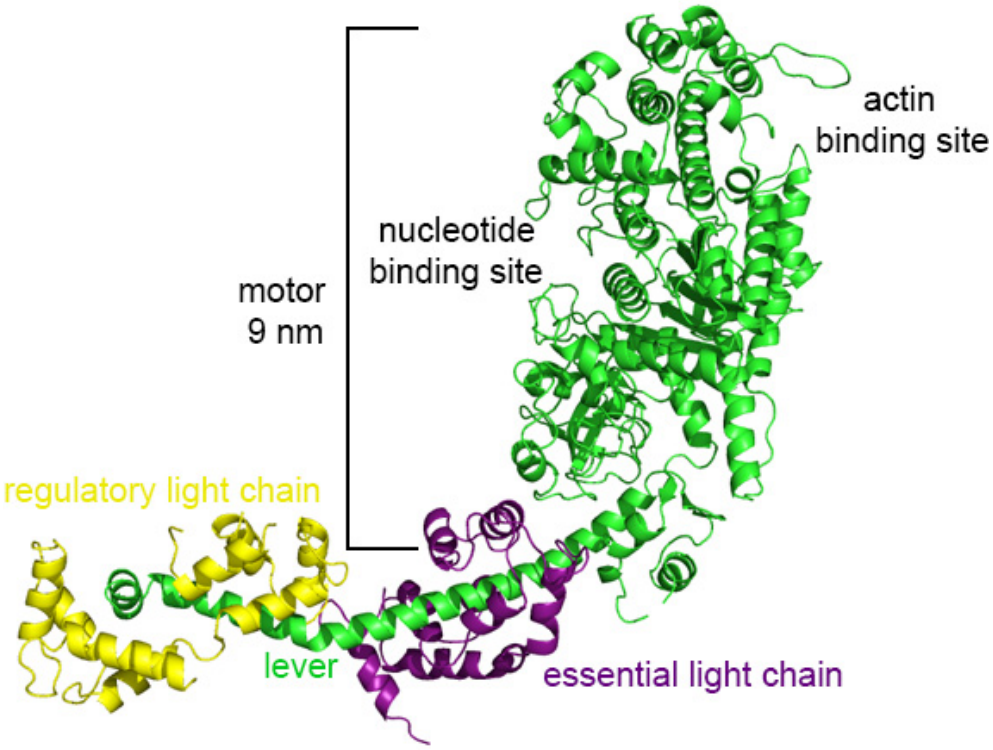

Figure 1.2. *Crystal structure of the muscle myosin-2 head with bound light chains and without bound nucleotide (PDB ID: 2MYS (Rayment et al., 1993), the presented crystal structure, that contains coordinates of all atoms of the light chains, was received from Prof. Ivan Rayment). Nucleotide and actin binding sites are shown in the motor domain. Protein is shown as cartoon representation.*

Historically, fragments of muscle myosin-2 were prepared by treating the myosin sample with proteases. The full length myosin-2 molecule consists of a pair of heavy chains which are dimerised through a long coiled-coil tail. Cleavage of this full length protein by trypsin (Lowey and Cohen, 1962) or by α-chymotrypsin (Weeds and Taylor, 1975) yields an HMM (heavy meromyosin) and an LMM (light meromyosin) fragment (Figure 1.3). The HMM comprises the heads and the first part of the coiled-coil. Further cleaving the HMM at the lever–coiled-coil junction by papain (Szent-Györgyi et al., 1973) or by α-chymotrypsin (Weeds and Taylor, 1975) yields the S1 and S2 subfragments: S1 is a monomeric subfragment that contains the head and retains ATPase activity, whereas S2 is a coiled-coil subfragment. For simplicity, the terms HMM and S1 have been retained for use when describing fragments of other myosins. The term HMM therefore describes a dimeric molecule which contains two motor domains, the subsequent levers and the coiled-coil dimerisation

region. The term S1 describes a molecule truncated prior to the coiled-coil that therefore remains monomeric. These terms can be used for proteolytic fragments of myosin or, as is more common today, for molecules produced via recombinant protein expression.

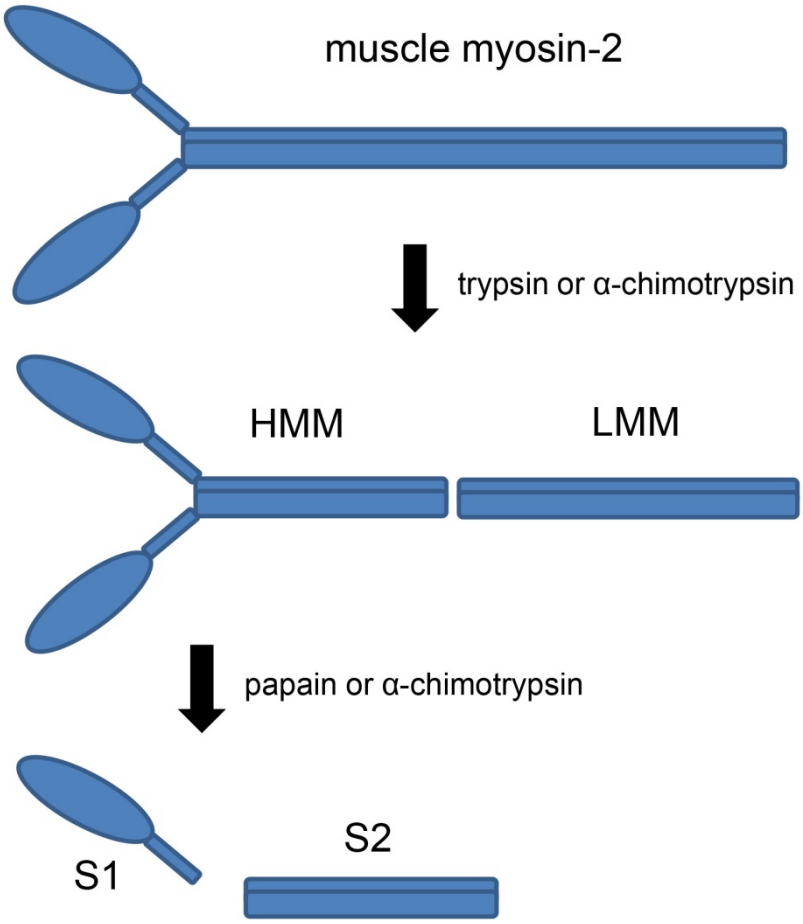

Figure 1.3. *Schematic representation of the muscle myosin-2 fragments prepared by proteolytic cleavage.*

1.1.2 Actomyosin ATPase cycle

The energy that drives myosin based motility is derived from the hydrolysis of ATP. Importantly, this ATPase activity is coupled to actin binding, as actin activates ATPase activity of myosin. This allows myosin to efficiently convert the chemical energy of ATPase hydrolysis into mechanical work when myosin is bound to actin. The specific enzymatic and mechanical properties of a given myosin are determined by the specific parameters of its ATPase cycle. A general scheme for this ATPase cycle is shown in Figure 1.4.

The starting point of the cycle can be defined as myosin strongly bound to actin in the absence of ATP (Lymn and Taylor, 1971). ATP binding to actomyosin (step 1, Figure 1.4) induces a conformational change in the myosin motor domain. This results in weakened actin binding affinity of the myosin motor, thus detachment from actin (step 2, Figure 1.4). Whilst unbound from actin, hydrolysis of ATP to ADP and P_i takes place along with a conformational change that rotates the lever and is termed the recovery stroke (step 3, Figure 1.4). The ADP–P_i bound myosin motor rebinds to actin (step 4, Figure 1.4) and then P_i release takes place along with the force-generating powerstroke (step 5, Figure 1.4). ADP dissociates (step 6, Figure 1.4) and the cycle is thus complete. Force results from a conformational change within the head, containing four subdomains connected by three flexible linkers, which occurs when the P_i leaves the active site. Little relative movement of three subdomains causes the lever to make a large, concerted movement, which is associated with the powerstroke.

As can be seen in Figure 1.4, the cycle consists of a number of states in which myosin is strongly bound to actin and a number of states in which the motor is detached. The fraction of time which myosin spends in the strong actin binding states with respect to the whole cycle is termed the duty ratio. Low duty ratio motors therefore spend a majority of the cycle detached from actin whilst high duty ratio motors spend a majority of the cycle attached to actin. Myosins where P_i release is rate limiting, tend to be low duty ratio motors whilst myosins where ADP release is rate limiting, tend to have a higher duty ratio (De La Cruz et al., 1999; El Mezgueldi et al., 2002).

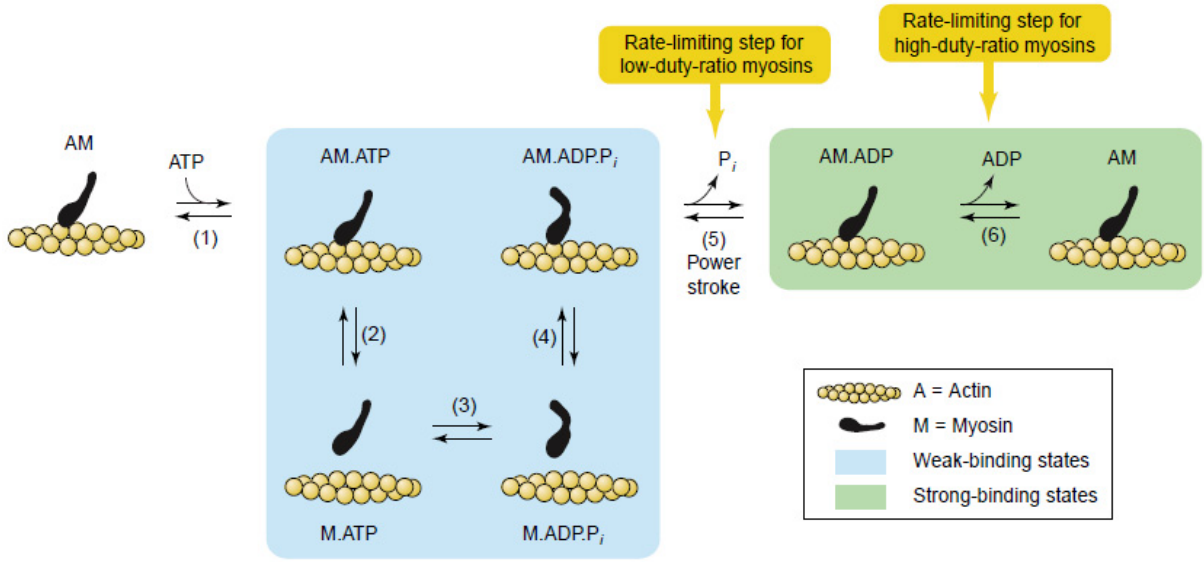

Figure 1.4. *Schematic representation of the actomyosin ATPase cycle showing strong and weak actin binding states of myosin. Figure is taken from (De La Cruz and Ostap, 2004).*

1.1.3 Myosin superfamily

Members of the myosin superfamily participate in a wide variety of cellular processes (Figure 1.1). Myosin-5, which is one of the most studied myosins (Nyitrai and Geeves, 2004; Sellers and Veigel, 2006; Trybus, 2008; Veigel and Schmidt, 2011), is involved in cargo transport, reviewed by (Hammer 3rd and Sellers, 2012). Besides myosin-5, members of myosin classes 1, 2, 6 and 7 are also involved in cargo transport in animal cells, reviewed by (Syamaladevi et al., 2012). In plants myosin-8 and myosin-11 are responsible for long-range movement of organelles (Sparkes, 2010). Myosin-19 transports mitochondria in human cells (Quintero et al., 2009), while myosin-11 transports them in plants (Wang and Pesacreta, 2004).

One of the functions of non-muscle myosin-2 is to help to separate daughter cells during cytokinesis (Vicente-Manzanares et al., 2009). Myosin-6 participates in vesicular membrane trafficking (Arden et al., 2007), and myosin-10 stimulates filopodia formation (Sousa and Cheney, 2005).

Many myosins localise to membrane extensions such as stereocilia in hair cells (Hasson et al., 1997; Belyantseva et al., 2003; Schneider et al., 2006) or microvilli in the intestines or in the kidney (Heintzelman et al., 1994; Benesh et al., 2010). Some myosins are associated with endosomes (Raposo et al., 1999; Hasson, 2003; Wang et al., 2008) or with phagosomes (Tuxworth et al., 2001; Cox et al., 2002). Most myosins are restricted to the cytoplasm, however some were found in the nucleus as well (Woolner and Bement, 2009).

As myosins are responsible for a wealth of different cellular processes, mutations in the myosin genes can lead to various diseases. Some examples are myosin-2, myosin-5a and myosin-7a. Mutations in myosin-7a can lead to deafness (Kremer et al., 2006), mutant myosin-5a can cause defects in pigmentation and neuronal malfunction (Van Gele et al., 2009), and defects in cardiac myosin-2 are responsible for cardiomyopathies (Walsh et al., 2010).

Non-muscle myosins interact with cargos through their C-terminal cargo binding domain. The tail region of different myosins is highly divergent, unlike their conserved motor domains, enabling them to interact with various cargos through association with adaptors and other binding proteins (Thompson and Langford, 2002). However, some myosins bind directly to lipids instead of interacting with adaptor proteins (McConnell and Tyska, 2010).

1.2 Actin

Actin is a 42 kDa globular protein (G-actin) with four subdomains (Figure 1.5A) that polymerises into filaments (F-actin) spontaneously under physiological salt conditions. The structure of the resulting filament (Figure 1.5B) can be viewed as either i) the right-handed double helix made up from strands of actin subunits that has a crossover length of 13 subunits, the rise per strand is 5.5 nm and the offset of subunits between the two helices is half a subunit. (Figure 1.5C left side) or as ii) the left-handed single helix with a pitch of 5.9 nm and a repeat period of 26 subunits and a 2.75 nm rise per subunit (Figure 1.5C right side). Since the actin filament is a polymer produced from asymmetric monomers, the actin filament is also polar. The filament is often defined as having a pointed end and a barbed end, like an arrowhead, due to the appearance of the filament when myosin heads are bound in the absence of nucleotide (Huxley, 1963; Pollard, 2016) (Figure 1.5D).

Nucleotide (ATP or ADP) can bind in the cleft between subdomains II and IV. The β- and γ-phosphate of ATP (or solely the β-phosphate of ADP) bind either Ca^{2+} or Mg^{2+} stabilizing the interaction between the nucleotide and the protein (Kabsch et al., 1990). Mg^{2+} and monovalent cations promote polymerisation of actin monomers as they enhance interaction between the subunits in the filament (Kang et al., 2013).

Upon polymerisation a conformational change takes place in subdomains I and III (Fujii et al., 2010), that increases the rate of ATP hydrolysis (Blanchoin and Pollard, 2002). Actin polymerisation from monomers starts with a slow lag phase as the formation of dimers and trimers are very slow, however the subsequent elongation is faster and polymers are much more stable (Sept and McCammon, 2001). Although actin filaments can elongate at both ends, the critical concentration (which is defined as the concentration above which there is net polymerisation and below which there is net depolymerisation) is not the same at both ends of the filament. The end of the filament that polymerises more rapidly is known as the plus end (equivalent to the barbed end described above) and the opposite end is known as the minus end (equivalent to the pointed end described above).

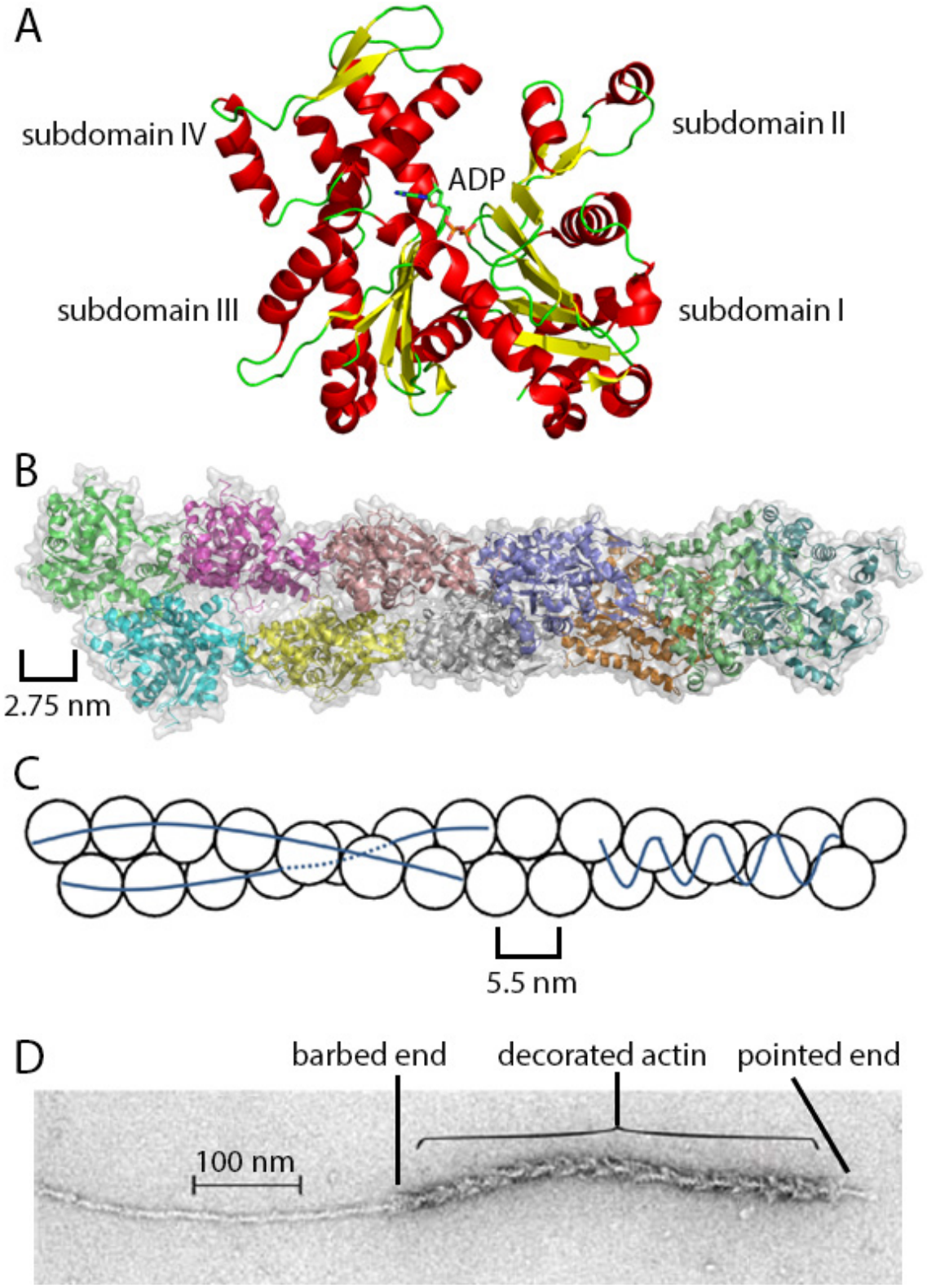

Figure 1.5. *Structures of actin. A) Crystal structure of G-actin complexed with ADP (PDB ID: 1J6Z (Otterbein et al., 2001)). Protein is shown as cartoon representation, secondary structure is colour coded (red: α-helix, yellow: β sheet, green: loop). ADP is denoted by sticks with atomic colouring. B) Cryo electron microscopy structure of F-actin (PDB ID: 3LUE (Galkin et al., 2010)). Protein is shown as both cartoon*

representation with colour coded subunits and as surface representation with transparent grey colour. CH1 domain of α-actinin is bound to F-actin in the structure, however that is omitted for clarity. C) Schematic representation of F-actin shows subunits as spheres. Lines on the left side show double helix interpretation of F-actin. Sinusoidal curve on the right side shows single helix interpretation of F-actin. D) Negative stain electron microscope image of F-actin decorated in part with myosin heads that show pointed and barbed end of an arrowhead structure. Image is taken from (Pollard, 2016).

Actin is essential in all eukaryotes. In muscle cells it makes up the thin filaments and along with muscle myosin-2, which makes up the thick filaments, is responsible for muscle contraction. In non-muscle cells actin has a wide range of functions as actin filaments are major component of the cytoskeleton and are responsible for maintaining cell structure and dynamics. During cytokinesis actin takes part in the contractile ring formation (Pelham and Chang, 2002). Actin dynamics in lamellipodia and filopodia plays a major role in cell migration. Actin is also found in focal adhesions and stress fibers that are involved in cell adhesion (Le Clainche and Carlier, 2008). Actin also provides track for cargo transport inside the cell. To carry out these various functions, a wide range of actin-binding proteins bind to the filaments. These protein often bind to the groove between actin subdomains I and III (Dominguez, 2004).

Actin is one of the most conserved proteins in eukaryotes (Gunning et al., 2015). Prokaryotes also encode actin homologue proteins, called MreB, FtsA and ParM that are responsible for distinct cellular processes, reviewed by (Pollard, 2016). Most eukaryotes utilise distinct actin isoforms for distinct cellular processes: α-actin in muscle cells, β- and one type of γ-actin in nonmuscle cells and another type of γ-actin in smooth muscle cells (Herman, 1993).

1.3 Myosin-5

1.3.1 Structure of myosin-5

The myosin-5 molecule contains two heavy chains that form a dimer. The dimer takes several 36 nm steps, before falling off actin, which makes it a processive molecular motor. It consists of a head and a tail domain (Cheney et al., 1993). The N-terminal head comprises the motor domain which binds actin and hydrolyses ATP and the α-helical lever, which has 6 IQ motifs, binding 6 calmodulin-like light chain molecules. The tail domain contains coiled-coil forming sequences, which are required for dimerisation. This is followed by sequences that are predicted to form coiled-coil and are interrupted by two loops, a proximal and a distal loop. The C-terminal region of the molecule is the cargo binding domain or globular tail domain (GTD) (Figure 1.6, 1.7). Alternative splicing yields the two isoforms of myosin-5a, found in melanocytes and brain cells containing exons A, C, D, E, F and A, B, C, E, respectively (Seperack et al., 1995). All exons are located at the tail domain, importantly exons B and D are located at the distal loop and exon F is located downstream compared to them (Figure 1.8) (Seperack et al., 1995; X. Wu et al., 2002).

Myosin-5a was first identified in mammalian brain tissue (Larson et al., 1988), then later on in yeast (Johnston et al., 1991) and also in mammalian melanocytes (Mercer et al., 1991). It was first purified from chicken brain tissue (Espreafico et al., 1992). Cheney *et al.* found that besides calmodulin two additional proteins co-purify with myosin-5a (Cheney et al., 1993), that were identified as L17 and L23 myosin-2 essential light chains, that are 17 and 23 kDa, respectively (Espindola et al., 2000). However these light chains were not found in myosin-5a purified from mouse brain (Wang, Chen, et al., 2000). A further 10 kDa light chain was found to bind both chicken and mouse brain myosin-5a (Espindola et al., 2000; Wang, Chen, et al., 2000). This light chain was identified to be the same that binds to cytoplasmic and axonemal dynein (King et al., 1996), thus its name, DLC8 dynein light chain, was retained. Exon B that is located on the distal loop in the tail domain of brain isoform myosin-5a was found to be responsible for dynein light chain binding and thus this molecules only binds to the brain isoform (Hodi et al., 2006; Wagner et al., 2006).

Myosin-5a was imaged with rotary shadowing electron microscopy, in which two heads, a tail and cargo binding domains were clearly visible (Figure 1.6) (Cheney et

al., 1993). The head is approximately 31 nm in size that consists of the motor domain (~10 nm) and of the lever with 6 IQ motifs (~21 nm) (Cheney et al., 1993). The size of the motor domain corresponds to that observed for muscle myosin-2 (~9 nm) using crystallography (Figure 1.2) (Rayment et al., 1993). A myosin-5 construct, which comprises only the motor domain and the lever with 6 IQ motifs is usually considered an S1 fragment. That is followed by a coiled-coil that is ~30 nm in chicken myosin-5a (Cheney et al., 1993). However in mouse myosin-5a the coiled-coil is ~26 nm as it is made up from 175 residues (Baboolal et al., 2009). The first part of the coiled-coil is followed by the proximal loop that contains a PEST site, which is rich in proline, glutamic acid, serine and threonine and is prone to cleavage by proteases. The HMM construct of myosin-5 comprises the head and the tail up to this point. The proximal loop is followed by another predicted coiled-coil segment that is ~13 nm in both chicken (Cheney et al., 1993) and mouse myosin-5a. This is followed by the distal loop, which encodes exon B that is 3 amino acids long (DDK) (Hodi et al., 2006; Wagner et al., 2006). The final, predicted coiled-coil segment just preceding the globular tail domain is ~13 nm in chicken (Cheney et al., 1993) and ~15 nm in mouse myosin-5a considering that it is ~100 residue-long and the length of a coiled-coil was measured to be 0.15 nm rise per amino acid (Chothia et al., 1981). C-terminal of the protein is the globular tail domain that is responsible for cargo binding.

Myosin-5a was first imaged bound to actin by negative stain electron microscopy (Figure 1.7A) (Walker et al., 2000). The two heads of the molecule were usually bound 13 actin subunits apart, that is 36 nm distance. However some molecules were bound 11 or 15 actin subunits apart (30 and 41 nm, respectively), suggesting that flexibility in the myosin heads enables it to vary the angle and distance it is attached to actin. The lead head was found to be curved, whereas the trail head is straighter. The short tail of the HMM construct that was used in this study was usually found to be angled in the direction of the trail head (arrow on Figure 1.7A). The trailing lever was found to be angled at 40º to the filament, whereas the leading lever angled at the average of 115º (values ranging from 90º to 150º) to the filament, resembling post- and pre-powerstroke conformations, respectively (Walker et al., 2000).

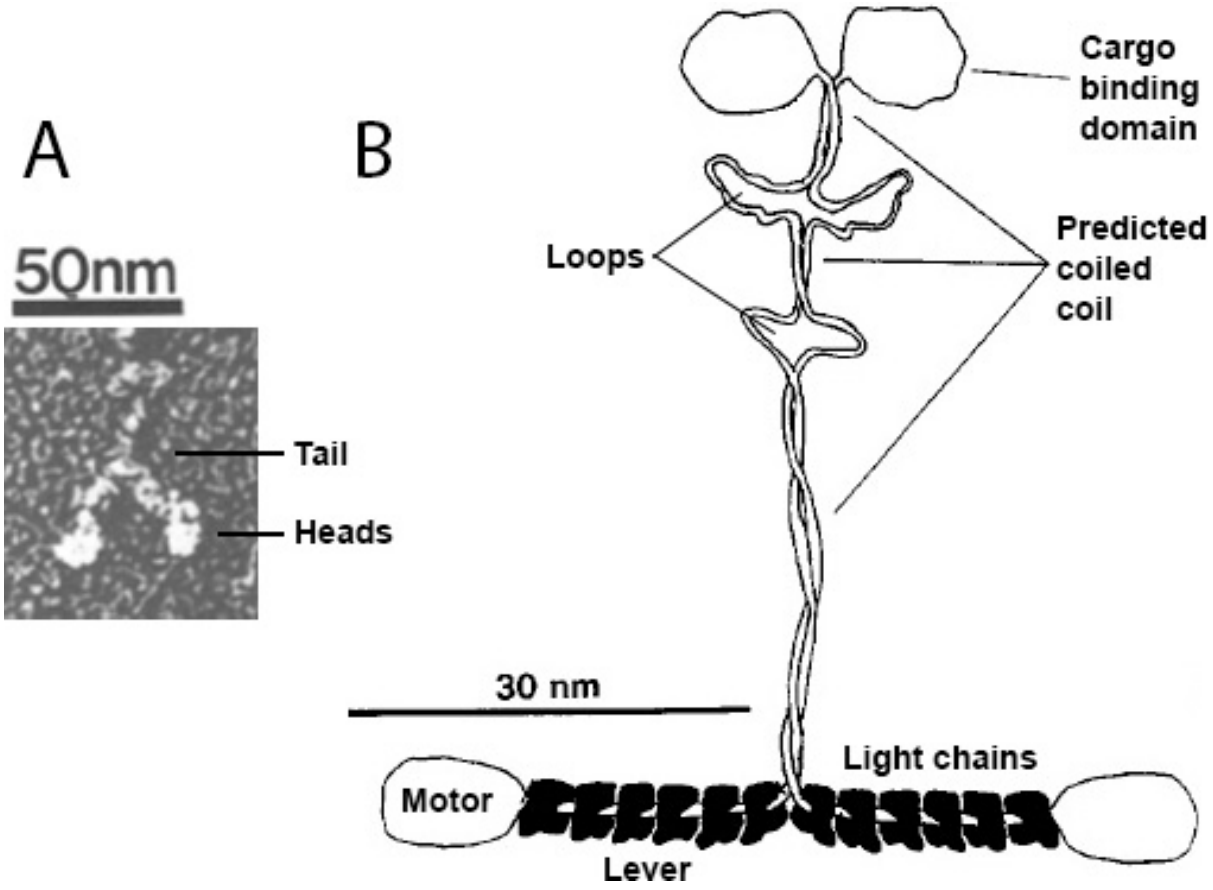

Figure 1.6. *Electron micrograph and schematic figure of myosin-5. Panel A) shows shadowing electron micrograph of myosin-5 with heads and tail domains. Scale bar is 50 nm. Panel B) shows schematic representation of myosin-5 observed in panel A. Calmodulins bound to the lever of myosin are represented black. Adapted from (Cheney et al., 1993).*

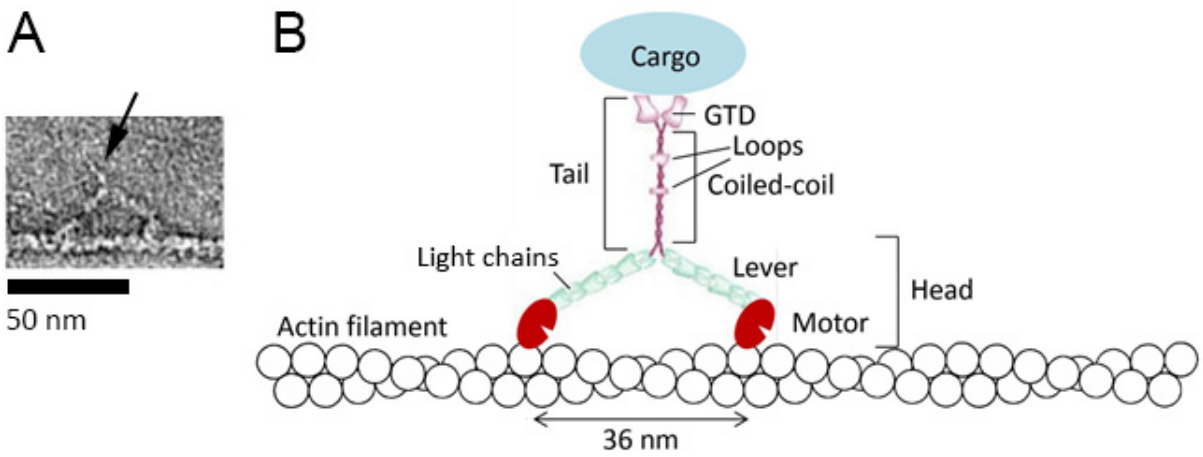

Figure 1.7. *Electron micrograph and schematic figure of myosin-5a bound to actin. Panel A) shows negative stain electron micrograph of myosin-5a bound to F-actin. Arrow points to the coiled-coil tail. Scale bar is 50 nm. Figure is taken from (Walker et al., 2000). Panel B) shows schematic representation of myosin-5a carrying cargo on an actin track. GTD stands for globular tail domain. The two myosin heads bind to actin 36 nm apart from each other spanning the helical pitch of the actin filament. There are 6 light chains bound to the 6 IQ motifs of the lever. The coiled-coil tail of myosin-5 is interrupted by loops. Adapted from a figure by Dr. James Sellers.*

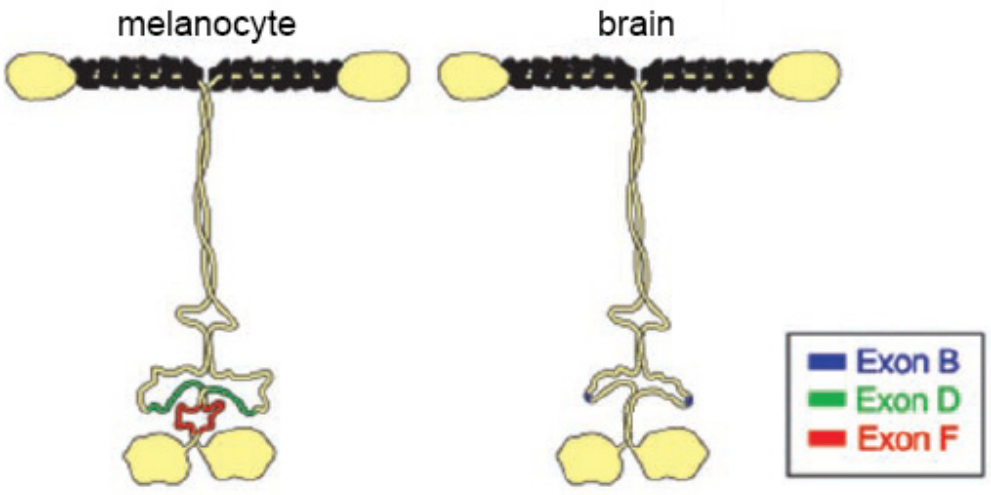

Figure 1.8. *Schematic figure of the two isoforms of myosin-5a. Exon B, D and F are denoted with blue, green and red colouring, respectively. Adapted from (X. Wu et al., 2002).*

1.3.2 Myosin-5a motor activity

Myosin-5a undergoes multiple enzymatic cycles without the molecule detaching from actin, which allows the processive movement of myosin along the actin track (Sakamoto et al., 2008; Nelson et al., 2009; Andrecka et al., 2015). This is required for the *in-vivo* function of myosin-5a, which is transporting various cargos, reviewed by (Hammer 3rd and Sellers, 2012).

Myosin-5 moves in a hand-over-hand fashion, where the two heads alternate position in every step (Walker et al., 2000; Yildiz et al., 2003; Warshaw et al., 2005; Sakamoto et al., 2008; Andrecka et al., 2015). Starting from the waiting state in the enzymatic cycle (A in Figure 1.9), myosin is attached to actin with bound ADP in both heads (Sakamoto et al., 2008). The intramolecular strain exerted on the trail head by the lead head accelerates the release of ADP from the trail head by two fold and inversely, the intramolecular strain exerted on the lead head by the trail head slows ADP release on the lead head by 50 fold (Rosenfeld and Sweeney, 2004; Veigel et al., 2005). This is then quickly followed by the binding of ATP and detachment of the trail head (B in Figure 1.9). The bound head then undergoes the powerstroke and the free head hydrolyses ATP (C in Figure 1.9). The free head then rebinds to actin (D in Figure 1.9) to become the new leading head and it releases P_i (E in Figure 1.9).

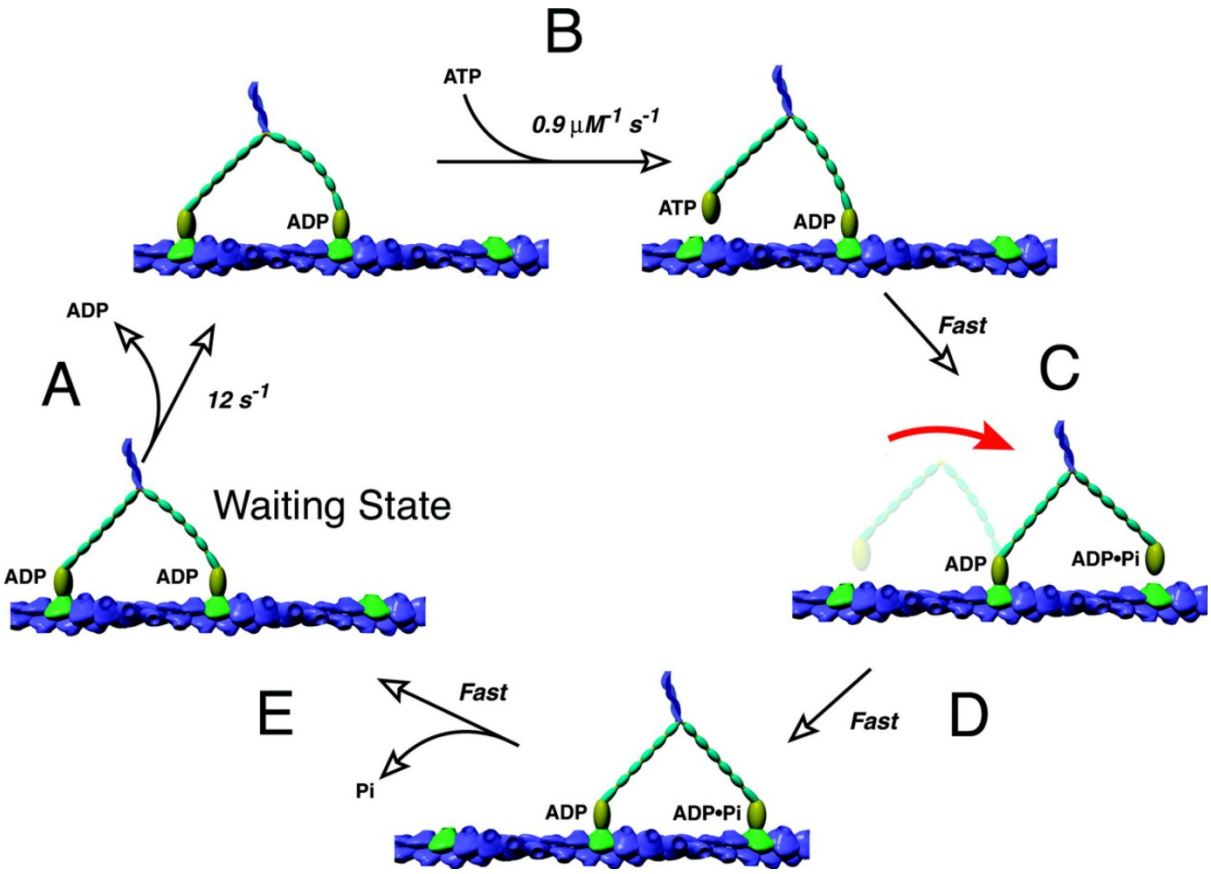

Figure 1.9. *Enzymatic cycle of myosin-5 processive motion. A) Waiting state, where both heads of myosin-5 is bound to actin and contain ADP. ADP dissociates from the trail head with a rate constant of 12 s^{-1}. B) ATP binds to the trail head with a rate constant of 0.9 μM^{-1} s^{-1}. C) The trail head lets go of actin, hydrolyses ATP and the lead head undergoes the powerstroke. The red arrow shows the displacement of the trail head and lever. D) The trail head binds to actin becoming the new lead head. E) P_i dissociates from the new lead head. Figure is taken from (Vale, 2003).*

Electron microscopy and X-ray crystallography revealed the two conformations of the lever being 60° apart from each other representing the two ends of the powerstroke (Walker et al., 2000; Coureux et al., 2003; Coureux et al., 2004). Burgess *et al.* compared the observed electron micrographs of the lead and trail heads with crystal structures of scallop myosin-2 docked onto actin (Figure 1.10). They demonstrated that the lead and the trail heads have their converter domains and thus their lever in different positions. The detached head undergoes the recovery stroke before binding again to actin (Burgess et al., 2002).

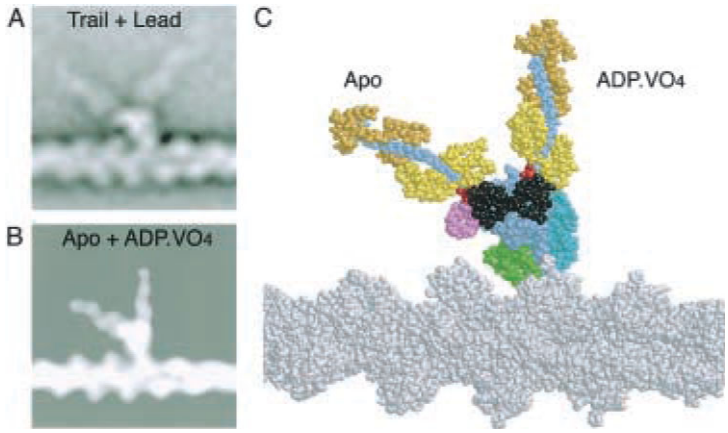

Figure 1.10. *The lead and the trail heads have their lever in different positions. Figure is taken from (Burgess et al., 2002) A) Superimposition of average lead and trail heads of myosin-5 considering that the molecule moves towards the pointed end (left) of the actin filament. B-C) Superimposition of apo and ADP.VO_4 containing scallop myosin-2 crystal structures docked onto the atomic model of the actin filament (Lorenz et al., 1993). B) Image has been filtered to 2 nm resolution. C) Actin filament is grey, myosin-2 heavy chain is blue, motor domains are light blue, green, magenta, converter region is black, light chains are yellow.*

A single molecule fluorescence study demonstrated the tight coupling between the ATPase cycle and the stepping motion of myosin-5 (Sakamoto et al., 2008). Sakamoto *et al.* used a fluorescent analogue of ATP (deac-aminoATP) and fluorescently labelled calmodulins bound to the lever of myosin-5. They simultaneously followed the two fluorescent signals and found that they move in the same direction with the same speed, however, myosin-5 was moving in 36 nm steps, whereas the nucleotide signal was moving in 18 nm steps. One step of the nucleotide signal happened together with the myosin-5 signal and the other step in the dwell time of myosin-5. Figure 1.11 shows the model built from the observations. In step 1, where both heads contain deac-aminoADP, the fluorescent nucleotide signal coincides with the myosin-5 signal. Then the trail head releases ADP (step 2), so the signal moves 18 nm, as it is now only coming from the lead head deac-aminoADP. In step 3 the trail head binds deac-aminoATP and dissociates from actin, the powerstroke happens in the leading head and the trail head becomes the lead head. Even though the ATP binding is partially rate limiting in this experiment as they used low concentrations of ATP, still the binding of nucleotide and the concomitant powerstroke is more rapid than the sampling rate in the experiments,

therefore no backwards stepping of the nucleotide signal was observed. Thus, in step 4 both the myosin-5 and the nucleotide signal move and coincide again. This study showed that the gating between the two heads is very strong, as the fluorescence signal coming from the nucleotide does not take a backward step, meaning that no nucleotide is released from the lead head as long as the trail head is attached.

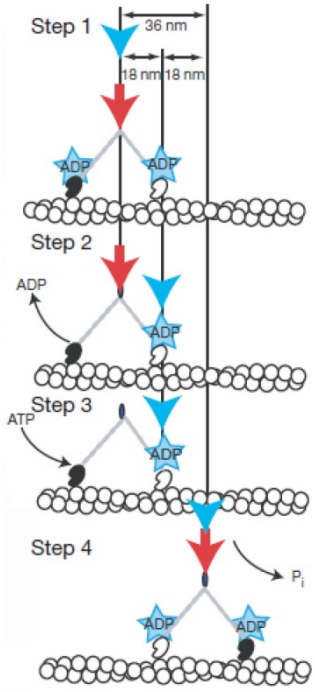

Figure 1.11. *ATPase mechanism and stepping motion of myosin-5. Step 1: Both myosin heads contain ADP, therefore the fluorescent signal coming from the myosin (red arrow) and nucleotides (blue arrow) coincide. Step 2: ADP dissociates from the trail head, thus the nucleotide signal moves 18 nm forward. Step 3: ATP binds to the trail head, which lets go of actin. This step is faster than the sampling rate of the experiment, therefore no movement of the signals is observed. Step 4: The trail head becomes the new lead head with bound ADP, so the myosin signal moved 36 nm, while the nucleotide signal 18 nm, and they coincide again. Figure is taken from (Sakamoto et al., 2008).*

Veigel *et al.* found that the working stroke of both single-headed recombinant myosin-5 and dimeric myosin-5 are 21–25 nm, however the stepping of the dimeric myosin-5 was found to be 36 nm, which is 13 actin subunits apart from the previous binding site (Veigel et al., 2002). They proposed that a forward-biased thermally driven diffusive movement adds the remaining 11 nm movement. According to the model, after the working stroke happens the new lead head has to go under a movement of 11 nm to bind preferentially 36 nm away from the trail head. In this conformation both heads can bind to actin with little or no twist compared to the actin filament axis. However, the heads can rotate at the head-tail junction to enable attachment to actin, thus attachment of 11 and 15 subunits apart was also found in the 13% and 10% of the observed molecules, respectively (Oke et al., 2010). Since the actin subunits in the filament have a helical path with crossover points every 36 nm (Figure 1.5C), this size of stepping, which is determined by the length of the lever and the angle through which it moves, enables myosin to linearly transport cargo along the actin filaments. It also facilitates myosin-5 to walk along bundles of actin, where following a helical track would not be possible.

Processive runs can be established via strain-dependent kinetic gating. Being a high duty ratio motor, a single-headed myosin-5 spends approximately 70% of its ATPase enzymatic cycle bound to actin at low actin and ADP concentrations (De La Cruz et al., 1999). The strain exerted on the lead head by the trail head dramatically slows the rate of ADP release from the lead head (Rosenfeld and Sweeney, 2004; Veigel et al., 2005; Sakamoto et al., 2008). This interhead strain facilitates that the trail head detaches before the lead head, and then it quickly rebinds to become the new leading head, however the two heads work independently in the absence of actin (Forgacs et al., 2008). This mechanism can ensure that myosin-5 does not detach from actin before transporting the vesicle to its target place (Forgacs et al., 2008). The kinetics of myosin-5 is also regulated by the external load, so that pulling and pushing forces increase and reduce the average lifetime of myosin-5 bound to actin, respectively (Veigel et al., 2005) and pulling forces can reduce the rate of the diffusive search of the new leading head (Clemen et al., 2005). A range of pulling forces does not affect the length of the step (Veigel et al., 2005). However, mutant molecules containing 4 or 8 IQ motifs in the lever, thus being 2 IQ shorter or longer than the wild type, walk in shorter or longer steps, respectively, leading to a helical path (Sakamoto et al., 2003; Sakamoto et al., 2005; Oke et al., 2010).

The IQ motifs present in the lever of myosin-5 can be substituted by single alpha helical (SAH) domains, and this structural motif can also act as a lever in myosin-6 and myosin-10. Baboolal et al found that the SAH domain containing myosin-5 chimera takes similar processive steps along actin as the wild-type, however no gating was found for the ADP release from the lead head. This observation questions if kinetic gating is required for the processivity of myosin-5 (Baboolal et al., 2009).

1.3.3 Myosin-5 tail and the organelle transport

In higher eukaryotic cells, organelles are usually being transported from the centre of the cell to the periphery by kinesins, while dyneins participate in retrograde transport directed towards the cell centre. Kinesins walk along microtubules from the minus end at the centrosome towards the plus end. When reaching the periphery of the cell, the cargo is switched to actin-based transport (Woolner and Bement, 2009). Myosin-5 is then involved in the local movement of the cargo.

Myosin-5 moves mRNA, pigment granules, neuronal vesicles, endoplasmic reticulum and other vesicles in the cells. Myosin-5a moves melanosomes in melanocytes and endoplasmic reticulum in Purkinje neurons, while myosin-5b carries endosomes in hippocampal neurons, reviewed by (Hammer 3rd and Sellers, 2012). Myo4 that is a myosin-5 homologue in budding yeast *Saccharomyces cerevisiae* moves mRNA into the bud tips (Shepard et al., 2003).

Mouse myosin-5a was found to transport melanosomes at 0.14 μm/sec speed in melanocytes (Wu et al., 1998) and to transport endoplasmic reticulum at 0.45 μm/sec speed in Purkinje neurons (Wagner et al., 2011). Since *in vitro* the number of the observed processive steps is between 20 and 60 (Veigel et al., 2002; Baker et al., 2004), myosin should transport its cargo over micrometre distances. It is also capable of switching between actin tracks to transport the cargo for long distances (Ali et al., 2007; Bao et al., 2013). It is currently not known how many myosins attach to one cargo to enable its transport inside the cell, however it has been estimated that more than 100 myosin-5 molecules are attached to a vesicle of a radius of 100 nm (Miller and Sheetz, 2000).

The C-terminal GTD is responsible for binding the cargo, however the cargo may also bind to the loops interrupting the coiled-coil domain (X.S. Wu et al., 2002).

Adaptor proteins are also involved in this process, which makes myosin-5 capable of binding different cargos and also different isoforms of myosin-5 bind different cargos. Exon F located at the tail domain of melanocyte isoform myosin-5 was found to be indispensable for myosin-5 localisation to melanosomes, as a mutant protein lacking this exon or the brain isoform of myosin-5 did not co-localise with melanosomes (X. Wu et al., 2002). Dynein light chain bound to exon B, present in the brain isoform of myosin-5 tail domain, is thought to be involved in cargo binding (Naisbitt et al., 2000; Navarro et al., 2004). When there is no cargo present, the globular tail domain tends to bind the motor domains and the molecule folds into a triangular conformation (Thirumurugan et al., 2006; Liu et al., 2006). In this conformation ATPase activity is inhibited, but increased level of Ca^{2+} can reactivate the molecule *in vitro* (Krementsov et al., 2004; Wang et al., 2004). However, the physiological activator of myosin-5 is presumably binding of an adaptor protein like melanophilin (Wu et al., 2006; Li et al., 2005; Sckolnick et al., 2013), since increased Ca^{2+} level would make calmodulins dissociate from the lever inhibiting myosin-5 stepping (Nguyen and Higuchi, 2005; Wu et al., 2006; Shen et al., 2016).

1.3.4 Properties enabling myosin-5 to transport cargo

To be able to transport cargo inside the cell, the physical properties of myosin-5 have to overcome the following issues. i) The size of the cargo transported along the actin filaments is ranging from 50 nm to 1 µm (Tabb et al., 1998), and therefore it might get stuck in the meshwork of cytoskeletal filaments and membranes within the cell. ii) The cytosol exhibits time-dependent deformation when stress is applied, as it is a viscoelastic medium (Canetta et al., 2005; Luby-Phelps, 2013; Goychuk et al., 2014), meaning that it has the properties of both viscous and elastic materials. The viscosity of the cell is in the range of 10^2 Pa.sec (Bausch et al., 1999), which is approximately five orders of magnitude higher than the viscosity of water. Moving of a relatively large cargo in a viscous medium would generate drag force on the myosin-cargo complex. iii) Given that the cell is a ‘crowded environment’ (Luby-Phelps, 2013) and a wide range of molecules can bind to actin, this can often mean that myosin-5 encounters obstacles while moving on actin filaments.

In cells, the behaviour of organelles trafficked by molecular motors is affected by the crowded environment. It has been shown that high densities of free kinesins can cause a ‘traffic jam’ on microtubules and hinder forward transport of cargo *in vitro*

(Conway et al., 2012). Results also suggested that cargos bind multiple kinesins that increase run length (Beeg et al., 2008), moreover cargos can also acquire new motors along the way enabling them to overcome obstacles or traffic jams (Conway et al., 2012). The transport of early endosomes by dynein was studied with live cell imaging and it was found that two-thirds of the early endosomes exhibited a confined motion, caged by the actin cytoskeleton (Zajac et al., 2013; Trybus, 2013). The motile subpopulation of the cargos showed directed movement with longer, diffusive pauses (Zajac et al., 2013). The site of the pauses co-localised with high density of microtubules, endoplasmic reticulum and other early endosomes, suggesting that these can regulate transport (Zajac et al., 2013; Trybus, 2013).

It has been previously proposed that if the tail region of myosin-5 is elastic, myosin-5 would step more regularly while moving cargo through a viscoelastic cytoplasm (Schilstra and Martin, 2006). The idea is that the motor could continue moving while the cargo is being squeezed through the meshwork, which can only be possible if the tail is able to extend over the force range that the cargo exerts on the motor. The coiled-coil tail of skeletal muscle myosin-2 (Schwaiger et al., 2002; Root et al., 2006) and that of mouse myosin-5 (Nagy et al., 2009) were studied using force spectroscopy and it was found that the tail domain of myosin-5 is much more elastic compared to the skeletal muscle myosin-2, most probably because various loops interrupt the coiled-coil segment (Nagy et al., 2009; Hammer 3rd and Sellers, 2012). The coiled-coil motif of myosin-2 is mechanically stable and relatively stiff compared to the loops. However, the coiled-coil motif is able to extend too and unfolds at forces of 25-40 pN (Schwaiger et al., 2002; Root et al., 2006). This force is much higher than the stall force of myosin-5, that is ~3 pN (Mehta et al., 1999; Uemura et al., 2004; Schilstra and Martin, 2006). Therefore the coiled-coil would not allow much movement of the heads in front of the cargo, thus if myosin-5 tail would only consist of coiled-coil segment, it would not be able to efficiently transport cargo along actin tracks. Force spectroscopy experiments revealed that first a low-force unfolding of the loops occurs and then the relative stiff coiled-coil structure extends while stretching the molecule (Nagy et al., 2009). Complete unfolding of the tail domain is not likely to occur *in vivo*, however the loops can extend even at low forces. This can be evidenced by the finding that the tail domain can be significantly longer (75 nm) than the sum of the coiled-coil domains (56 nm) as observed for chicken brain myosin-5a (Cheney et al., 1993). Presumably the loop motifs interrupting the coiled-

coil (Figures 1.6 and 1.7) enable the tail domain to extend elastically and absorb the force generated when the cargo is being stuck.

The potential 'backward' force applied to the cargo, combined with the forward movement bias of the motor is likely to result in an applied load on the motor (Schilstra and Martin, 2006). Imaging of molecular motors *in vitro* tends to use conditions where there is no load (Walker et al., 2000). Since the role of myosin-5 is to move cargo within the cell, it is of utmost importance to study the protein in circumstances mimicking load. Therefore the aim of this study was to investigate the effect of strain on the biophysical properties of myosin-5.

The challenge was to devise a methodology by which strain is introduced on myosin-5 *in vitro* as it walks along actin. To do this, I have generated recombinant myosins in which the tail of myosin-5 was modified so that it would strongly attach to the actin filament. When the tail engages with the actin filament as the myosin walks along it, it would be expected to exert a load on the motor. As the motor continues to walk along the filament, the load will increase until eventually the motor will stall at ~3 pN.

1.3.5 Tethering the tail using the biotin-avidin interaction

The initial approach I used to attach the tail to the actin filament exploited the avidin-biotin interaction. Biotin, also known as vitamin B_7 or vitamin H, is a carboxylic acid that serves as a coenzyme for carboxyl transferase enzymes (György et al., 1940). Avidin is a homotetrameric glycoprotein that is found in the egg white of birds (Eakin et al., 1940). Each subunit of avidin binds biotin with an approximate dissociation constant of 10^{-15} M (Green, 1963), which makes the avidin-biotin interaction the strongest known protein-ligand interaction. NeutrAvidin, a non-glycosylated and neutral derivative of avidin, has since been isolated (Hiller et al., 1987). The molecular weight of a NeutrAvidin subunit is 15 kDa and its β-barrel structure is made up from 8 antiparallel β-strands (Livnah et al., 1993). The biotin binding site is inside the β-barrel, positioned close to one end (Figure 1.12). The NeutrAvidin tetramer is a globular, 60 kDa molecule that has a diameter of ~5.8 nm, which is close to that of actin (5.5 nm). NeutrAvidin retains the binding properties of the native avidin glycoprotein, but has a reduced non-specific binding due to nonglycosylation, and a lack of positively charged residues (Hiller et al., 1987; Marttila et al., 2000). NeutrAvidin binding to surface-immobilised biotin has a

dissociation constant of approximately 2 pM and a binding rate constant of $2*10^8$ M^{-1} s^{-1} (Wayment and Harris, 2009).

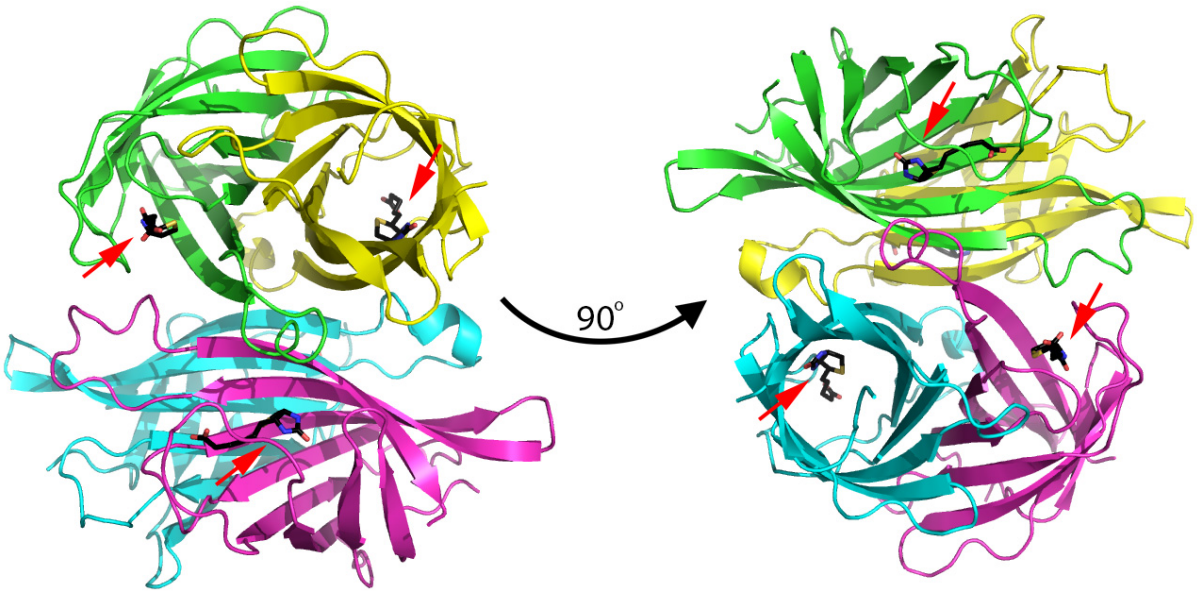

Figure 1.12. *Crystal structure of the deglycosylated avidin tetramer with bound biotin (PDB ID: 2AVI (Livnah et al., 1993)). Protein is shown as cartoon representation with colour coded monomers. Red arrows point to biotin that is shown with stick representation and atomic colouring with black carbons. The structure on the right side has been rotated 90º right around the vertical axis with respect to the structure on the left side.*

A biotinylation tag at the N-terminus of myosin-5a HMM has previously been used to attach quantum dots via streptavidin to myosin-5a (Hodges et al., 2007; Nelson et al., 2009; Andrecka et al., 2015). The 15 amino acid Avi-tag on purified myosin-5a was specifically biotinylated by the purified *E. coli* biotin ligase (BirA) enzyme *in vitro* (Beckett et al., 1999). In our experiments, the Avi-tag was introduced at the C-terminal end of a myosin-5a construct (Figure 1.13). The aim was to biotinylate the purified myosin, mix it with biotinylated F-actin, in which 5-10% of the actin monomers are biotinylated, and then add avidin to crosslink the biotinylated myosin tail to the actin filament. By tethering the tail to the actin filament in this way, this was expected to apply a load to the motor as it walks along the actin filament away from the site of tail attachment, and thus enable us to visualise any effects on the coiled-coil tail and on the motor domains (Figure 1.13).

The extent of the coiled-coil domain was assessed using the COILS webserver (http://embnet.vital-it.ch/software/COILS_form.html), which predicts the probability of coiled-coil formation (Lupas et al., 1991). The prediction suggests that residues 900 to 1100, 1150 to 1240 and 1310 to 1430 form coiled-coil (Figure 1.14), whereas residues 1100 to 1150 and 1240 to 1310 form loops. This agrees with earlier published predictions (Cheney et al., 1993). Previously, HMM constructs of mouse myosin-5a have been studied. This construct is 1,091 residues long (Wang, Chen, et al., 2000) and contains a ~26 nm long coiled-coil (e.g. the first region of coiled-coil predicted to exist in the tail) (Baboolal et al., 2009). The present construct is 350 amino acids longer than the HMM construct, and additionally contains the loops and both of the predicted distal coiled-coil motifs.

The C-terminal cargo binding globular tail domain (GTD) of myosin-5a is not included in this construct, as the main focus of this study was the investigation of the coiled-coil tail. Including the GTD in the construct would have increased its size by an additional 44 kDa, making the construct more difficult to express. Moreover, a full length construct containing the GTD tends to adopt an auto inhibitory conformation without the cargo being present (Thirumurugan et al., 2006), and this may have interfered with achieving the aims of this study.

The myosin-5a Avi-tag construct contains an N-terminal GFP followed by the first 1,440 amino acids of the mouse myosin-5a brain isoform, which includes the motor domain and coiled-coil motifs, but excludes the cargo binding domain. This is followed by an Avi-tag sequence (15 amino acids long (GLNDIFEAQKIEWHE)) (Beckett et al., 1999) and a Flag tag for affinity purification. The heavy chain of the construct is 1,721 residues long (Figure 1.16). The predicted molecular weight is 200 kDa and it is expected to bind six calmodulin molecules per heavy chain. For simplicity, this construct is called Myo5-Avi.

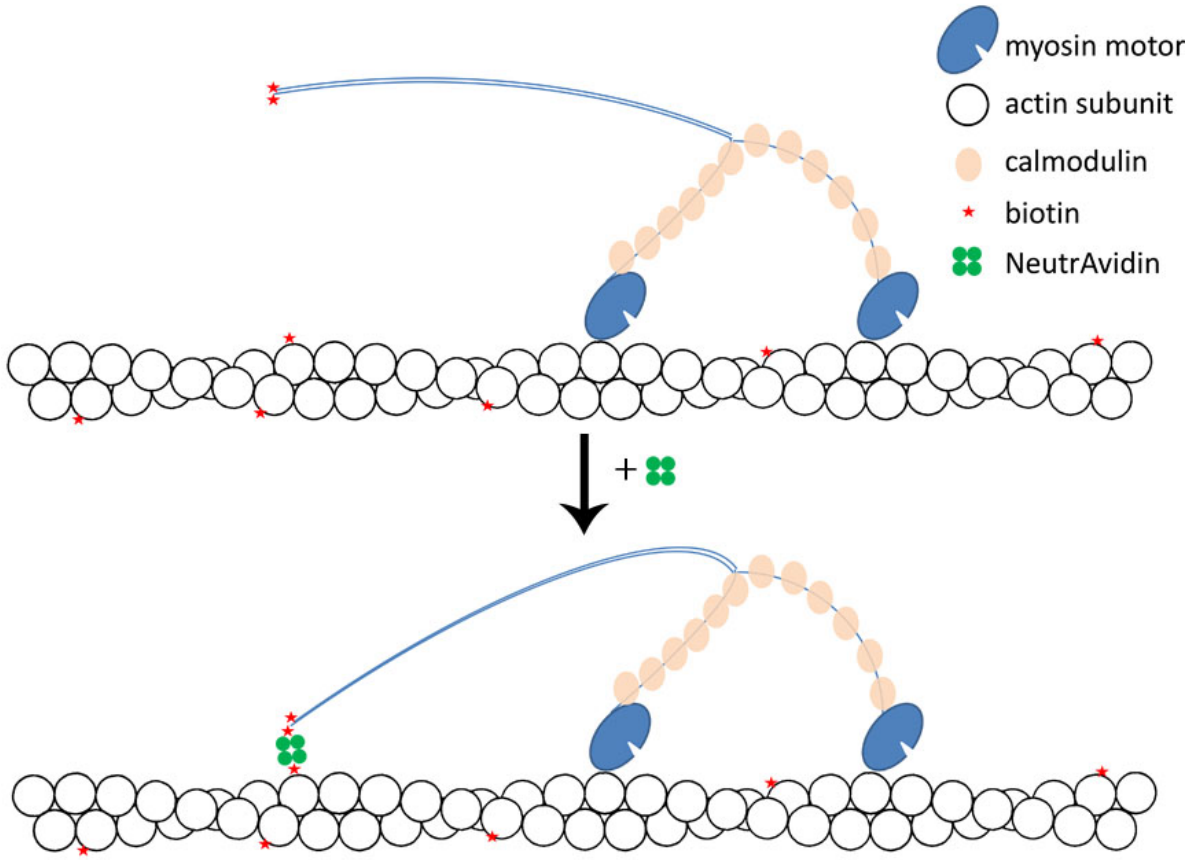

Figure 1.13. *Schematic representation shows how the biotin-actin interaction is planned to be applied to attach the tail of myosin-5 to actin.*

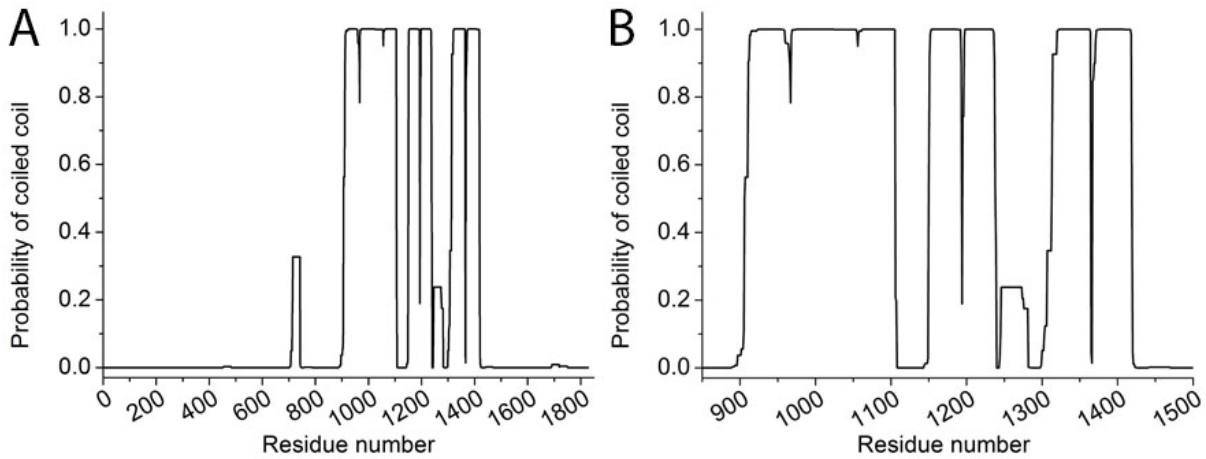

Figure 1.14. *Result of the coiled-coil prediction by COILS webserver, using a scanning window of 28 amino acids. Probability of coiled-coil formation is shown as a function of the residue numbers of the brain isoform of mouse myosin-5a. Panel A) shows all residues of mouse myosin-5a. Panel B) shows only the coiled-coil region for easier assessment.*

1.3.6 Making the coiled-coil tail longer

Attaching the tail of the previously described Myosin-5-Avi construct to actin might not work well if the tail is not long enough or not flexible enough to attach to the same actin filament as the myosin motors are walking on. To overcome this possible issue, the tail was designed to be longer in a second, Myosin-5-cc construct compared to the Myosin-5-Avi construct.

The myosin-5a HMM construct contains the first region of coiled-coil, equating to 189 amino acids, that makes the tail of this molecule 28 nm long (0.15 nm rise per amino acid (Chothia et al., 1981; Baboolal et al., 2009)). A second construct was engineered in which this region of coiled-coil was almost doubled. This is achieved by adding an additional 175 residues of coiled-coil sequence from the first region of coiled-coil. This is expected to increase the length of the coiled-coil by 26 nm. The planned construct was also assessed by the COILS webserver and prediction suggested that this doubled region still forms coiled-coil (Figure 1.15). The inserted region of coiled-coil is then followed by the remaining 350 amino acids of the tail, Avi-tag and Flag tag sequences as in the Myo5-Avi construct. This construct is 1,896 residues long (Figure 1.16). The predicted molecular weight is 220 kDa and it binds six calmodulin molecules per heavy chain. For simplicity, this construct is named Myo5-cc.

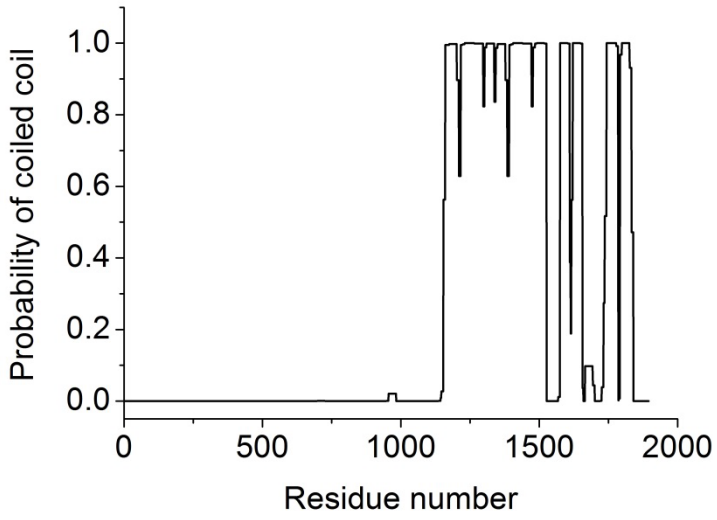

Figure 1.15. *Result of the coiled-coil prediction of Myo5-cc by COILS webserver, using a scanning window of 28 amino acids. Probability of coiled-coil formation is shown as a function of the residue numbers.*

1.3.7 Use of an Adhiron to tether myosin-5a to actin via its tail

A further myosin-5a construct was also designed using Myo5-cc, in which the sequence for the Avi-tag at the end of the tail, was replaced by the sequence for Adhiron14. As shown in chapter 3, Adhiron14 binds to F-actin with a high affinity, and therefore its inclusion at the end of the myosin-5a tail should enable the binding of the tail to F-actin without any need to modify the protein. This construct contains an N-terminal Avi-tag that could potentially be used to label this construct with a Q-dot. GFP is also included in this construct downstream of the sequence for Adhiron14, to monitor expression of this protein in *Sf9* cells, and for use as a fluorescent reporter of the isolated protein in *in-vitro* studies. The whole construct is 1,993 residues long and the predicted molecular weight is 232 kDa (Figure 1.16). This construct is also expected to bind six calmodulin light chains per heavy chain. For simplicity, this construct is called Myo5-Ad.

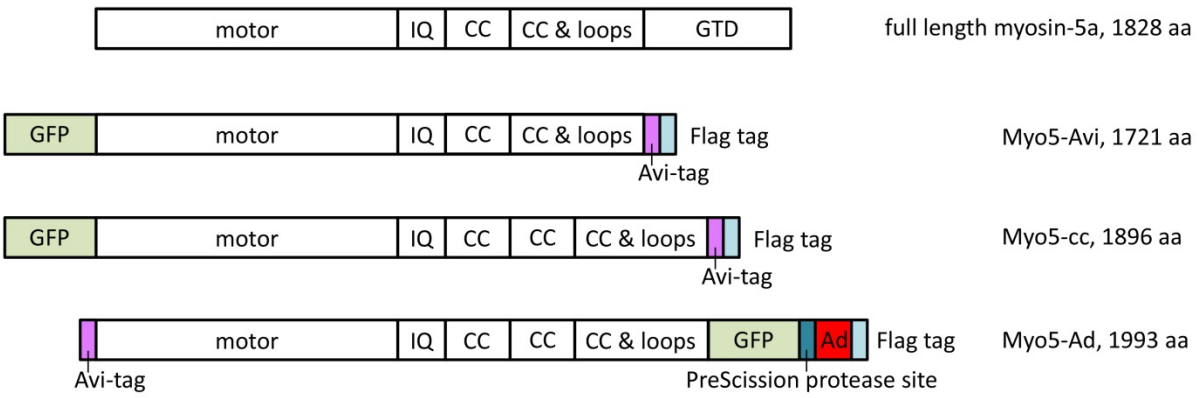

Figure 1.16. *Schematic representation of the full length wild type myosin-5a and of the designed constructs. Labelling is the following. Motor: motor domain of myosin-5a; IQ: lever with the 6 IQ motifs; CC: 175 amino acids long coiled-coil; CC & loops: 350 amino acids long tail domain that contains predicted coiled-coil and loops; GTD: globular tail domain; GFP: enhanced GFP; Ad: Adhiron14.*

1.3.8 Use of chaperones to improve folding and expression of myosin-5a constructs

Co-expression of specific chaperones has recently been shown to increase the yield of recombinant myosin motor constructs (Bird et al., 2014; Bookwalter et al., 2014). These chaperones are normally associated with proper folding of the motor domain (Barral et al., 2002; Liu et al., 2008). In particular, heat shock protein chaperones

(Hsc70 and Hsp90) and their co-chaperone (Unc45b) are required for proper folding of striated muscle myosin motor domain (Barral et al., 2002; Liu et al., 2008). Hsc70 and Hsp90 are general chaperones, while members of the Unc45 family are myosin specific co-chaperones. Unc45b is only expressed in skeletal and cardiac tissues, whereas Unc45a can be found in every vertebrate tissue (Price et al., 2002). The N-terminal tetratricopeptide repeat (TPR) motif of Unc45 proteins is responsible for the protein-protein interaction of Unc45 with Hsp90, while the C-terminal UCS domain interacts with the myosin motor (Srikakulam et al., 2008). The UCS domain is named after the proteins that were found to contain this domain: Unc45 from *Caenorhabditis elegans*, Cro1 from *Podospora anserina* and She4p from *Saccharomyces cerevisiae* (Barral et al., 2002). These chaperones are required to express soluble and active myosin-14 (Bookwalter et al., 2014) and myosin-15 (Bird et al., 2014) in *Sf9* cells. Co-expression of both Hsp90 and Unc45b increased the yield of soluble myosin-15 in *Sf9* cells, even though there is some endogenous expression of Hsp90 in these cells (Bird et al., 2014).

The myosin-5a constructs used here are larger than the usual HMM constructs that were designed and expressed previously (Andrecka et al., 2015; Zimmermann et al., 2015). I therefore wanted to test if their co-expression with chaperones might increase protein expression levels to obtain high yields for the downstream biochemical and *in-vitro* studies.

1.4 Actin binding molecules

1.4.1 Phalloidin

Phalloidin, which is the toxin of death cap mushroom (*Amanita phalloides*), is a cyclic peptide that causes severe liver damage in humans (Wieland and Faulstich, 1978). It binds tightly with a 1:1 stoichiometry in the proximity of the nucleotide binding site of actin (Barden et al., 1987) with a dissociation constant of 22 nM (Cooper, 1987). Phalloidin decreases the rate of actin filament depolymerisation (Estes et al., 1981) by blocking the nucleotide exchange in actin subunits (Barden et al., 1987). Binding of phalloidin to actin decreases the critical concentration of filament formation as it shifts the equilibrium between actin monomers and filaments towards the filamentous state (Estes et al., 1981). The cell membrane is impermeable for phalloidin, thus it was microinjected into live cells and results showed that phalloidin

perturbs actin dynamics and cell growth (Wehland et al., 1977). Therefore fluorescent derivatives of phalloidin have only been applied to stain actin in fixed cells a long since (Wulf et al., 1979). As phalloidin binds inbetween the actin subunits (Steinmetz et al., 1998), it usually does not interfere with actin-binding proteins. However, exemptions include nebulin that competes with phalloidin for the same binding site (Ao and Lehrer, 1995) and both cofilin and gelsolin, that change the actin organisation, so that phalloidin is unable to bind (Nishida et al., 1987; Allen and Janmey, 1994). The interaction between the motor domain of some non-muscle myosin-2 isoforms and actin can also be perturbed in the presence of phalloidin that should be considered in the experimental design of *in-vitro* experiments (Diensthuber et al., 2011).

1.4.2 Actin-binding proteins and their use in imaging actin

A plethora of actin-binding proteins exist in the cell, that regulate actin assembly by various processes like nucleating actin for polymerisation, elongating, severing, capping, crosslinking and bundling actin filaments, reviewed by (Pollard, 2016).

Crystallographic studies showed that some actin-binding proteins, including gelsolin, cofilin, the WH2 (Wiskott-Aldrich syndrome homology region 2) motif containing proteins, profilin and FH2 (formin homology) motif bind to the hydrophobic pocket in subdomain I (Figure 1.5A) (Dominguez, 2004; Ferron et al., 2007; Park et al., 2015). This hydrophobic pocket is at the barbed end groove, which is still accessible when actin is polymerised into filaments. The actin-binding motif that is responsible for binding to the hydrophobic pocket was found to contain an α-helix with hydrophobic residues, but without consensus sequence similarity (Dominguez, 2004).

The interaction and the binding site between the myosin motor and F-actin have been recently explored in detail by a high resolution cryo electron microscopy study (von der Ecken et al., 2016). The motor domain was found to interact with subdomains I and II of one actin subunit and also with the loop of subdomain II of the adjacent actin subunit.

The spectrin superfamily that includes fimbrin, α-actinin, utrophin and dystrophin actin-binding proteins, bind with a calponin homology (CH) domain to actin. Cryo electron microscopy studies suggested that the tandem CH repeat domains interact with subdomains I and II in an actin subunit (Galkin et al., 2002; Galkin et al., 2010). Utrophin and dystrophin are homologue proteins, the latter was identified as the

defective protein in Duchenne and Becker muscular dystrophies (Monaco et al., 1986).

As actin is involved in various fundamental processes inside the cell including cytokinesis, migration and adhesion, there has always been a need to image actin structures and dynamics in living cells. As it was described above (in section 1.4.1), phalloidin was one of the first compounds used to study actin labelling in live cells. However, it is usually not applied anymore in living cells as i) it stabilises actin filaments and thus perturbs actin dynamics, ii) it requires microinjection which may have adverse effects on the behaviour of the cell. Another approach was to express or microinject fluorescent G-actin into cells (Kreis et al., 1982). However, expression of fluorescent G-actin altered actin assembly (Aizawa et al., 1997) and it was found to be excluded from formin-bound F-actin structures (Kovar et al., 2006; Chen et al., 2012).

One of the most widely used probes for staining actin in cells is Lifeact (Riedl et al., 2008), a fluorescently-tagged 17 residues long peptide from the N-terminus of the yeast actin-binding protein Abp140. It exhibits tight binding to both F-actin and G-actin, while it does not interfere with actin severing, nucleation, elongation or with the binding of myosin or α-actinin (Riedl et al., 2008). However Lifeact molecules rapidly exchange on F-actin (Riedl et al., 2008) and it was reported that Lifeact does not bind to stress induced cofilin-bound actin rods (Munsie et al., 2009).

Another widely used probe is F-tractin, the N-terminal, alpha-helical 66 amino acids of Inositol 1,4,5-Trisphosphate 3-Kinase A fused to a fluorophore (Schell et al., 2001). It was found to bind tightly to F-actin with a similar K_d (~2 μM) compared to Lifeact (Schell et al., 2001; Riedl et al., 2008). However it was also reported to dimerise and bundle actin filaments *in vitro* (Johnson and Schell, 2009) and modify F-actin structure *in vivo* (Schell et al., 2001; Johnson and Schell, 2009).

The CH domain of utrophin, that is the N-terminal 261 amino acids of the full length molecule, that binds to actin with a K_d of ~18 μM (Rybakova and Ervasti, 2005). Fluorescently-tagged version of this domain was found to label actin in variety of cell types without disturbing actin assembly (Burkel et al., 2007).

Recent studies compared the available fluorescent actin-binding probes in their localisation to different actin structures (Belin et al., 2014; Lemieux et al., 2014; Spracklen et al., 2014). The CH domain of either utrophin or filamin appeared to

have limited distribution (Belin et al., 2014; Lemieux et al., 2014), and do not recognise lamellipodial actin networks of spreading cells (Belin et al., 2014). Lifeact also failed to recognise lamellipodial structures and additionally is excluded from formin-bound actin filaments (Belin et al., 2014). The CH domain of utrophin and Lifeact were expressed in the *Drosophila* germline and found to cause sterility and severe actin defects (Spracklen et al., 2014). In contrast, F-tractin was found to label actin structures well, while not causing sterility or actin defects, when expressed in the *Drosophila* germline (Spracklen et al., 2014). The distribution of F-tractin resembled the distribution observed by phalloidin staining (Belin et al., 2014). However, it was also found that the choice of the fluorescent protein fused to the actin-binding probe and also the peptide linker between the probe and the fluorescent protein can alter the subset of F-actin labelled by the probe in the cells (Lemieux et al., 2014).

1.4.3 Single molecule motility assay setup

The motility of single molecules of motor proteins can be studied in a fluorescence-based *in-vitro* assay using TIRF (total internal reflection fluorescence) microscope. In this assay actin filaments are attached to the surface of a coverslip, then myosin is added and the translocation of single fluorescently labelled myosin molecules can be tracked.

Even though actin binds loosely to the surface of the coverslip, this does not attach actin properly as in this case the filaments were observed to move. Proper attachment of actin to the surface is crucial, so it does not interfere with myosin walking, especially since some myosins have been shown to follow a helical path around actin (Ali et al., 2002; Sun et al., 2007). Therefore it is best to have the actin filament tethered to the surface via an attachment protein only at certain intervals. Traditionally, actin is attached to the surface of the coverslip in these assays using either one of two possible techniques. In the first, biotinylated BSA is applied to the surface of the coverslip, streptavidin or NeutrAvidin is then bound to this, and then biotinylated F-actin is added, which binds to the avidin (Toepfer and Sellers, 2014). The biotinylated actin filaments are formed using approximately 10-20% of biotinylated actin monomers, that are polymerised with unmodified G-actin. However some experiments use biotinylated myosins with streptavidin attached Q-dot (Warshaw et al., 2005) or beads. In these experiments biotinylated myosin can

potentially attach to NeutrAvidin that was used to attach actin to the surface. Moreover, streptavidin Q-dots can potentially attach to the biotinylated actin subunits. In the second technique, NEM-treated skeletal muscle myosin-2 HMM is applied to the surface and then actin is added (Warshaw et al., 1990; Guilford et al., 1997; Warshaw et al., 2005). N-ethyl-maleimide (NEM) treatment of myosin chemically inactivates the myosin's ATPase activity, however its strong actin binding affinity is retained. In fact, the NEM treatment produces a variety of myosin molecules considering their activity. This leads to a group of molecules, where some myosin molecules are still active and moving actin, while being attached to the surface; some myosin molecules are inactivated and attach actin to the surface; and some myosin molecules are inactivated to lose even their actin binding affinity. In other words there is a fine line between inactivating the myosin's ATPase activity and still retaining strong actin binding activity (Warshaw et al., 1990). Moreover, during storage by freezing, the strong, ATP-insensitive actin binding of NEM-treated myosin declines with time. However, this method still provides a way for label-free actin tethering to the coverslip, enabling the use of biotinylation for myosin labelling.

1.4.4 Adhirons

As an alternative to actin-binding domains, we wanted to explore the possibility of raising Adhirons against actin that we could use to tether myosin-5 to actin. Adhirons are small, artificial, non-antibody binding proteins, that were developed by the groups of Dr. Tomlinson and Prof. McPherson at the University of Leeds (Tiede et al., 2014). The core of this scaffold protein is based on a consensus phytocystatin, a plant cysteine inhibitor, sequence that was derived by aligning 57 sequences. Consensus proteins are often exploited as the scaffold of artificial binding proteins (Devi et al., 2004; Main et al., 2003), due to their enhanced structural stability. The Adhiron scaffold was found to be extremely stable with a T_m of 101 ºC, and is the most stable artificial binding protein scaffold to date (Tiede et al., 2014). Crystallisation and structure determination of the Adhiron core shows that the scaffold is made up from four β-strands and an α-helix (Figure 1.17). Two variable, 9 amino acids long loops are present in this scaffold, loop1 is inserted between the 1^{st} and 2^{nd} β-sheet and loop2 between the 3^{rd} and 4^{th} β-sheet. A large phage display library was developed, comprising more than $3*10^{10}$ clones that are expected to only differ in the amino acid composition of their two loops. Screening of random clones showed that 86% of

them were full length and that the prevalence rate of each amino acid (except Cys) are similar, indicating that the library is of high quality. Cysteine was not included in the library to prevent Adhirons from disulphide bond induced dimerisation. These proteins are 12 kDa and easy to express in *E. coli* with reasonably high yields of 50-100 mg/l. All these properties of the Adhirons make them as an artificial alternative to antibodies, but they are easier to express and have much higher thermal stability compared to antibodies.

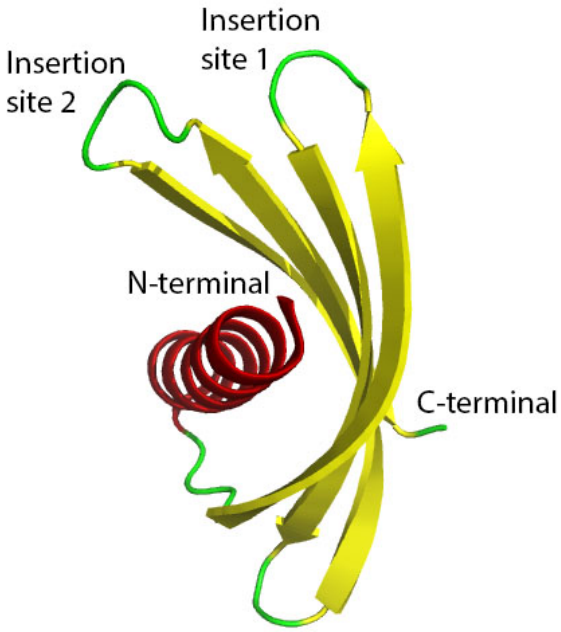

Figure 1.17. *Crystal structure of the Adhiron scaffold at 1.75 Å resolution (PDB ID: 4N6T (Tiede et al., 2014)) is shown as cartoon representation. Secondary structure is colour coded (red: α-helix, yellow: β-sheet, green: loop), termini and insertion sites are shown on the figure. Note that this Adhiron scaffold only has the insertion sites (3 and 4 residues loop, respectively), whereas the loops of the binders are 9 residues long. There are 4 residues at the N-terminal, that are disordered and 6 at the C-terminal, followed by the single Cys residue and the His-tag.*

Using phage display assay, Adhirons can be raised against any protein (Tiede et al., 2014). The phage display technique applies phage that displays a protein on the outside of their packing. A phage library is required, that contains numerous clones that differ in the sequence of the displayed protein. In our case Adhirons are displayed on the outer protein shell of the virus, and are thus available to bind to

proteins of interest, that is fixed to a surface. Non-binders are washed off, binders are eluted and further amplified. Usually three selection rounds are performed yielding specific binders.

Actin-binding Adhirons were raised by Dr. Christian Tiede using biotinylated rabbit skeletal muscle G-actin (Cytoskeleton) that was bound to streptavidin-coated wells of a 24-well plate. As the screening is performed in PBS, it is likely that the actin used in the screen polymerises to F-actin, even though there was no Mg^{2+} or ATP present (Pollard, 2016).

Once Adhirons have been isolated that show potential binding to the protein of interest, the coding sequence for the Adhiron is subcloned into a bacterial expression plasmid which codes for a C-terminal His-tag, to facilitate Ni-resin purification. The protein is then expressed using *E. coli*, and the purified Adhiron characterised for its ability to bind the protein of interest. Adhirons have been raised against yeast Small Ubiquitin-like Modifier (SUMO), growth factor FGF1, receptor CD31, SH2 domain of Grb2 (Tiede et al., 2014), fibrinogen (King et al., 2015) and against hypoxia-inducible transcription factor (HIF-1α) (Kyle et al., 2015) so far. Typically, they have 7–140 nM binding affinities to their binding partners and have 87–95 ºC T_m (Tiede et al., 2014; Kyle et al., 2015). In addition, a single cysteine residue can be added to the C-terminal of the Adhiron sequence that can be used for biotinylation or other types of labelling. Fluorescent streptavidin can be added to biotinylated Adhirons for use in fluorescent studies such as staining of fixed cells (e.g. in a similar way to antibodies). The DNA sequence of the Adhirons can also be subcloned into a GFP expression vector and cells can be transfected with this plasmid. Expression of GFP-tagged Adhirons raised against a given protein in live cells enables studying the localisation of the target protein *in vivo*.

Therefore, we isolated Adhirons to actin, and tested their properties in a variety of assays to determine if they are suitable for tethering myosin-5 to actin by its tail. We measured the binding affinities of the Adhirons to actin, determined their ability to recognise and bind to actin in fixed cells, and tested the ability of Adhirons fused to GFP to bind to actin in live mammalian cells. We also tested if Adhirons are able to attach actin filaments to microscopy slides used in TIRF microscopy single molecule motility assays.

2. General Materials and Methods

2.1 Materials

Molecular biology reagents were from Thermo Fisher Scientific. Restriction enzymes and buffers were from New England BioLabs®. Buffers and reagents for cell culture work were from Gibco® Life Technologies™. All other reagents and chemicals were from Sigma-Aldrich® if not stated otherwise. Stock concentrations of reagents used to make up buffers are listed in Table 2.1. 1 M HCl and 1 M NaOH stock solutions and their dilutions were used to adjust pH of buffers. Deionised water was used to make buffers and for other procedures. Composition of PBS buffer used for non-sterile applications was 154 mM NaCl, 5.6 mM Na_2HPO_4,1.06 mM KH_2PO_4, pH 7.4.

Reagent	**Stock concentration**
Na_2ATP	100 mM pH 7.0
$CaCl_2$	2 M
EDTA	100 mM pH 8.0
EGTA	100 mM pH 7.2
KCl	2 M
$MgCl_2$	1 M
MOPS	1 M pH 7.0
NaCl	5 M
NaN_3	1 M
PMSF	100 mM in anhydrous ethanol

Table 2.1. *Stock concentration of the reagents used to make up buffers.*

2.2 Molecular biology techniques

2.2.1 PCR

Appropriate DNA was amplified using Pfx DNA polymerase and gene-specific primers. The reagents for the PCR reaction (Table 2.2) were mixed in 100 µl final volume. Pfx DNA polymerase was used as it has 3’ to 5’ proofreading exonuclease activity, high specificity and sensitivity (Cline et al., 1996). The DNA polymerase was activated by a ‘hot start’ (3 minutes at 94 ºC), which denatured the Platinum®

antibody specifically binding to and inhibiting the polymerase (Sharkey et al., 1994). Following this, 35 cycles of i) 94 ºC for 1 minute (to denature the DNA) ii) 1 minute at 55 ºC (to anneal the primers) and iii) x minutes at 68 ºC (for extension) were used to amplify the DNA. Pfx DNA polymerase extends 1 kb DNA per minute, and thus x was calculated to cover the full length of the PCR product. Following the 35 cycles, there was a final extension step of 10 minutes. Details of the PCR cycle are shown in Table 2.3.

Reagent	**Final concentration**
Pfu Amplification buffer	20 mM Tris-HCl pH 8.8, 2 mM $MgSO_4$, 10 mM KCl, 10 mM $(NH_4)_2SO_4$, 0.1% v/v Triton™ X-100, 0.1 mg/ml nuclease-free BSA
dNTP mix	0.2 mM each
$MgSO_4$	1 mM
Forward primer	1 µM
Reverse primer	1 µM
Template DNA	1 µg/ml
Platinum® Pfx DNA polymerase	10 unit/ml

Table 2.2. *Concentration of the reagents used in the PCR reactions.*

94 ºC	3 min	94 ºC	1 min	35x	68 ºC	5 min
		55 ºC	1 min			
		68 ºC	x min			

Table 2.3. *Temperatures and times used in the PCR amplification. Pfx DNA polymerase extends 1 kb DNA per minute, and thus x was calculated to cover the full length of the PCR product.*

2.2.2 Restriction digest

DNA was digested using restriction enzyme in a total volume of 50 µl for 1 hour at 37 ºC. The mixture contained 20 µg/ml DNA and 200 unit/ml restriction enzyme in CutSmart® buffer (20 mM Tris acetate pH 7.9, 50 mM Potassium acetate, 10 mM

Magnesium acetate, 100 µg/ml BSA). If double digest was performed the concentration of both restriction enzymes was 200 unit/ml.

2.2.3 Agarose gel electrophoresis

After PCR or restriction digest DNA samples were separated on an agarose gel according to size. 1% w/v agarose gel was made by adding agarose (Bioline) to TAE buffer (40 mM Tris base, 20 mM acetic acid and 1 mM EDTA). Mixture was microwaved for 1–2 minutes to get agarose dissolved in the solution. Then the mixture was left to cool down to ~40 ºC and ethidium bromide was added to a final concentration of 0.7 µg/ml. Solution was poured into casts and was left to solidify. DNA loading dye was added to the samples to have a final concentration of 1.7 mM Tris-HCl pH 7.6, 10 mM EDTA, 0.005% w/v bromophenol blue, 0.005% w/v xylene cyanol FF and 10% v/v glycerol. Samples were loaded in the wells and electrophoresis was run at 100 V for 30 minutes. GeneRuler 1 kb DNA ladder (Thermo Fisher Scientific) was used for size estimation. Ethidium bromide facilitates visualization by intercalating into DNA and fluorescing in UV light. Images were taken by Kodak Image Station or by UVIdoc Gel Documentation System (UVItec).

2.2.4 DNA purification

To purify DNA from solution after PCR or restriction digest NucleoSpin® Gel and PCR Clean-up kit (Mackerey-Nagel) was used. Alternatively DNA was run on an agarose gel and appropriate sized band was excised and DNA was recovered using QIAquick® Gel Extraction Kit (QIAGEN®) or NucleoSpin® Gel and PCR Clean-up Kit (Mackerey-Nagel), following the manufacturer's instructions. The concentration of the purified DNA was measured using a NanoDrop® Spectrophotometer set to a wavelength of 260 nm.

2.2.5 Transformation after cloning

The ligation mixture was transformed into Stellar™ Competent Cells (Clontech Laboratories). 1 µl of the mixture containing the ligated plasmid was added to 50 µl of cells and incubated on ice for 30 minutes. Then cells were heat shocked at 42 ºC for 45 s to facilitate DNA entry into the cells. The mixture was then incubated on ice for 3 minutes, before adding 150 µl room temperature SOC medium (Invitrogen™). The cells were then incubated at 37 ºC for 1 hour while shaking at 230 rpm. 100 µl of

the cells were plated onto LB agar plates containing selective antibiotics to select for cells containing the ligated vector. Plates were incubated at 37 °C for 16–18 hours. Individual colonies were picked from the plates and used to inoculate 5 ml LB cultures, containing antibiotics, and grown overnight with shaking at 37 °C. Plasmids were purified from these cultures using the QIAprep® Spin Miniprep Kit (QIAGEN®), following the manufacturer's instructions. The construct sequence was verified by DNA sequencing at Eurofins Genomics.

2.2.6 Protein concentration measurement

Protein concentration was measured by UV absorbance at 280 nm wavelength using a NanoDrop® or a Cary Spectrophotometer. The extinction coefficient of the different constructs was calculated using the ProtParam tool webserver (http://web.expasy.org/protparam) (Wilkins et al., 1999). Protein concentration was calculated according to the Beer-Lambert law:

$$A = \varepsilon c l$$

where A is the absorbance, ε is the extinction coefficient, c is the concentration of the protein and l is the path length of the solution.

2.2.7 SDS-PAGE

To perform SDS gel electrophoresis, self-made 12% or 15% w/v acrylamide or commercial 4-12% gradient NuPAGE® Bis-Tris pre-cast gels (Novex®) were used and also two different buffer systems were applied accordingly. The first was the standard 'Tris' buffer, containing 25 mM Tris base, 192 mM glycine pH 8.0, 0.1% w/v SDS. The second was an MES buffer, containing 50 mM MES (2-(N-Morpholino)ethanesulfonic acid), 50 mM Tris base pH 7.3, 0.1% w/v SDS, and 1 mM EDTA, which is optimised for resolving small proteins on the pre-cast gels. Protein samples were diluted in Laemlli buffer (50 mM Tris pH 6.8, 2% w/v SDS, 10% v/v glycerol, 5% v/v β-mercaptoethanol, 0.005% w/v bromophenol blue) and incubated at 98 ºC for 5 minutes to ensure proteins become denatured through the binding of SDS.

Mini gels (8 cm x 8 cm) were run at 180 V for 30-40 minutes in Bio-Rad Mini-PROTEAN® gel tank. To estimate approximate molecular masses of proteins in the samples, protein ladders were used. These included: PageRuler Plus, BenchMark™, unstained BenchMark™ or SeeBlue Plus2. All protein ladders were from Thermo

Fisher Scientific. After running the gels, they were submerged in stain solution (0.25% w/v Coomassie Brilliant Blue R-250, 10% v/v acetic acid, 50% v/v methanol) for 1-2 hours, while rocking, to stain the proteins. Then gels were washed with destain solution (7.5% v/v acetic acid, 27.5% v/v methanol for 12 hours). Destained gels were imaged with Odyssey® Imaging System (LI-COR Biosciences) at 700 nm wavelength.

During the course of my experiments, I discovered that proteins of similar molecular mass in the BenchMark pre-stained protein ladder and PageRuler Plus ladders run at different positions on NuPAGE® Bis-Tris pre-cast gels. In particular, proteins in the BenchMark ladder run faster on the gel than the PageRuler Plus ladders. To directly compare the two, both PageRuler Plus and BenchMark ladders were run on the same NuPAGE® Bis-Tris pre-cast gel (Figure 2.1A). Migration of a protein band on an SDS gel is inversely proportional to the logarithm of its molecular weight in gels that have fixed acrylamide content. However, here gradient gels were used that have a complex correlation between molecular weight and migration, especially because exact acrylamide content at a distinct point in the gel is indefinable. Therefore the results were treated as if they were obtained from a gel with fixed acrylamide content and the logarithmical correlation was applied as follows. The migration of each protein was measured from the top of the gel using ImageJ. Then the logarithm of the molecular mass was plotted as a function of the migration (Figure 2.1B) for the PageRuler Plus ladder. The data points were fitted with a linear function that had the equation of $y = 5.48 – 0.24x$, where x is the migration and y is the logarithm of the molecular weight. Putting the migration values of BenchMark ladder into this equation gave the apparent molecular weight of the bands. These corrected values will be showed throughout the Results.

Note that the linear equation that was fitted to the data points of PageRuler Plus do not fully fit the dataset, which is most probably due to the neglect of the properties of the gradient gel. This leads to contrary, e.g. the 77 kDa band of BenchMark still runs faster than the 70 kDa band of PageRuler Plus. However, as in this study the ladders serve to estimate size and not to determine exact molecular weight, keeping this in mind, the ladders can still be used with caution.

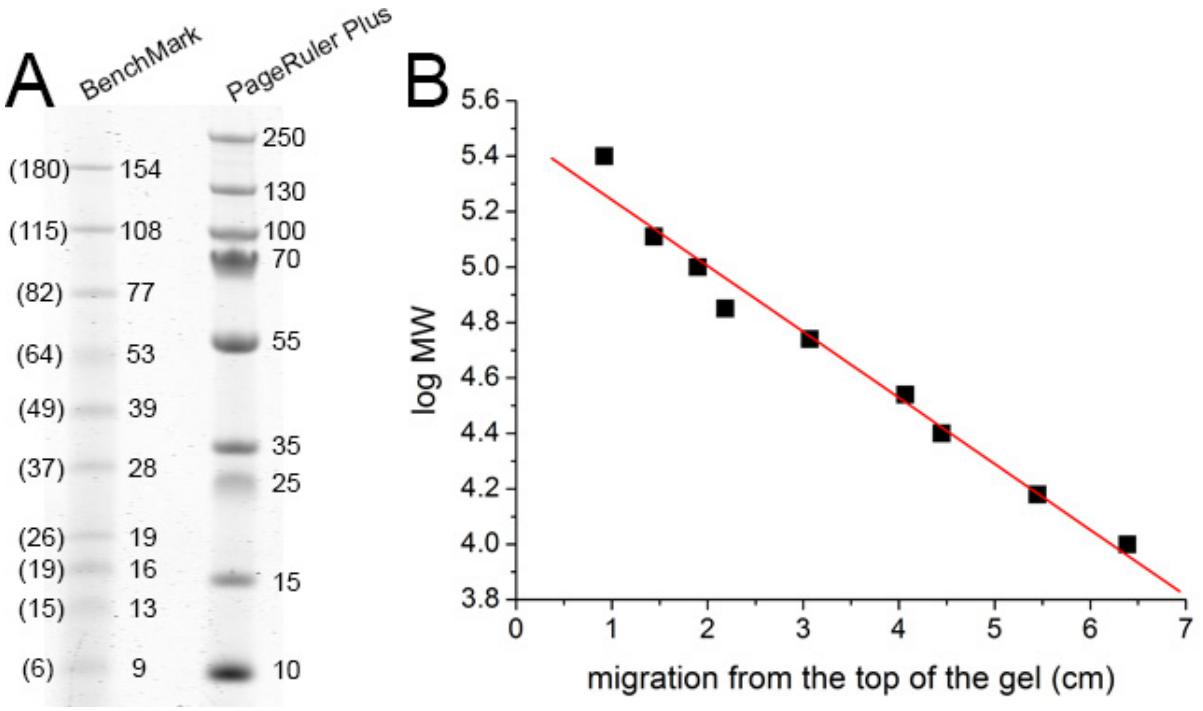

Figure 2.1. *Calibration of BenchMark pre-stained protein ladder in 4-12% gradient NuPAGE® Bis-Tris pre-cast gels. A) Coomassie-stained SDS-PAGE gel showing both BenchMark and PageRuler Plus pre-stained ladders. Numbers in brackets show the nominal molecular weight in kDa of the BenchMark protein bands. Numbers on the right side of the lanes show actual molecular weight in kDa. B) Logarithm of molecular weight of the bands of PageRuler Plus from panel A as a function of their migration. Equation y = 5.48 – 0.24x was fitted to the data points.*

2.2.8 Western blot

Western blotting using specific antibodies was performed to identify proteins. To perform a Western blot, proteins were transferred from the SDS gel to either a PVDF or nitrocellulose membrane. For the PVDF membrane, the iBlot® Dry Blotting System (Invitrogen™) was used on program P2 (23 V) for 7 minutes (iBlot® Gel Transfer Stacks PVDF Mini from Novex®). For the nitrocellulose membrane, proteins were blotted onto Amersham™ Hybond™-ECL nitrocellulose membrane (GE Healthcare) at 250 mA for 2 hours in Transfer Buffer (Pierce™) using Mini Trans-Blot® cell apparatus (Bio Rad Laboratories). After transferring the proteins onto the membrane, the membrane was blocked with PBS containing 0.05% v/v Triton™ X-100 (PBST) and 3% w/v skimmed milk powder or BSA. Membranes were either blocked at room temperature for 1 hour or at 4 ºC for 16-18 hours. After blocking, the membrane was washed with PBST, 3 times, for 3 minutes each at

room temperature, and then incubated with primary antibody (for dilutions, see Table 2.4), diluted into blocking solution either for 1 hour at room temperature, or at 4 ºC for 16-18 hours. Primary antibody was then removed by washing with PBST, 3 times, for 3 minutes each at room temperature. The membrane was then incubated with secondary antibody, diluted into blocking buffer for 1 hour at room temperature. Finally, the blot was washed with PBST, 3 times, for 3 minutes each at room temperature.

To detect the binding of the primary antibody, either horseradish peroxidase (HRP) linked or IRDye® linked secondary antibodies were used. For HRP-linked antibodies, the membrane was developed using the Pierce™ ECL Western Blotting kit (Thermo Fisher Scientific), following the manufacturer's instructions. Chemiluminescence was detected by exposing the membrane to Kodak X-Ray film and the film was processed using a Xograph Compact X2 instrument. When IRDye® linked secondary antibodies were used, the incubation was performed in a case protected from light as this dye is light-sensitive. After incubation the membrane was scanned with Odyssey® Imaging System (LI-COR Biosciences) at 700 nm wavelength.

Primary antibody	Secondary antibody
Mouse anti-calmodulin (clone 6D4, Sigma-Aldrich®) in 1:2,000 dilution	Goat anti-mouse HRP-linked (Thermo Fisher Scientific) in 1:5,000 dilution
Mouse anti-GFP (clone 9F9.F9, Abcam) in 1:3,000 dilution	Goat anti-mouse IRDye® 680-linked (LI-COR®) in 1:50,000 dilution
Rabbit anti-Myo5a (clone H-90, Santa Cruz Biotechnology®) in 1:100 dilution	Goat anti-rabbit IRDye® 680-linked (LI-COR®) in 1:50,000 dilution
Mouse anti-Flag (clone M2, Sigma-Aldrich®) in 1:1,000 dilution	Goat anti-mouse IRDye® 680-linked (LI-COR®) in 1:50,000 dilution
Mouse anti-biotin (clone Z021, Invitrogen™) in 1:1,000 dilution	Goat anti-mouse IRDye® 680-linked (LI-COR®) in 1:50,000 dilution
Rabbit anti-GFP (polyclonal, Millipore) in 1:2,000 dilution	Goat anti-rabbit HRP-linked (Thermo Fisher Scientific) in 1:5,000 dilution
Rabbit anti-Myo5a (clone H-90, Santa Cruz Biotechnology®) in 1:200 dilution	Goat anti-rabbit HRP-linked (Thermo Fisher Scientific) in 1:5,000 dilution
Mouse anti-Flag (clone M2, Sigma-Aldrich®) in 1:2,000 dilution	Goat anti-mouse HRP-linked (Sigma-Aldrich®) in 1:5,000 dilution

Table 2.4. *Pairs of primary and secondary antibodies that were used in Western blots.*

2.3 Actin techniques

2.3.1 Preparation of acetone-dried muscle powder

Preparation of acetone-dried powder was performed according to (Pardee and Spudich, 1982) using approximately 400 grams of fresh rabbit skeletal muscle. All procedures were carried out at 4 °C. The muscle was minced, and then added to 1.5 litres of 0.1 M KCl, 0.15 M potassium phosphate pH 6.5, and stirred for 10 minutes. The solution was filtered through sterile gauze, and the mince added to 3 litres of 0.05 M $NaHCO_3$, stirred for 10 minutes, and then filtered again. The mince was then added to 1.5 litres of 1 mM EDTA pH 7.0, stirred for 10 minutes and filtered. A further two extractions were then performed with 2 litres of H_2O, stirring for 5 minutes each time, then filtered. The mince was then added to 1 litre of acetone,

and stirred for 10 minutes, before filtering. This was repeated 4 more times. All the steps with acetone were performed in the fume hood on ice. This procedure removes all the water from the extract. The resulting acetone-dried powder was allowed to dry in the fume hood for 16-18 hours and then stored at -20 °C.

2.3.2 Isolation of actin

Isolation of actin from acetone-dried powder was performed according to (Spudich and Watt, 1971). To extract actin and depolymerise it, 8 grams of acetone-dried powder made from rabbit muscle was dissolved in 160 ml Buffer A (2 mM Tris base pH 8.0, 0.2 mM $CaCl_2$, 1 mM DTT, 0.5 mM NaN_3, 0.2 mM ATP) at 0 °C and stirred for 30 minutes. After sedimentation at 31,500 *g* for 45 minutes, the supernatant was filtered through a 0.22 µm pore size filter. Then a final concentration of 5 mM Tris-HCl, 50 mM KCl, 2 mM $MgCl_2$ and 1 mM ATP were added to the solution and actin was allowed to polymerise for 2 hours at room temperature. To dissociate contaminant tropomyosin and troponin from actin, a high salt step was performed, by increasing the salt concentration to 800 mM KCl, and stirring for 30 minutes at room temperature. After sedimentation at 111,000 *g* for 2 hours, the pellet was resuspended in 10 ml Buffer A. The solution was then dialysed to depolymerise actin. First it was dialysed against 700 ml Buffer A at 4°C for 5 hours, then a fresh 1.5 litres Buffer A was used for 16-18 hours at 4°C. Before freezing, another sedimentation step was carried out at 67,000 *g* for 1 hour to get rid of contaminants. Supernatant was kept and concentration was measured. The resulting G-actin was drop frozen in liquid nitrogen, the frozen drops transferred to a cryo-tube, which was then stored in liquid nitrogen. Effectiveness of the preparation and purification steps was checked with SDS-PAGE.

2.3.3 Measurement of actin concentration

G-actin concentration was measured according to (Houk Jr. and Ue, 1974) using a Cary Spectrophotometer. Absorbance at 290 nm was corrected for scattering by subtracting the absorbance at 320 nm. Protein concentration was calculated from the corrected absorbance with an extinction coefficient of 0.63 ml mg^{-1} cm^{-1} (Houk Jr. and Ue, 1974).

F-actin concentration was calculated by measuring absorbance at 280 nm with the NanoDrop® Spectrophotometer and using extinction coefficient of 45,840 M^{-1} cm^{-1} as described in section 2.2.6.

2.3.4 Polymerisation of actin

Actin polymerisation was carried out as described by (Burgess et al., 2002) using exchange and polymerisation buffers (Table 2.5). 1 µl of exchange buffer was added to 10 µl of G-actin stock (50-80 µM), and the solution was left on ice for 5 minutes. Then 1 µl of polymerisation buffer was added and the mixture incubated on ice for 1 hour. To generate biotin labelled F-actin, biotin labelled rabbit skeletal muscle G-actin (Cytoskeleton) was mixed with non-labelled G-actin before polymerisation, so that 5-20% of the actin monomers were biotinylated.

Final concentration of the buffer F-actin was in is the following: 10 mM MOPS, 25 mM KCl, 1.25 mM $MgCl_2$, 1 mM EGTA, 1.67 mM Tris, 0.17 mM $CaCl_2$, 0.83 mM DTT, 0.42 mM NaN_3, 0.17 mM ATP.

Exchange buffer	3 mM $MgCl_2$, 11 mM EGTA pH 7.0
Polymerisation buffer	300 mM KCl, 12 mM $MgCl_2$, 1 mM EGTA, 120 mM MOPS pH 7.0

Table 2.5. *Buffers used for actin polymerisation.*

2.4 Myosin techniques

2.4.1 Cloning of the Myosin-5-Avi construct

The recombinant Myosin-5-Avi construct in pFastBac™ vector (Invitrogen™) was made using an In-Fusion® cloning protocol (Clontech Laboratories) following the manufacturer's recommendations (Figure 2.2). First a linearised vector was created by cleaving the donor pFastBac plasmid at the multiple cloning site (MCS) with a restriction endonuclease. The appropriate DNA insert was amplified by PCR using primers which have at least 15 bp 5' extension complementary to the linearised donor vector ends. After purification the PCR product was cloned into the vector using In-Fusion® HD EcoDry™ recombinase. The mixture was incubated, then transformed into competent cells and colonies were selected on plates containing ampicillin (Figure 2.2).

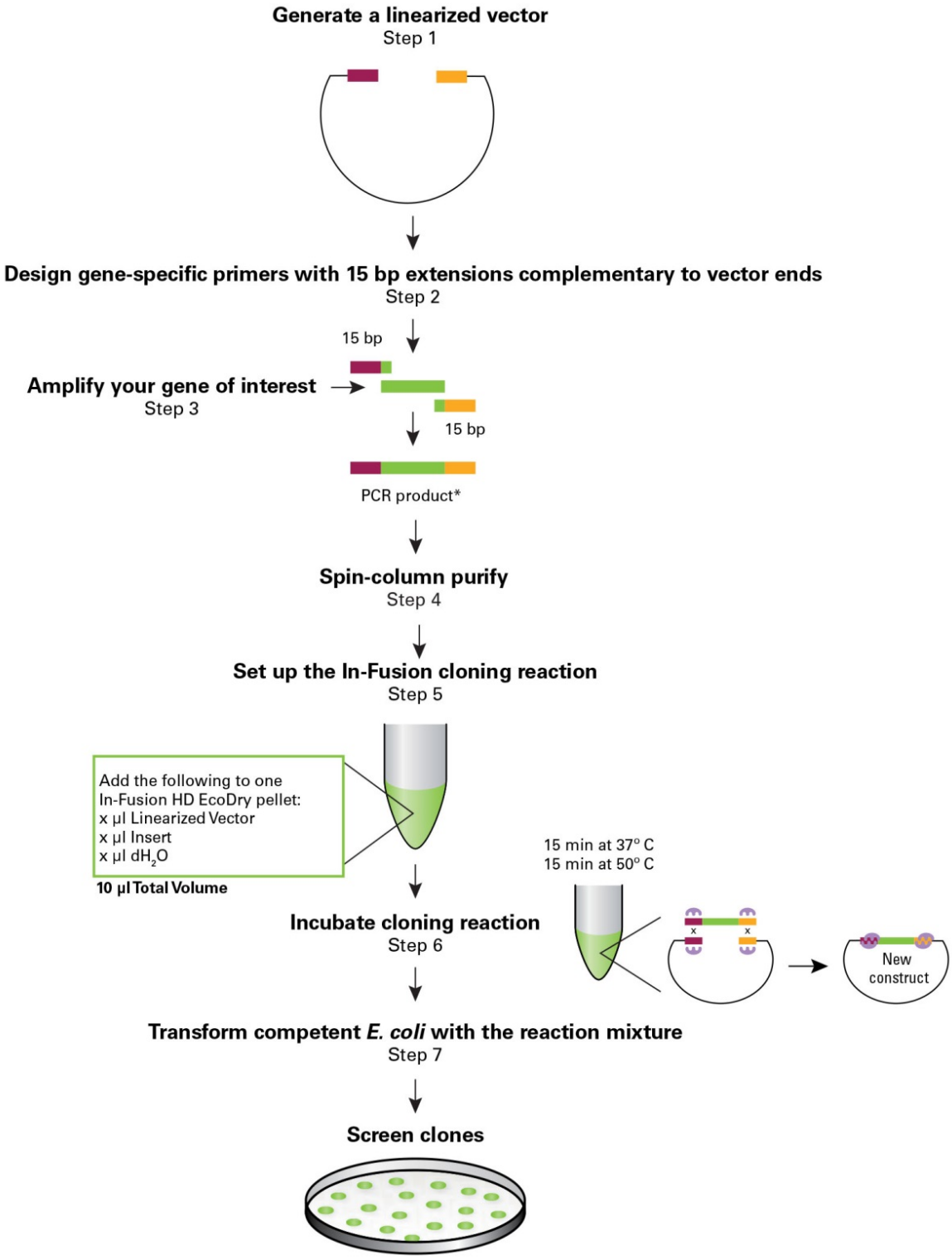

Figure 2.2. *Generalised In-Fusion® cloning protocol. Figure is taken from In-Fusion® HD EcoDry™ Cloning Kit User Manual.*

The resulting Myo5-Avi construct contains the coding sequence for the first 1,440 amino acids of the mouse myosin-5a, with a C-terminal Avi-tag™. The forward primer contained sequence that matched that of the vector at the EcoR I/Stu I sites and the first 16 bases of the coding sequence for myosin-5a (Figure 2.3). The reverse primer contained sequence that matched that of the vector at the Stu I /Sal I sites, the Avi-tag sequence, and the coding sequence for residues 1335 to 1440 (i.e. 18 bases; Figure 2.3). The pFastBac plasmid already contained eGFP cloned into the BssH II site and Flag tag sequence (DYKDDDDK) cloned into the Not I site by Dr. Attila Nagy (Dr. Sellers' laboratory at NIH, NHLBI). Enhanced GFP (eGFP) is a point mutant of GFP that exhibits much higher fluorescent intensity compared to GFP (Cormack et al., 1996). The GFP tag at the N-terminus of myosin-5 enables monitoring protein expression by *Sf9* cells and is required for fluorescence microscopy studies. The C-terminal Flag tag is required for Flag affinity purification of the protein. The source of the myosin-5 cDNA was the brain isoform of mouse (*Mus musculus*) myosin-5a (NCBI Reference Sequence: XM_006510832.3). Both the source and the donor plasmids were kind gifts from Dr. Attila Nagy (Dr. Sellers' laboratory at NIH, NHLBI).

To generate the construct, the coding sequence for the first 1,440 amino acids of the mouse myosin-5a was PCR-amplified from the source plasmid using the primers described (Figure 2.3), applying an extension time of 5 minutes. This is a suitable length of time to fully amplify the insert DNA (total length of 4.3 kb DNA). Both primers were designed according to the In-Fusion® cloning protocol. PCR was performed as described in section 2.2.1.

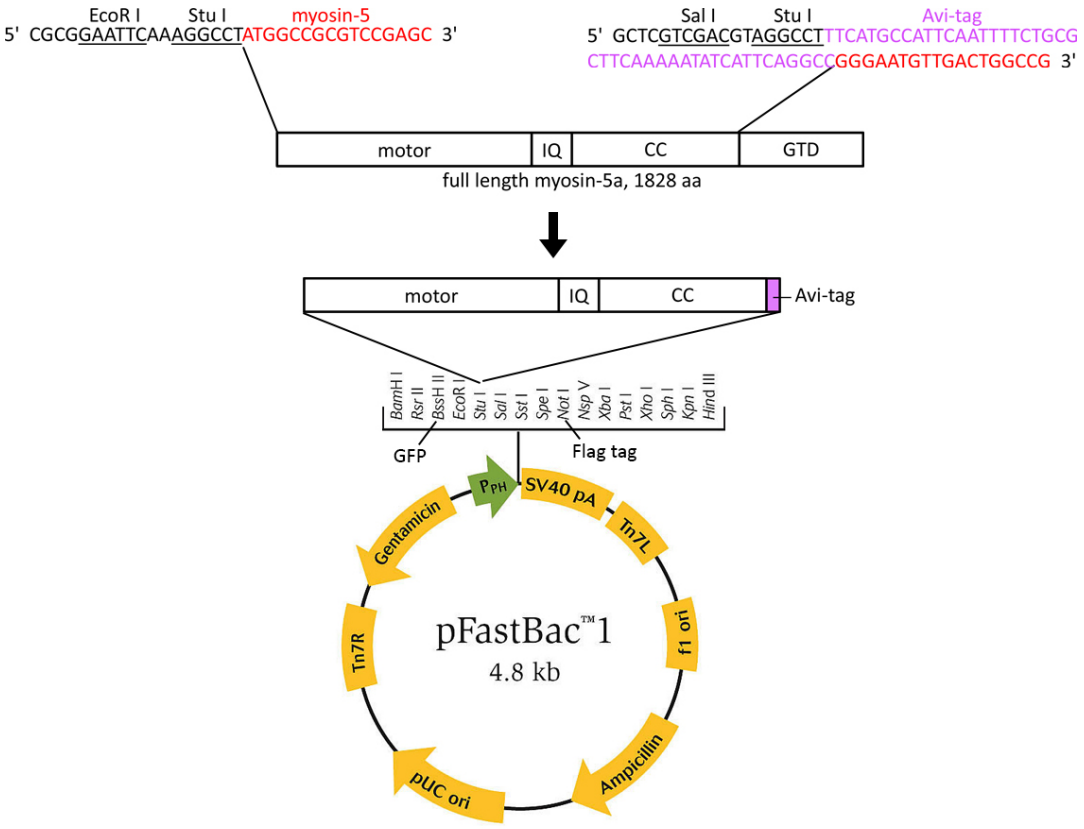

Resulting sequence:

```
          GFP sequence                    BssH II   EcoR I    Stu I
1   ATG GTG AGC AAG ... GAG CTG TAC AAG GCG CGC GGA ATT CAA AGG CCT
1    M   V   S   K  ...  E   L   Y   K   A   R   G   I   Q   R   P

          Myo5 sequence                        Avi-tag sequence
739  ATG GCC GCG TCC ... GTC AAC ATT CCC GGC CTG AAT GAT ATT TTT
247   M   A   A   S  ...  V   N   I   P   G   L   N   D   I   F

          Avi-tag sequence                    Stu I     Sal I
5077 GAA GCG CAG AAA ATT GAA TGG CAT GAA AGG CCT ACG TCG AC
1693  E   A   Q   K   I   E   W   H   E   R   P   T   S   T

     Sst I   Spe I     Not I     Flag-tag sequence
5118 G AGC TC A CTA GTC GCG GCC GCA GAC TAC AAG GAC GAC GAT
1707   S    S    L   V   A   A   A   D   Y   K   D   D   D

     Flag   Stop
5158 GAT AAG TAG
1720  D   K   X
```

Figure 2.3. *Cloning strategy, primer sequences and the resulting DNA and amino acid sequence of the Myosin-5-Avi construct with numbering. Restriction sites are shown where GFP, the myosin sequence, Avi-tag and Flag tag were cloned into the multiple cloning site of the pFastBac vector. Motor, IQ and CC stand for the DNA sequence coding for the myosin-5 motor domain, the lever with the 6 IQ motifs, and the predicted coiled-coil tail with the loops, respectively. Nucleic acid and amino acid sequences are shown with single letter code.*

After amplification, the PCR reaction was run on a 1% w/v agarose gel, and the amplified cDNA was gel purified as described (sections 2.2.3 and 2.2.4). The pFastBac vector was digested with Stu I restriction enzyme, and purified as described (sections 2.2.2 through 2.2.4). The concentrations of both insert and vector were measured, and the In-Fusion® reaction set up using the amount of 100 ng for both the vector and the insert in a total volume of 10 µl to the lyophilised pellet of the recombinase. The mixture was incubated for 15 minutes at 37 ºC, followed by 15 minutes at 50 ºC and then transformed as described (section 2.2.5). Cells were plated on LB agar plates containing 100 µg/ml ampicillin (KD Medical) to select for cells containing the pFastBac vector.

Colonies were picked and plasmid was purified as described (section 2.2.5). Plasmids were screened by running them on an agarose gel as described (section 2.2.3) and checking for an increased size of 4.3 kb in plasmids that contained an insert. The pFastBac vector containing the eGFP sequence is 5.5 kb and the size of the insert is 4.3 kb. Colonies containing a DNA insert were sequenced (Eurofins Genomics) to confirm the identity and fidelity of the inserted sequence (Figure 2.3). Ten different primers (Table 2.6) were used for sequencing to cover the entire sequence of the construct, and a Myo5-Avi construct was obtained in which the sequence was that expected (full length sequence of this construct is provided in the supplementary materials (S2)).

Primer name	Primer sequence	Location (bp)
pFBfor	TCCGGATTATTCATACCGTCCC	
FOR1	ACTACCAGCAGAACACCCCC	545
FOR2	CGCAGTAGCTGAAGAGGCTT	1158
FOR3	CATCTCGGGATTCAGACAGC	1760
FOR4	CCGCATGTCAAACAAAGC	2361
FOR5	CAAGGATAAATACCAGTTTGGTAAGA	2949
FOR6	GACTACAAATGCCTCATGGAGA	3562
FOR7	ACCAAGAACAGAGGAGCCAA	4149
FOR8	GGGGAGATCCAGAGCCTAAA	4762
pFBrev	CCTCTACAAATGTGGTATGGCTG	

Table 2.6. *Primers used for sequencing of Myosin-5-Avi construct. pFBrev to For8 primers are forward primers and pFBrev is a reverse primer annealing to the backbone of the pFastBac plasmid. Numbers in the Location column show the start of each primer in bp considering the Myo5-Avi sequence.*

2.4.2 Re-cloning of the Myosin-5-Avi construct

Expression trials for the initial Myo5-Avi construct were unsuccessful (see section 4.1.3). As this was likely due to the backbone vector used, I subcloned the entire coding region for Myo5-Avi, including the N-terminal eGFP and the C-terminal Flag tag, into the EcoR I and Xho I sites of an unmodified pFastBac™ vector (Invitrogen™) (Figure 2.4) using In-Fusion® cloning (as described above in section 2.4.1). The pFastBac vector was digested with EcoR I and Xho I (section 2.2.2), and the reaction was stopped by incubating it at 65 ºC for 20 minutes. The insert was amplified using the primers shown (Figure 2.4) applying the same conditions as described above (section 2.4.1). The resulting constructs were sequenced (Eurofins Genomics). The pFastBac vector was a kind gift from Dr. Jonathan Bird (Dr. Friedman's laboratory at NIH, NIDCD). Sequence of this Myo5-Avi construct is identical to the original construct presented in section 2.4.1.

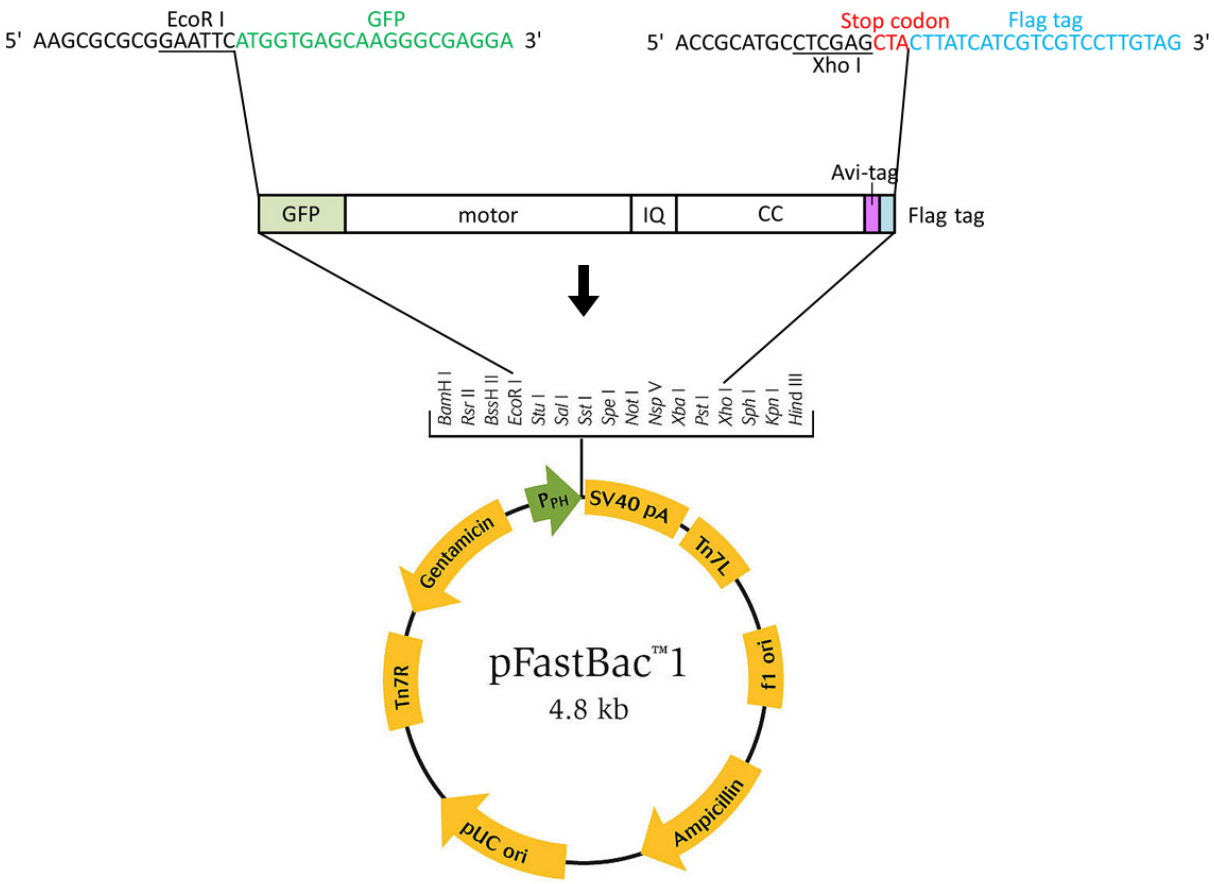

Figure 2.4. *Cloning strategy and primer sequences used to amplify the myosin-5 construct for re-cloning into a new pFastBac vector. Restriction sites are shown where the construct was cloned into the multiple cloning site of the pFastBac vector. Motor, IQ and CC stand for the DNA sequence coding for the myosin-5 motor domain, the lever with the 6 IQ motifs, and the predicted coiled-coil tail with the loops, respectively.*

2.4.3 Cloning of the Myosin-5-cc construct

The recombinant Myosin-5-cc construct in pFastBac™ vector (Invitrogen™) was made using the GeneArt® Seamless cloning protocol (Invitrogen™) following the manufacturer's recommendations. First a linearised vector was created by cleaving the donor pFastBac plasmid with restriction endonuclease. Then the appropriate DNA insert was amplified by PCR using primers which have at least 15 bp 5' extension complementary to the linearised donor vector ends. After purification the PCR product was cloned into the vector using the GeneArt® Seamless enzyme. The mixture was incubated, then transformed into competent cells and colonies were selected on plates containing ampicillin.

The pFastBac vector containing the Myosin-5-Avi construct in between the EcoR I and Xho I restriction sites, which was created during the re-cloning of the Myosin-5-Avi construct, was used as a donor vector. This plasmid was linearised using Afe I restriction enzyme that cuts the plasmid at the AGCGCT sequence coding for Arg1337 according to Myosin-5-Avi numbering (Arg1091 according to wild type mouse myosin-5a numbering). This residue is the last amino acid of the proximal part of coiled-coil and also the last residue of the HMM construct.

The coding sequence for 175 amino acids of the mouse myosin-5a coiled-coil starting with Arg917 and ending with Arg1091 according to the wild type myosin-5a numbering was PCR-amplified from the source plasmid using the primers described (Figure 2.5), applying an extension time of 30 seconds. This is a suitable length of time to fully amplify the insert DNA (total length of 0.5 kb DNA). Both primers were designed according to the GeneArt® Seamless cloning protocol. PCR was performed as described in section 2.2.1. The source plasmid was the brain isoform of mouse (*Mus musculus*) myosin-5a (NCBI Reference Sequence: XM_006510832.3).

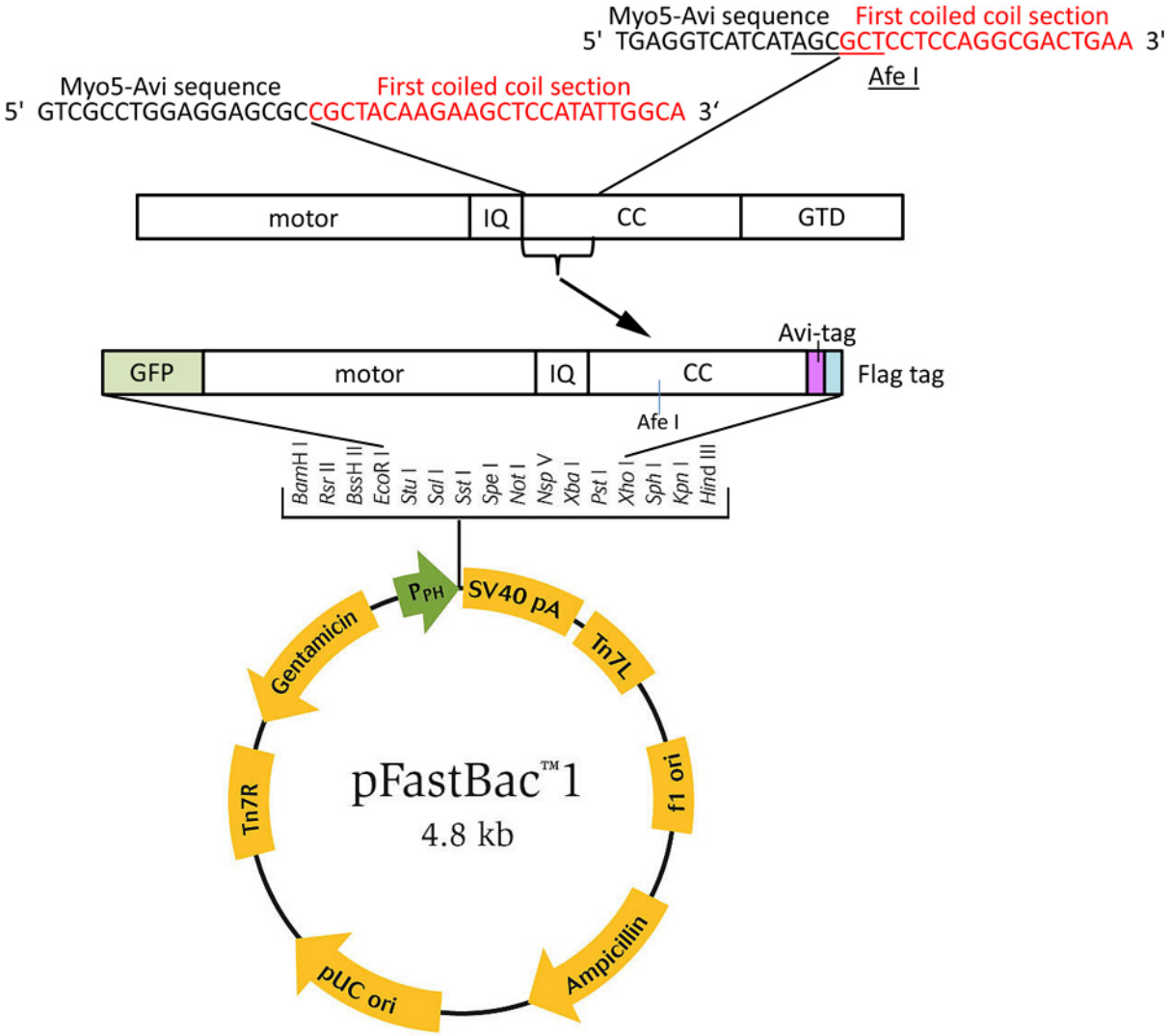

Figure 2.5. *Cloning strategy and primer sequences used to amplify the coding sequence of the 175 amino acid coiled-coil section. Afe I restriction site is shown where the insert was cloned into the Myosin-5-Avi sequence. Motor, IQ and CC stand for the DNA sequence coding for the myosin-5 motor domain, the lever with the 6 IQ motifs, and the predicted coiled-coil tail with the loops, respectively.*

The PCR product and the digestion product were run on a 1% w/v agarose gel, and the DNA was gel purified as described (sections 2.2.3 and 2.2.4). The concentrations of both insert and vector were measured, and the GeneArt® Seamless reaction set up using the amount of 50 ng for both the vector and the insert in a total volume of 20 µl. The final mixture also contained 4 µl enzyme buffer (from a 5x stock, provided in the cloning kit) and 2 µl enzyme mix (from a 10x stock, provided in the cloning kit). The mixture was incubated for 30 minutes at room temperature, and then transformed as described in section 2.2.5. Cells were plated on LB agar plates containing 100 µg/ml ampicillin to select for cells containing the pFastBac vector.

Colonies were picked and colony PCR was performed as described in section 2.2.1. The colonies were touched with the tip of the pipette tip and the cell suspension attached to the tip was then transferred to the PCR mixture tube. The first, hot start step of the PCR (3 minutes at 94 ºC) enables the DNA to be released from the cells. For5 and Rev7 primers (Table 2.7) were used for the amplification, which yields a PCR product of 1,300 bp for the negative control and 1,800 bp if the colony contains the insert. After the amplification, the PCR products were run on an agarose gel as described in section 2.2.3, checking for a possible size difference of 500 bp. Colonies containing the insert were sequenced (Eurofins Genomics) to confirm the identity and fidelity of the inserted sequence (Figure 2.5). The sequencing primers listed in Table 2.6 and Table 2.7 were used for sequencing to cover the entire sequence of the construct. The amino acid sequence of the whole construct is in the supplementary materials (S3).

The resulting construct contains the coding sequence for an eGFP and then the first 1,091 amino acids of the mouse myosin-5a that would be a regular HMM. This is followed by 175 amino acids of coiled-coil that was doubled from the HMM and then the remaining 350 amino acids of the coiled-coil tail that is predicted to form both loops and coiled-coil. The sequence ends with a C-terminal Avi-tag™ (Avidity) (GLNDIFEAQKIEWHE), followed by a Flag tag sequence (DYKDDDDK). Enhanced GFP (eGFP) is a point mutant of GFP that exhibits much higher fluorescent intensity compared to GFP (Cormack et al., 1996). The GFP tag at the N-terminus of myosin-5 enables monitoring protein expression by *Sf9* cells and is required for fluorescence microscopy studies. The C-terminal Flag tag is required for Flag affinity purification of the protein. The source of the myosin-5 cDNA was the brain isoform of mouse (*Mus musculus*) myosin-5a (NCBI Reference Sequence: XM_006510832.3),

that was a kind gift from Dr. Attila Nagy (Dr. Sellers' laboratory at NIH, NHLBI). This construct is 1,896 residues long and the molecular weight is 220 kDa. Like Myosin-5-Avi, this construct also binds six calmodulin light chains per heavy chain.

Primer name	Primer sequence	Location (bp)
FOR5	CAAGGATAAATACCAGTTTGGTAAGA	2949
FOR5.5	CCTTCAGTGCTGCTTCCGGCG	3411
REV7	AGCTGCTTCTCCTGTTCCAG	4777

Table 2.7. *Primers used for colony PCR and sequencing of the Myosin-5-cc construct. For5 and Rev7 were used for colony PCR. All primers along with primers in Table 2.6 were used for sequencing. Numbers in the Location column show the start of each primer in bp considering the Myo5-cc sequence.*

2.4.4 Cloning of the Myosin-5-Ad construct

The recombinant Myosin-5-Ad construct was cloned into the EcoR I and Xho I sites of the multiple cloning site of pFastBac plasmid by GenScript®. DNA sequence was codon optimised for expression in insect cells by GenScript, therefore DNA sequence differs from NCBI Reference Sequence XM_006510832.3. The construct contains an N-terminal Avi-tag for potential labelling with a Q-dot. This is followed by a mouse myosin-5a HMM molecule, that comprises the motor domain, the lever with 6 IQ motifs and 175 amino acids of the coiled-coil. These 175 amino acids are then doubled to lengthen the tail of the molecule. This is followed by the remaining parts of the tail comprising the coiled-coil and loop motifs, but excluding the globular tail domain as in the previous Myosin-5-cc construct. Then the sequence continues with a GFP to monitor expression and also to use the molecule later on in fluorescent studies, and then with the sequence of the actin-binding Adhiron14. For potential removal of the actin-binding Adhiron14, a PreScission protease site (GE Healthcare, LEVLFQGP) is inserted between the GFP and the Adhiron14 sequence. The sequence ends with a C-terminal Flag tag that allows purification of the molecule on a Flag affinity resin. The whole construct is 1,993 residues long and the molecular weight is 232 kDa (Figure 1.16). Like Myosin-5-Avi, this construct also binds six calmodulin light chains per heavy chain. Sequence of the construct in

pFastBac plasmid was verified by GenScript and can be found in the Supplementary Materials (S4).

2.4.5 Bacmid DNA generation

Generation of recombinant baculovirus was carried out according to the Bac-to-Bac® Baculovirus Expression Systems protocol (Invitrogen™). The recombinant donor pFastBac™ plasmid was transformed into DH10Bac™ competent cells (Invitrogen™) as follows. 50 ng plasmid was added to 100 µl of freshly thawed cells on ice and incubated on ice for 30 minutes. The tube was transferred to a water bath, set to a temperature of 42 ºC, for 45 s to facilitate the DNA entering the cells, then transferred back to ice for 3 minutes. 900 µl SOC medium was added, and the tube was transferred to the incubator at 37 ºC for 4 hour with shaking at 230 rpm before plating the cells onto bacmid plates.

Bacmid plates were prepared using LB medium + 1.5% w/v Agar (KD Medical), supplemented with 50 µg/ml kanamycin (Gibco® Life Technologies™), 7 µg/ml gentamicin (Gibco® Life Technologies™), 10 µg/ml tetracycline (Sigma-Aldrich®), 100 µg/ml Bluo-gal (Invitrogen™, stock solution dissolved in DMSO) and 40 µg/ml IPTG (Sigma-Aldrich®). 100 µl of the bacterial cells were plated onto the bacmid plates and the plates were incubated at 37 ºC for 48 hours. Cells, in which the DNA from the pFastBac plasmid was transposed into the bacmid, appeared white on these selective plates. Other cells, in which the lacZ gene was not disrupted by the transposition, express β-galactosidase which cleaves Bluo-gal producing a blue product turning these colonies blue. As these colonies are small and often hard to distinguish if they are blue or white, multiple colonies were picked and restreaked onto a fresh bacmid plate and incubated at 37 ºC for 16-18 hours, to enable clear blue/white selection.

Multiple white colonies and one blue colony as a negative control were picked from the plates, used to inoculate 5 ml LB containing 50 µg/ml kanamycin, 7 µg/ml gentamicin and 10 µg/ml tetracycline and incubated at 37 ºC for 24 hours, while shaking at 230 rpm. Bacmid purification was then performed according to the Bac-to-Bac® bacmid purification protocol as follows, using solutions P1, P2 and N3 from the QIAprep® Spin Miniprep Kit (QIAGEN®). The cell culture was centrifuged at 3,800 *g* and the pellet resuspended in 300 µl of solution P1. 300 µl of solution P2 was added, and the mixture incubated at room temperature for 5 minutes. 300 µl of

solution N3 was then added and the mixture was incubated on ice for 10 minutes. The mixture was then centrifuged at 16,000 *g* for 10 minutes and the supernatant transferred to fresh tube containing 800 µl isopropanol. The tube was incubated on ice for 10 minutes, then centrifuged again at 16,000 *g* for 15 minutes. After removing the supernatant the pellet was washed with 500 µl 70% v/v ethanol and centrifuged at 16,000 *g* for 5 minutes. After air drying the pellet for 15 minutes 40 µl H_2O was added and bacmid stored at 4 ºC.

2.4.6 Verification of transposition

The large size of the bacmid DNA (>135 kb) makes it difficult to verify that transposition has occurred simply based on its size on an agarose gel. Instead, PCR using M13 primers (Table 2.8) were used, following the protocol described above (section 2.2.1) with an extension time of 8 minutes. These primers anneal to either side of the specific site within the lacZ gene where the transposition is expected to occur. A negative control PCR amplification was also performed using the bacmid from a blue colony, in which no transposition should have occurred. Using these primers, the PCR product is expected to be the size of the gene of interest plus an additional 2.3 kb if the transposition occurred, or 2.3 kb if not.

Forward	5'-CCCAGTCACGACGTTGTAAAACG-3'
Reverse	5'- AGCGGATAACAATTTCACACAGG-3'

Table 2.8. *M13 primers used to verify transposition of the construct into the bacmid.*

2.4.7 Culturing *Sf9* cells

Previously prepared and frozen *Sf9* (*Spodoptera frugiperda*) cells (Invitrogen™) are kept in the liquid nitrogen. A cryovial containing 1 ml *Sf9* cells (usually ~$8x10^6$ cells/ml) was thawed by hand. Then 9 ml room temperature Sf-900 II SFM medium (Invitrogen™) supplemented with 2.5% v/v heat inactivated FBS and 1x GlutaMAX™ (both from Gibco® Life Technologies™) was added to the cells and it was centrifuged at 180 *g* for 10 minutes. Pellet was resuspended in 2 ml fresh medium to eliminate the 10% v/v DMSO that is used as a cryoprotectant, when freezing the cells. Cells were counted using Trypan blue stain and a haemocytometer, and diluted to $0.5x10^6$ cells/ml density. Suspension cultures were

grown while shaking with 120 rpm at 27 ºC. Cells usually double every 24 hours, therefore they were usually passaged every 2-3 days, when cell density reached ~6x10^6 cells/ml, then cells were diluted to ~1x10^6 cells/ml. Cells were usually left growing and adapting to culture conditions for a week before using them for virus amplification or protein expression. After cells recovered, some of them were frozen down as follows. Cells were centrifuged and resuspended in the above described medium containing also 10% v/v DMSO, to a density of ~8x10^6 cells/ml. 1 ml of cells were transferred to cryovials, that were placed in the -80 ºC freezer and after 3 days were transferred into the liquid nitrogen storage.

2.4.8 Myosin-5 baculovirus generation

Baculovirus generation and virus amplification were first carried out according to the Bac-to-Bac® Baculovirus Expression System protocol. *Sf9* cells were transfected with the bacmid DNA using Cellfectin® reagent. Prior to transfection, 10^5 *Sf9* cells were seeded into a single well of a 6-well plate in 2 ml of Sf-900 II SFM medium containing 50 units/ml penicillin and 50 µg/ml streptomycin (PenStrep from Gibco® Life Technologies™) and left at 27 ºC for 1 hour to attach. 5 µl of bacmid DNA was mixed with 6 µl of Cellfectin® reagent (Invitrogen™) in 200 µl of the same medium without antibiotics and incubated at room temperature for 30 minutes. After washing the cells with 2 ml of medium without antibiotics, the DNA mixture, diluted to 1 ml with Sf-900 II SFM medium, was pipetted onto the cells and the cells incubated at 27 °C for 5 hours. The cells were then washed with medium containing antibiotics, 2 ml of medium with antibiotics was added, and the cells were then incubated at 27 °C. After 72 hours of incubation, the medium and the cells were centrifuged, and the supernatant containing the P1 virus was harvested. However, this method only provides 2 ml of P1 virus, all of which has to be used to amplify the virus further. To obtain high enough titre, this meant performing 4 or 5 rounds of amplification, and this did not provide good results in expression trials. Therefore, I switched to a different approach.

In an improved approach to generating virus (Bird et al., 2014), 25 µg bacmid DNA was added to 300 µl sterile PBS (Gibco® Life Technologies™). In a separate tube, 300 µl of polyethyleneimine (PEI from Polysciences, stock concentration: 1 mg/ml) was added to 300 µl PBS. Then the bacmid solution was mixed with the PEI solution and incubated at room temperature for 10 minutes. 100 ml of 10^5 *Sf9* cells/ml grown

in suspension in Sf-900 II SFM medium supplemented with 2.5% v/v heat inactivated FBS and 1x GlutaMAX™ were then transfected using this bacmid mixture. The culture was incubated at 27 °C while shaking at 120 rpm, and virus replication followed by fluorescence microscopy, as the construct contains eGFP. Virus was harvested when ~80% of the cells were eGFP positive, usually after 4-5 days. This method provided 100 ml of high titer P1 virus, which required only one further amplification to have enough virus for expression.

2.4.9 Calmodulin baculovirus generation

Since myosin-5a needs to be co-expressed with a calmodulin (CaM) expressing virus, to ensure that there is enough CaM to bind to the myosin lever, a fresh baculovirus for CaM was also generated. The original plasmid (pVL1392) which contains the *Xenopus laevis* CaM (Uniprot: P62155) was used. The sequence of *Xenopus* CaM is identical to that of mouse. In this case, the bacmid DNA is co-transfected with the plasmid, and the transposition takes place in the *Sf9* cells. This approach uses the BaculoGold™ Transfection Kit (BD Biosciences), which includes the bacmid DNA. The plasmid was a kind gift from Dr. Attila Nagy (Dr. Sellers' laboratory at NIH, NHLBI).

$2x10^6$ *Sf9* cells were seeded into a single well of 6-well plate, in 2 ml of Sf-900 II SFM medium, and incubated at 27 ºC for 15 minutes to allow the cells to attach. The medium was then removed and 1 ml of Transfection Buffer A added to the cells. 0.5 µg BD BaculoGold™ Baculovirus DNA was mixed with 2 µg of the pVL1392 plasmid containing the CaM gene, and incubated at room temperature for 5 minutes, before adding 1 ml of Transfection Buffer B. This mixture was then added dropwise to the cells, while gently rocking the plate. The cells were then incubated at 27 °C for 4 hours, before removing the transfection solution from the cells and adding 3 ml Sf-900 II SFM medium. The cells were incubated at 27 °C and P1 virus was harvested after 4-5 days.

2.4.10 Virus harvesting and storage

To harvest the virus, the cells were centrifuged at 400 *g* for 15 minutes. The supernatant was filtered through a sterile filter with a 0.22 µm pore size (Millipore). Filtered virus were kept at 4 ºC, protected from light as they are light-sensitive.

2.4.11 Virus titre determination

The titre is a measure of how many infective particles there are per volume unit, and is used to add the appropriate amount of virus to *Sf9* cells for expression (using MOI: multiplicity of infection). The titre was measured using an end-point assay (Hopkins and Esposito, 2009), which uses a novel cell line named *Sf9* Easy Titer (*Sf9*-ET). This cell line has an eGFP gene under the control of the baculovirus polyhedrin promoter. Thus, if these cells are infected with baculovirus, they will turn green. The medium used to grow the *Sf9*-ET cells must contain Geneticin® (G418 from Gibco® Life Technologies™) to select for cells that contain the eGFP plasmid. The *Sf9*-ET cell line was a kind gift from Dr. Dominic Esposito (NIH, NCI).

Using a 96-well plate, 100 µl of Sf-900 II SFM medium containing 0.1 mg/ml G418, 2.5% v/v FBS and 1x GlutaMAX™ was pipetted into wells A2 through H10 (i.e. in all wells from column 2 to column 10). The viral stock was diluted 1:500 into medium containing G418 and 125 µl of this mixture was added into wells A1–H1. 25 µl of the solution in A1-H1 was removed and added to wells A2–H2, resulting in a 1:5 dilution. This was then repeated for each subsequent set of wells (A3–H3 and so on), resulting in a dilution of 1:5 each time. After adding 25 µl to the wells in column A9–H9 and mixing, 25 µl was removed, to ensure that each well had the same volume (100 µl). Virus was not added to the wells in the final column (A10–H10), to provide a negative control. Finally, 100 µl of *Sf9*-ET cells at a density of $7.4x10^5$ cells/ml, in medium containing G418, were pipetted into each well. This approach provides 8 parallel serial dilutions, each of which can be assessed to calculate the titre. The plate was incubated at 27 °C and the number of eGFP positive wells in every column was counted after 4-5 days. The data was transferred to an Excel spreadsheet to calculate the titre as described (Reed and Muench, 1938). A titre of $1\text{-}5x10^8$ infective particles/ml is considered to be good for subsequent experiments.

2.4.12 Baculovirus amplification

To generate a high titre virus stock, the virus has to be further amplified after its first round of amplification (P1). To amplify the virus $1.5–2x10^6$ *Sf9* cells/ml growing suspension in medium supplemented with 2.5% v/v FBS and 1x GlutaMAX™, were infected with the appropriate virus using an MOI (multiplicity of infection) of 0.1. An MOI of 0.1 indicates that there should be one infective virus particle for every 10

Sf9 cells. After infection, the cells were incubated at 27 °C, shaking at 120 rpm, and the eGFP fluorescence monitored by fluorescence microscopy each day. The virus was harvested when ~80% of the cells were eGFP positive, usually after 3 days. The virus titre was then determined. In most cases the viruses were only amplified once (to P2) or twice (to P3). Further amplification of the viruses can lead to fragmentation of DNA incorporated into the viral particles and/or the acquisition of mutations.

2.4.13 Cell extraction for calmodulin Western blot

Calmodulin expression of *Sf9* cells was checked by Western blotting. *Sf9* cells that were either non-infected or infected with calmodulin baculovirus at MOI of 5, were incubated for 2 days while shaking (as described in section 2.4.12). 500 µl of the cells were centrifuged at 400 *g* for 15 minutes. The cell pellet was resuspended in 500 µl extraction buffer comprising 150 mM NaCl, 50 mM Tris-HCl pH 8.0, 1 mM EDTA, 1% v/v Triton™ X-100 and 1x Halt™ Protease Inhibitor Cocktail (Thermo Fisher Scientific). The mixture was incubated on ice for 30 minutes, then centrifuged at 16,000 *g* for 20 minutes at 4 °C. Supernatant was mixed with Laemlli buffer (as described in section 2.2.7), 15 µl loaded and run on an SDS-PAGE gel and Western blotting was performed (as described in section 2.2.8).

2.4.14 Myosin expression

To express the myosin-5 constructs, 1.5 litres of 1.5-2x10^6 *Sf9* cells/ml in a medium supplemented with 2.5% v/v FBS and 1x GlutaMAX™ were co-infected with both myosin-5 and CaM baculoviruses at MOI of 5. The infected culture was shaken at 27 °C at 90 rpm until ~70% of the cells were eGFP positive as followed by fluorescence microscopy (usually 2 days). The cell culture was then centrifuged at 400 *g* for 15 minutes, and the pellet flash frozen in liquid nitrogen.

In some cases, chaperones were additionally co-expressed with the myosin-5 constructs, to help improving expression. P2 virus of Unc45b/Hsp90 was provided as a kind gift from Dr. Jonathan Bird (Dr. Friedman's laboratory at NIH, NIDCD). Both chaperones, (UNC45 and HSP90; *Mus musculus)*, were cloned into the same pFastBac™ Dual vector (Bird et al., 2014) and P1 virus had been generated as described (section 2.4.8). The P2 virus was amplified further (to P3 as described in 2.4.12) to provide enough virus for co-expression at an MOI of 5.

2.4.15 Cell extraction for Myosin-5-Ad Western blot

Myosin-5-Ad expression in *Sf9* cells was checked by Western blotting. 200 ml of *Sf9* cells that were infected with Myosin-5-Ad, calmodulin and Unc45b baculoviruses, all at MOI of 5, were incubated for 3 days while shaking (as described in section 2.4.14). 1 ml sample was taken 1, 2 and 3 days after the infection and these were centrifuged at 400 *g* for 15 minutes. The cell pellet was resuspended in 100 µl boiling 1x Laemlli buffer. 10 µl from that mixture was loaded and run on an SDS-PAGE gel (as described in section 2.2.7). Western blotting was performed using anti-Flag and anti-Myo5a antibodies (as described in section 2.2.8).

2.4.16 Myosin purification

Proteins were purified as described previously (Wang, Harvey, et al., 2000; Nagy et al., 2013) using the same protocol. Each step was performed on ice or in the cold room at 4 °C. Frozen cell pellets from 1.5 litres of cell culture were extracted in 300 ml extraction buffer (Table 2.9) using a manual glass homogeniser. The cell lysate was sonicated using a microtip on a Misonix Sonicator Controller XL2020. Sonication was performed in ~150 ml volume for 3 minutes using 1 s cycles of sonication/no sonication. This 3 minute cycle was applied 2-3 times, then the lysate was centrifuged at 48,000 *g* for 15 minutes.

Myosin-5a constructs were purified from the supernatant using Flag affinity chromatography, applying a resin in which Flag antibodies are attached to M2 agarose beads (Sigma-Aldrich®). 2 ml Flag resin was added to ~300 ml supernatant and incubated for 3 hours, while rocking. The mixture was then centrifuged at 200 *g* for 4 minutes and the pelleted resin was washed 3 times with 50 ml Mary's buffer (Table 2.9), then once with 50 ml HMM buffer (Table 2.9) as follows. Supernatant was pipetted off from the resin carefully not to lose any resin, and then buffer was mixed with the resin and the mixture was centrifuged at 200 *g* for 4 minutes. The resin was transferred into a 10 ml chromatography column (Bio-Rad Laboratories) and myosin-5a constructs eluted with elution buffer (Table 2.9). 1 ml elution fractions were collected, and analysed using SDS-PAGE. The fractions that had high concentration of myosin-5a constructs were dialysed, by placing the fractions into Spectra/Por® dialysis tubing (cut-off: 20,000 Da) and dialysing against 2 litres dialysis buffer (Table 2.9) for 16-18 hours. The dialysis buffer was exchanged for fresh dialysis buffer, and dialysis continued for an additional 3-4 hours. Protein was

concentrated 5-10 fold using Amicon® Ultra filter tubes (cut-off: 30,000 Da). The tubes were first centrifuged with dialysis buffer alone to activate the filter and prevent protein sticking to it, and then the protein sample was added. The tubes were centrifuged at 3,800 *g* for 20-40 minutes using a swing out rotor. Purified myosin-5a constructs were flash frozen in liquid nitrogen, by adding 20 µl drops of the purified protein to liquid nitrogen. The frozen beads were transferred to a cryo-tube on dry ice, and then stored at -80 °C.

Extraction buffer	10 mM MOPS pH 7.3, 200 mM NaCl, 10 mM $MgCl_2$, 1 mM EGTA, 3 mM NaN_3, 0.1 mM DTT, 0.1 mM PMSF, 2 mM ATP, 1 mg/l leupeptin, protease inhibitor mixture comprising 2 mg/l chymostatin, 1 mg/l pepstatin, 1 mg/l N_α-Tosyl-L-lysine-chloromethylketone-HCl, 1 mg/l N-*p*-Tosyl-L-phenylalanine chloromethylketone
Mary's buffer	10 mM MOPS pH 7.2, 500 mM NaCl, 0.1 mM EGTA, 3 mM NaN_3, 0.1 mM DTT, 0.1 mM PMSF, 1 mg/l leupeptin, 1 mM ATP, 5 mM $MgCl_2$
HMM buffer	10 mM MOPS pH 7.2, 0.1 mM EGTA, 3 mM NaN_3, 0.1 mM DTT, 0.1 mM PMSF, 1 mg/l leupeptin
Elution buffer	10 mM MOPS pH 7.2, 100 mM KCl, 0.1 mM EGTA, 3 mM NaN_3, 0.1 mM DTT, 0.1 mM PMSF, 1 mg/l leupeptin, 0.3 mg/ml Flag peptide
Dialysis buffer	10 mM MOPS pH 7.2, 100 mM KCl, 0.1 mM EGTA, 3 mM NaN_3, 1 mM DTT

Table 2.9. *Buffers used in myosin purification.*

2.4.17 Measurement of Myo5 constructs concentration

The extinction coefficient of the myosin constructs with 6 calmodulin molecules (Table 2.10) obtained from ProtParam was used for calculating protein concentration as described (section 2.2.6). Protein concentration is given as concentration of heads.

Construct name	Extinction coefficient
Myo5-Avi	186,575 M^{-1} cm^{-1}
Myo5-cc	192,650 M^{-1} cm^{-1}
Myo5-Ad	219,120 M^{-1} cm^{-1}

Table 2.10. *Extinction coefficients of the Myo5-constructs with 6 calmodulins bound, obtained by ProtParam.*

2.4.18 Biotinylation of Myo5-Avi

Biotinylation of the recombinant Myosin-5-Avi construct was carried out using the Biotinylation kit from Avidity. Usually 10 µl of 2 µM recombinant myosin-5 was mixed with 1.25 µl of Biomix-A buffer (10x stock concentration: 0.5 M bicine buffer pH 8.3) and 1.25 µl of Biomix-B buffer (10x stock concentration: 100 mM ATP, 100 mM Mg oxaloacetate, 500 µM d-biotin) and 0.2 µl of BirA biotin ligase enzyme (stock concentration: 3 mg/ml). All solutions and the enzyme were included in the kit from Avidity. The mixture was incubated at 30 °C for 45 minutes or on ice for 16-18 hours. As the biotinylation reaction by BirA is specific to Avi-tag sequences (GLNDIFEAQKIEWHE), the reaction is expected to stop when all the available Avi-tag sequences are biotinylated. Biotinylation was checked by Western blotting using an anti-biotin antibody (section 2.2.8) and also by mass spectrometry as described below (section 2.4.19). Biotinylated myosin-5 construct was either used in experiments after biotinylation or stored at -80 °C as described (section 2.4.16).

2.4.19 Mass spectrometry of Myo5-Avi and actin

Biotinylated and non-biotinylated myosin-5a constructs and actin samples were analysed with reverse phase HPLC linked to a mass spectrometer as described (Taggart et al., 2000; Liu et al., 2014). 2-3 µl of a ~1 mg/ml protein was introduced into the HPLC. The initial solvent was 0.05% trifluoroacetic acid with gradient elution by acetonitrile, 0.05% trifluoroacetic acid increasing at 2% v/v per minute with a flow rate of 0.2 ml/min. The fractionated protein samples were then introduced into the mass spectrometer. Positive-ion electrospray ionisation mass spectra of the samples were obtained with an Agilent 6224 mass spectrometer equipped with an ion electrospray ionisation interface and a time-of-flight mass detector. Mass spectra

were analyzed and deconvolved using the MassHunter software (Agilent). The non-biotinylated and biotinylated actin samples contained only one peak analysed by HPLC. The non-biotinylated and biotinylated myosin samples contained more peaks analysed by the HPLC, but only one of those contained the full length myosin construct. Mass spectrometry and data analysis were carried out with the help of Dr. Duck-Yeon Lee (director of Biochemistry Core NHLBI, NIH).

2.5 Adhiron techniques

2.5.1 Phage ELISA

Phage ELISA was performed by Dr. Christian Tiede as described (Tiede et al., 2014) to check if there were any potential binders. Streptavidin-coated plates were first blocked with casein blocking buffer (Sigma-Aldrich®), and then biotinylated actin was bound to the wells. After that growth medium, containing cells, helper phage and Adhiron phage, were added to the wells. After washing, bound phage was detected using an HRP-linked anti-phage antibody (Seramun). The antibodies, and thus the phage bound to actin, were visualised by adding 3,3',5,5'-tetramethylbenzidine (TMB) substrate to the wells and absorbance was measured at 620 nm after 2 minutes of incubation. Phage which binds to actin will not be washed away during the washing step and therefore will be recognised by the antibody and thus, by the absorbance of the TMB substrate. Controls were also performed in a similar way as described, but without adding biotinylated actin to check if there is any non-specific binding of the phage in this experimental setup.

2.5.2 Cloning of Adhirons

The screen resulted in the isolation of four potential actin-binding Adhirons, and the DNA encoding these Adhirons was provided to us in a phagemid vector between the Nhe I and Pst I restriction sites (Figure 2.6) by Dr. Christian Tiede. These were named Adhiron2, Adhiron6, Adhiron14 and Adhiron24 according to their location on the 24-well plate.

First, the cDNA sequence for each Adhiron was subcloned from the phagemid into a pET11a vector (provided by Dr Christian Tiede) using the Nhe I and Not I restriction sites. This introduces a C-terminal His-tag to allow Ni-NTA resin affinity purification of the expressed protein. In addition, another subcloning step was performed for all

four Adhirons to generate a second expression construct for each one, in which there was a Cys at the end of the Adhiron sequence. This single Cys residue can be used for biotinylation or other kinds of labelling, and is at the C-terminus preceding the His-tag.

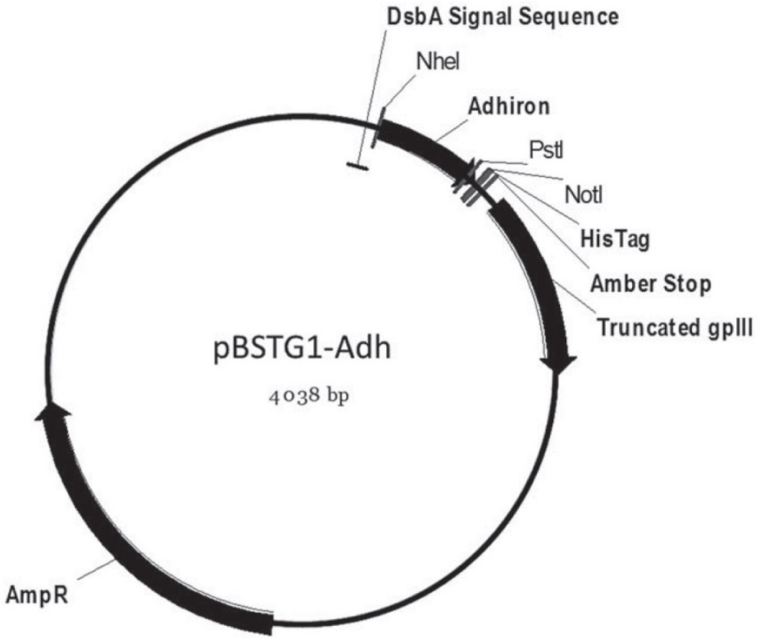

Figure 2.6. *pBSTG1 phagemid vector containing the coding region for Adhiron. Figure was taken from (Tiede et al., 2014).*

To achieve this, the pET11a plasmid was digested with Nhe I and Not I enzymes (section 2.2.2). After digestion, Antarctic Phosphatase (to a final concentration of 50 unit/ml) was added to the digested pET11a DNA in Antarctic Phosphatase Reaction Buffer (final concentration: 50 mM Bis-Tris-Propane-HCl pH 6, 1 mM $MgCl_2$, 0.1 mM $ZnCl_2$) and the mixture incubated at 37 ºC for 15 minutes. This removes 5' phosphate from the digested linear DNA to prevent self-ligation (Sambrook et al., 1989). The reaction was then heat inactivated at 65 ºC for 5 minutes. The DNA of the plasmid (pET11a) was purified as described (section 2.2.4).

Adhiron sequences were PCR amplified (primers in Table 2.11 and PCR as described in section 2.2.1). To generate Adhirons with a C-terminal cysteine residue, the reverse primer named Cys-Reverse (Table 2.11) was used, to introduce the codon for the cysteine residue. An extension time of only 30 s was used, as the

coding sequences for the Adhirons are only ~300 bp. The amplified DNA was purified, double digested with Nhe I and Not I, and then re-purified. The purified vector and insert (Adhiron sequences) were used in a ligation reaction in a total volume of 20 µl as shown (Table 2.12). The ligation reaction was incubated at room temperature for 16-18 hours, before transforming the ligation mixture into *E. coli*, isolating colonies, and purifying the resulting plasmid DNA, as described (section 2.2.4). The DNA sequence of the constructs was verified by Sanger sequencing (Source BioScience).

Forward	5'-ATGGCTAGCAACTCCCTGGAAATCGAAG-3'
Reverse	5'-TACCCTAGTGGTGATGATGGTGATGC-3'
Cys-Reverse	5'-TTACTAATGCGGCCGCACAAGCGTCACCAACCGGTTTG-3'

Table 2.11. *Primers used to amplify the Adhiron constructs. Forward and reverse primers were used for non Cys-Adhirons. Forward and Cys-Reverse primers were used for Cys-Adhirons. Colour coded background indicates the sequence and the restriction sites (Green: Nhe I site, grey: stop codon, magenta: His-tag, light blue: Not I site, yellow: Cys).*

Reagent	**Final concentration**
T4 DNA ligase buffer	50 mM Tris-HCl pH 7.5, 10 mM $MgCl_2$, 1 mM ATP, 10 mM DTT
Donor vector	3.75 ng/µl
Insert	1.25 ng/µl
T4 DNA ligase	20 unit/µl

Table 2.12. *Concentration of the reagents used in the ligation reaction.*

2.5.3 Transformation for Adhiron expression

After confirming the correct sequence, 100 ng of the plasmids was transformed into 50 µl BL21-CodonPlus(DE3)-RP *E. coli* competent cells (Agilent Technologies) for expression as described above (section 2.2.5), and colonies grown on LB agar plates containing 100 µg/ml ampicillin (KD Medical) to select for cells containing the pET11a vector.

2.5.4 Expression of Adhirons

For each Adhiron, a single colony was picked from the agar plate and inoculated into 5 ml sterile 2YT medium (16 g/l Bacto™ tryptone, 10 g/l Bacto™ yeast extract, 5 g/l NaCl, pH 7.0) supplemented with 1% w/v glucose and 100 µg/ml ampicillin. The culture was incubated at 37 °C for 16–18 hours while shaking at 230 rpm. Then 250 ml LB medium (KD Medical) containing also 100 µg/ml ampicillin was inoculated with the overnight culture and incubated at 37 °C while shaking at 230 rpm. The optical density of the culture at 600 nm wavelength was monitored (to estimate cell density) and when it reached 0.7, usually after 2.5–3 hours, the culture was induced with a final concentration of 0.1 mM IPTG. Then cells were incubated at 25 °C for 16–18 hours while shaking at 150 rpm. Cells were harvested using centrifugation for 15 minutes at 3500 *g* and cell pellets were kept at -80 °C until the protein purification step.

2.5.5 Adhiron purification

Cell pellets were resuspended in a 5 ml solution comprising 4.5 ml lysis buffer (Table 2.13), 500 µl 10x BugBuster (Novagen) and 5 µl Benzonase (25 unit/µl stock concentration, Novagen). Resuspended cells were then incubated at room temperature for 30 minutes while shaking. To heat denature the low stability *E. coli* proteins, the samples were incubated at 50 °C for 20 minutes. Adhirons are not affected by this step, as they are stable at 50 °C. Then the suspension was centrifuged for 20 minutes at 4 °C with 3,000 *g* and the rest of the purification was carried out at room temperature. The supernatant was loaded onto 1–1.5 ml Ni-NTA resin in 10 ml chromatography column (Bio-Rad Laboratories), which was already equilibrated with wash buffer (Table 2.13). The mixture was incubated for 1 hour with occasional shaking and mixing to ensure the resin binds all the Adhiron molecules. Then the flow through was collected and the resin was washed with 10–15 ml wash buffer, and again the flow through was collected. The resin was incubated for 15 minutes first with 10 ml elution buffer (Table 2.13), and then the protein was eluted, collecting 1 ml fractions. The elute was monitored for its protein content using Bradford reagent and usually it showed that there is still protein in the last elution fraction, therefore additional 5 ml elution buffer was added to the resin, incubated and then eluted. Samples of the supernatant, pellet from centrifugation, flow through and wash fraction, along with the elution fractions were run and analyzed by SDS gel

electrophoresis. The elution fractions that contained most of the Adhiron, and the least contamination with other proteins, were combined. These fractions, usually 10–13 ml, were then dialyzed using 7 kDa cut-off dialysis cassettes (Thermo Scientific) against 3–4 litres buffer comprising PBS (Quality Biological™) pH 7.4 and 1 mM DTT for 16–18 hours at 4 °C. Typical concentration of Adhirons and yield of the expression varied between 10–170 µM (2–120 mg Adhirons/litre of *E. coli* cells). Purified Adhirons were flash frozen in liquid nitrogen and stored at -80 °C.

Lysis buffer	50 mM NaH_2PO_4, 300 mM NaCl, 20 mM imidazole, 10% glycerol, pH 7.4
Wash buffer	50mM NaH_2PO_4, 500 mM NaCl, 20 mM imidazole, 10% glycerol, pH 7.4
Elution buffer	50mM NaH_2PO_4, 500 mM NaCl, 300 mM imidazole, 10% glycerol, pH 7.4

Table 2.13. *Buffers used in Adhiron purification. pH was adjusted to 7.4 by adding drops of 1 M HCl solution to the buffer containing all ingredients except glycerol.*

2.5.6 Adhiron concentration

Protein concentration was calculated from the UV absorbance at 280 nm wavelength (see section 2.2.6), using the calculated extinction coefficients (Table 2.14). Cys-Adhirons have the same extinction coefficient as Cys-free ones.

Adhiron2	18,450 M^{-1} cm^{-1}
Adhiron6	26,470 M^{-1} cm^{-1}
Adhiron14	26,470 M^{-1} cm^{-1}
Adhiron24	18,450 M^{-1} cm^{-1}

Table 2.14. *Extinction coefficients of Adhirons.*

2.5.7 Biotinylation of Adhirons

Cys-Adhirons can be covalently biotinylated at their cysteine residue using biotin maleimide. As this solvent-exposed Cys residue is highly reactive, first any cystine was reduced to cysteine, using a tris(2-carboxyethyl)phosphine (TCEP) disulphide reducing gel (Thermo Scientific), which was washed twice with equal volume of PBS

and centrifuged at 1,000 *g* for 2 minutes before adding to the Adhirons. Equal volumes of TCEP resin and Adhirons (still in elution buffer) were mixed and incubated at room temperature for 1 hour while rocking. The mixture was then centrifuged at 1,000 *g* for 2 minutes and the supernatant was mixed with 0.5 mM biotin-maleimide (50 mM stock concentration, dissolved in DMSO) and incubated on ice for 4 hours. Biotinylated Adhirons were then dialysed as described (section 2.5.5). Biotinylation of the Adhirons were done by Dr. Christian Tiede.

2.5.8 Actin spin down assay

Various actin spin down assays were performed with Adhirons to study their binding affinities and possible binding sites on F-actin. To determine the dissociation constant of the Adhirons to F-actin, stock F-actin (prepared as described in section 2.3.4) and Adhiron solutions were mixed and adjusted to a final volume of 200 µl, that contained 2.5 µM actin and 1-10 µM Adhiron in a buffer comprising 25 mM MOPS pH 7.0, 50 mM KCl, 2 mM $MgCl_2$, and 1 mM DTT. After mixing the components, the mixture was incubated at room temperature for 30 minutes, and then centrifuged at 4 ºC for 1 hour at 110,000 *g* using a TLA100 fixed angle rotor. Samples from both the supernatant and the pellet were mixed with Laemlli buffer (as described in section 2.2.7). 50 µl supernatant was mixed with 50 µl 2x Laemlli buffer. The pellet was dissolved in 200 µl boiling hot 1x Laemlli buffer. 50 µl of this solution was further mixed with 50 µl 1x Laemlli buffer. Equal volumes of the supernatant and the pellet were loaded into separate wells of two, 10-well 4-12% gradient NuPAGE® Bis-Tris pre-cast SDS PAGE gels, and subjected to gel electrophoresis together in the same tank. Three independent sets of binding assays were run for each Adhiron and average of the three measurements with the standard deviation were plotted against the concentration.

Additional experiments were performed to determine if Adhirons bind to the same binding site (Adhiron competition assay), or to the same binding site as the motor of myosin (myosin competition assay) on actin. In the Adhiron competition assay, stock F-actin, AdhironA and AdhironB were mixed to have a final concentration of 2.5 µM for all. All Adhirons have the same molecular weight, thus they are indistinguishable on an SDS gel. By using equimolar F-actin and Adhirons at concentrations well above the K_d, the sites on F-actin for each Adhiron will be nearly saturated.

In mixtures containing pairs of Adhirons, if the Adhirons do not compete, almost all the added Adhirons will pellet with the F-actin, with little in the supernatant. If they do compete, the amount in the pellet will be very similar to as with one Adhiron, and the rest will be in the supernatant.

In the myosin competition assay, stock F-actin, Adhiron and *Mus musculus* myosin-5a subfragment 1 (S1) were mixed to have a final concentration of 2.5 µM F-actin, 2.5 µM Adhiron and 0.2-2.5 µM S1. The S1 prep, which consists of the motor domain and the 6 IQ motif lever, was made previously in Dr. Sellers' laboratory (Wang, Chen, et al., 2000) and the extinction coefficient of S1 with 6 calmodulin molecules (141,420 M^{-1} cm^{-1}) was used for calculating protein concentration. After mixing, the samples were centrifuged as described for the Adhiron-actin binding assay.

To determine binding, the gel was stained and imaged as described (section 2.2.7). When two gels were used to analyse all data points, the images were combined and the intensity of the bands were determined using ImageJ. Boxes were drawn around the band of interest so that the whole band fits in it and the additional intensity of the band compared to the background was calculated. F-actin and everything that is bound to it, pellet during the centrifugation. As the pellet is transparent and only approximately 2 mm in size on the bottom of the 200 µl tube, it is challenging to fully recover it. Therefore samples loaded into the wells of the SDS gel will vary in the amount of actin they have, even though actin amount was kept equal in all assays. To account for the variation in recovery of the pellet, Adhiron band intensities were normalised according to the variation in the actin band intensities. Intensities of actin in the pellet were determined and lower intensities were multiplied to have equal intensity for all lanes. The same multiplication was performed for Adhiron (and S1) pellet intensities. The intensities in the supernatant were not affected. Adhiron (and S1) band intensity was determined in the pellet and in the supernatant and the bound Adhiron (and S1) concentration was calculated for each data point using the following equation:

$$Bound\ Adhiron = Total\ Adhiron * \frac{Pellet\ intensity}{(Pellet\ intensity + Supernatant\ intensity)}$$

Bound Adhiron concentrations were plotted as a function of the total Adhiron concentration and the following quadratic equation (Pollard, 2010) was fitted to the data points to determine the dissociation constant:

$$y = \frac{(c + x + K) - \sqrt{(c + x + K)^2 - 4cx}}{2}$$

where x is the total Adhiron concentration, and y is the bound Adhiron concentration, c is the total F-actin concentration and K is the dissociation constant (K_d). Parameters c and K were allowed to float during the fitting.

2.5.9 Generation of GFP-tagged Adhirons

The Adhiron sequences were subcloned into the pEGFP-C1 mammalian expression vector (Clontech) using the method described (section 2.5.2). Using PCR, the Adhiron sequences were amplified without the His-tag and Cys using the primers shown (Table 2.15). The cDNA were inserted into the EcoR I and BamH I restriction sites, placing the sequence downstream of that for eGFP (Figure 2.7). After ligation, the mixture was transformed as described (section 2.2.5), and cells plated onto LB agar plates containing 30 µg/ml kanamycin (KD Medical) to select for cells containing the pEGFP-C1 vector. The sequence of the constructs was verified by DNA sequencing at Eurofins Genomics (see S1 supplementary materials).

Plasmids with the correct sequences in the pEGFP-C1 vector were amplified and purified to provide a high enough concentration and quality DNA for transfection of mammalian cells, using the Plasmid Maxiprep Kit (QIAGEN®) according to the manufacturer's protocol.

Forward	5'- GAATTCTGCTAGCAACTCCCTGGAAATCGAAG -3'
Reverse	5'- GGATCCCGCAGCGTCACCAACCGG -3'

Table 2.15. *Primers used to amplify the Adhiron constructs to subclone them into pEGFP-C1 vector. Colour coded background indicates the restriction sites (Yellow: EcoR I site, green: BamH I site).*

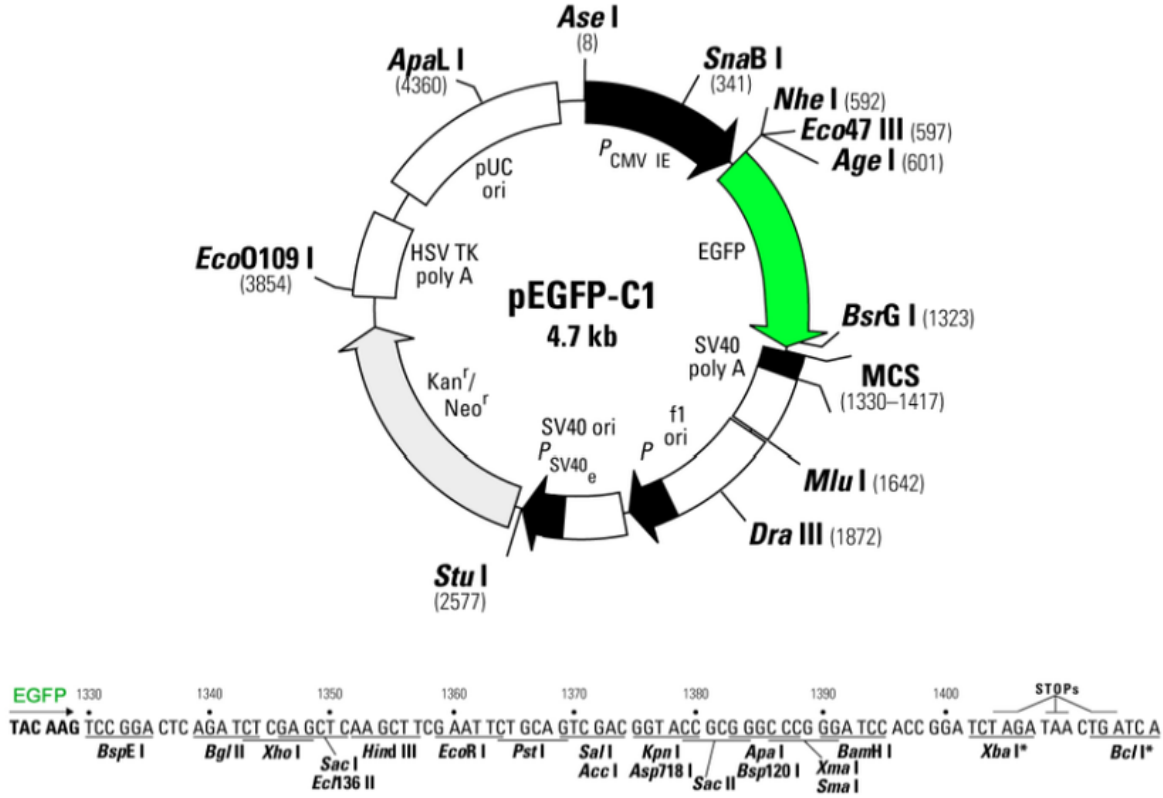

Figure 2.7. *Map and restriction sites of pEGFP-C1 plasmid. The DNA coding for the Adhiron was cloned between the EcoR I and BamH I restriction sites in the multiple cloning site (MCS) of the vector. Details of the restriction sites of the MCS are also shown. Figure is taken from the Addgene website.*

2.5.10 Cell culture experiments with Adhirons

HeLa cells were obtained from ATCC. They were cultured in DMEM + GlutaMAX™-I medium (Thermo Fisher Scientific) supplemented with 100 unit/ml penicillin, 100 µg/ml streptomycin and 10% v/v FBS. Cells were grown as adherent cell culture at 37 ºC and 5% CO_2. To passage the cells usually after 3 days, when confluency reached approximately 75%, the growth medium was removed from the cells and replaced with 1 ml TrypLE Express (Thermo Fisher Scientific) and incubated for 3 minutes to dissociate the cells. Cells were monitored with a light microscope to check if they are rounding up and detaching from the surface. When this was complete, 9 ml medium was added and the cells were centrifuged at 1,000 *g* for 5 minutes. The pelleted cells were resuspended to a density of 10^4 cells/ml in fresh medium. To freeze cells for long term storage, the cells were centrifuged and resuspended in medium containing 10% v/v DMSO up to a density of 10^6 cells/ml.

They were aliquoted in 2 ml cryo-tubes that were placed in the -80 º C freezer and after 3 days were transferred into the liquid nitrogen storage.

For imaging, cells were plated onto 13 mm diameter glass coverslips, that were cleaned by washing with hydrochloric acid, rinsing with H_2O ten times and then with 70% v/v ethanol. They were allowed to dry in the tissue culture hood and then placed one in each well of a 6-well plate. To prepare the cells for transfection with eGFP-tagged Adhirons, HeLa cells were passaged as described above and cells were diluted to a density of 10^5 cells/ml. 300 µl of the cell suspension was added to cleaned coverslips, and incubated at room temperature for 3 minutes. Then 2 ml of growth medium was added to the wells and the plate was incubated at 37 ºC and 5% CO_2 for 24 hours.

To transfect the cells 3 µl room temperature FuGENE® HD Transfection Reagent (Promega) was added to 97 µl DMEM and the mixture was incubated at room temperature for 5 minutes. Then 2 µg high quality (as described in section 2.5.9) DNA was added to the mixture and incubated at room temperature for 15 minutes. Finally, this mixture was pipetted onto the cells and the plate was incubated at 37 ºC and 5% v/v CO_2 for 1-2 days before fixing and staining the cells.

To fix the cells, the growth medium was aspirated from the wells and replaced with 1 ml of 4% w/v paraformaldehyde (dissolved in PBS) at room temperature. After 15 minutes incubation at room temperature, this solution was removed and the cells were washed 3x with 2 ml PBS. 1 ml of PBS was left in each well, the plates were sealed with Parafilm and the cells were stored at 4 ºC before staining.

To stain the cells, the coverslips were removed from the 6-well plate and PBS + 0.2% v/v Triton™ X-100 was added to permeabilise the cells. Alexa Fluor® 546 labelled phalloidin and DAPI (both from Thermo Fisher Scientific) were diluted to 66 nM and 2 µg/ml in PBS, respectively. 100 µl of this staining solution was pipetted onto the coverslips and allowed to incubate for 20 minutes at room temperature. Then the coverslip was washed 3x with PBS + 0.2% v/v Triton™ X-100 and then 3x with PBS. 3 µl ProLong® Diamond Antifade Mountant (Molecular Probes™) was pipetted onto a slide and the coverslip inverted onto the slide. The slide was incubated at room temperature for 1 hour to allow the mountant to set before imaging. Prepared slides were imaged using the DeltaVision deconvolution microscope. Cell culture experiments and imaging were performed with the help of Prof. Michelle Peckham.

To determine if any of the Adhirons bind to actin in non-transfected HeLa cells, biotinylated Cys-Adhirons were used. Cys-Adhirons were biotinylated as described (section 2.5.7). Fixed cells on 13 mm diameter glass coverslips were permeabilised with PBS containing 0.2% v/v Triton™ X-100 for 5 minutes. The Adhirons were diluted to 5 mg/ml in PBS, added to the cells, and incubated for 1 hour. The coverslips were washed 5x in PBS, and then Alexa Fluor® 647 labelled streptavidin in PBS, together with Alexa Fluor® 488 labelled phalloidin (1/50 dilution), and DAPI (1/500 dilution) was added and incubated for another hour. Coverslips were washed, mounted onto glass slides using Prolong antifade, and imaged with the DeltaVision deconvolution microscope.

2.6 Assays of interaction between myosin and actin

2.6.1 ATPase activity assay

Actin-activated steady-state MgATPase activity of myosin-5 was measured using a continuous NADH-coupled assay (Figure 2.8). Usually 30 nM myosin-5 was mixed with a buffer comprising 20 mM MOPS pH 7.0, 3 mM $MgCl_2$, 50 mM KCl, 1 mM DTT, 0.05 mM EGTA, 40 units/ml lactate dehydrogenase, 200 units/ml pyruvate kinase, 200 µM NADH, 1 mM PEP and 1 mM ATP in a total volume of 200 µl. To measure maximal velocity (V_{max}) of the ATPase reaction, saturating concentrations (20 µM) of F-actin were used. The measurement was started by adding ATP to the reaction mixture. Oxidation of NADH, which indirectly shows the rate of the ATPase reaction, was measured by following the fall in absorbance at a wavelength of 340 nm using a Cary Spectrophotometer. The experiments were carried out at 25 °C. Since ADP produced by ATP hydrolysis is converted back to ATP by the pyruvate kinase, product inhibition by ADP will not occur.

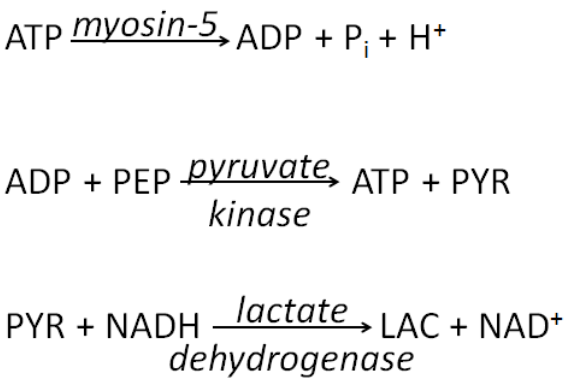

Figure 2.8. *Reactions in the NADH-coupled ATPase assay. Abbreviations are the following, PEP: phospho(enol)pyruvate, PYR: pyruvate, LAC: lactate.*

2.6.1.1 ATPase activity of Myo5-Avi

ATPase activity assays were performed using 30 nM myosin-5 and 20 µM F-actin as described (section 2.6.1). Both biotinylated and non-biotinylated actin and myosin were used. Biotinylated myosin was kept in the biotinylation buffer, non-biotinylated myosin was kept in the dialysis buffer and 2.5-3 µl of the concentrated protein stock was added to 200 µl of reaction mix. To make up biotinylated F-actin, a mixture of actin monomers of which 5% were biotinylated (Cytoskeleton) were mixed and allowed to polymerise as described (section 2.3.4).

Activities were corrected for the ATPase of Myo5-Avi (both biotinylated and non-biotinylated) measured in the absence of F-actin and also for the ATPase activity of F-actin (both biotinylated and non-biotinylated) measured in the absence of myosin. To test the effect of NeutrAvidin, the reaction was started with Myo5-Avi and F-actin. After obtaining a stable slope corresponding to constant ATPase rate, 5 µl of 80 µM NeutrAvidin (Thermo Fisher Scientific, dissolved in H_2O) was mixed into the 200 µl reaction mixture to obtain a final concentration of 2 µM. NeutrAvidin concentration is given in tetramers.

2.6.1.2 Adhirons in the ATPase activity assay

To determine the effect of the Adhirons on actin-activated MgATPase activity of *Mus musculus* myosin-5 S1, ATPase activity assays were performed as described (section 2.6.1). Stock F-actin, S1 and Adhiron were mixed to have a final concentration of 30 nM S1 and 1-40 µM Adhirons in a buffer containing 25 mM KCl

and all the additional components (section 2.6.1). A lower concentration of F-actin (4 µM, as compared to 20 µM) was used so that not all myosin heads will be bound to F-actin. At this actin concentration, ATPase activity will depend on the available concentration of actin in a quasilinear manner (Wang, Chen, et al., 2000). This way if Adhirons occupy the binding site of the myosin motor on F-actin, the observed reduction in ATPase activity would reflect the reduction of concentration of available actin. Three experiments were performed, and the data were averaged. The measured activities were corrected for S1 activity measured without F-actin.

2.6.2 Motility assay

The movement of myosin-5 on F-actin was visualised using total internal reflection fluorescence (TIRF) microscopy. Alexa Fluor® 647 labelled biotinylated F-actin was attached to the coverslip and the translocation of GFP-tagged myosin was tracked at room temperature (~23 °C) by imaging it using the green channel (emission wavelength of 488 nm) on the Nikon® Eclipse Ti microscope. The position of the F-actin filaments was imaged in the far-red channel (emission wavelength of 640 nm). 100x oil TIRF objective was used, with a numerical aperture of 1.49 (Nikon®).

Biotinylated F-actin, where 20% of the monomers are biotinylated, was prepared as described in section 2.3.4. Alexa Fluor® 647 Phalloidin (Molecular Probes™) was dissolved in methanol and added to biotinylated F-actin (final methanol concentration was 5% v/v). The final concentration of the dye was double compared to F-actin to ensure full labelling that is important for imaging actin filaments. Labelled F-actin was left protected from light on ice for 2 hours before using it.

To prepare the coverslips (22 x 30 mm), 3 µl of 0.1% w/v nitrocellulose (diluted in amyl acetate) was applied onto the surface and allowed to dry for 15 minutes at room temperature. To prepare the flow chamber, double-sided adhesive tape was attached to the long edges of a microscope slide and then coverslip was attached to the slide onto the tape, with the treated side facing down. The volume of the flow chamber was 20-30 µl as the channel between the tapes is 7-10 mm wide. Next, 30 µl biotinylated BSA (1 mg/ml in H_2O, Sigma-Aldrich®) was added into the chamber, and then incubated at room temperature for 2 minutes. The chamber was then washed with 200 µl motility buffer (MB: 20 mM MOPS pH 7.4, 5 mM $MgCl_2$, 0.1 mM EGTA). Filter paper was applied to suck the liquid from the opposite side of

the chamber as to the side where liquid was introduced to the chamber. 50 µl of NeutrAvidin (1 mg/ml, 16.7 µM in tetramers, in H_2O) was then added into the chamber to bind to the biotinylated BSA, and incubated at room temperature for 2 minutes, before washed again with 200 µl MB. 40 µl of Alexa 647 labelled biotinylated F-actin (50 nM in MB) was then added into the chamber to bind to NeutrAvidin, incubated for 1 minute at room temperature, then washed with 200 µl MB. The surface was then blocked by adding 100 µl BSA (1 mg/ml in MB), incubation at room temperature for 2 minutes and then the flow cell was washed with 100 µl MB. The final myosin-containing mixture (100 µl) comprised 50 mM DTT, 50 mM KCl, 1 mM ATP, 0.01 mg/ml BSA, 200 unit/ml glucose oxidase (Sigma-Aldrich®), 1150 unit/ml catalase (Roche), 20 mM glucose, and 5 nM Myo5-Avi in MB. After adding this mixture into the flow chamber, I started to image the slide.

Frame rate was 0.21 sec^{-1} and pixel size was 0.13 µm/pixel. The software Fiji with plugin Trackmate v2.8.1 was used to analyse run length and speed of the single molecules (Tinevez et al., 2016). When analysing and identifying the tracks, no gaps were allowed, meaning that if a molecule disappeared for a frame and reappeared at the same place, it was considered as a separate track. Molecules that were visible for less than 4 frames and molecules that translocated less than 3 pixels (0.4 µm) from their initial site were omitted to have data only from processive movement (Sakamoto et al., 2008). Bin size was set 0.2 for both run length (µm) and for velocity (µm/sec). Run length distribution was fitted with a first order exponential decay function. Velocity distribution was fitted with a Gaussian function (Hodges et al., 2007). Mean values show the fitted parameter and error of the fitting.

2.6.2.1 Myo5-Avi motility assay

To study the effect of NeutrAvidin on Myosin-5 motility, first the assay was set up using biotinylated GFP-tagged Myo5-Avi as described in section 2.6.2. After imaging the slide for 3 minutes, additional 30 µl of the following solution was introduced into the chamber, while being imaged continuously. This solution had the same composition as described in section 2.6.2, but it contained additional 16.7 µM NeutrAvidin tetramers. This way, myosin movement on the same filaments were tracked and additional myosin was added to the chamber to compensate for the

molecules that were washed away, when introducing the new mixture into the chamber.

Acquisition time was 3 minutes for control assays and 6 minutes for NeutrAvidin assay. Velocity exhibited an unusual distribution after the addition of NeutrAvidin, therefore in that case average and standard deviation was calculated.

2.6.2.2 Adhirons in the TIRF assay

Adhirons were tested for the ability to fix actin to a glass surface and allow myosin movement in a TIRF assay. 0.5 or 5 µM Adhirons in motility buffer (MB) were added to the glass coverslips in the flow chamber (section 2.6.2), and incubated at room temperature for 5 minutes, before washing with 200 µl MB for 1 minute, and then adding Alexa Fluor® 647 labelled biotinylated F-actin. The remainder of the assay was performed as described (section 2.6.2).

Anti-His antibodies (6x-His Epitope Tag Antibody, Thermo Fisher Scientific) were also tested for their ability to bind Adhirons and thus, actin to the surface. As Adhirons have a C-terminal His-tag, they could potentially be attached to the surface using these antibodies. 10 µg/ml antibodies were added to the flow chamber, then 1 mg/ml BSA (in MB) and then 5 µM Adhirons (in PBS), with wash steps in between and further steps as described above and in section 2.6.2.

Run length distribution could not be fitted with a first order exponential decay function, therefore average and standard deviation was calculated.

2.6.3 Negative stain electron microscopy

First, myosin at a final concentration of 100 nM and 100 µM ATP was added to a buffer comprising 12.5 mM MOPS pH 7.2, 2 mM $MgCl_2$, 0.1 mM EGTA and 100 mM KCl. Then, F-actin (final concentration of 1 µM, containing 50 nM biotinylated actin) was mixed with NeutrAvidin (final concentration of 80 nM). Next the mixture of biotinylated myosin (final concentration of 100 nM) and ATP (final concentration of 1 µM) was added to the solution containing F-actin and NeutrAvidin, all diluted in the buffer described above. 30 seconds after mixing, 3 µl of the sample was applied to a carbon-filmed 200 mesh copper grid (Ted Pella), which had been UV treated for 30 minutes prior.

Grids were UV treated as a broad range of UV light wavelengths and ozone makes the surface of the grid more hydrophilic, and thus proteins will attach better to these

grids (Burgess et al., 2004). The grids were placed ~3 cm from the lamp (low pressure mercury vapour type R51, UV Products) in a cardboard box to retain the ozone that is generated in the air by the UV radiation.

After applying protein to the grids, they were then stained with 1% w/v uranyl acetate by adding a few drops of the stain to the protein on the grid, and then blotting the excess liquid with filter paper (Whatman® grade 42).

Micrographs were recorded at nominal magnification of 40,000 on a JEOL 1200EX II microscope with an AMT XR-60 CCD camera (2816x2528 pixels). Actual pixel size was calibrated by Dr. Neil Billington using the lattice spacing of bovine liver catalase crystals (Ted Pella) (Wrigley, 1968) and determined to be 0.46 nm/pixel.

2.7 Data and figure analysis

Data were plotted and analysed with OriginPro 7.5 (OriginLab Corp.). Figures were created using Photoshop CS6 (Adobe Systems Inc.). Microscope images and gel images were analysed by ImageJ. Protein structure images were created with Pymol (Schrödinger, LLC). T test were carried out using GraphPad (GraphPad Software Inc.).

3. Characterisation of actin-binding Adhirons

3.1 Results

3.1.1 Selection of Adhirons that bind to actin

The phage ELISA assay showed that several clones bound to actin (Figure 3.1). Several wells showed high levels of absorbance, indicating binding of the phage to actin. None of the control wells, in which actin was not present, showed high absorbance levels and the absorbance for all control wells was less than 0.05. Phages with the ID numbers 2, 6, 10, 11, 13, 14, 15, 16, 19 and 24 gave absorbance levels of 0.2 or greater for wells containing actin. These clones were sequenced and four unique binders were identified. These were Adhiron2, Adhiron6, Adhiron14 and Adhiron24 according to their physical location on the 24-well plate. Adhiron2 was present in phages ID number 2, 13 and 15 and Adhiron6 in phages ID number 6, 11, 16 and 19. Phage ID number 10 was not analysed as the sequencing results were of low quality for this clone. The amino acid sequence of the four potential actin-binding Adhirons is identical except for the two variable loops (Figure 3.2). Cys-Adhirons have the additional cysteine residue just preceding the His-tag.

Amino acid sequence comparisons were performed on the variable loops using the BLAST webserver (Altschul et al., 1997) and the protein-protein BLAST algorithm with default parameter settings. No clear alignment with any known actin-binding domain was recognised. The sequence of loop1 of Adhiron6 and Adhiron14 are similar, therefore it is expected that they will have similar properties. No other sequence similarity was found in the loops.

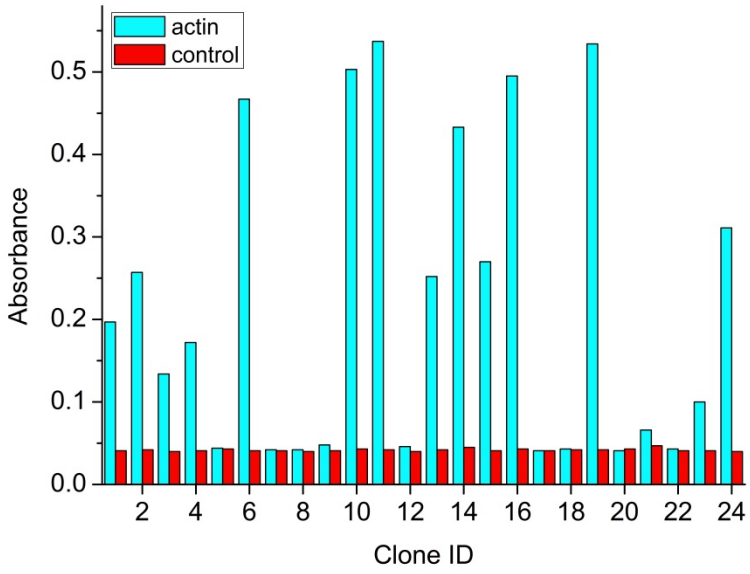

Figure 3.1. *Screening Adhiron clones for actin binding using ELISA. 24 clones were tested in wells coated with actin and in wells containing only buffer and absorbance of oxidised TMB at 620 nm was recorded.*

```
Adhiron2        MASNSLEIEELARFAVDEHNKKENALLEFVRVVKAKEQWIYIHPRKVTMYYLTLEAKDGG 60
Adhiron6        MASNSLEIEELARFAVDEHNKKENALLEFVRVVKAKEQSSVPHWWWTTMYYLTLEAKDGG 60
Adhiron14       MASNSLEIEELARFAVDEHNKKENALLEFVRVVKAKEQSDTPHWWWTTMYYLTLEAKDGG 60
Adhiron24       MASNSLEIEELARFAVDEHNKKENALLEFVRVVKAKEQMDMIGEYVSTMYYLTLEAKDGG 60

Adhiron2        KKKLYEAKVWVKTHKYQNMSDNFKELQEFKPVGDAAAAHHHHHHHH 106
Adhiron6        KKKLYEAKVWVKRDPNMIFKINFKELQEFKPVGDAAAAHHHHHHHH 106
Adhiron14       KKKLYEAKVWVKESPVHPKRLNFKDLQEFKPVGDAAAAHHHHHHHH 106
Adhiron24       KKKLYEAKVWVKGWMPLYSRQNFKELQEFKPVGDAAAAHHHHHHHH 106
```

Figure 3.2. *Sequence alignment of the actin-binding Adhirons, using the ClustalW webserver (Larkin et al., 2007). The amino acids in the variable loops lie between residue numbers 39–47 and 73–81, are denoted by the red boxes.*

3.1.2 Expression and purification of Adhirons

Adhiron sequences were cloned from the phagemid vector into a pET11a *E. coli* expression vector. All four Adhirons and also their Cys version were expressed and then purified using Ni-NTA resin, as they all bear a C-terminal His-tag (section 2.5.5). Typically, the purity of the Adhirons in the elution fractions was very high (Figure 3.3A). Occasionally (as shown in Figure 3.3A), there is Adhiron in the flow through suggesting that the amount of resin used in that purification was not enough to bind all of the Adhiron molecules or the resin incubation with the cell lysate was not performed appropriately.

After expressing, purifying and dialysing all four Adhirons, their concentration was measured and they were analysed on an SDS gel (Figure 3.3B). This expression yielded concentrations of 33, 15, 56 and 39 μM for Adhiron2, 6, 14 and 24, respectively. Figure 3.3B shows that the preparations are clean, only Adhiron2 and 14 contain small amount of contaminants. As expected all Adhirons have the same size according to the SDS gel. Band intensities correspond to the measured concentrations.

Cys-Adhirons, which contain a single cysteine residue at the C-terminus of the protein, just preceding the His-tag can be specifically biotinylated on this residue. As the cysteine residue is solvent-exposed it is prone to oxidisation to cystine that dimerises the Cys-Adhirons via a disulphide bond.

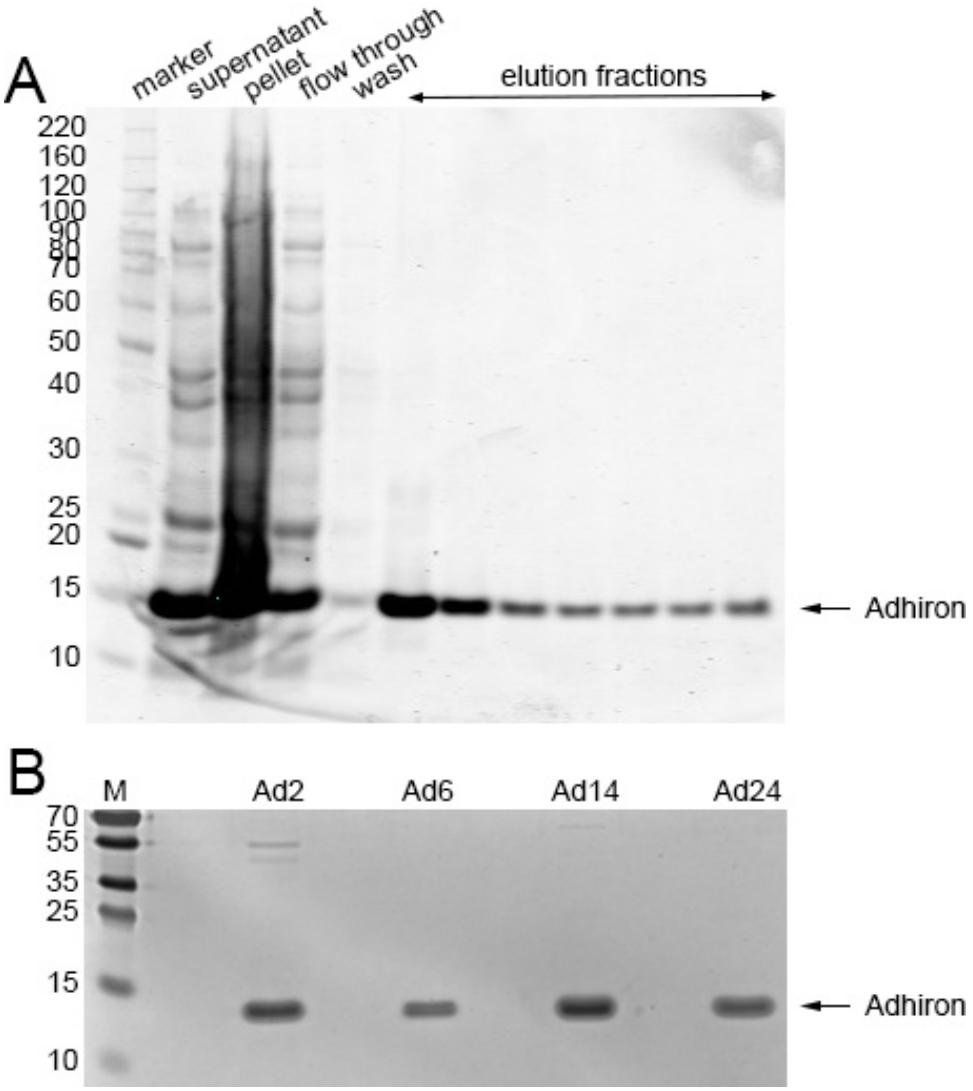

Figure 3.3. *Coomassie-stained SDS-PAGE gels of Cys-Adhiron14 purification steps and of the purified Adhirons. A) SDS-PAGE gel shows the steps of Cys-Adhiron14 purification. Lanes are the following. Marker: BenchMark protein ladder, numbers denote molecular mass in kDa corresponding to the bands of the lane. Supernatant: taken after centrifuging the cell lysate. Pellet: taken after centrifuging the cell lysate. Flow through: taken after incubation with Ni-NTA resin. Wash: flow through taken after washing the Ni-NTA resin. Elution fractions: samples taken from each 1 ml elution fraction. B) SDS-PAGE gel of all four purified Adhirons. Lanes are the following. M: PageRuler Plus pre-stained protein ladder, numbers denote molecular mass in kDa corresponding to the bands of the lane. Ad2, Ad6, Ad14 and Ad24 denote the four different Adhirons. Equal volumes of the purified protein were loaded in all wells. Arrows point out the Adhirons.*

3.1.3 Measuring the binding of Adhirons to actin

Phage ELISA results indicated that Adhiron2, 6, 14 and 24 bind to actin, however this has to be validated by direct measurement of the binding. As F-actin is a viscous polymer, standard biophysical methods for determining the binding constant (e.g. isothermal titration calorimetry), are not applicable. However, as the molecular weight of the F-actin polymer is high, it sediments in the ultracentrifuge, whereas Adhirons do not (Figure 3.4). Thus, we can exploit this property of actin to distinguish between free Adhiron and actin-bound Adhiron (Hertzog and Carlier, 2005).

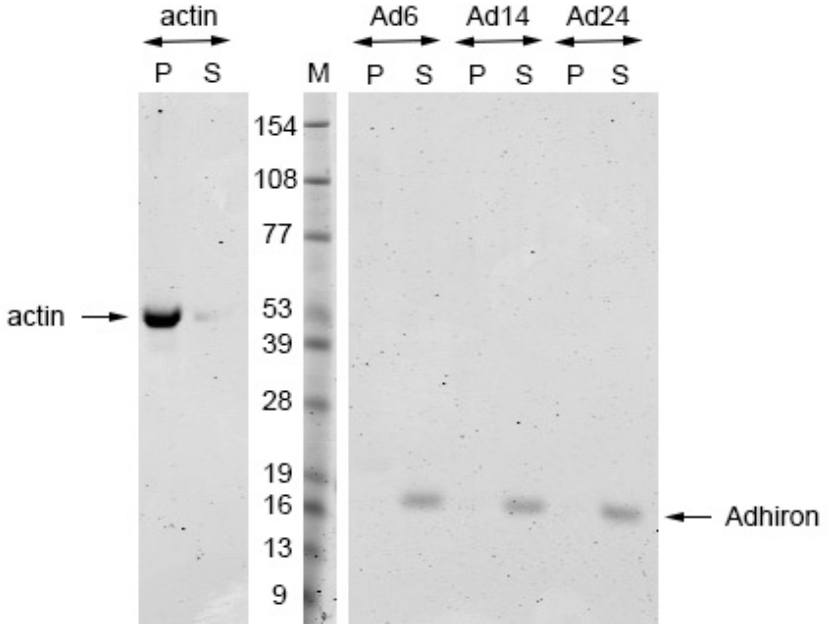

Figure 3.4. *Coomassie-stained SDS gels showing results of centrifugation of F-actin and Adhirons alone. 2.5 µM concentrations were used for all proteins in the centrifugation and then equal volumes were loaded in all wells. Lanes are the following. M: BenchMark pre-stained protein ladder, numbers denote molecular mass in kDa corresponding to the bands of the lane. P: pellet after centrifugation. S: supernatant after centrifugation. Arrows point out actin and the Adhirons.*

To be able to quantify the information obtained from the spin down assays, I had to make sure that the intensity of the Adhiron bands on SDS gels is linearly related to the amount of protein loaded onto the gel in the concentration range used in the experiments (Figure 3.5). Band intensities from SDS gels of varying concentrations of Adhirons (Figure 3.5A) were quantified with ImageJ and plotted against the amount of protein loaded (Figure 3.5B). The data points could be fitted using a linear

function, which was only used as an initial check point, not as a calibration curve for subsequent assays.

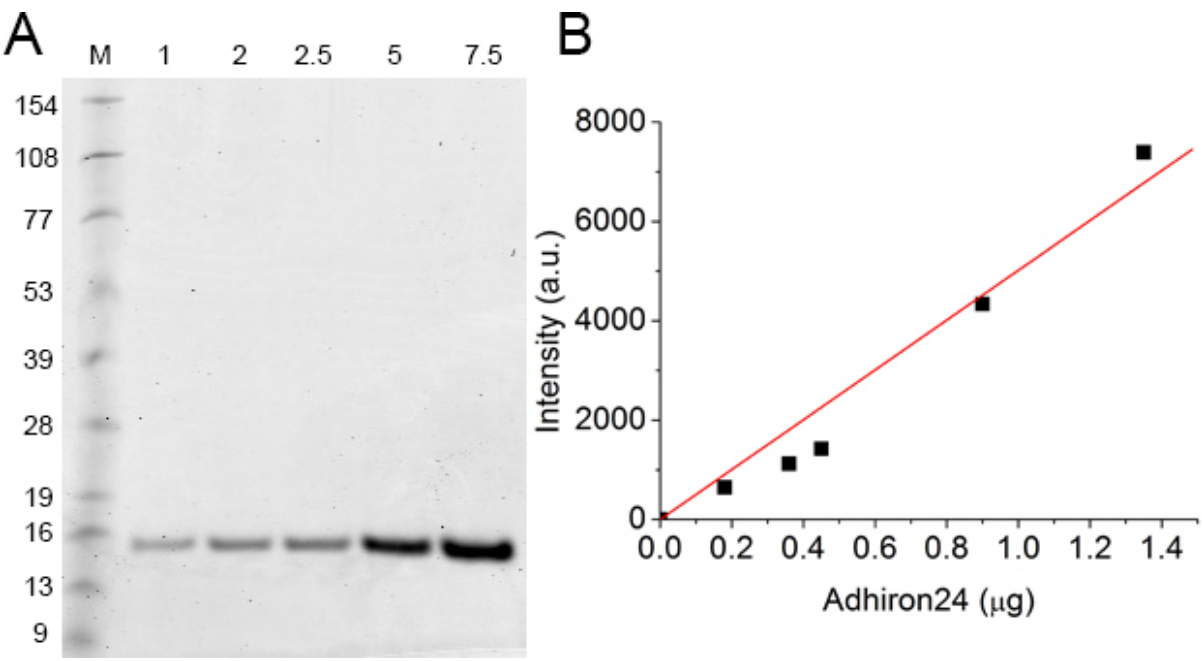

Figure 3.5. *Calibration of Adhiron amount and band intensity on SDS gels. A) Coomassie-stained SDS gel showing increasing concentrations of Adhiron24. Lanes are the following. M: BenchMark pre-stained protein ladder, numbers denote molecular mass in kDa corresponding to the bands of the lane. 1, 2, 2.5, 5 and 7.5 denote concentrations of Adhiron24 in µM. Adhiron samples were diluted in 2x Laemlli buffer and 30 µl mixture was loaded in each well. B) The intensities of the bands from gel A) were plotted versus the amount of protein loaded onto the SDS gel. Intensity is in arbitrary units. A linear function was fitted to the data with the following parameters: y = 5017x.*

SDS-PAGE gel of the Adhiron24 spin down assay shows that the ratio between actin in the pellet and in the supernatant did not change due to Adhiron binding, suggesting that Adhiron24 does not cause actin depolymerisation (Figure 3.6). The amount of Adhiron24 in the pellet appears to saturate, suggesting that the conditions used for the binding assay were appropriate. The amount of Adhiron24 in the supernatant increases above the saturating concentration, whereas its amount in the pellet is unchanged (Figure 3.6).

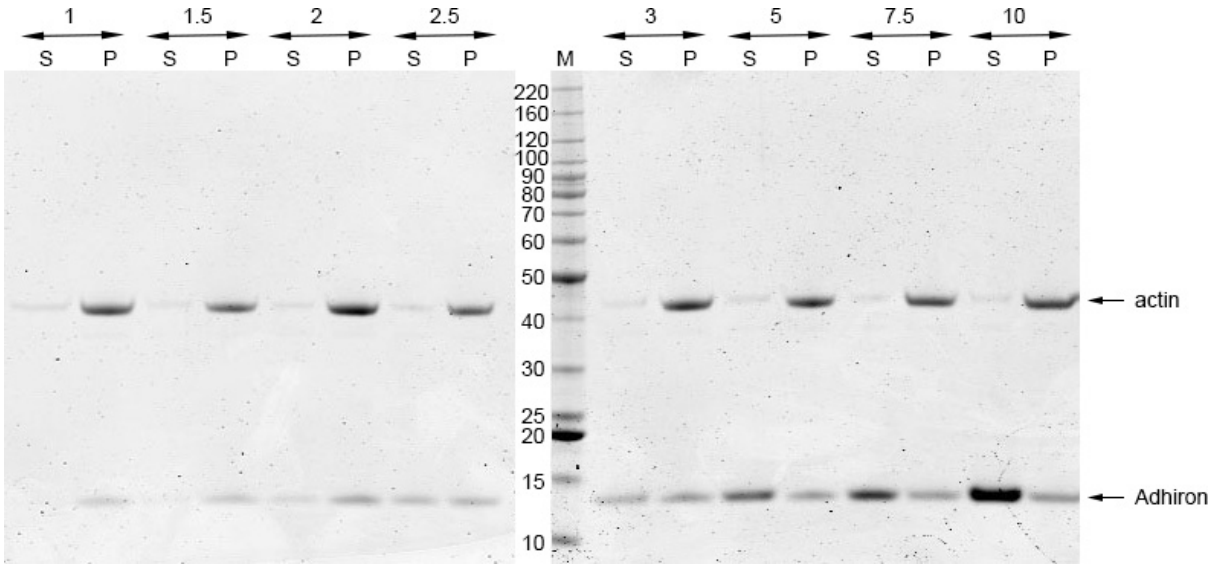

Figure 3.6. *Coomassie-stained SDS gels of the result of a spin down assay using 2.5 µM F-actin and Adhiron24. Lanes are the following. M: BenchMark protein ladder, numbers denote molecular mass in kDa corresponding to the bands of the lane. P: pellet after centrifugation. S: supernatant after centrifugation. Numbers above S and P denote concentration of Adhiron24 in that data point. Samples were diluted in 2x Laemlli buffer and 30 µl mixture was loaded in each well. Arrows point out actin and the Adhirons.*

Binding assays show that Adhiron6, Adhiron14 and Adhiron24 all bind to actin with a high affinity (Figure 3.7). Fits to the data points of Adhiron6, 14 and 24 gave values for the dissociation constants (Table 3.1) that were all close to 0.3 µM, indicating tight binding. In contrast, while Adhiron2 bound to actin, its binding curve did not show saturation for the concentration range used in this assay (Figure 3.7) and therefore the dissociation constant could not be determined.

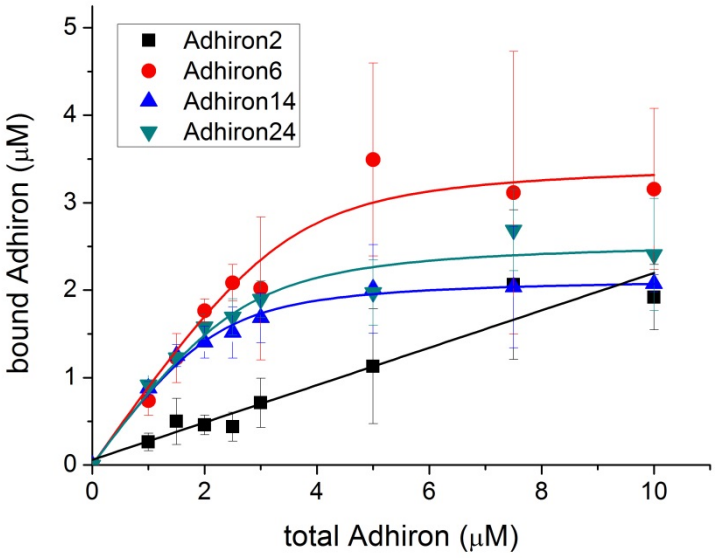

Figure 3.7. *Results of the actin spin down assay measured with all four Adhirons. Data points show mean of three independent measurements and error bars indicate the standard deviation. Quadratic curves were fitted to Adhiron6, 14 and 24. A linear function was fitted to the data points of Adhiron2 that could potentially fit the initial range of a quadratic data distribution.*

	K_d (μM)
Adhiron6	0.31 ± 0.17
Adhiron14	0.30 ± 0.05
Adhiron24	0.38 ± 0.14

Table 3.1. *Dissociation constants of Adhirons binding to F-actin. Data were obtained from fitting the results of the actin spin down assays. Colours represent the same colours used in Figure 3.7. Numbers show mean of the fitting and confidence values.*

3.1.4 Testing competition between Adhirons

To test if the Adhirons bind to the same or overlapping binding sites on F-actin, further spin down assays were performed, using a mixture of two different Adhirons to determine if they can both bind, or if they interfere with binding of the second Adhiron. A mixture of three different Adhirons was also tested (Figure 3.8).

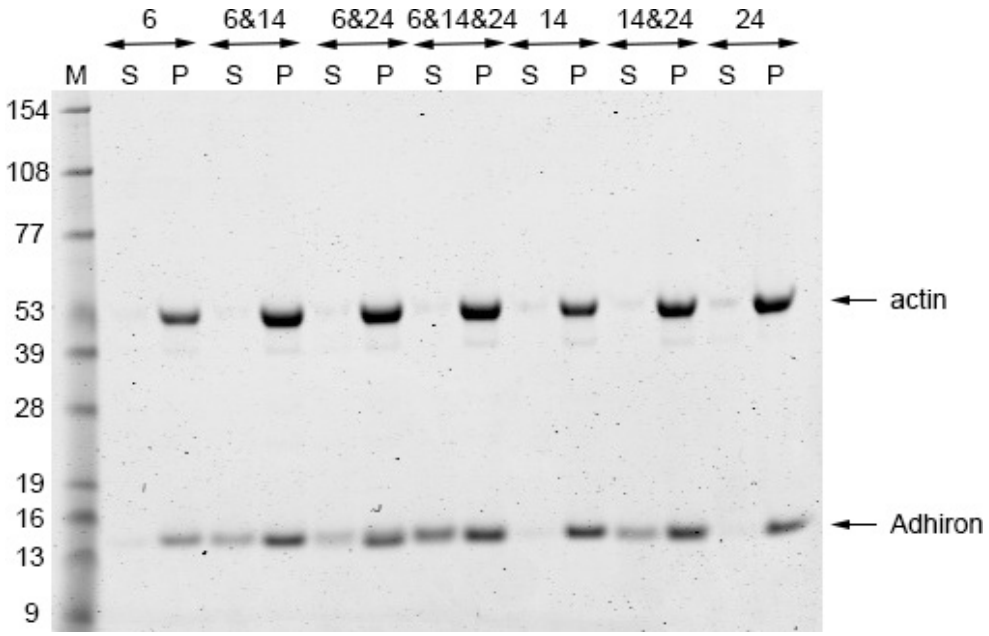

Figure 3.8. *Coomassie-stained SDS gel showing the results of one of the competition spin down assays performed. 2.5 µM F-actin and equimolar concentrations of 2.5 µM Adhirons were used in these experiments. The Adhiron concentrations used are well above the K_d, to ensure that the sites on F-actin for each Adhiron will be nearly saturated. Three independent sets of assays were performed including controls of single Adhiron binding the actin and also a mixture of three Adhirons and actin. Lanes are the following. M: BenchMark pre-stained protein ladder, numbers denote molecular mass in kDa corresponding to the bands of the lane. P: pellet after centrifugation. S: supernatant after centrifugation. Numbers above S and P denote the type of Adhiron that was added to the mixture in that data point. Samples were diluted in 2x Laemlli buffer and 15 µl mixture was loaded in each well. Arrows point out actin and the Adhirons. Band intensities were analysed and bound Adhiron concentrations are shown in Table 3.2.*

Analysing the intensity of the bands for each of the competition assays shows that approximately 2.5 µM Adhiron is always found in the pellet for all experiments (single, double or triple Adhirons), which would be expected if these Adhirons compete for the same binding site (Table 3.2). Some of the values are however exceeding 2.5 µM, but are still far from the total Adhiron concentration, which would be expected if these Adhirons bind to independent binding sites on actin. These results suggest that the binding sites of Adhiron6, 14 and 24 on actin are either identical or at least these sites are overlapping.

	Total Adhiron concentration (µM)	**Bound Adhiron concentration (µM)**
Ad6	2.5	2.30 ± 0.09
Ad14	2.5	2.35 ± 0.00
Ad24	2.5	2.23 ± 0.20
Ad6+Ad14	5.0	2.45 ± 0.44
Ad6+Ad24	5.0	2.69 ± 0.54
Ad14+Ad24	5.0	2.51 ± 0.52
Ad6+Ad14+Ad24	7.5	3.14 ± 0.03

Table 3.2. *Results of the Adhiron competition spin down assays. Data shows average concentration of bound Adhirons with standard deviations.*

3.1.5 Testing competition between Adhirons and myosin head in binding to actin

To test if any of the Adhirons bind to the same or overlapping regions on actin to that of the motor domain of myosin, competition assays were performed using a mixture of Adhirons and myosin-5a subfragment 1, which contains the motor and the lever. Control experiments showed that under the conditions used, myosin-5a S1 only sediments in the presence of actin (Figure 3.9). Myosin-5a S1 binds to actin in the absence of ATP with a very high affinity (5 pM (De La Cruz et al., 1999)). Therefore, if Adhirons bind to the same site on F-actin, they will be displaced by myosin S1 as they bind with weaker affinity. Even though the data are scattered (Figure 3.10), all three Adhirons appear to be displaced from actin as the S1 concentration increases. This suggests that the binding site of these three Adhirons on actin may overlap with that of the motor domain of myosin-5.

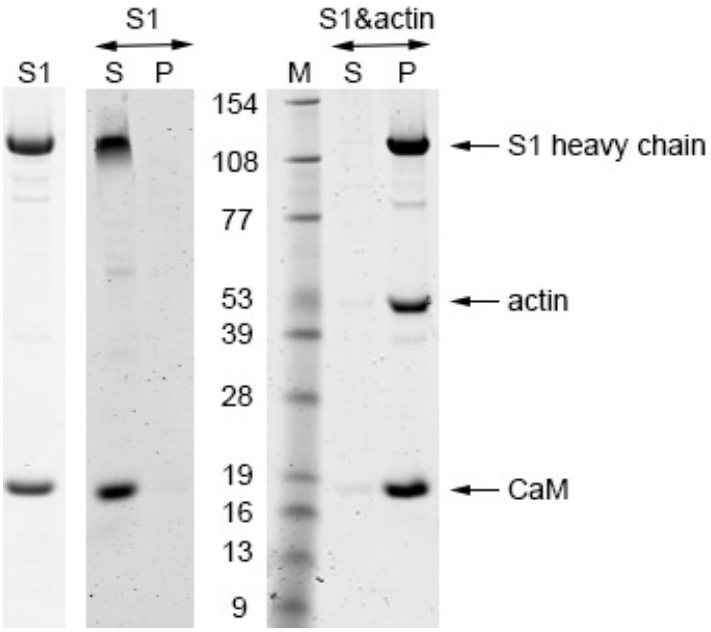

Figure 3.9. *Coomassie-stained SDS gels showing myosin-5 S1 with bound calmodulins and the result of centrifugation of myosin-5 S1 alone and myosin-5 S1 with actin. Myosin-5 S1 only sediments in the presence of actin. Lanes are the following. M: BenchMark pre-stained protein ladder, numbers denote molecular mass in kDa corresponding to the bands of the lane. P: pellet after centrifugation. S: supernatant after centrifugation. Samples were diluted in 2x Laemlli buffer and 15 µl mixture was loaded in each well. Arrows point out actin, the heavy chain of S1 and the calmodulin light chain.*

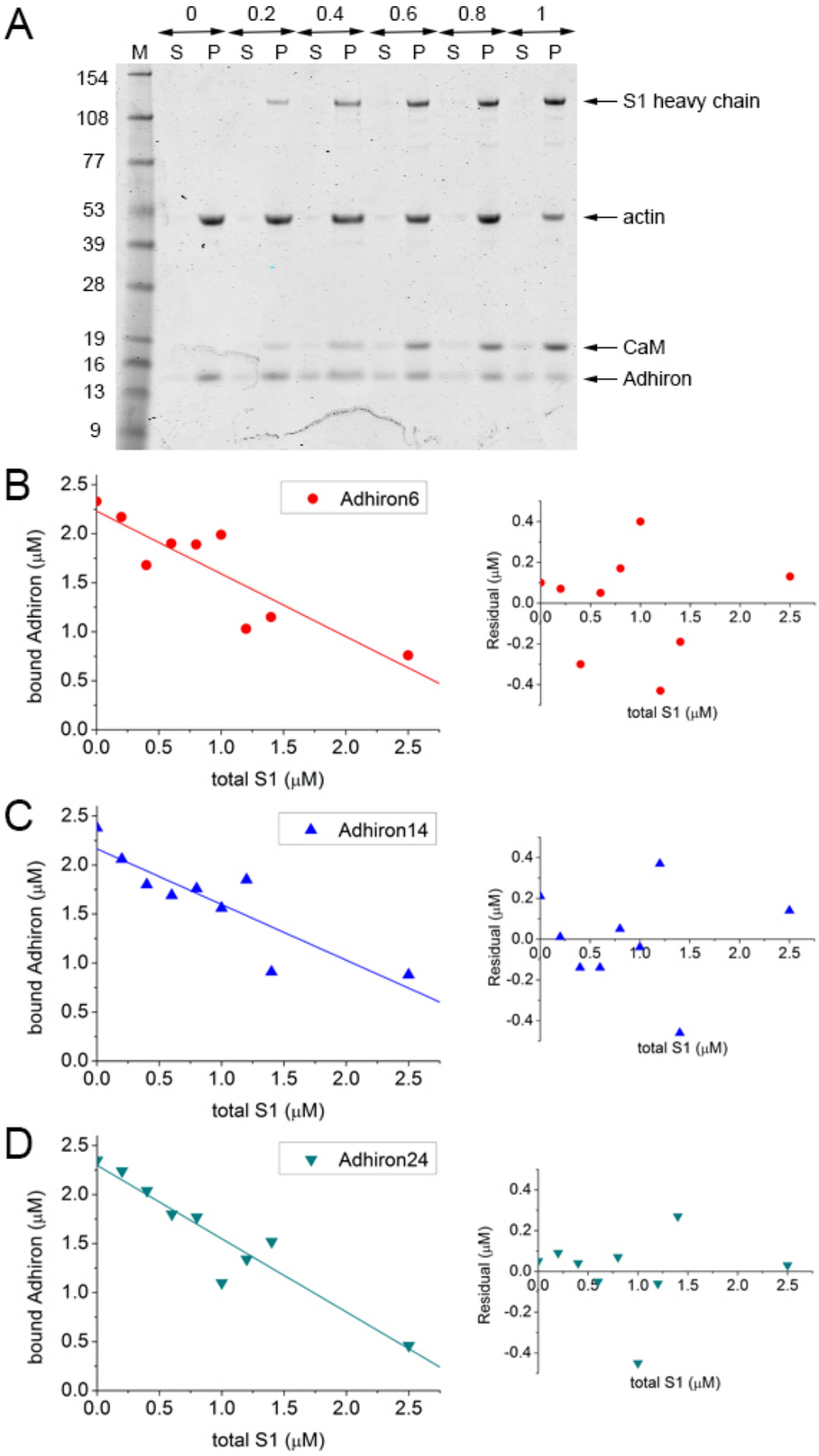
A
0
0.2
0.4
0.6
0.8
1
M S P S P S P S P S P S P
154
108
77
53
39
28
19
16
13
9
S1 heavy chain
actin
CaM
Adhiron
B
Adhiron6
bound Adhiron (μM)
total S1 (μM)
Residual (μM)
C
Adhiron14
D
Adhiron24

Figure 3.10. *SDS gel of a single experiment for the Adhiron6-S1 competition spin down assay and result of all of the experiments. A) Coomassie-stained SDS gel of the result of a single experiment for the Adhiron6-S1 competition spin down assay. 2.5 μM actin was mixed with 2.5 μM Adhiron and increasing concentrations of S1 (0-1 μM). Lanes are the following. M: BenchMark pre-stained protein ladder, numbers denote molecular mass in kDa corresponding to the bands of the lane. P: pellet after centrifugation. S: supernatant after centrifugation. Numbers above S and P denote concentration of S1 in that data point. Samples were diluted in 2x Laemlli buffer and 15 μl mixture was loaded in each well. Arrows point out the heavy chain of S1, calmodulin light chain, actin and Adhiron. B) Data points measured with Adhiron6 (B), Adhiron14 (C) and Adhiron24 (D) were plotted against total S1 concentration. Only one set of experiments were carried out due to a limited supply of myosin-5 S1. The data points were fitted with a linear function. Deviations from the fit are also shown for each Adhiron.*

3.1.6 Effect of the Adhirons on ATPase activity

If Adhirons bind to the same site on actin as the motor domain of myosin their binding may inhibit myosin actin-activated ATPase activity. To test this, the actin-activated ATPase activity of myosin-5 S1 was measured at increasing concentrations of Adhirons. The data shows that the ATPase activity of myosin-5 S1 decreases upon addition of Adhiron6, 14 and 24 reducing to zero at equimolar concentration of actin and Adhiron (Figure 3.11). However, Adhiron2 has no effect on the ATPase activity over this concentration range suggesting that Adhiron2 does not bind to the same binding site on actin as the other three Adhirons.

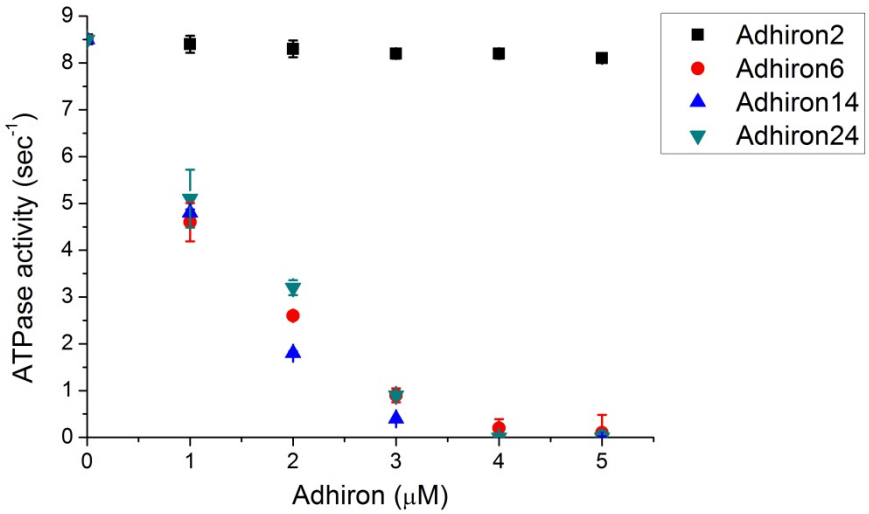

Figure 3.11. *Results of the ATPase activity assay as a function of Adhiron concentration. 30 nM myosin-5a S1, 4 μM F-actin and 1-5 μM Adhirons were mixed and ATPase activity was measured. Data show the mean values and standard deviation for three measurements.*

3.1.7 Using Adhirons to bind F-actin to coverslips

As these Adhirons display binding to actin, they could potentially be used to attach actin to a coverslip for the TIRF single molecule *in-vitro* motility assay. As described above in section 1.4.3, the present methods to attach actin to the coverslip, involving biotinylated actin or NEM-treated myosin, have their drawbacks. Therefore Adhirons could yield an alternative, label-free way to attach actin to the surface.

All four Adhirons were tested for their ability to bind F-actin to coverslips in *in-vitro* motility assays. After attaching the filaments, myosin-5 was also added to the flow chamber to test if Adhirons binding to actin interfere with single molecule myosin-5 translocation.

A concentration of 5 µM Adhiron firmly attached F-actin (50 nM) to the coverslip, and this was the case for all four Adhirons (Figure 3.12). A lower concentration of 0.5 µM Adhiron was however not sufficient to firmly attach the actin filaments as they were observed to be wiggling when imaged. Actin filaments that were attached to the coverslip surface by Adhiron2 appear shorter, than the actin filaments that were attached to the coverslip surface by either Adhiron6 or 14 and 24 (Figure 3.12). Alterations in the flow chamber, e.g. different flow speed or imaging the slide at the edge could result in the observed differences that are not due to the different nature of the binding proteins.

Next, the ability of Myosin-5-Avi (described in section 1.3.5) to move along F-actin was investigated. GFP-tagged myosin-5-Avi was able to move along F-actin only when Adhiron2 was used to attach F-actin to the surface. Myosin-5-Avi had a characteristic run length of 1.05 ± 0.72 µm (mean ± s.d.) (Figure 3.13A) and the particles were observed to move with a velocity of 0.59 µm/sec (Figure 3.13B).

Interestingly, a large number of immobile Myosin-5-Avi molecules were observed to be not co-localised with actin (Figure 3.12). These particles could possibly bind either to the surface of the coverslip or to the Adhirons, even though Adhirons were raised to bind actin.

No myosin-5 movement was detected when F-actin was bound to the surface with either Adhiron6, 14 or 24, whereas 59 motile events were observed when Adhiron2 was used. This could be due to the detachment of Adhirons from the surface, and rebinding to F-actin at sites that block movement of myosin-5a. Adhiron2 does not bind as tight as the other three Adhirons and it might also have a different binding site compared to that of the myosin motor domain, thus no inhibition effect is

apparent in this case.To try to overcome this problem, anti-His antibodies were first applied to the surface, followed by the Adhirons. This should ensure a more effective binding of Adhirons to the surface via the antibody, which should bind to the Adhirons through their C-terminal His-tag. Adhiron14 and 24 were both tested using this approach. However, while this promoted the binding of F-actin, myosin-5 movement was still not detected. Most probably Adhirons still attach to the coverslip surface as they attached to it without the antibodies and then got washed off and reattached to actin.

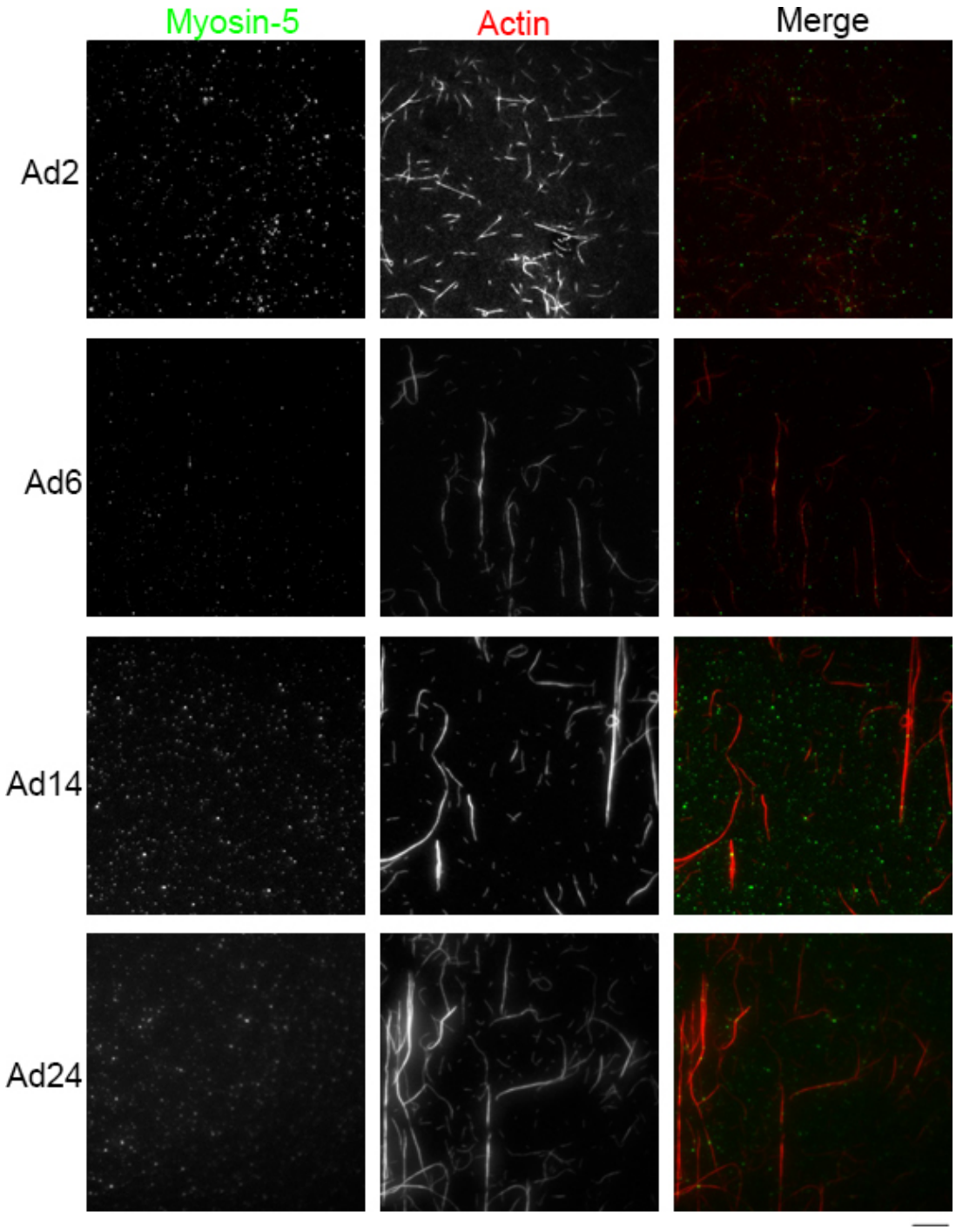

Figure 3.12. *TIRF microscope images of F-actin attached to the surface using Adhirons. Each row shows slides, where one Adhiron (Ad) was used to attach F-actin onto nitrocellulose coated coverslips and Myosin-5-Avi was also added to the flow chamber. GFP-tagged myosin-5 fluorescence and Alexa 647 phalloidin labelled F-actin fluorescence are shown in each row, together with the merged image in colour. In the merged image, myosin-5 is shown in green and F-actin is shown in red. Scale bar is 10 µm.*

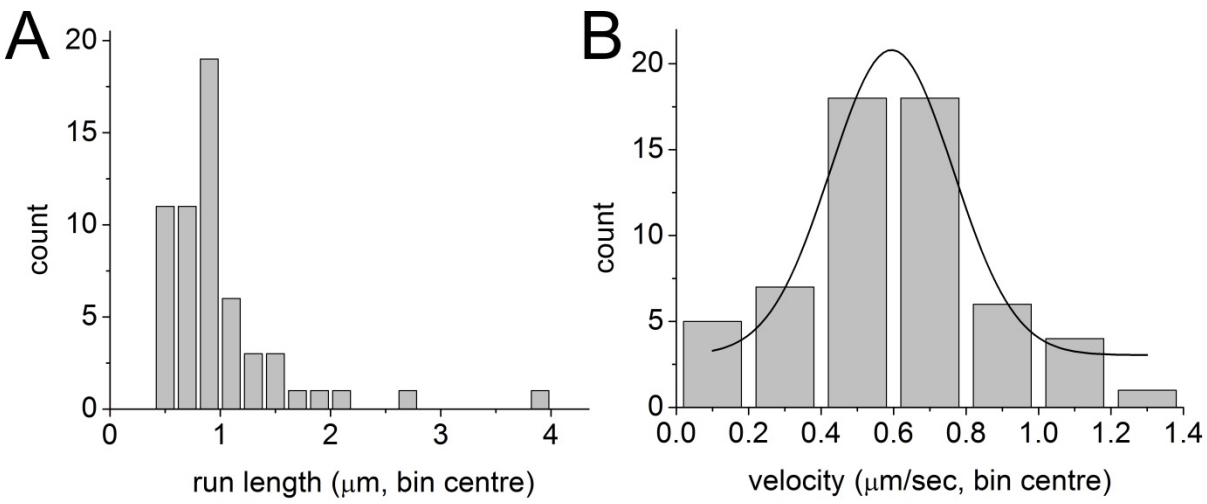

Figure 3.13. *Run length (A) and velocity (B) distribution of Myo5-Avi on actin, when actin was fixed to the coverslip using Adhiron2. Run length distribution could not be fitted with a first order exponential decay function, therefore mean and standard deviation were calculated, yielding characteristic run length of 1.05 ± 0.72 μm. Velocity distribution was fitted with a Gaussian function, yielding average speed of 0.59 ± 0.02 μm/sec, where numbers represent mean of the fitting and confidence values. Numbers of the observed molecules were 59.*

3.1.8 Actin imaging in cells transfected with Adhirons

GFP-tagged Adhiron constructs were cloned into a mammalian expression vector and HeLa cells were transfected. After incubation, they were fixed and co-stained with fluorescent phalloidin, which serves as an actin binding control. GFP is at the N-terminus of the Adhirons, whereas the target binding loops are in the middle of the molecule. Therefore change in the affinity of the Adhirons to actin is not expected when GFP-Adhirons are used.

In four separate experiments 59, 85, 92 and 102 cells were imaged for Adhiron2, 6, 14 and 24, respectively. GFP-Adhiron6, 14 and 24 localised to F-actin based structures, when expressed in the cells, whereas Adhiron2 did not (Figure 3.14). GFP-Adhiron6 and 14 both showed good co-localisation with F-actin structures that stained positively with fluorescent phalloidin. Analysis of the images using ImageJ showed that GFP-Adhiron6 and 14 exhibit 80% and 82% co-localisation with phalloidin, respectively. Adhiron6 additionally appeared to localise to vesicular structures, which were also co-stained for actin with fluorescent phalloidin. Adhiron24 showed a discrete localisation at the ends of actin bundles in structures that resemble focal adhesion. As this is only a small fraction of the phalloidin stained actin structures, Adhiron24 exhibits only 13% co-localisation with phalloidin. These differences in the observed localisation for GFP-Adhirons may reflect differences in their binding properties.

Co-staining of the GFP-Adhiron expressing cells with fluorescent phalloidin, allows the assessment of the overall F-actin organisation, and whether it is disturbed by expressing the GFP-Adhirons. There did not appear to be any clear differences in actin organisation in GFP-Adhiron expressing cells, compared to adjacent non-transfected cells. However, it is also possible that the GFP-Adhirons do have minor effects on the organisation of F-actin.

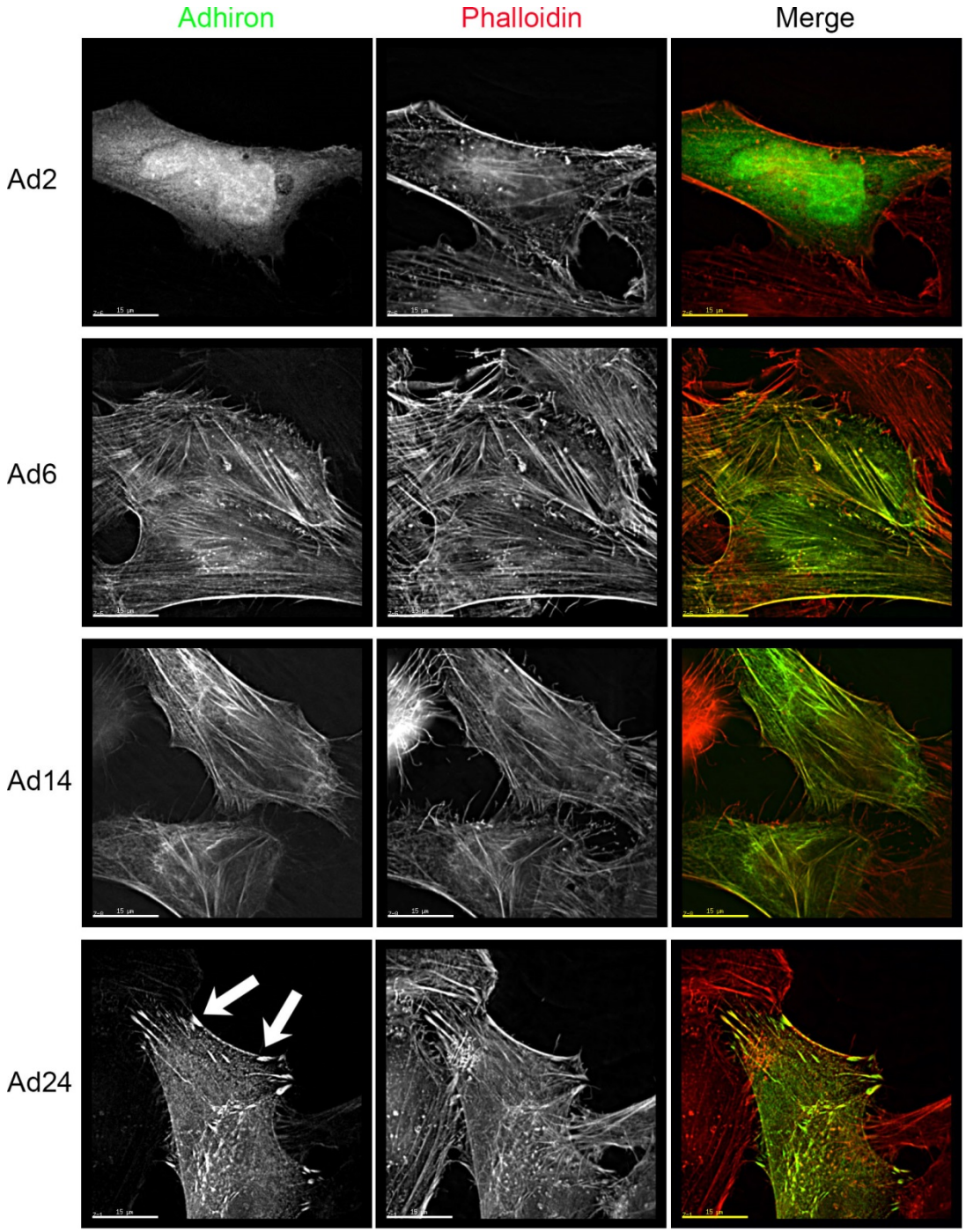

Figure 3.14. *Fluorescent images of HeLa cells transfected with GFP-tagged Adhirons. Each row shows HeLa cells that were transfected with one GFP-tagged Adhiron (Ad). GFP-Adhiron fluorescence and the staining for F-actin (using Alexa 546 phalloidin) are shown in each row, together with the merged image in colour. In the merged image, Adhiron staining is shown in green and phalloidin staining is shown in red. Arrows point to putative focal adhesions stained by Adhiron24. Images were taken using the DeltaVision deconvolution microscope. Scale bar is 15 µm.*

3.1.9 Actin imaging in fixed cells using Adhirons

Finally, we tested if any of the Adhirons were able to localise to F-actin in fixed cells, using biotinylated Adhirons and fluorescent streptavidin. Cells were co-stained with fluorescent phalloidin, to visualise the F-actin organisation.

In two separate experiments 37, 14, 24 and 15 cells were imaged for Adhiron2, 6, 14 and 24, respectively. In these experiments only Adhiron14 was able to label F-actin in HeLa cells (Figure 3.15) and it showed a similar staining pattern with 86% co-localisation to fluorescent phalloidin. Adhiron2, 6 and 24 did not localise to F-actin. In the example shown here, Adhiron6 appeared to show weak F-actin binding, and appeared to be localised to a membrane ruffle (arrows, Figure 3.15).

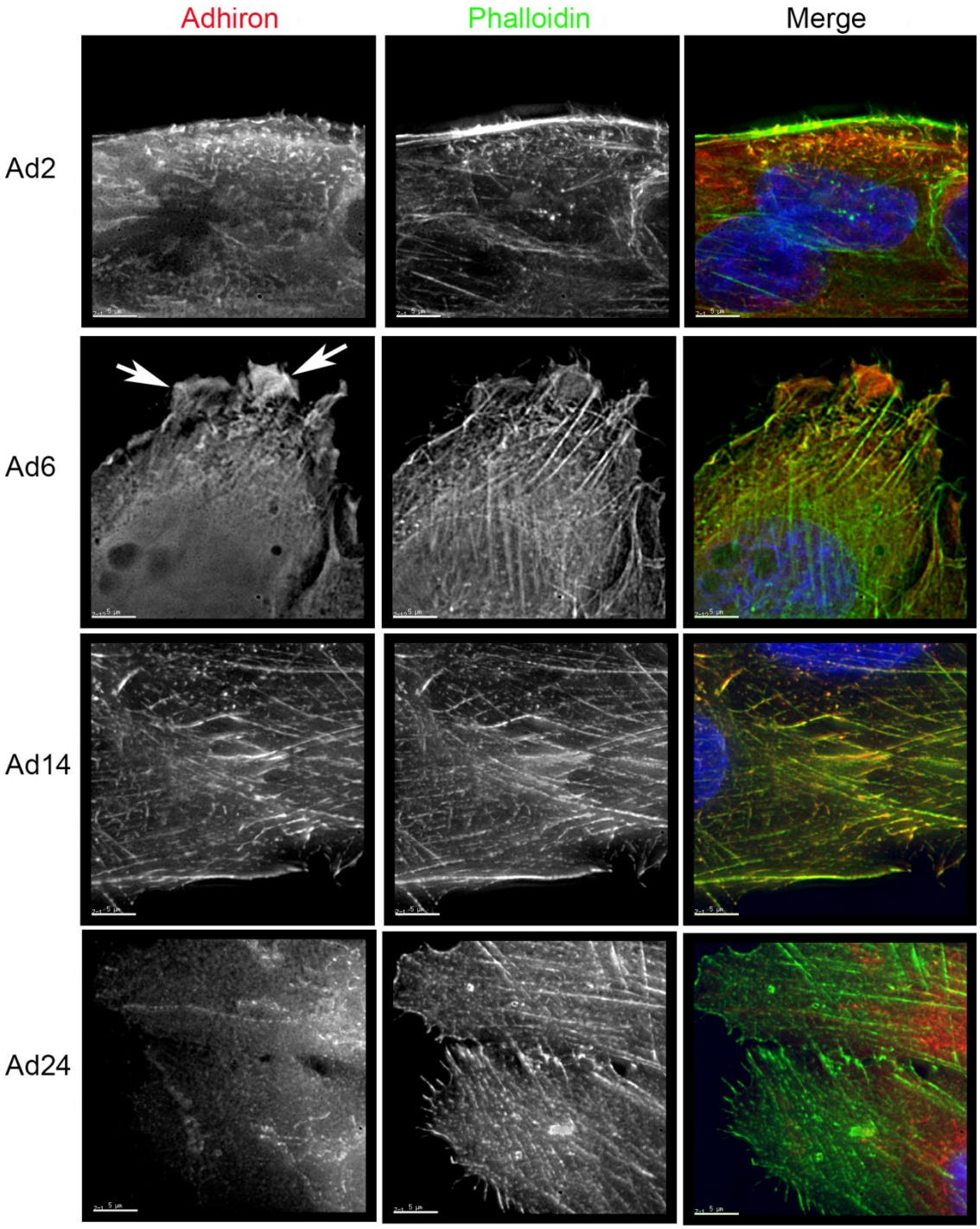

Figure 3.15. *Fluorescent images of non-transfected HeLa cells stained with Adhirons and phalloidin. Each row shows HeLa cells stained with one fluorescent Adhiron (Ad). Biotinylated Adhiron staining (using Alexa 647 streptavidin) and staining for F-actin (using Alexa 488 phalloidin) are shown in each row, together with the merged image in colour. In the merged image, Adhiron staining is shown in red, phalloidin staining is shown in green and DAPI staining is shown in blue. Arrows point to membrane ruffle stained by Adhiron6. Images were taken using the DeltaVision deconvolution microscope. Scale bar is 5 µm.*

3.2 Discussion

Four potential actin-binding molecules were raised with phage display assay, named Adhiron2, 6, 14 and 24. These proteins are small and share the same core structure; they only differ in their two, 9 residues long variable loops. Adhiron6, 14 and 24 showed submicromolar dissociation constant to actin and additional experiments suggest that they may share the same binding site with the myosin motor domain, as all three of these Adhirons inhibited myosin's actin-activated ATPase activity. Adhiron2 showed much weaker binding to F-actin, and did not inhibit the ATPase activity. Adhiron2 was the only Adhiron that both bound F-actin to the coverslip surface, and allowed myosin-5 to walk along it in *in-vitro* motility TIRF assays. Adhiron14 stained F-actin in fixed, non-transfected HeLa cells. In contrast, GFP-Adhiron6, 14 and 24 all bind to actin when expressed in HeLa cells, with each Adhiron showing a different localisation pattern.

Adhiron6, 14 and 24 showed tight binding to actin and may share the same binding site with the myosin motor domain. One possible explanation is that these actin-binding Adhirons occupy the potential binding sites on actin and therefore the weak initial binding of S1.ADP.P_i complex is inhibited and it cannot progress to P_i release. Even though Adhirons were raised to bind to actin, it cannot be ruled out that they bind non-specifically to the myosin motor domain, and therefore prevent either binding of ATP or binding of the myosin head to actin. This hypothesis however is challenging to be tested using ATPase activity assays, as myosin-5a S1 exhibits a low ATPase activity in the absence of actin (0.2 sec^{-1}). Moreover, some experiments made by other groups at the University of Leeds using other, non-actin binding Adhirons suggest that Adhirons dimerise (Dr. Christian Tiede, personal communication). If these actin-binding Adhirons dimerise too, they could potentially bundle actin. If actin filaments are tightly bundled, binding sites for the myosin head sterically will not be available.

There is an apparent contradiction in the S1-Adhiron competition spin down assay and in the actin-activated ATPase assay results as S1 displaced Adhirons off actin in the spin down assay, whereas Adhirons inhibited the actin-activated ATPase activity of S1. A possible explanation is that S1 has a very high affinity to actin in the absence of ATP (i.e. spin down assay conditions), whereas in the presence of the nucleotide S1 has a lower affinity to actin (i.e. ATPase assay conditions). Further

competition spin down assays, where ATP is also added to the mixture, could prove this explanation.

Adhiron2 could be useful as an alternative method for binding F-actin to coverslips in *in-vitro* motility assays, in which myosin is visualised as it is walking along actin using TIRF microscopy. Adhiron2 could serve as a label-free actin attaching method that can be produced easily, thus it has advantages over both of the currently used methods involving biotinylation or NEM-myosin. It is unclear why Adhiron6, 14 and 24 inhibit the movement of myosin-5 in TIRF assays, when they are applied to bind F-actin to the surface. It is possible that even though Adhirons are attached to the surface of the coverslip, they are washed off during the wash steps. After detaching from the surface, they might rebind elsewhere to F-actin and therefore block myosin-5 binding and movement. While Adhiron2 binds less tightly to F-actin compared to the other Adhirons it also does not appear to interfere with the actin-activated ATPase activity of myosin-5 in solution. Therefore, even if Adhiron2 is similarly washed away from the surface in this assay, and rebinds to F-actin, it would not be expected to inhibit myosin-5 motility.

Only Adhiron14 is useful for labelling F-actin in fixed cells, while GFP-Adhiron6, 14 and 24 showed some localisation to the F-actin cytoskeleton when expressed in HeLa cells, although with differences. Adhiron6 appeared to have the least effect on actin organisation, with fewer actin bundles observed in transfected cells, compared to 14 or 24. Adhiron24 appeared to be excluded from F-actin bundles, and localised strongly to structures resembling focal adhesions. This suggests that Adhirons, while apparently having similar effects on myosin-5 ATPase activity, exhibit differences in their actin binding characteristics in live cells.

Comparing Adhiron14 to previously described actin binding probes highlights the outstanding binding affinity of Adhiron14 to actin. Whereas F-tractin and Lifeact bind to F-actin with a K_d of ~2 µM (Schell et al., 2001; Riedl et al., 2008) and the CH domain of utrophin with a K_d of ~18 µM (Rybakova and Ervasti, 2005), Adhiron14 has a K_d of ~0.3 µM in binding to F-actin. Even though the affinity of the GFP-tagged Adhirons have not been measured so far, the higher affinity of Adhiron14 compared to other actin-binding probes could potentially result in better recognition and localisation to F-actin structures. However, localisation of an actin binding probe to actin in live cell depends also on the size of the probe and also on the spatial availability of the actin filaments and the presence of other actin binding proteins.

Higher affinity could potentially result in perturbing the actin assembly or it might prevent binding of other actin-binding molecules as it inhibited the actin-activated ATPase activity of myosin-5. Further experiments are needed using various cell lines to explore if Adhiron14 could serve as a general actin-binding probe.

4. Characterisation of recombinant myosin-5 constructs with actin-binding tail domains

4.1 Results

4.1.1 Myosin-5-Avi cloning

Myosin-5-Avi construct was cloned as described (section 2.4.1). Both digested pFastBac and the PCR product of the coding sequence for the first 1,440 amino acids of mouse myosin-5a brain isoform were run on an agarose gel to check the efficiency of both the digestion and the amplification. The estimated sizes of the PCR product and the digested vector are 4.3 kb and 5.5 kb, respectively. Agarose gel electrophoresis confirmed the sizes of the vector and PCR product (Figure 4.1A).

After ligation, an analysis of undigested plasmids purified from selected colonies, run on an agarose gel (Figure 4.1B) showed that only one out of ten colonies contained an insert. Subsequent sequencing verified that this plasmid has the correct sequence expected for Myo5-Avi (Supplementary Materials S2).

PCR analysis of a bacmid purified from a white colony, obtained from a transposition of the Myo5-Avi (section 2.4.6) showed that transposition had been successful (Figure 4.1C). The size of the band obtained by PCR using the M13 forward and reverse primers was ~7 kb, consistent with the expected size of 7.4 kb (5.1 kb for the inserted DNA, plus an additional 2.3 kb from the bacmid backbone). A control PCR on a bacmid purified from a blue colony, which is not expected to contain an insert, generated a smaller sized band (2.3 kb), as expected (Figure 4.1C).

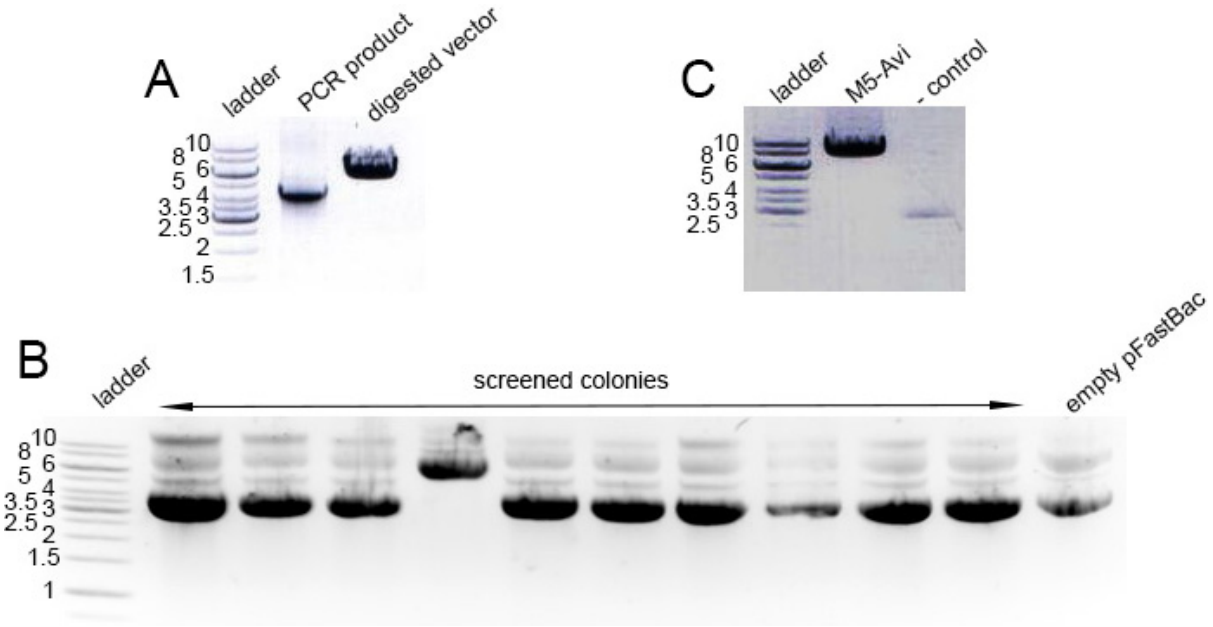

Figure 4.1. *Agarose gels showing the steps of Myo5-Avi cloning. Ladder lanes stand for GeneRuler 1 kb DNA ladder, numbers denote size in kb corresponding to the bands of the lane. A) Result of the PCR amplification and digestion of the donor vector. Lanes are the following. PCR product: of amplifying the coding sequence for the first 1,440 amino acids of mouse myosin 5a. Digested vector: pFastBac vector, containing also the coding sequence of eGFP, digested by Stu I. B) Plasmid samples purified from 10 colonies. Lanes are the following. Screened colonies: purified pFastBac plasmid from 10 randomly picked colonies, plasmid from colony No. 4 has a significantly larger size compared to the other plasmids. Empty pFastBac: donor vector that was used for the cloning. C) Result of the M13 PCR amplification. Lanes are the following. M5-Avi: PCR product from a bacmid that was purified from a white colony. –control: PCR product from a bacmid that was purified from a blue colony.*

4.1.2 Calmodulin baculovirus

Western blotting of *Sf9* cells infected with CaM baculovirus, together with control non-infected cells showed that CaM was successfully expressed from the new CaM virus (Figure 4.2). Anti-calmodulin antibody recognised a single band, with an approximate molecular weight of 17 kDa, in the cell lysate of infected cells, and in the positive control containing purified CaM protein. No band was detected for CaM in the lysate of control, uninfected cells.

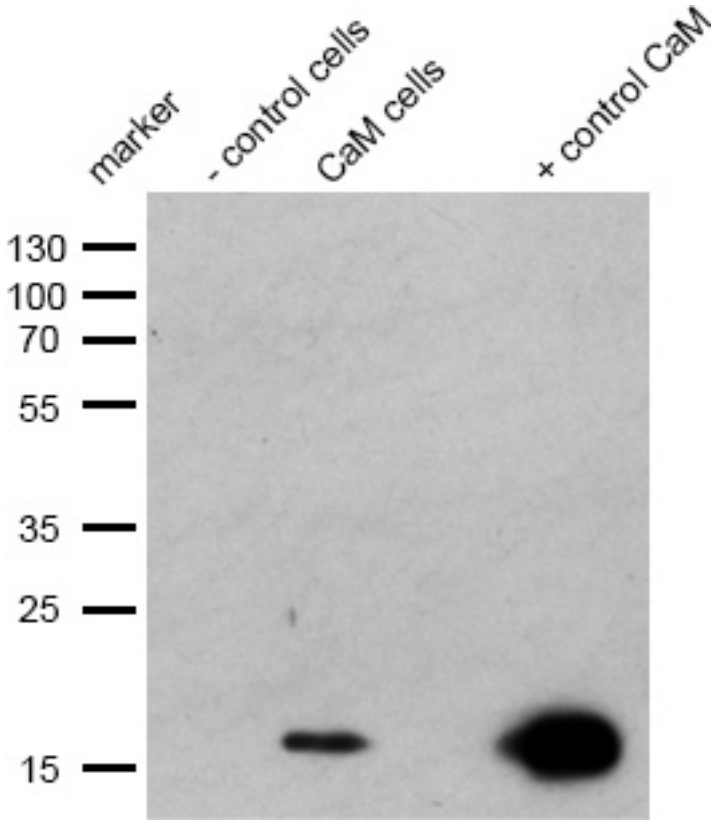

Figure 4.2. *Anti-calmodulin Western blot of Sf9 cell lysate infected with calmodulin baculovirus and appropriate controls. Lanes are the following. Marker: PageRuler Plus pre-stained protein ladder, numbers denote size in kDa corresponding to the bands of the lane. – control cells: cell lysate of non-infected Sf9 cells. CaM cells: cell lysate of Sf9 cells infected with calmodulin baculovirus. + control CaM: 5 µM purified calmodulin protein. 20 µl was loaded to the wells from all three samples.*

4.1.3 Myosin-5-Avi expression trials

Myosin-5-Avi was co-expressed with calmodulin light chain in *Sf9* insect cells and protein expression was followed by monitoring GFP fluorescence in *Sf9* cells using fluorescence microscopy. Cells were harvested after 2-3 days, when 70-80% of the cells showed GFP fluorescence. Cell pellets were extracted and myosin-5 was purified on a Flag affinity resin.

Myo5-Avi was successfully purified from the first protein expression trial run. A band of the expected molecular mass for Myo5-Avi was observed on an SDS-PAGE gel in each of the elution fractions (200 kDa; Figure 4.3A) together with a band of the expected size for calmodulin (17 kDa, Figure 4.3A). Two bands of the same size are also found in the purified, concentrated sample (Figure 4.3B). However, additional bands can also be observed.

The protein yield for this purification was relatively low. The average yield was 38 µg protein/litre of *Sf9* cells from 5 expression runs. This value was calculated from measurements of absorbance at 280 nm, using the extinction coefficient for the full length construct with 6 calmodulins (Table 2.10). The additional bands observed in the concentrated protein sample suggest that the real protein yield may be even lower.

Several expression and purification trials were carried out to improve the levels of expression and reduce the levels of additional bands, but without much success.

Six calmodulin light chains bind to the lever of myosin-5a and therefore it is important to have enough calmodulin baculovirus during expression. As calmodulin is smaller than myosin-5a, it is expressed faster and thus, usually an identical MOI of myosin and calmodulin baculoviruses ensures that enough calmodulin is expressed. However, the exact myosin:calmodulin molecular ratio could potentially be assessed by densitometry using purified calmodulin as calibration or by mass spectrometry.

I suspected that there could be an issue with the pFastBac plasmid used in cloning, as this DNA stock has been amplified, digested and cloned multiple times in the past it might have acquired mutations in the pFastBac backbone. Therefore I decided to re-clone the construct into a fresh pFastBac plasmid.

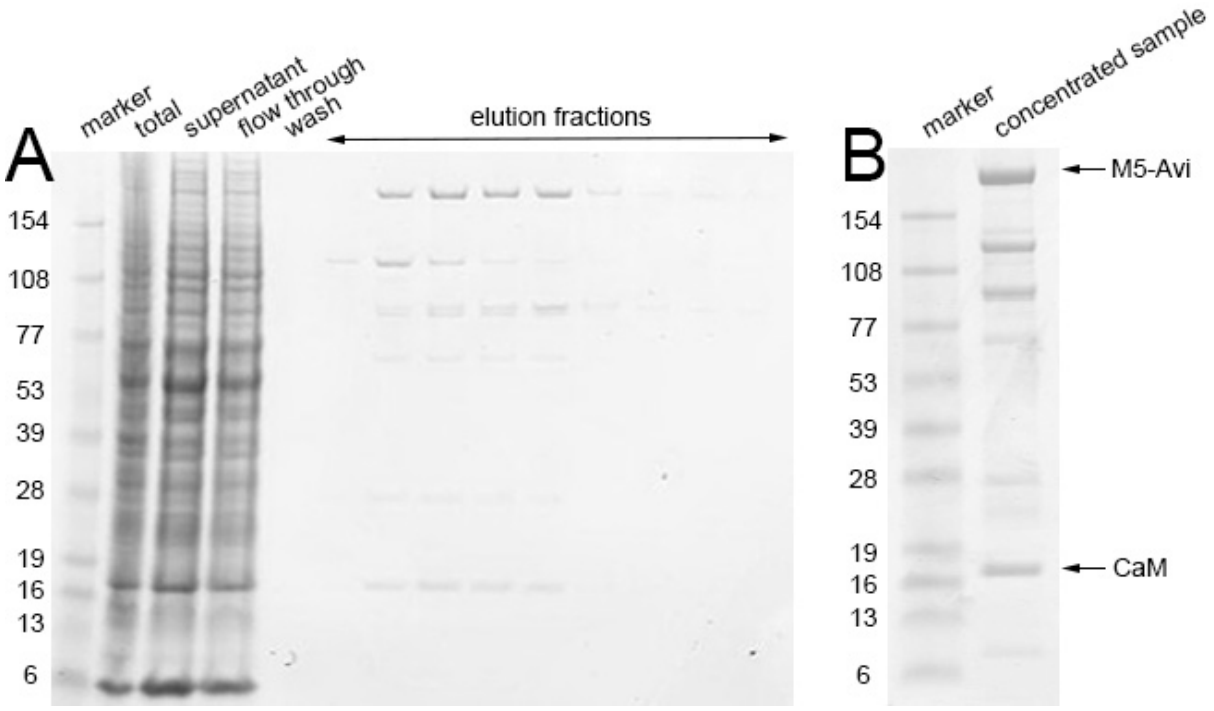

Figure 4.3. *Coomassie-stained SDS-PAGE gels of Myosin-5-Avi purification. A) SDS-PAGE gel shows the steps of Myosin-5-Avi purification. Lanes are the following. Marker: BenchMark pre-stained protein ladder, numbers denote molecular mass in kDa corresponding to the bands of the lane. Total: cell lysate taken after extraction and sonication of the cell pellet and before centrifugation. Supernatant: taken after centrifuging the cell lysate. Flow through: supernatant taken after incubation with Flag resin. Wash: supernatant taken after washing the Flag resin. Elution fractions: samples taken from each 1 ml elution fraction. B) SDS-PAGE gel of the concentrated eluted sample. Arrows point out the full length construct and the calmodulin light chain.*

4.1.4 Re-cloning the Myosin-5-Avi construct

To overcome the problem of the poor expression yield, the Myosin-5-Avi construct was re-cloned into a fresh pFastBac plasmid as described (section 2.4.2). The PCR product of the coding sequence for the 1,721 amino acids of the entire construct was run on an agarose gel to check the efficiency of the amplification, and the size of the DNA generated. The PCR product was ~5 kb, consistent with the expected size of 5.1 kb (Figure 4.4A).

After cloning the PCR product into the backbone vector, 4 out of 6 colonies picked showed an increased size when analysed by agarose gel electrophoresis, suggesting that the PCR product had been successfully cloned into each of these plasmids (Figure 4.4B). Sequencing verified that colonies No. 3 and 4 contained inserts with the correct sequence. Successful transposition for plasmid No. 4 was verified by PCR amplification (Figure 4.4C), as described before.

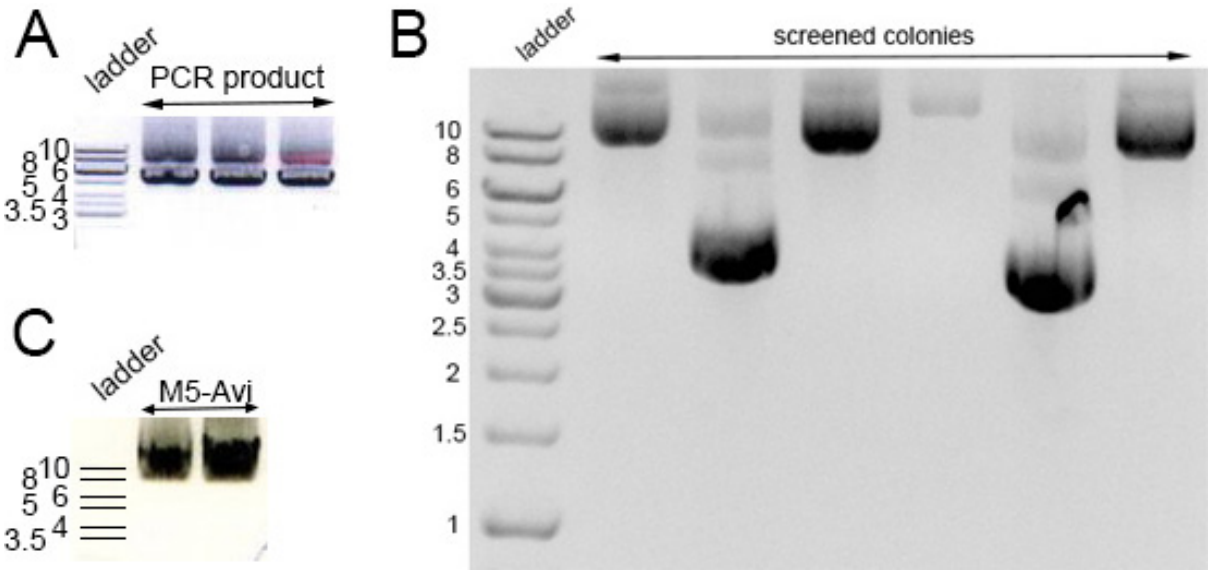

Figure 4.4. *Agarose gels showing the steps of Myo5-Avi re-cloning. Ladder lanes stand for GeneRuler 1 kb DNA ladder, numbers denote size in kb corresponding to the bands of the lane. A) Result of the PCR amplification. Lanes are the following. PCR product: of amplifying the 1,721 amino acids of the entire construct. B) Plasmid samples purified from 6 colonies. Lanes are the following. Screened colonies: purified pFastBac plasmid from 6 randomly picked colonies, plasmid from colonies No. 1, 3, 4 and 6 have a significantly larger size compared to the other plasmids. C) Result of the M13 PCR amplification. Lanes are the following. M5-Avi: PCR product from bacmids that were purified from white colonies.*

Expression using amplified virus from this new construct showed that higher levels of protein were produced than for the original construct (Figure 4.5A-B). The yields from two expression trials were 148 and 258 µg protein/litre of *Sf9* cells. As the purified protein contained additional bands, the actual protein yield for the full length protein is likely to be lower than 203 µg protein/litre of *Sf9* cells. In particular, there was a prominent band with an approximate size of 110 kDa. The protein preparation was purified on a Flag affinity column as it bears a Flag tag at the C-terminus, suggesting that this degraded construct had a cleavage at the motor domain and contains the coiled-coil tail.

Co-expression of chaperones as reported (Bird et al., 2014) with the Myosin-5-Avi improved the expression yield still further. Unc45b together with Hsp90 were co-expressed at MOI of 5 with Myosin-5-Avi and calmodulin and protein was purified on Flag resin (Figure 4.5C-D). The level of purified Myosin-5-Avi was significantly higher than in the previous expression trials with the yields of 3.36 and 3.78 mg protein/litre of *Sf9* cells from two expression runs.

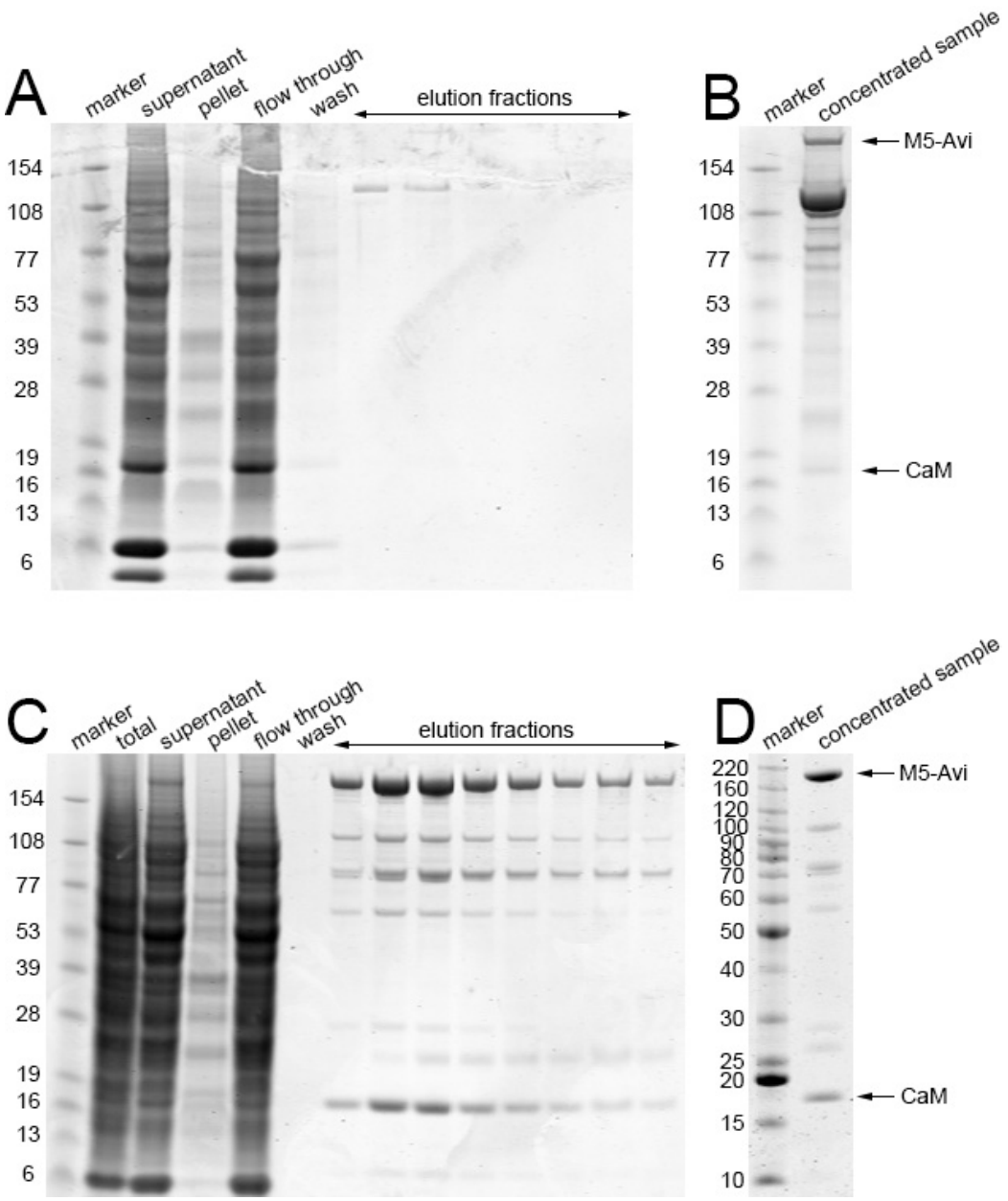

Figure 4.5. *Coomassie-stained SDS-PAGE gels showing the purification steps and concentrated eluted Myosin-5-Avi samples, that were expressed without (A and B) or with (C and D) Unc45b and Hsp90 chaperones. Lanes are the following. Marker: BenchMark pre-stained (A to C) and BenchMark unstained (D) protein ladders were used as marker, numbers denote size in kDa corresponding to the bands of the lanes. Total: cell lysate taken after extraction and sonication of the cell pellet and before centrifugation. Supernatant: taken after centrifuging the cell lysate. Pellet: taken after centrifuging the cell lysate and resuspending the pellet. Flow through: supernatant taken after incubation with Flag resin. Wash: supernatant taken after washing the Flag resin. Elution fractions: samples taken from each 1 ml elution fraction. Arrows indicate the full length construct and the calmodulin light chain.*

4.1.5 Identifying the additional bands in the Myosin-5-Avi preparation

While co-expressing chaperones with the myosin-5a construct markedly increased the yield, there were still additional bands on the SDS gel of the purified protein preparation. To identify these bands, Western blotting was performed using anti-GFP, anti-Myo5a and anti-Flag antibodies (Figure 4.6). The anti-Myo5a antibody was raised against the amino acids 981-1070 of the human myosin-5a, which correspond to the same residue number in mouse myosin-5a, which is located at the first coiled-coil section of the tail.

The band with a molecular weight of approximately 200 kDa was recognised by all the antibodies, suggesting that this band is the full length construct as GFP is at the N-terminus, the Flag tag is at the C-terminus and the anti-Myo5a antibody recognises a region in the middle of the protein.

The anti-Myo5a antibody also recognised a band with a molecular weight of ~90 kDa. This band was apparently not recognised by either the anti-GFP or anti-Flag antibody. However, the band for the full length construct on the anti-GFP blot was faint, and given the lower intensity of this band on the SDS gel, its levels may have been too low to have been detected by the anti-GFP antibody. The lack of reactivity with the anti-Flag antibody suggests that this band may contain a degraded construct that does not contain GFP, nor part of the tail, including the Flag tag.

The third prominent band of approximately 70 kDa was only recognised by the anti-Flag antibody, suggesting this degraded protein no longer contains GFP, or the epitope recognised by the anti-Myo5a antibody (e.g. residues up to aa1070, wild type numbering). However, its size is larger than expected if this were the case.

Two more bands approximately 55 and 30 kDa were recognised by the anti-Flag antibody that could correspond to tail fragments having cleavage at the first coiled-coil section or at the distal section, respectively. This also suggests that the 55 kDa protein could have been recognised by the anti-Myo5a antibody too. However that blot is also faint and according to the SDS gel, the intensity of this band is much lower compared to the full-length construct, thus this band could have been recognised by the anti-Myo5a antibody, but is not visible on the blot.

Note that the 198 and 98 kDa markers run slower on both the SDS gel and the blot (Figure 4.6) compared to the heavy chain of myosin-5 and to the first additional band seen on the gel that were identified to be approximately 200 and 110 kDa in the previous gels (Figure 4.5), respectively. In this case SeeBlue Plus2 protein ladder

was used that was expected to run at the appropriate speed. Reason for this anomaly is not known, however this means that exact size of the bands seen in the myosin-5 sample are uncertain.

In summary the additional bands seen on the expression gels (Figure 4.6) are most probably degradation products of the Myosin-5-Avi construct, however results of the Western blots are inconclusive.

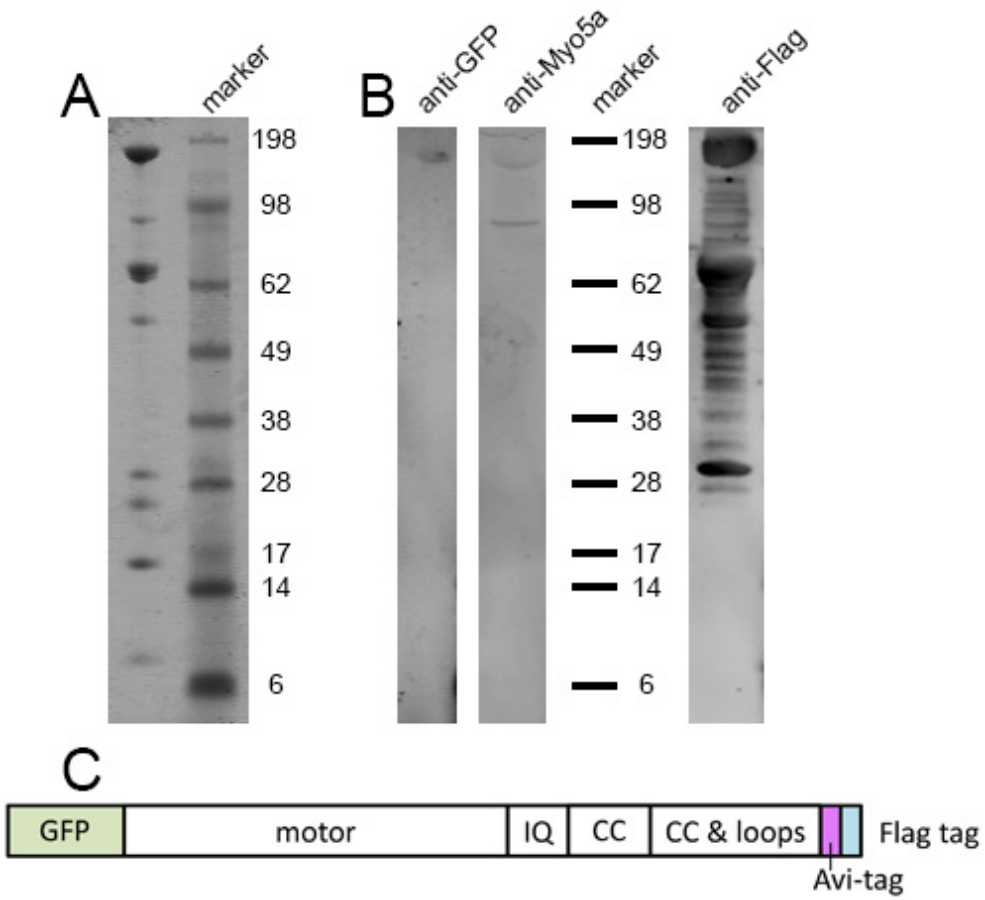

Figure 4.6. *Coomassie-stained SDS gel (A) and Western blots (B) showing the Myosin-5-Avi protein preparation. Marker lane shows SeeBlue Plus2 pre-stained protein ladder, numbers denote size in kDa corresponding to the bands of the lane. Equal volumes of Myosin-5-Avi were loaded to all wells. C) Schematic representation of Myosin-5-Avi. Labelling is the following. GFP: enhanced GFP; Motor: motor domain of myosin-5a; IQ: lever with the 6 IQ motifs; CC: 175 amino acids long coiled-coil; CC & loops: 350 amino acids long tail domain that contains predicted coiled-coil and loops.*

4.1.6 Myosin-5-cc cloning

Myosin-5-cc construct was cloned as described in section 2.4.3. Both digested pFastBac containing the Myosin-5-Avi sequence and the PCR product of the coding sequence for the 175 amino acids of coiled-coil were run on an agarose gel to check the efficiency of both the digestion and the amplification. Estimated size of the digested vector and the PCR product are 9.8 kb and 0.5 kb, respectively, which are verified by the result of the agarose gel electrophoresis (Figure 4.7A).

Gel purified PCR product and digested vector were ligated using the GeneArt® Seamless cloning method, and then transformed into competent cells. Colonies were picked and colony PCR was performed, then PCR products were run on agarose gel to check for plasmids containing the coiled-coil insert (Figure 4.7B). The PCR product was expected to be 1,300 bp for the negative control (i.e. Myosin-5-Avi) and 1,800 bp if a colony contains the insert. Colonies No. 2, 3, 5, 6, 9, 12 and 14 seemed to contain the insert. Sequencing confirmed that colony No. 14 indeed has the correct sequence.

Bacmid DNA was generated as described in section 2.4.5. The pFastBac plasmid isolated from colony No. 14 was transposed into the bacmid and transposition was verified by PCR amplification using M13 primers as described in section 2.4.6. Bacmid was isolated from a white colony and PCR was run (Figure 4.7C). PCR product of this myosin-5 construct is expected to be 8 kb (5.7 kb for the construct, plus additional 2.3 kb from the bacmid backbone). Agarose gel verifies that the bacmid contains the insert of the expected size.

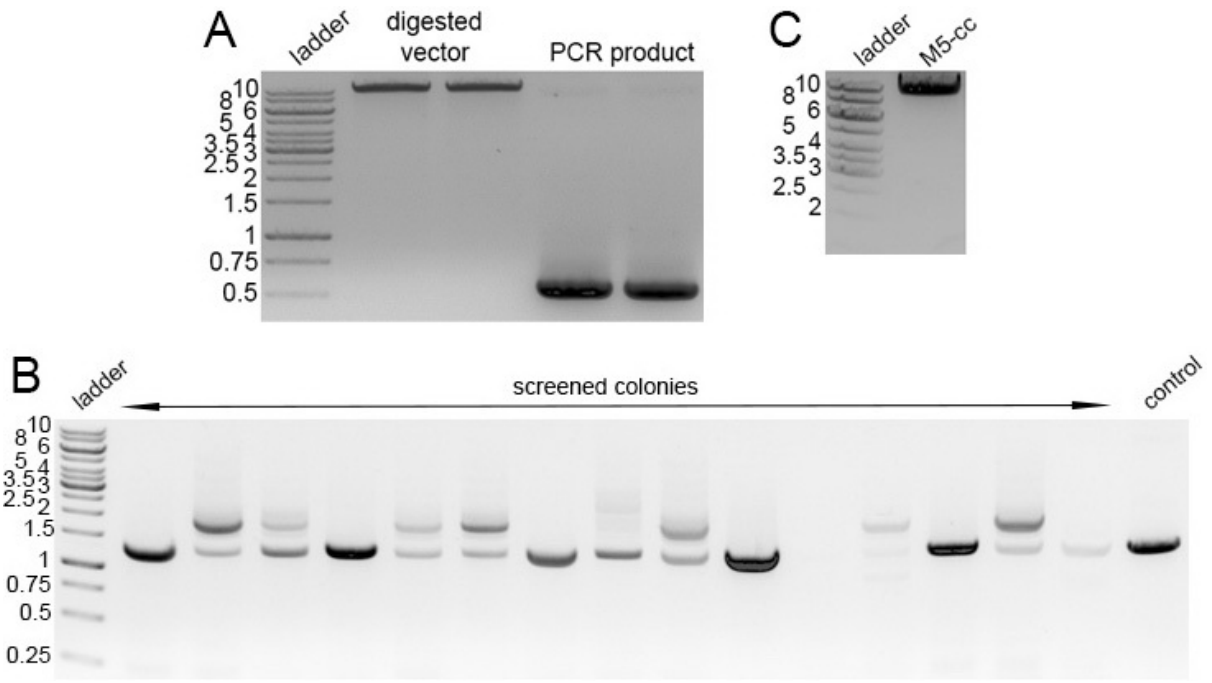

Figure 4.7. *Agarose gels showing the steps of Myo5-cc cloning. Ladder lanes stand for GeneRuler 1 kb DNA ladder, numbers denote size in kb corresponding to the bands of the lane. A) Result of the digestion of the donor vector and the PCR amplification. Lanes are the following. Digested vector: pFastBac vector, containing the Myosin-5-Avi sequence digested by Afe I. PCR product: of amplifying the coding sequence for 175 amino acids of coiled-coil. B) Colony PCR results from 15 colonies. Lanes are the following. Screened colonies: PCR product from 15 randomly picked colonies. Control: PCR product from Myosin-5-Avi construct. PCR product from colonies No. 2, 3, 5, 6, 9, 12 and 14 are larger compared to the control PCR product. C) Result of the M13 PCR amplification. Lanes are the following. M5-cc: PCR product from a bacmid that was purified from a white colony.*

4.1.7 Myosin-5-cc expression trial

SDS-PAGE gels of the purification steps and of the concentrated protein show multiple bands, but a band corresponding to the full length Myosin-5-cc construct is not visible (Figure 4.8). The concentration of protein in the purified sample was 85 µg protein/litre of *Sf9* cells, which was only calculated as estimation, using the extinction coefficient of the full length construct (Table 2.10).

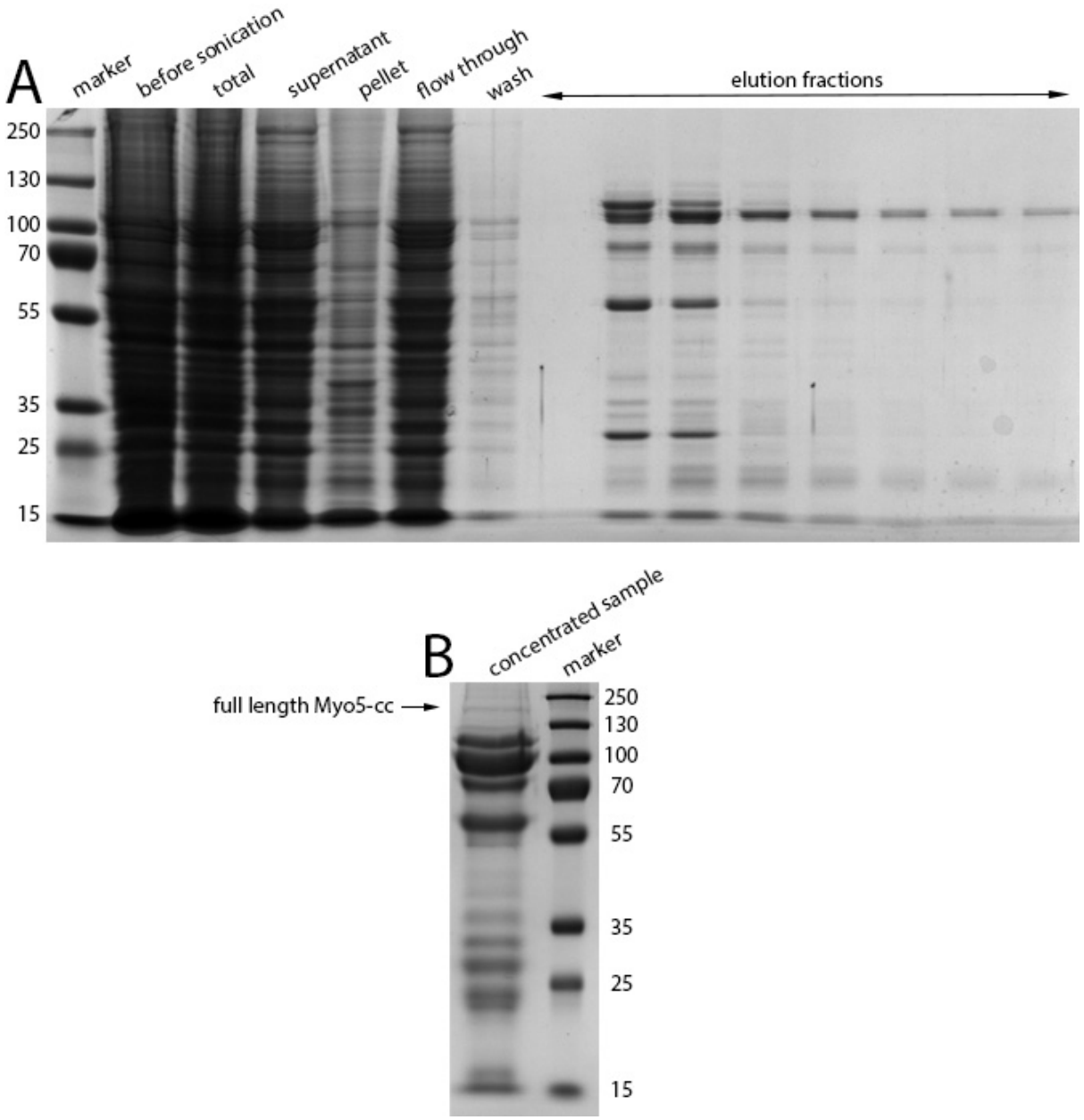

Figure 4.8. *Coomassie-stained SDS-PAGE gels of Myosin-5-cc purification. A) SDS-PAGE gel shows the steps of Myosin-5-cc purification. Lanes are the following. Marker: PageRuler Plus pre-stained protein ladder, numbers denote molecular mass in kDa corresponding to the bands of the lane. Before sonication: cell lysate taken after extraction and before sonication of the cell pellet. Total: cell lysate taken after sonication of the cell pellet and before centrifugation. Supernatant: taken after centrifuging the cell lysate. Flow through: supernatant taken after incubation with Flag resin. Wash: supernatant taken after washing the Flag resin. Elution fractions: samples taken from each 1 ml elution fraction. B) SDS-PAGE gel of the concentrated eluted sample.*

4.1.8 Identifying the bands in the Myosin-5-cc expression

The full length construct was not visible on the purification gel of Myosin-5-cc, however there are multiple bands approximately 60, 80, 100 and 110 kDa (Figure 4.8). Western blotting was performed using anti-GFP, anti-Myo5a and anti-Flag antibodies to identify these bands (Figure 4.9).

The highest molecular weight band on the anti-GFP blot is approximately 140 kDa. GFP is at the N-terminus of the protein, but the affinity tag, according to which the purification was carried out, is at the C-terminus. This protein fragment was purified on a Flag affinity column, therefore it could correspond to a protein that is full length in native conditions, but has a cleavage at the proximal part of the coiled-coil and thus, in the denaturing SDS-PAGE conditions it appears as a 140 kDa fragment.

The second highest molecular weight band is approximately 100 kDa and is visible on both the anti-Myo5a and the anti-Flag blots. This corresponds to a degraded C-terminal protein that was cleaved at the lever.

There are bands on all 3 blots approximately 80 kDa molecular weight, that could not all correspond to the same protein, as that would be the full length construct with 220 kDa size. The 80 kDa band seen on the anti-GFP blot could be an N-terminal protein that was cleaved at the motor domain. The 80 kDa protein that is seen on the anti-Myo5a and anti-Flag blots could be an N-terminal protein fragment that had a cleavage at the proximal part of the coiled-coil. It is possible that this fragment is paired with the 140 kDa fragment seen on the anti-GFP blot in native conditions.

There are more bands on the anti-GFP blot with ~70, ~50 and ~40 kDa size. That could all arise from cleavages within the motor domain. These proteins made it through the Flag-resin, therefore they could be full length protein in native conditions, but have cleavages various sites at the motor.

There are ~50 and ~20 kDa molecular weight bands on the anti-Myo5a blot. These could be fragments that had cleavage both at the lever and at the distal part of the coiled-coil tail.

There are ~60 and ~25 kDa molecular weight bands on the anti-Flag blot, that could correspond to N-terminal fragment that had cleavage at the doubled coiled-coil part (that is in the middle) or at the distal coiled-coil part.

In summary, Western blotting identified the bands seen on the purification SDS gel of Myosin-5-cc. This prep was heavily degraded and the full length construct was not

visible. Expression optimisation is needed to get the full length Myosin-5-cc construct.

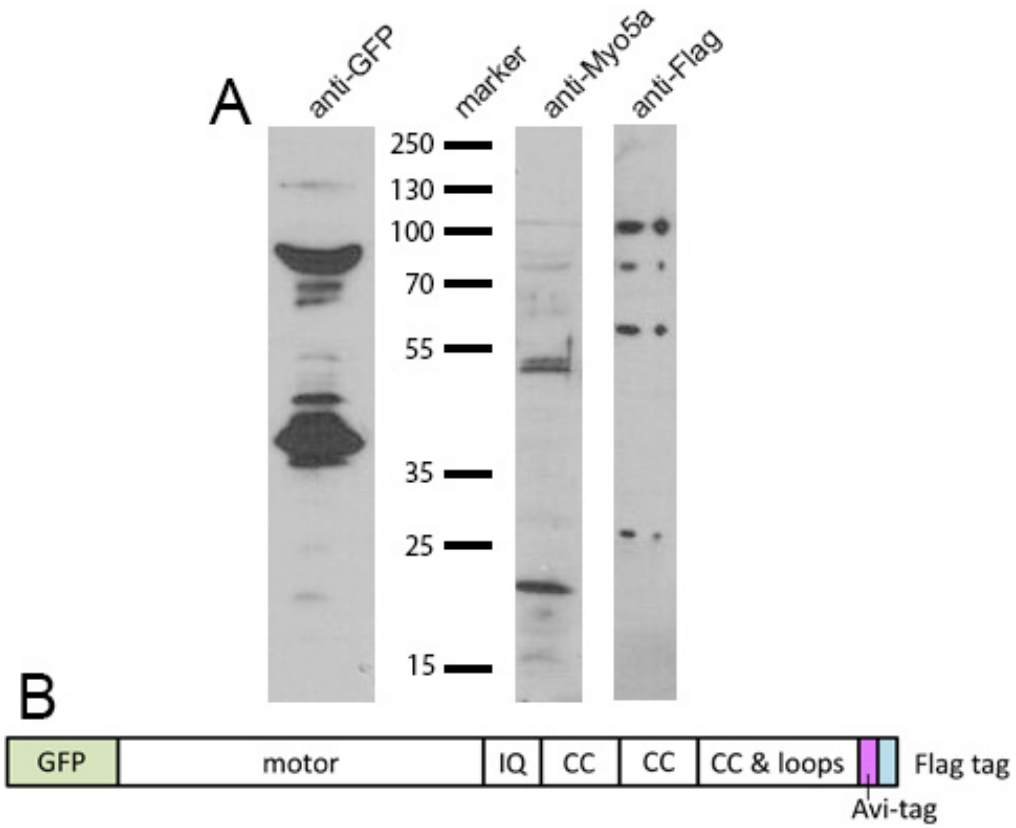

Figure 4.9. *A) Western blots showing the Myosin-5-cc protein preparation. Marker lane shows PageRuler Plus pre-stained protein ladder, numbers denote size in kDa corresponding to the bands of the lane. Equal volumes of Myosin-5-cc were loaded to all wells. B) Schematic representation of Myosin-5-cc. Labelling is the following. GFP: enhanced GFP; Motor: motor domain of myosin-5a; IQ: lever with the 6 IQ motifs; CC: 175 amino acids long coiled-coil; CC & loops: 350 amino acids long tail domain that contains predicted coiled-coil and loops.*

4.1.9 Myosin-5-Ad cloning

The recombinant Myosin-5-Ad construct was cloned into pFastBac plasmid by GenScript®. Bacmid DNA was generated from this pFastBac plasmid as described in section 2.4.5. Transposition into the bacmid was verified by PCR amplification using M13 primers as described in section 2.4.6. PCR was run on two colonies that were supposed to contain the Myosin-5-Ad construct (Figure 4.10). PCR product of this myosin-5 construct is expected to be 8.3 kb (6 kb for the construct, plus additional 2.3 kb from the bacmid backbone). Agarose gel verifies that the bacmid from colony No. 2 contains the insert of the expected size.

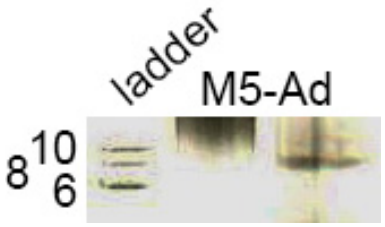

Figure 4.10. *Agarose gel showing the result of the M13 PCR amplification of the Myosin-5-Ad construct. Lanes are the following. Ladder: GeneRuler 1 kb DNA ladder, numbers denote size in kb corresponding to the bands of the lane. M5-Ad: PCR product from bacmids that were purified from white colonies.*

4.1.10 Myosin-5-Ad expression trials

SDS-PAGE gel of the purification steps and of the concentrated protein sample show a small amount of protein that is approximately 120 kDa in size (Figure 4.11), inconsistent with the length of the full size protein construct. Either this is a degraded C-terminal cleavage product or a cleaved full length protein. However, no full length protein appears to be present.

The yields from two expressions were 237 and 259 µg protein/litre of *Sf9* cells, which was only calculated as estimation, using the extinction coefficient of the full length construct (Table 2.10).

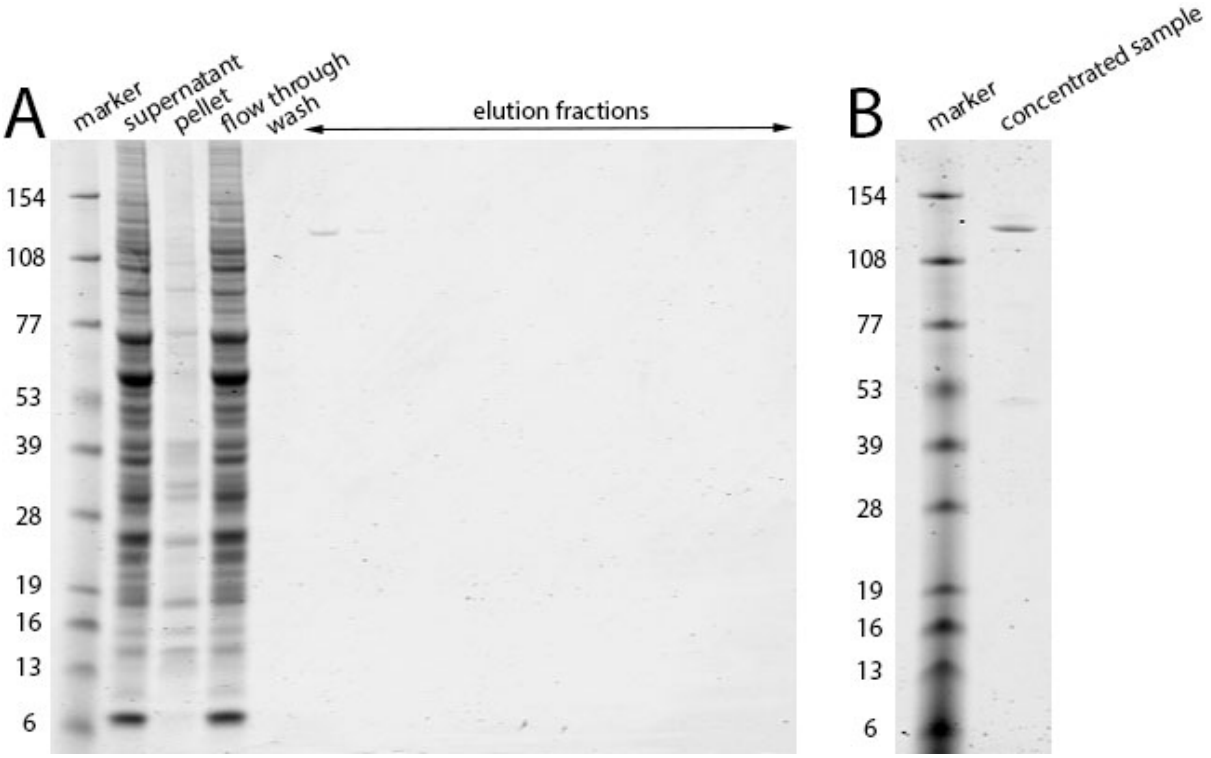

Figure 4.11. *Coomassie-stained SDS-PAGE gels of Myosin-5-Ad purification. A) SDS-PAGE gel shows the steps of Myosin-5-Ad purification. Lanes are the following. Marker: BenchMark pre-stained protein ladder, numbers denote size in kDa corresponding to the bands of the lane. Supernatant: taken after centrifuging the cell lysate. Pellet: taken after centrifuging the cell lysate. Flow through: supernatant taken after incubation with Flag resin. Wash: supernatant taken after washing the Flag resin. Elution fractions: samples taken from each 1 ml elution fraction. B) SDS-PAGE gel of the concentrated eluted sample.*

4.1.11 Identifying the bands in the Myosin-5-Ad expression

The full length construct was not visible on the purification gel of Myosin-5-Ad, however there are two bands approximately 120 and 50 kDa (Figure 4.11). Western blotting was performed using anti-Myo5a and anti-Flag antibodies to identify these bands (Figure 4.12). The anti-Myo5a antibody was raised against the amino acids 981-1070 of the human myosin-5a, that corresponds to the same residue number in mouse myosin-5a. This section of the protein (i.e. 175 amino acids of the coiled-coil) was doubled in the current construct.

There is only one major band recognised on the anti-Flag blot (Figure 4.12A), that is in the day1 sample and approximately 120 kDa. As the Flag tag is at the C-terminus of the construct, this could be an N-terminal fragment that had a cleavage at the lever. Interestingly this band is not visible on day2. There are some very faint bands appearing on day3 approximately 130, 120, 110, 60 and 40 kDa. Considering that these all have a Flag tag, these could be N-terminal fragments that had cleavage at the lever, two different sites at the proximal part of the coiled-coil, at the distal part of the coiled-coil and just before the GFP, respectively. The full length construct is not visible on the blot.

The anti-Myo5a blot shows two bands in all samples approximately 60 and 30 kDa (Figure 4.12B). These could be coiled-coil fragments that have cleavages at the lever or at the motor and at the distal coiled-coil or at the loops that interrupt the predicted coiled-coil. The 130, 120 and 110 kDa bands that are visible in the day3 sample on the anti-Flag blot, should have been recognised on the anti-Myo5a blot too, but they are not present there.

The anti-Flag blot shows less protein on day2 and day3 compared to day1. The anti-Myo5a blot shows similar amounts of protein on day1 and day2, however less protein on day3. However, it is possible that either the cell extraction or the loading of the day3 sample into the well of the SDS gel was less efficient compared to the day1 and day2 samples. In summary, the protein sample looks degraded and the full length construct was not discovered.

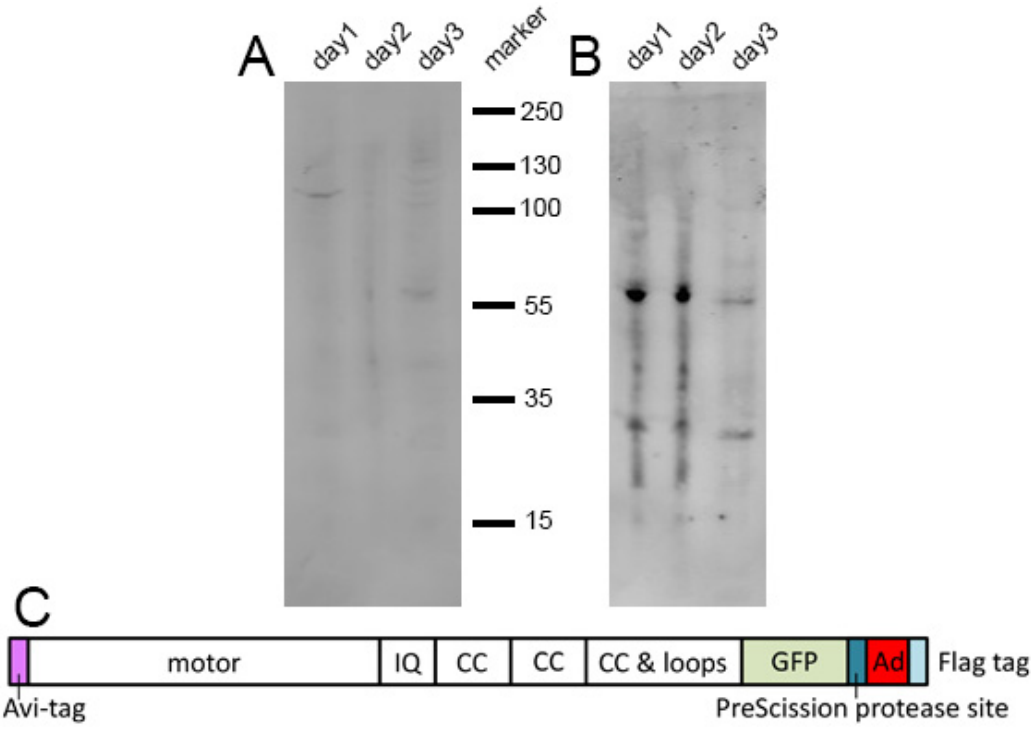

Figure 4.12. *Western blot showing the cell lysate of Sf9 cells expressing Myosin-5-Ad after 1, 2 and 3 days of infection. Anti-Flag (A) and anti-Myo5a (B) antibodies were used for blotting. Marker lane shows bands of PageRuler Plus pre-stained protein ladder, numbers denote size in kDa corresponding to the bands of the lane. 10 µl was loaded to the wells from all samples.* C) *Schematic representation of Myosin-5-Ad. Labelling is the following. Motor: motor domain of myosin-5a; IQ: lever with the 6 IQ motifs; CC: 175 amino acids long coiled-coil; CC & loops: 350 amino acids long tail domain that contains predicted coiled-coil and loops; GFP: enhanced GFP; Ad: Adhiron14.*

4.1.12 Biotinylation of the Myosin-5-Avi construct

Western blotting of the purified Myosin-5-Avi after biotinylation confirmed that the myosin was biotinylated (Figure 4.13B). Full length Myosin-5-Avi construct and some of the additional bands seen also on the purification gel (Figure 4.5) were recognised by the anti-biotin antibody suggesting that these additional bands are degradation products of the myosin-5 construct that still contain the Avi-tag. The ~110 kDa band is not recognised by the anti-biotin antibody in agreement with the previous anti-Flag blot results (Figure 4.6). The ~70 kDa band is recognised by the anti-biotin antibody also in agreement with the previous anti-Flag blot results (Figure 4.6). An additional band with 35 kDa molecular weight was detected on the SDS gel in the biotinylated

Myosin-5-Avi sample that is not visible in the untreated sample (Figure 4.13A). This band was recognised by the anti-biotin antibody and most probably corresponds to the biotin ligase that is used for the biotinylation. Biotin ligase binds biotin, however covalent attachment is not supposed to happen, therefore this results is unexpected. None of the bands in the untreated sample were recognised. Biotinylated actin that was used as a positive control is recognised by the anti-biotin antibody at the approximate molecular weight of 42 kDa.

Note that the 250 kDa marker runs faster on both the SDS gel and the blot (Figure 4.13) compared to the heavy chain of myosin-5 that is expected to be 200 kDa. In this case, the PageRuler Plus protein ladder was used and this was expected to run at the appropriate speed. Reason for this anomaly is not known, however this means that exact size of the bands seen in the biotinylated myosin-5 sample are uncertain.

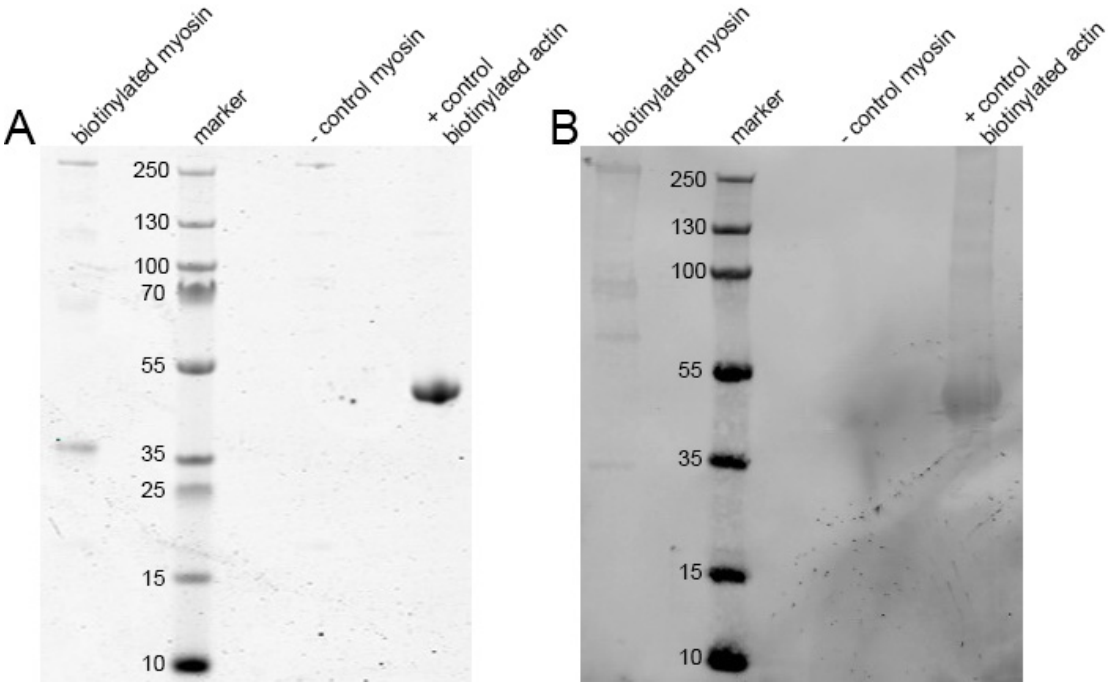

Figure 4.13. *SDS gel (A) and anti-biotin Western blot (B) showing biotinylated Myosin-5-Avi and appropriate controls. Lanes are the following. Biotinylated myosin: 1 µM Myosin-5-Avi treated with biotin ligase. Marker: PageRuler Plus pre-stained protein ladder, numbers denote size in kDa corresponding to the bands of the lane. – control myosin: 1.25 µM untreated Myosin-5-Avi. + control biotinylated actin: 3 µM biotinylated actin (Cytoskeleton). 8 µl was loaded to the wells from all samples. Note that the 70 kDa and 25 kDa marker bands are only showing up on the SDS gel (A).*

4.1.13 Checking biotinylation with mass spectrometry

As western blotting does not yield quantitative information on the efficiency of the biotinylation, mass spectrometry has been applied to analyse the protein preparation. The Myosin-5-Avi construct was incubated with the biotin ligase enzyme two different ways. In method 1, the construct was incubated with the ligase mixture at a temperature of 30 °C for 45 minutes according to the manufacturer's protocol and in method 2 the construct was incubated on ice for 16–18 hours. As a control, similar incubation reactions were set up in the biotinylation buffer using the Myosin-5-Avi construct, but without adding the biotin ligase. All samples were analysed by mass spectrometry.

Accurate mass determination for big molecules like myosin-5 is a challenge, however the obtained mass of the non-biotinylated myosin-5 construct (202,922.9 and 202,923.4 Da for non-biotinylated myosin-5 controls using method 1 and 2, respectively) is only 1.5% different from the mass expected (199,539.4 Da) (Table 4.1). Post-translational modifications and artefacts arising from the ionisation method used in the mass spectrometer could account for the difference between the two values, which appears to be systematic for all samples.

Molecular masses of the biotinylated myosin-5 increased by 679.1 Da (method 1) and by 441.5 Da (method 2) compared to non-biotinylated myosin-5 (Table 4.1). When a single molecule of biotin is covalently attached to a molecule, the mass of the molecule is expected to increase by 226 Da. Thus method 1 adds three biotins per myosin-5 heavy chain, whereas method 2 adds two. That is unexpected as the myosin heavy chain was only expected to be biotinylated at the Avi-tag. This mass spectrometry analysis does not show where the biotins get attached to. However protein fragmentation and subsequently performed mass spectrometry could analyse the sequence of the protein and therefore could potentially identify the additional residues that got biotinylated using method 1 or method 2. Site directed mutagenesis targeting these additional biotinylated residues could eliminate them from the sequence and thus, could avoid that additional biotinylation occur. As the extent of biotinylation is sufficient with method 2, which is expected to be gentler than method 1, this method was used for the remainder of this study.

The biotinylation levels of the commercially available biotinylated G-actin (Cytoskeleton) were also checked using mass spectrometry. The expected mass of

rabbit skeletal α-actin is 41,785 Da (Elzinga et al., 1973). The measured mass of control non-biotinylated G-actin, prepared from rabbit skeletal muscle had a mass of 41,872.8 Da, close to that expected. The biotinylated G-actin sample had multiple peaks with ~452.6 Da differences in mass (Table 4.2). Cytoskeleton Inc. used the compound Biotin-XX, SE (Thermo Fisher Scientific) for biotinylation that adds 452.6 Da mass per biotin to the protein mass. Therefore, these results suggest that the sample contains actin monomers with either 0, 1, 2, 3, 4 or 5 biotin molecules with prevalence rates of 7%, 17%, 29%, 30%, 15% and 1%, respectively, according to a peak area analysis (Table 4.2). This gives an average of 2.3 biotins per actin monomer that is generally in agreement with that reported by the technical support of Cytoskeleton Inc. (i.e. ~1 biotin per actin monomer). In this case, biotin attaches to surface lysine residues of G-actin, in a random manner. If adding 2 to 5 biotin molecules does not interfere with polymerisation of G-actin to F-actin, then the resulting filament will contain more biotins than 1 biotin/subunit.

Sample	**myo30**	**myo0**	**bmyo30**	**bmyo0**
Mass (Da)	202,922.9	202,923.4	203,602.0	203,364.4
Difference in mass (Da)			679.1	441.5
Number of biotins (226 Da)			3.00	1.95

Table 4.1. *Molecular mass results from mass spectrometry of the non-biotinylated and biotinylated Myosin-5-Avi. Samples were treated at 30 °C for 45 minutes (myo30 and bmyo30) or incubated on ice for 16–18 hours (myo0 and bmyo0).*

Peak No.	Measured masses (Da)	Difference in masses (Da)	Number of biotins (calculated)	Number of biotins	Proportion (%)
1	41,873.8		0	0	7.4
2	42,325.7	451.9	0.99845	1	17.1
3	42,778.4	904.6	1.99867	2	29.1
4	43,230.9	1357.1	2.99845	3	30.2
5	43,684.2	1810.4	4.00000	4	14.8
6	44,137.2	2263.4	5.00088	5	1.4

Table 4.2. *Analysis of the mass spectrometry results of biotinylated actin. Multiple peaks observed on the mass spec deconvolution graph are associated with G-actin having 0 to 5 biotin molecules. The column 'Number of biotins (calculated)' shows the mass difference value divided by 452.6 Da. Calculating the area of the peaks suggests the prevalence rates of the compounds shown in the last column.*

4.1.14 ATPase activity of the Myosin-5-Avi construct

In the absence of NeutrAvidin, ATPase assays showed that biotinylation of myosin affected the actin-activated ATPase activity (Figure 4.14A). The ATPase activity of the biotinylated myosin-5 construct was significantly reduced by about 50% compared to the non-biotinylated protein ($p=0.0001$), when the ATPase assays are performed with non-biotinylated actin (Table 4.3). Similarly, a decrease of about 40% in the ATPase activity for biotinylated myosin compared to non-biotinylated protein was also observed when biotinylated actin was used ($p=0.0011$). It is possible that either the biotinylation treatment or the biotinylation buffer conditions decreased the activity of the biotinylated myosin. The measured ATPase rates were somewhat similar for non-biotinylated myosin when either actin or biotinylated actin was used. However interestingly there was a significant ($p=0.0001$) 30% increase in the rate of biotinylated myosin with biotinylated actin compared to non-biotinylated actin. The reason underlying this is not understood. It is also notable that the activity of this construct (1.1 sec^{-1}) is lower than 3.8 sec^{-1} that was reported for mouse myosin-5 HMM at 25 ºC (Wang, Chen, et al., 2000). The presented construct, however, contains an additional N-terminal GFP that could potentially result in decreased activity, especially considering that the GFP is close to the motor domain.

Adding NeutrAvidin in each of these four conditions showed that the largest decrease in the ATPase activity of Myosin-5-Avi was when both biotinylated myosin and biotinyated actin was used (Figure 4.14B) (Table 4.4). This reduced the rate compared to non-biotinylated myosin and actin ATPase valued to 40% ($p=0.0001$). Smaller, but significant reductions were seen when either myosin and biotinylated actin ($p=0.0477$) or biotinyated myosin and actin ($p=0.0001$) were used. NeutrAvidin had no effect on the ATPase activity when non-biotinylated myosin and actin were used. The inhibitory effect of NeutrAvidin on biotinylated myosin and biotinylated actin is greater than the sum of the effects measured with the controls. This indicates that crosslinking the tail to actin via the avidin linkage may affect the ATPase rates of acto-myosin.

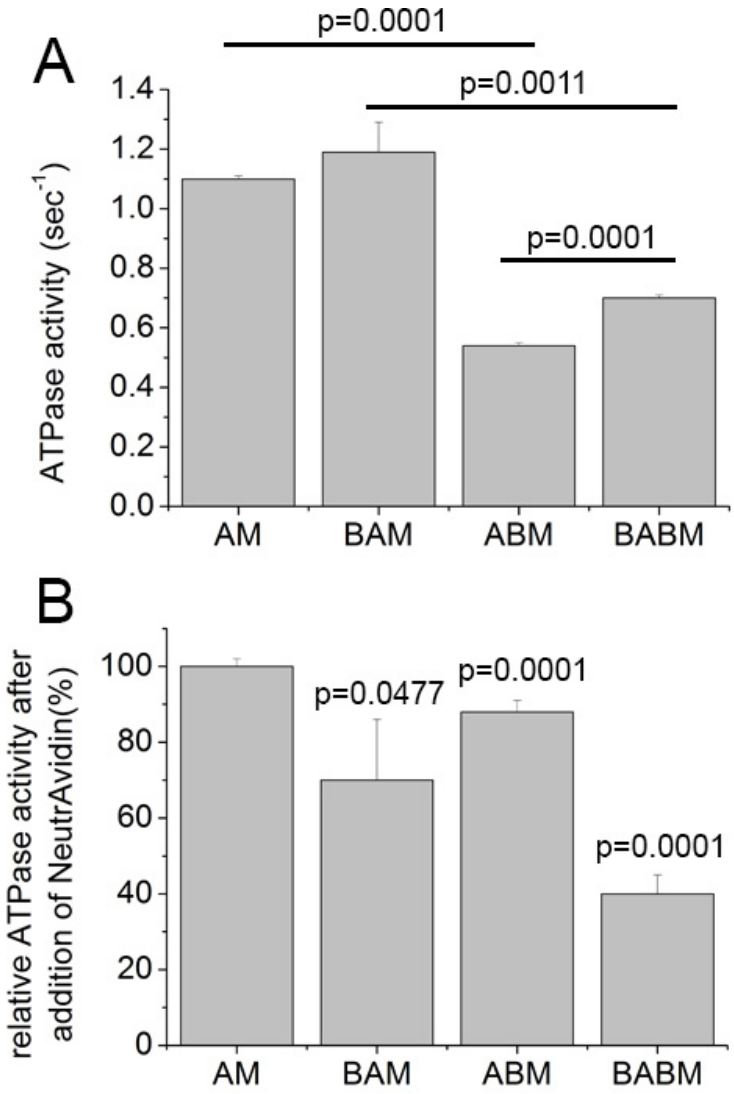

Figure 4.14. *Bar graphs showing the results of the actin-activated ATPase activity of Myosin-5-Avi. Abbreviations are the followings. AM: non-biotinylated actin with non-biotinylated myosin. BAM: biotinylated actin with non-biotinylated myosin. ABM: non-biotinylated actin with biotinylated myosin. BABM: biotinylated actin with biotinylated myosin. 20 μM F-actin was used in the measurements, biotinylated F-actin had 5% of the actin subunits biotinylated. Bars show average and standard deviation of three measurements. P values showing significance are presented on the graphs.*

Panel A shows results of the actin-activated ATPase activity in sec^{-1} myosin $head^{-1}$. Values corresponding to the graph are presented in Table 4.3. Panel B shows results of the actin-activated ATPase activity after addition of NeutrAvidin compared to the activity measured before NeutrAvidin addition, in percentage. Values corresponding to the graph are presented in Table 4.4.

	Actin	Biotinylated actin
Myosin	1.10 ± 0.01	1.19 ± 0.10
Biotinylated myosin	0.54 ± 0.01	0.70 ± 0.01

Table 4.3. *Values of the actin-activated ATPase activity of Myosin-5-Avi in* sec^{-1} *myosin* $head^{-1}$*. 20 μM F-actin was used in the measurements, biotinylated F-actin had 5% of the actin subunits biotinylated. Numbers show average and standard deviation of three measurements.*

	Actin	Biotinylated actin
Myosin	100 ± 2	71 ± 16
Biotinylated myosin	87 ± 3	40 ± 5

Table 4.4. *Percentage of the actin-activated ATPase activity of Myosin-5-Avi after addition of NeutrAvidin compared to the activity measured before NeutrAvidin addition. Actual values are 1*1.1=1.1; 0.71*1.19=0.84; 0.87*0.54=0.47 and 0.4*0.7=0.28. 20 μM F-actin was used in the measurements, biotinylated F-actin had 5% of the actin subunits biotinylated. Numbers show average and standard deviation of three measurements.*

4.1.15 Electron microscopy images of Myosin-5-Avi on actin

Negative stain electron micrographs of non-biotinylated Myosin-5-Avi, in the presence of ATP and in the absence of NeutrAvidin, showed molecules in which the motor domain, lever and coiled-coil tail of the molecule were visible (Figure 4.15). Negative stain electron micrographs of biotinylated actin mixed with NeutrAvidin to which biotinylated Myosin-5-Avi was then added together with ATP showed the attachment of Myosin-5-Avi to actin filaments via its motor domains (Figure 4.16). However, the tail of the myosin construct was almost never seen to be attached to actin. There was only one single molecule, where both the motor domains and the tail were attached to actin. However, in this case, the tail was not attached to the same actin filament as the motor domains, but to an adjacent filament.

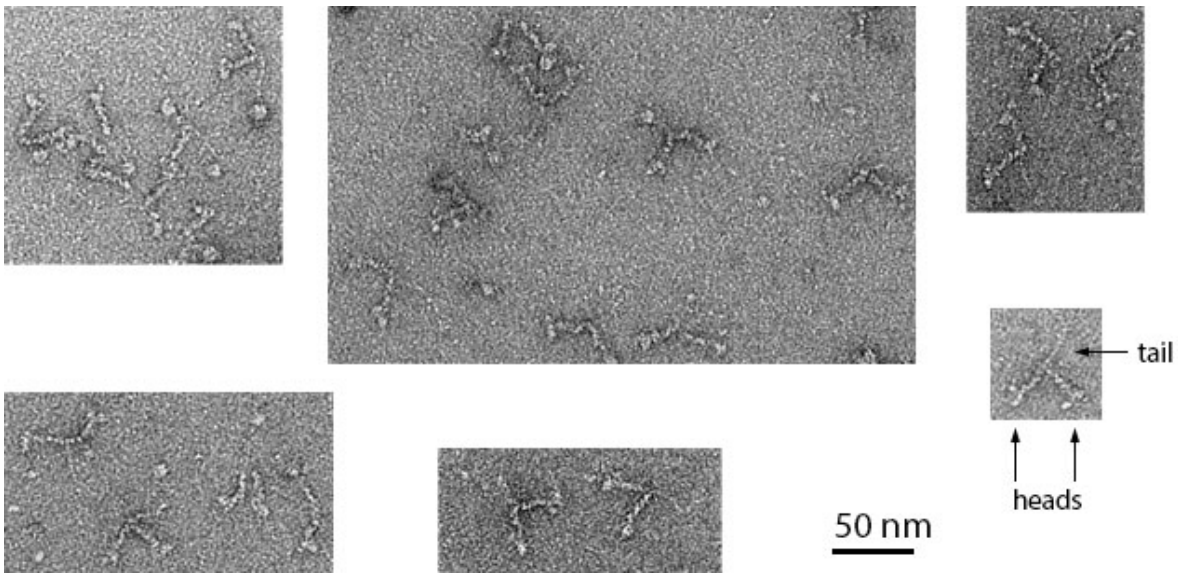

Figure 4.15. *Negative stain electron microscope images of the Myosin-5-Avi construct. 50 nM myosin-5 dimer molecules with 100 µM ATP was mixed and applied to the carbon coated grids. Arrows point to show lever arm and motor domain of Myosin-5-Avi and also to show the coiled-coil tail. Scale bar corresponds to 50 nm.*

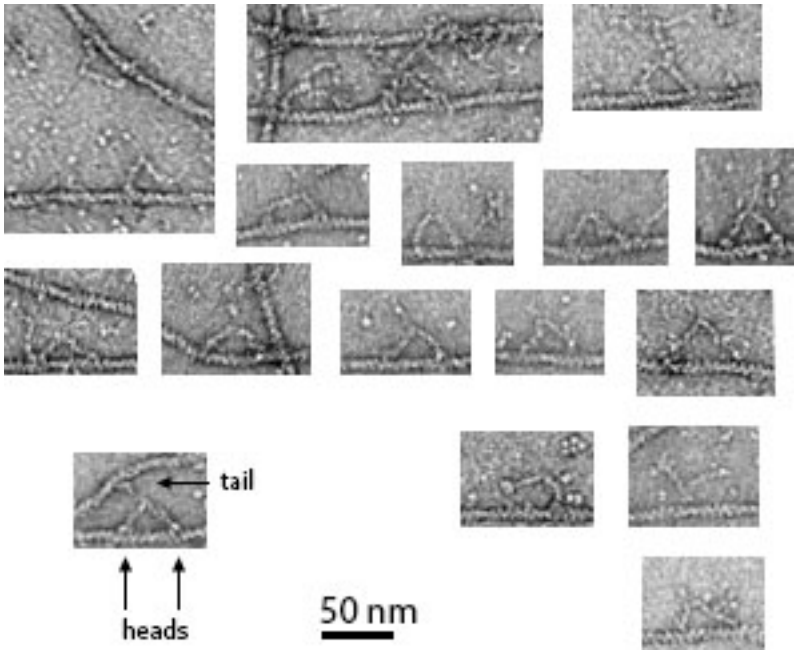

Figure 4.16. *Negative stain electron microscope images show biotinylated Myosin-5-Avi construct on biotinylated actin. 50 nM biotinylated Myosin-5-Avi with 1 μM ATP was mixed with 1 μM biotinylated actin (50 nM biotinylated actin subunits as 5% of the subunits are biotinylated) and 80 nM NeutrAvidin tetramers. Arrows point to show lever arm and motor domain of Myosin-5-Avi and also to show the coiled-coil tail. Scale bar corresponds to 50 nm.*

4.1.16 Single molecule motility assay

In the absence of NeutrAvidin the non-biotinylated and biotinylated Myosin-5-Avi constructs moved along fluorescent biotinylated actin in TIRF microscopy based *in-vitro* motility assays with similar characteristic run length of 0.61 ± 0.14 μm (Figure 4.17A) and 0.55 ± 0.06 μm (Figure 4.17C), respectively. The average speed of the observed Myo5-Avi particles were 0.88 ± 0.01 μm/sec (Figure 4.17B) and 0.83 ± 0.01 μm/sec (Figure 4.17D) for non-biotinylated and biotinylated Myo5-Avi, respectively. Numbers represent mean of the fitting and confidence values. Numbers of the observed molecules were 183 and 1,001 for non-biotinylated and biotinylated Myo5-Avi, respectively. These numbers were compared to literature data measured using mouse myosin-5 HMM constructs by different laboratories and by different methods (Table 4.5). Even though it is not straightforward to compare results that were measured at different temperature using different salt concentrations, interestingly results suggest that the characteristic run lengths are shorter, whereas

velocity values are faster compared to literature data (Sakamoto et al., 2003; Baker et al., 2004; Hodges et al., 2007; Ortega Arroyo et al., 2014).

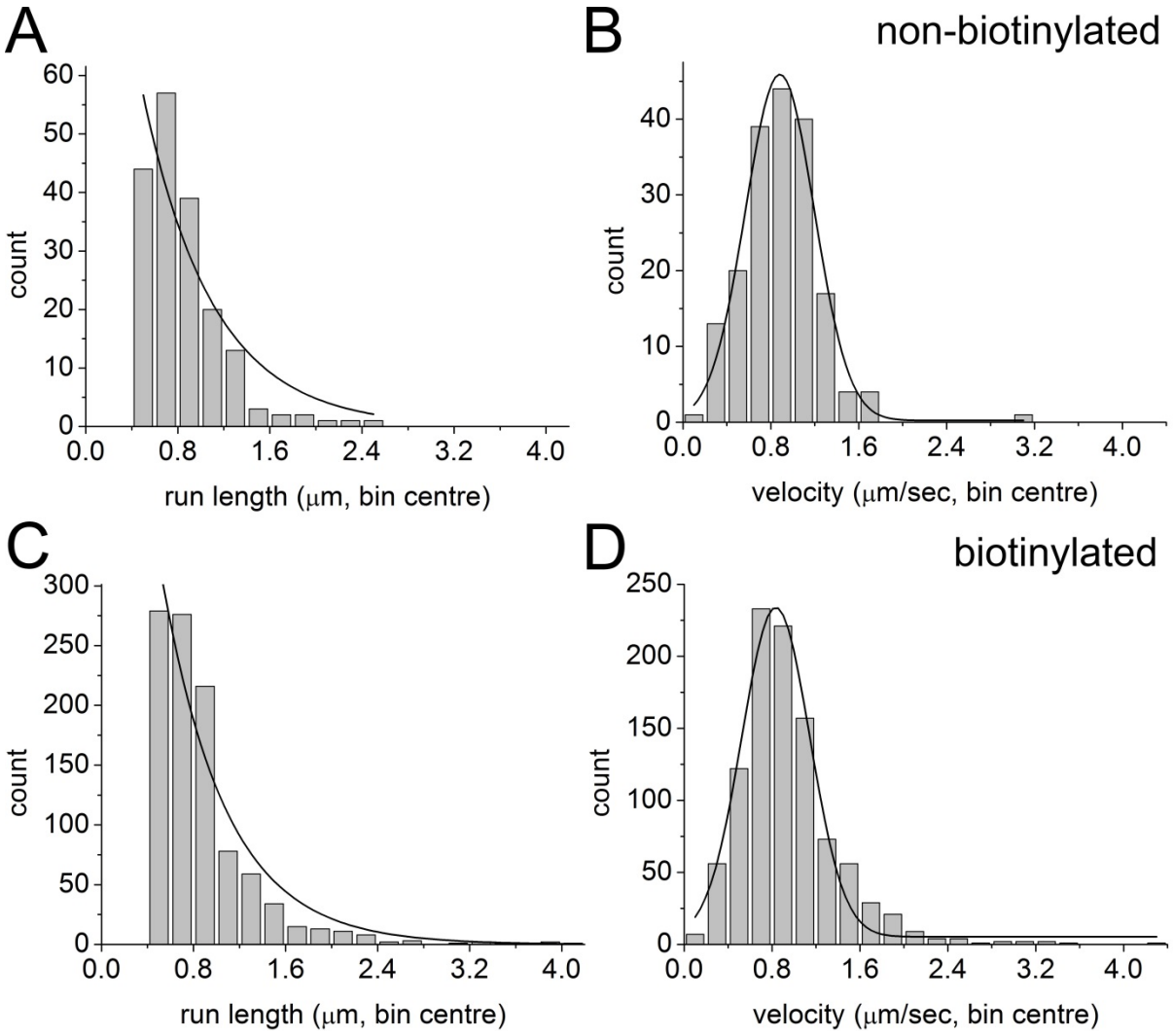

Figure 4.17. *Run length and velocity distribution of the Myo5-Avi construct on actin without NeutrAvidin. Panels A and B show data of the non-biotinylated Myo5-Avi, whereas panels C and D show data of the biotinylated Myo5-Avi. Run length distributions were fitted with a first order exponential decay function, yielding characteristic run lengths of 0.61 ± 0.14 µm (A) and 0.55 ± 0.06 µm (C). Velocity distributions were fitted with a Gaussian function, yielding average speed of 0.88 ± 0.01 µm/sec (B) and 0.83 ± 0.01 (D). Numbers represent mean of the fitting and confidence values. Numbers of the observed molecules were 183 and 1,001 for non-biotinylated and biotinylated Myo5-Avi, respectively.*

Study	Temperature (ºC)	KCl (mM)	Run length (µm)	Velocity (µm/sec)	Number of tracked molecules
(Sakamoto et al., 2003)	30	25	1.81	0.3 ± 0.1*	~153**
(Baker et al., 2004)	25	25	1.3 ± 0.2	0.38 ± 0.04	>72
(Baker et al., 2004)	25	100	0.8 ± 0.2	0.55 ± 0.04	>54
(Hodges et al., 2007)	30	50	1.8 ± 0.2	0.94 ± 0.32	~117***
(Ortega Arroyo et al., 2014)	23	40	0.86 ± 0.35	0.43 ± 0.15	91
This thesis	23	50	0.61 ± 0.14	0.88 ± 0.01	183

Table 4.5. *Run length and velocity data taken from the literature, measured using mouse myosin-5 HMM constructs and data on the non-biotinylated Myosin-5-Avi construct presented above in Figure 4.17.*

**Velocity value is not stated in the paper. Estimated values are given here according to Figure 6 in (Sakamoto et al., 2003).*

***Number of observed molecules is not stated in the paper. An estimate number is given here according to Figure 5 in (Sakamoto et al., 2003).*

****Number of observed molecules is not stated in the paper. An estimate number is given here according to Figure 4 in (Hodges et al., 2007).*

There is an apparent controversy in the data of the steady state ATPase activity and the single molecule motility assay. Steady state ATPase assay showed that the activity is decreased compared to the literature data (Wang, Chen, et al., 2000) and it also showed decreased activity for the biotinylated myosin compared to the non-biotinylated myosin. Whereas in the single molecule motility assay velocity of the non-biotinylated and biotinylated myosin were similar and it was also similar or even higher compared to the literature data (Sakamoto et al., 2003; Baker et al., 2004; Hodges et al., 2007; Ortega Arroyo et al., 2014). This could be explained that some fraction of the myosin molecules is not active in the preparation and that the biotinylation method even decreased the number of the active molecules. The steady state activity describes a population average activity, therefore if only 30% of the molecules are active, the steady state activity will be 30% of that expected. However, in the single molecule motility assay, the inactive molecules are not taken into account and only those molecules are analysed that are actually moving. Therefore this assay could potentially give an activity that is much higher than the steady state activity.

The effect of NeutrAvidin on the motility of biotinylated Myo5-Avi was also tested. The distribution of both the run length and the velocity of the single particles altered after the addition of NeutrAvidin (Figure 4.18), even though the average did not change significantly. Characteristic run length was found to be 0.55 ± 0.03 μm (Figure 4.18A) without NeutrAvidin and 0.51 ± 0.11 μm (Figure 4.18C) after NeutrAvidin addition. Numbers represent mean of the fitting and confidence values. Velocity distribution after NeutrAvidin addition could not be fitted with a Gaussian curve, therefore average was calculated and was found to be 0.92 ± 0.46 μm/sec (mean ± s.d.) (Figure 4.18B) without NeutrAvidin and it was 0.97 ± 0.57 μm/sec (mean ± s.d.) (Figure 4.18D) after addition of NeutrAvidin. Numbers of the observed molecules were 336 and 261 for without NeutrAvidin and after NeutrAvidin addition, respectively.

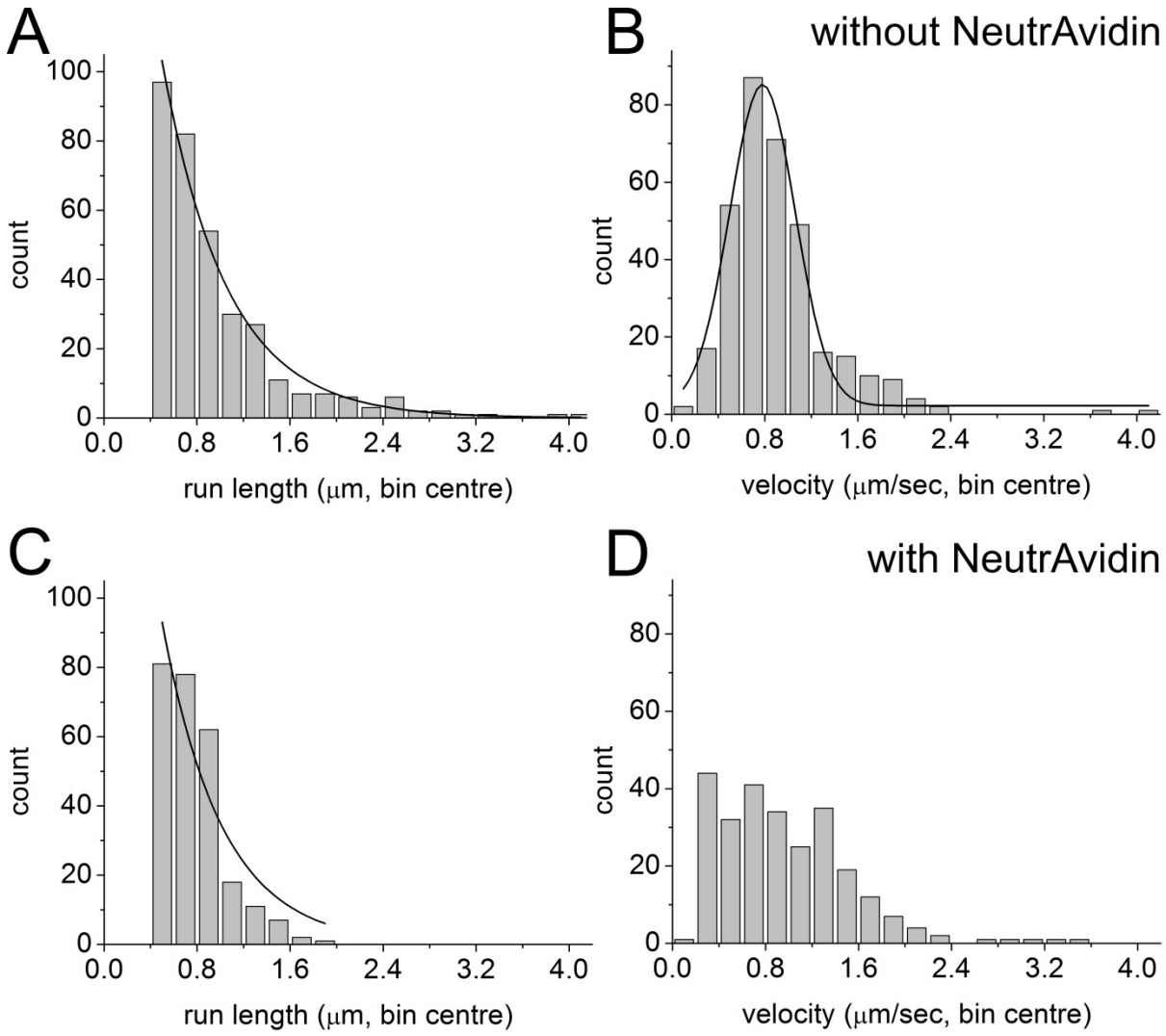

Figure 4.18. *Run length and velocity distribution of biotinylated Myo5-Avi before and after NeutrAvidin addition. Panels A and B show data before, whereas panels C and D show data after NeutrAvidin addition. Run length distributions were fitted with a first order exponential decay function, yielding characteristic run lengths of 0.55 ± 0.03 µm (A) and 0.51 ± 0.13 µm (C). Velocity distribution without NeutrAvidin was fitted with a Gaussian function, yielding average velocity of 0.78 ± 0.01 µm (B). Numbers represent mean of the fitting and confidence values. Numbers of tracked molecules were 338 and 261 for without NeutrAvidin and after NeutrAvidin addition, respectively.*

Results show that NeutrAvidin addition had some effect on biotinylated Myo5-Avi. Run length distribution (Figure 4.18C) could not be fitted properly with a single exponential decay function as there were no molecules observed with run length above 2 µm. However, proportionally more molecules had shorter run length compared to the molecules observed before NeutrAvidin addition (Figure 4.18A). The Gaussian distribution (Figure 4.18B) of the velocity changed after NeutrAvidin addition and similar number of molecules were observed with velocities 0.3 to 1.3 µm/sec (Figure 4.18D). NeutrAvidin was in a large excess (16.7 µM) compared to Myo5-Avi (5 nM) and biotinylated actin subunits (10 nM), therefore most probably every biotinylated molecule had NeutrAvidin bound to them. NeutrAvidin molecules bound to actin could act as obstacles that myosin-5 either i) has to bypass or ii) it dissociates from actin. Increased ratio of slower velocities and short run lengths could be explained by i) and ii), respectively.

4.2 Discussion

A myosin-5 construct that contains the whole coiled-coil tail of the full length myosin-5a molecule, but missing the C-terminal globular tail domain, was designed, cloned, expressed and purified. Yield and purity of the expression was low, thus chaperones were employed that helped to achieve higher yield and also less impurity in the protein preparation. Biotinylation of the myosin decreased the acto-myosin ATPase activity by ~50% in the absence of NeutrAvidin, suggesting that the process of biotinylation may affect myosin ATPase. Crosslinking of biotinylated myosin to actin using NeutrAvidin further decreased the ATPase activity. However, electron micrographs did not show the presence of molecules in which the motor and the tail domain were attached to the same actin filament. Moreover, single molecule motility of the individual biotinylated myosin-5 molecules were not affected by the addition of NeutrAvidin.

This study is the first to employ chaperones to help with expression of myosin-5. Previously, myosin-5 has been shown to express well even in the absence of chaperones. This includes full length constructs (Krementsov et al., 2004; Wu et al., 2006) as well as the myosin-5 HMM construct that is more typically expressed (Andrecka et al., 2015; Zimmermann et al., 2015; Iwaki et al., 2015). The chaperones are thought to bind to and interact with the motor domain to promote folding (Barral et al., 2002; Liu et al., 2008), and have been shown to improve expression levels of other myosin isoforms including myosin-14 and myosin-15 (Bookwalter et al., 2014; Bird et al., 2014). In the case of Myosin-5-Avi construct, chaperones increased yield of expression by one order of magnitude and they also helped to reduce the intensity of the additional bands seen on the SDS gel of myosin-5 preparation. Therefore applying chaperones to express this and further myosin-5 constructs is beneficial to get good quality protein for downstream biochemical and biophysical studies.

The reduced ATPase activity following myosin biotinylation suggests that the process of biotinylation may affect myosin. In previous reports, the Avi-tag was added to the N-terminus of myosin-5, and decrease in the actin-activated ATPase was not reported after biotinylation of the myosin (Hodges et al., 2007; Nelson et al., 2009; Andrecka et al., 2015). It is unlikely that this is due to the positioning of the tag, or the smaller size of the myosin-5 constructs used in those experiments (Hodges et

al., 2007; Nelson et al., 2009; Andrecka et al., 2015). An N-terminal biotinylation is close to the motor, where the ATP hydrolysis takes place, therefore could interfere with that, whereas a C-terminal biotinylation is spatially far from the active site. However, mass spectrometry analysis showed that the Myo5-Avi construct gets biotinylated at 2 or 3 sites depending on the incubation circumstances. If the motor gets non-specifically biotinylated, that could decrease ATPase activity explaining the observed results.

Moreover, the measured actin-activated ATPase activity is ~3 fold lower than previously reported (Wang, Chen, et al., 2000). It is possible that the active fraction of the molecules is only ~30% and therefore the steady state activity is 30% compared to what was observed before. That could be tested with active site titration using a stopped flow instrument. However the observed difference might also be due to the fact that this construct is 350 residues longer than an HMM. Overestimation of the protein concentration due to the additional bands seen on the SDS gel might also lead to lower activity. Exact protein concentration could be measured using mass spectrometry, however inaccurate protein concentration cannot account for 70% of the activity loss compared to the literature results.

NeutrAvidin decreased the ATPase activity of biotinylated myosin-5 on biotinylated actin, suggesting that the tail of myosin-5 might be bound to actin. However, electron microscope images did not show the hypothesised myosin-actin conformation, in which the motor and the tail are tethered to the same actin filament (Figure 1.13). In the one example where Myosin-5-Avi was attached to F-actin by both of its motor domains and via its tail, the motors were on a different filament to that to which the tail was bound. Different experimental setup might explain the difference observed in the ATPase assay and the EM images. Moreover EM images are 2D projections of the molecules present in solution, which limits the number and variety of molecules and structures to be observed.

Single molecule motility experiments showed that Myo5-Avi construct moves with similar or even higher speed compared to previous literature data on mouse myosin-5 HMM. This was unexpected as steady state activity of the molecules was found to be lower than that of previously reported. However as explained above, it is possible that a huge fraction of the Myo5-Avi molecules are inactive, therefore their population average (i.e. steady state) activity is low. Whereas in single molecule

experiments individual, motile molecules are analysed and inactive molecules that do not move are filtered out.

Single molecule experiments also revealed that non-biotinylated and biotinylated Myo5-Avi molecules display similar run length and velocity. It is however still possible that the biotinylation process affects some Myo5-Avi molecules and renders them inactive. But it might be more likely that the biotinylation buffer affected the steady state ATPase activity measurement as there was ~1% v/v biotinylation buffer in the final reaction mixture. In the single molecule experiments there is only 0.1% v/v biotinylation buffer in the final reaction mixture.

Considering that the tail of myosin-5 was never observed to be tethered to the same actin filament as it is walking on, and that NeutrAvidin did not affect the single molecule motility of biotinylation Myo5-Avi, it is possible that lever and the coiled-coil junction is not flexible enough to allow that attachment. If the predicted coiled-coil sections of the myosin-5 tail indeed form coiled-coil, that would add up to a 54 nm (26+13+15 nm (Chothia et al., 1981; Baboolal et al., 2009)) long tail. Assuming that the loops are not extending, this coiled-coil tail would be able to attach to the actin filament if the tail is able to meet at a ~27º to the lever and then the N-terminal end of the tail would be bound 30 nm away from the trailing motor (Figure 4.19). If the loops are able to extend, both the angle and the distance would be larger. If the tail is only able to make a wider angle to the lever, we either need a construct with a longer tail or a construct with some flexible regions in the tail. Even though the loops that interrupt the predicted coiled-coil structure were thought to be flexible, this flexibility is apparently not sufficient for our study.

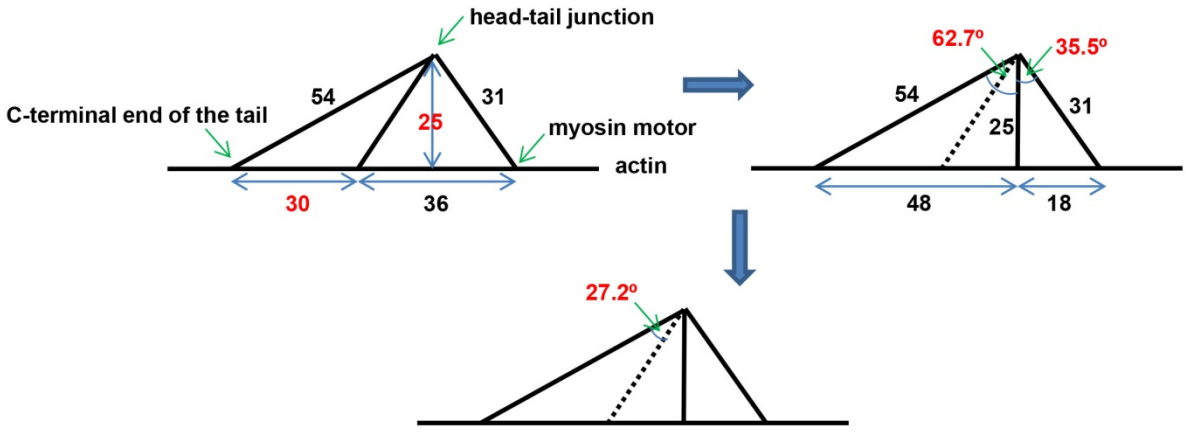

Figure 4.19. *Calculating distances and angles in the schematic myosin-5 structure bound to actin. Blue arrows indicate the steps of the calculations. Distances are in nm. Step size (36 nm) (Walker et al., 2000), length of the head domain (31 nm) (Cheney et al., 1993) and length of the coiled-coil tail (54 nm) (Chothia et al., 1981) are taken from the literature. Numbers denoted with red were calculated using simple algebra in the given step. Final step shows that the tail meets at a 27º angle with the trailing head to attach to actin.*

Results suggest that the present Myosin-5-Avi construct is not appropriate to study the elasticity of the tail domain as hypothesised (Figure 1.13). Therefore two new constructs, Myosin-5-cc and Myosin-5-Ad, were designed that have a longer coiled-coil tail. 175 amino acids of the coiled-coil were doubled in these constructs, making the tail 26 nm longer compared to Myosin-5-Avi. In the previous chapter a new method, Adhirons, were explored that could substitute the biotin-avidin interaction, thus avoid the biotinylation process. The sequence of an actin binding Adhiron molecule was added to the C-terminus of the Myosin-5-Ad construct, whereas Myosin-5-cc contains a C-terminal Avi-tag such as Myosin-5-Avi.

The expression trials of neither Myosin-5-cc, nor Myosin-5-Ad were successful as the full length constructs were not obtained. The DNA sequence of the constructs was correct as checked by sequencing. Western blots confirmed that the protein bands seen in the protein purification prep were fragments of the full length protein. It is possible that the extended coiled-coil of 350 amino acids (doubling the 175 amino acids) is prone to cleavage by proteases. Furthermore, it is also possible that the Adhiron at the C-terminus of the Myosin-5-Ad construct binds to actin in *Sf9* cells that makes it prone to cleavage by proteases. Due to these or due to other reasons the molecules can get cleaved during expression in the insect cells. Further expression optimisation is needed to obtain the full length protein constructs.

5. Concluding remarks

5.1 Characterisation of actin-binding Adhirons

5.1.1 Summary

Four new actin-binding molecules were raised with phage display assay. These new proteins are small, easy to express and bind tightly to actin, making them potentially useful in wide variety of applications. These molecules are named Adhiron2, Adhiron6, Adhiron14 and Adhiron24. Adhiron14 binds with a submicromolar affinity to actin and, when labelled with a fluorophore, can be used to label actin in live cells or in fixed cells. Adhiron2 binds with a micromolar affinity to actin and could potentially be used to attach actin to the coverslip in TIRF single molecule motility assay.

5.1.2 Future directions

Future experiments will explore the exact binding affinity of Adhiron2 to actin using further spin down assays. The potential difference in binding due to biotinylation of the Adhirons will also be studied using similar spin down assays.

The presented results suggest that Adhiron6, Adhiron14 and Adhiron24 bind to the same or overlapping sites on actin. This will be further studied using competition spin down assays of pairs of Adhirons, where one Adhiron is biotin labelled and the other Adhiron is non-labelled. Western blotting will be performed and using an anti-biotin antibody, the amount of one of the Adhirons in the pellet and in the supernatant will specifically be determined.

Competition between the myosin motor domain and the Adhirons will also be further studied using competition spin down assays. It will also be tested if S1 competes Adhirons off actin in the presence of ATP.

The properties of Adhiron2 in attaching actin to the coverslips will also be further studied. Myosin movement on actin attached to the surface by Adhiron2 and by NeutrAvidin will be compared, run length and velocity distribution will be analysed.

The application of Adhiron14 in cell staining will be further studied using more, different cell lines. On and off rates of Adhiron will be measured and these properties along with Adhiron distribution in binding to various actin structures will be compared with present methods used for actin staining. Adhiron24 was implied to stain focal adhesions when expressed in HeLa cells, which will be tested using anti-vinculin or

anti-paxillin antibodies. Exact nature of Adhiron24 binding to actin will be determined, as the reason behind targeting to focal adhesions remains to be resolved.

The potential actin bundling properties of Adhirons will be studied by electron microscopy. The use of Adhirons will be explored in optical trapping and also in iSCAT systems.

A mutational analysis on the Adhirons could be performed to discover which residues in the variable loops are responsible for binding to actin. These residues could be selectively mutated, then the mutant Adhirons expressed and studied in spin down assays.

Structure prediction of the Adhirons could be performed using homology modelling, then Adhirons could be docked to the structure of F-actin to discover potential binding site of Adhirons on F-actin.

5.2 Characterisation of recombinant myosin-5 constructs with actin-binding tail domains

5.2.1 Summary

Multiple myosin-5 constructs were designed and cloned that contain an actin-binding motif at their C-termini. Myosin-5-Avi that contains the entire predicted coiled-coil motif was expressed and purified successfully. Even though steady state actin-activated ATPase activity indicated low activity of this construct, single molecule motility assay results showed that individual molecules move along actin with a faster speed than was reported earlier. The presented experiments did not show that the tail of this construct is able to bind to the same actin filament as the motors are walking on. Expression of Myosin-5-cc and Myosin-5-Ad constructs, where the coiled-coil tail of myosin-5 is longer to allow attachment of the tail to actin, only proceeded successfully as far as the creation of baculoviruses and expression trials are currently in progress.

5.2.2 Future directions

Expression optimisation will be performed to get full length constructs of Myosin-5-cc and Myosin-5-Ad and study if their tail is able to bind to the same actin filament as the heads are bound to. Negative staining electron microscopy will be used to image the motor domains and levers of stalled myosin-5 and their structures will be

compared to those of myosin-5 molecules moving under unloaded conditions. It is likely that the predicted coiled-coil tail of myosin-5 is elastic and might extend under these conditions, which will be measured. In addition, a fluorescent-analogue of ATP will be applied to determine how strain affects the kinetics of the two heads of myosin under stalled conditions.

Future experiments will also explore further properties of Myosin-5-Avi.

Adding NeutrAvidin to the single molecule motility assay did not change the average velocity and run length of biotinylated Myosin-5-Avi, even though the distribution of the velocities and run lengths of the single molecules altered. Control experiment using non-biotinylated Myosin-5-Avi could clarify whether the distribution change was due to the binding of NeutrAvidin to the biotinylated myosin or due to NeutrAvidin attachment to biotinylated actin. Adhiron2 will also be explored to attach actin to coverslips and to study the difference between using biotinylated or non-biotinylated actin in Myosin-5-Avi motility assays.

Detailed analyses of electron micrographs can show the length of the first coiled-coil part of the tail, as loop motifs following this segment are usually not visible in negative stain EM. The angle between the tail and the lever will also be measured that could suggest if there is enough flexibility at the head-tail junction to allow the attachment of the tail to the same actin filament as the heads are bound to.

Supplementary Materials

S1. Amino acid sequences of the GFP-Adhiron constructs

legend:
GFP
Adhiron
linker

GFP-Adhiron2

```
         10          20          30          40          50          60
MVSKGEELFT GVVPILVELD GDVNGHKFSV SGEGEGDATY GKLTLKFICT TGKLPVPWPT

         70          80          90         100         110         120
LVTTLTYGVQ CFSRYPDHMK QHDFFKSAMP EGYVQERTIF FKDDGNYKTR AEVKFEGDTL

        130         140         150         160         170         180
VNRIELKGID FKEDGNILGH KLEYNYNSHN VYIMADKQKN GIKVNFKIRH NIEDGSVQLA

        190         200         210         220         230         240
DHYQQNTPIG DGPVLLPDNH YLSTQSALSK DPNEKRDHMV LLEFVTAAGI TLGMDELYKS

        250         260         270         280         290         300
GLRSRAQASN SASNSLEIEE LARFAVDEHN KKENALLEFV RVVKAKEQWI YIHPRKVTMY

        310         320         330         340         350
YLTLEAKDGG KKKLYEAKVW VKTHKYQNMS DNFKELQEFK PVGDAAGSTG SR
```

GFP-Adhiron6

```
         10          20          30          40          50          60
MVSKGEELFT GVVPILVELD GDVNGHKFSV SGEGEGDATY GKLTLKFICT TGKLPVPWPT

         70          80          90         100         110         120
LVTTLTYGVQ CFSRYPDHMK QHDFFKSAMP EGYVQERTIF FKDDGNYKTR AEVKFEGDTL

        130         140         150         160         170         180
VNRIELKGID FKEDGNILGH KLEYNYNSHN VYIMADKQKN GIKVNFKIRH NIEDGSVQLA

        190         200         210         220         230         240
DHYQQNTPIG DGPVLLPDNH YLSTQSALSK DPNEKRDHMV LLEFVTAAGI TLGMDELYKS

        250         260         270         280         290         300
GLRSRAQASN SASNSLEIEE LARFAVDEHN KKENALLEFV RVVKAKEQSS VPHWWWTTMY

        310         320         330         340         350
YLTLEAKDGG KKKLYEAKVW VKRDPNMIFK INFKELQEFK PVGDAAGSTG SR
```

GFP-Adhiron14

```
         10          20          30          40          50          60
MVSKGEELFT GVVPILVELD GDVNGHKFSV SGEGEGDATY GKLTLKFICT TGKLPVPWPT

         70          80          90         100         110         120
LVTTLTYGVQ CFSRYPDHMK QHDFFKSAMP EGYVQERTIF FKDDGNYKTR AEVKFEGDTL
```

```
       130        140        150        160        170        180
VNRIELKGID FKEDGNILGH KLEYNYNSHN VYIMADKQKN GIKVNFKIRH NIEDGSVQLA

       190        200        210        220        230        240
DHYQQNTPIG DGPVLLPDNH YLSTQSALSK DPNEKRDHMV LLEFVTAAGI TLGMDELYKS

       250        260        270        280        290        300
GLRSRAQASN SASNSLEIEE LARFAVDEHN KKENALLEFV RVVKAKEQSD TPHWWWTTMY

       310        320        330        340        350
YLTLEAKDGG KKKLYEAKVW VKESPVHPKR LNFKDLQEFK PVGDAAGSTG SR
```

GFP-Adhiron24

```
        10         20         30         40         50         60
MVSKGEELFT GVVPILVELD GDVNGHKFSV SGEGEGDATY GKLTLKFICT TGKLPVPWPT

        70         80         90        100        110        120
LVTTLTYGVQ CFSRYPDHMK QHDFFKSAMP EGYVQERTIF FKDDGNYKTR AEVKFEGDTL

       130        140        150        160        170        180
VNRIELKGID FKEDGNILGH KLEYNYNSHN VYIMADKQKN GIKVNFKIRH NIEDGSVQLA

       190        200        210        220        230        240
DHYQQNTPIG DGPVLLPDNH YLSTQSALSK DPNEKRDHMV LLEFVTAAGI TLGMDELYKS

       250        260        270        280        290        300
GLRSRAQASN SASNSLEIEE LARFAVDEHN KKENALLEFV RVVKAKEQMD MIGEYVSTMY

       310        320        330        340        350
YLTLEAKDGG KKKLYEAKVW VKGWMPLYSR QNFKELQEFK PVGDAAGSTG SR
```

S2. Amino acid sequence of Myosin-5-Avi construct

Sequence alignment was performed using the ClustalW webserver (Larkin et al., 2007). First line shows the DNA sequence of the brain isoform of mouse myosin-5a (NCBI Reference Sequence: XM_006510832.3). Second line shows the DNA sequence of the Myosin-5-Avi construct. Third line shows the amino acid sequence corresponding to the Myosin-5-Avi construct. Colouring of the amino acid sequence represents the distinct domains and motifs of the protein according to the legend. Numbers at the end of the lines represent the number of nucleic acids or amino acids up to that point in the sequence.

Legend:

GFP
Restriction sites: BssH II, EcoR I and Stu I
Mouse myosin-5a brain isoform with the whole coiled-coil domain, 1440 aa
Avi-tag
Restriction sites: Stu I, Sal I, Sst I, Spe I and Not I
Flag tag

```
XM_00651  ------------------------------------------------------------
M5-Avi    ATGGTGAGCAAGGGCGAGGAGCTGTTCACCGGGGTGGTGCCCATCCTGGTCGAGCTGGAC 60
            M  V  S  K  G  E  E  L  F  T  G  V  V  P  I  L  V  E  L  D  20

XM_00651  ------------------------------------------------------------
M5-Avi    GGCGACGTAAACGGCCACAAGTTCAGCGTGTCCGGCGAGGGCGAGGGCGATGCCACCTAC 120
            G  D  V  N  G  H  K  F  S  V  S  G  E  G  E  G  D  A  T  Y  40

XM_00651  ------------------------------------------------------------
M5-Avi    GGCAAGCTGACCCTGAAGTTCATCTGCACCACCGGCAAGCTGCCCGTGCCCTGGCCCACC 180
            G  K  L  T  L  K  F  I  C  T  T  G  K  L  P  V  P  W  P  T  60

XM_00651  ------------------------------------------------------------
M5-Avi    CTCGTGACCACCCTGACCTACGGCGTGCAGTGCTTCAGCCGCTACCCCGACCACATGAAG 240
            L  V  T  T  L  T  Y  G  V  Q  C  F  S  R  Y  P  D  H  M  K  80

XM_00651  ------------------------------------------------------------
M5-Avi    CAGCACGACTTCTTCAAGTCCGCCATGCCCGAAGGCTACGTCCAGGAGCGCACCATCTTC 300
            Q  H  D  F  F  K  S  A  M  P  E  G  Y  V  Q  E  R  T  I  F  100

XM_00651  ------------------------------------------------------------
M5-Avi    TTCAAGGACGACGGCAACTACAAGACCCGCGCCGAGGTGAAGTTCGAGGGCGACACCCTG 360
            F  K  D  D  G  N  Y  K  T  R  A  E  V  K  F  E  G  D  T  L  120

XM_00651  ------------------------------------------------------------
M5-Avi    GTGAACCGCATCGAGCTGAAGGGCATCGACTTCAAGGAGGACGGCAACATCCTGGGGCAC 420
            V  N  R  I  E  L  K  G  I  D  F  K  E  D  G  N  I  L  G  H  140

XM_00651  ------------------------------------------------------------
M5-Avi    AAGCTGGAGTACAACTACAACAGCCACAACGTCTATATCATGGCCGACAAGCAGAAGAAC 480
            K  L  E  Y  N  Y  N  S  H  N  V  Y  I  M  A  D  K  Q  K  N  160

XM_00651  ------------------------------------------------------------
M5-Avi    GGCATCAAGGTGAACTTCAAGATCCGCCACAACATCGAGGACGGCAGCGTGCAGCTCGCC 540
            G  I  K  V  N  F  K  I  R  H  N  I  E  D  G  S  V  Q  L  A  180

XM_00651  ------------------------------------------------------------
M5-Avi    GACCACTACCAGCAGAACACCCCCATCGGCGACGGCCCCGTGCTGCTGCCCGACAACCAC 600
            D  H  Y  Q  Q  N  T  P  I  G  D  G  P  V  L  L  P  D  N  H  200

XM_00651  ------------------------------------------------------------
M5-Avi    TACCTGAGCACCCAGTCCGCCCTGAGCAAAGACCCCAACGAGAAGCGCGATCACATGGTC 660
            Y  L  S  T  Q  S  A  L  S  K  D  P  N  E  K  R  D  H  M  V  220

XM_00651  ------------------------------------------------------------
M5-Avi    CTGCTGGAGTTCGTGACCGCCGCCGGGATCACTCTCGGCATGGACGAGCTGTACAAGGCG 720
            L  L  E  F  V  T  A  A  G  I  T  L  G  M  D  E  L  Y  K  A  240

XM_00651  ------------------ATGGCCGCGTCCGAGCTCTACACCAAGTTTGCCAGGGTTTGG 42
M5-Avi    CGCGGAATTCAAAGGCCTATGGCCGCGTCCGAGCTCTACACCAAGTTTGCCAGGGTTTGG 780
            R  G  I  Q  R  P  M  A  A  S  E  L  Y  T  K  F  A  R  V  W  260
```

```
XM_00651  ATCCCTGATCCTGAGGAAGTGTGGAAATCGGCAGAGTTGCTCAAGGATTATAAGCCTGGA 102
M5-Avi    ATCCCTGATCCTGAGGAAGTGTGGAAATCGGCAGAGTTGCTCAAGGATTATAAGCCTGGA 840
           I  P  D  P  E  E  V  W  K  S  A  E  L  L  K  D  Y  K  P  G  280

XM_00651  GATAAAGTGCTCCTGCTTCACCTCGAGGAAGGGAAGGATTTGGAATACCGTCTAGACCCA 162
M5-Avi    GATAAAGTGCTCCTGCTTCACCTCGAGGAAGGGAAGGATTTGGAATACCGTCTAGACCCA 900
           D  K  V  L  L  L  H  L  E  E  G  K  D  L  E  Y  R  L  D  P  300

XM_00651  AAGACCGGTGAGCTCCCTCACTTACGGAACCCTGACATACTTGTTGGAGAAAATGACCTC 222
M5-Avi    AAGACCGGTGAGCTCCCTCACTTACGGAACCCTGACATACTTGTTGGAGAAAATGACCTC 960
           K  T  G  E  L  P  H  L  R  N  P  D  I  L  V  G  E  N  D  L  320

XM_00651  ACAGCCCTCAGCTACCTTCACGAGCCCGCTGTGCTACATAATCTCCGAGTTCGCTTCATC 282
M5-Avi    ACAGCCCTCAGCTACCTTCACGAGCCCGCTGTGCTACATAATCTCCGAGTTCGCTTCATC 1020
           T  A  L  S  Y  L  H  E  P  A  V  L  H  N  L  R  V  R  F  I  340

XM_00651  GATTCCAAACTTATTTATACGTATTGTGGAATAGTTCTGGTAGCTATAAATCCCTATGAG 342
M5-Avi    GATTCCAAACTTATTTATACGTATTGTGGAATAGTTCTGGTAGCTATAAATCCCTATGAG 1080
           D  S  K  L  I  Y  T  Y  C  G  I  V  L  V  A  I  N  P  Y  E  360

XM_00651  CAGCTGCCTATTTATGGAGAAGATATTATTAATGCCTACAGTGGCCAGAACATGGGTGAC 402
M5-Avi    CAGCTGCCTATTTATGGAGAAGATATTATTAATGCCTACAGTGGCCAGAACATGGGTGAC 1140
           Q  L  P  I  Y  G  E  D  I  I  N  A  Y  S  G  Q  N  M  G  D  380

XM_00651  ATGGATCCTCACATCTTCGCAGTAGCTGAAGAGGCTTACAAGCAAATGGCAAGGGATGAA 462
M5-Avi    ATGGATCCTCACATCTTCGCAGTAGCTGAAGAGGCTTACAAGCAAATGGCAAGGGATGAA 1200
           M  D  P  H  I  F  A  V  A  E  E  A  Y  K  Q  M  A  R  D  E  400

XM_00651  CGAAATCAGTCCATCATTGTAAGTGGAGAGTCAGGCGCAGGGAAGACGGTCTCTGCTAAG 522
M5-Avi    CGAAATCAGTCCATCATTGTAAGTGGAGAGTCAGGCGCAGGGAAGACGGTCTCTGCTAAG 1260
           R  N  Q  S  I  I  V  S  G  E  S  G  A  G  K  T  V  S  A  K  420

XM_00651  TATGCCATGCGGTACTTCGCAACTGTAAGTGGCTCTGCCAGTGAGGCCAATGTTGAGGAA 582
M5-Avi    TATGCCATGCGGTACTTCGCAACTGTAAGTGGCTCTGCCAGTGAGGCCAATGTTGAGGAA 1320
           Y  A  M  R  Y  F  A  T  V  S  G  S  A  S  E  A  N  V  E  E  440

XM_00651  AAGGTCTTGGCCTCCAACCCCATCATGGAGTCAATTGGAAATGCCAAAACAACCAGGAAT 642
M5-Avi    AAGGTCTTGGCCTCCAACCCCATCATGGAGTCAATTGGAAATGCCAAAACAACCAGGAAT 1380
           K  V  L  A  S  N  P  I  M  E  S  I  G  N  A  K  T  T  R  N  460

XM_00651  GATAATAGCAGCCGGTTTGGAAAATATATTGAAATTGGTTTTGACAAGAGGTACAGAATC 702
M5-Avi    GATAATAGCAGCCGGTTTGGAAAATATATTGAAATTGGTTTTGACAAGAGGTACAGAATC 1440
           D  N  S  S  R  F  G  K  Y  I  E  I  G  F  D  K  R  Y  R  I  480

XM_00651  ATCGGTGCCAATATGAGAACTTACCTTTTAGAGAAATCCAGAGTGGTGTTCCAGGCAGAA 762
M5-Avi    ATCGGTGCCAATATGAGAACTTACCTTTTAGAGAAATCCAGAGTGGTGTTCCAGGCAGAA 1500
           I  G  A  N  M  R  T  Y  L  L  E  K  S  R  V  V  F  Q  A  E  500

XM_00651  GAGGAGAGAAACTACCATATCTTCTATCAGCTCTGTGCTTCGGCAAAGTTACCTGAGTTT 822
M5-Avi    GAGGAGAGAAACTACCATATCTTCTATCAGCTCTGTGCTTCGGCAAAGTTACCTGAGTTT 1560
           E  E  R  N  Y  H  I  F  Y  Q  L  C  A  S  A  K  L  P  E  F  520

XM_00651  AAAATGCTGCGGTTAGGAAATGCAGATAGTTTTCATTACACGAAGCAAGGAGGCAGCCCT 882
M5-Avi    AAAATGCTGCGGTTAGGAAATGCAGATAGTTTTCATTACACGAAGCAAGGAGGCAGCCCT 1620
           K  M  L  R  L  G  N  A  D  S  F  H  Y  T  K  Q  G  G  S  P  540

XM_00651  ATGATAGAAGGAGTAGATGATGCGAAGGAGATGGCGCACACCAGGCAGGCCTGCACTCTG 942
M5-Avi    ATGATAGAAGGAGTAGATGATGCGAAGGAGATGGCGCACACCAGGCAGGCCTGCACTCTG 1680
           M  I  E  G  V  D  D  A  K  E  M  A  H  T  R  Q  A  C  T  L  560
```

```
XM_00651  CTGGGAATTAGTGAATCTTACCAAATGGGAATTTTTCGAATACTTGCTGGCATTCTTCAC 1002
M5-Avi    CTGGGAATTAGTGAATCTTACCAAATGGGAATTTTTCGAATACTTGCTGGCATTCTTCAC 1740
           L  G  I  S  E  S  Y  Q  M  G  I  F  R  I  L  A  G  I  L  H  580

XM_00651  TTAGGCAATGTTGGATTTGCATCTCGGGATTCAGACAGCTGCACAATACCTCCCAAGCAC 1062
M5-Avi    TTAGGCAATGTTGGATTTGCATCTCGGGATTCAGACAGCTGCACAATACCTCCCAAGCAC 1800
           L  G  N  V  G  F  A  S  R  D  S  D  S  C  T  I  P  P  K  H  600

XM_00651  GAACCTCTTACCATCTTCTGTGACCTTATGGGTGTGGATTATGAAGAGATGTGTCACTGG 1122
M5-Avi    GAACCTCTTACCATCTTCTGTGACCTTATGGGTGTGGATTATGAAGAGATGTGTCACTGG 1860
           E  P  L  T  I  F  C  D  L  M  G  V  D  Y  E  E  M  C  H  W  620

XM_00651  CTCTGCCACCGAAAGCTGGCTACTGCCACAGAGACATACATCAAGCCCATCTCCAAGCTG 1182
M5-Avi    CTCTGCCACCGAAAGCTGGCTACTGCCACAGAGACATACATCAAGCCCATCTCCAAGCTG 1920
           L  C  H  R  K  L  A  T  A  T  E  T  Y  I  K  P  I  S  K  L  640

XM_00651  CAGGCCACAAATGCCCGAGATGCTTTAGCAAAGCACATCTATGCAAAGCTCTTTAACTGG 1242
M5-Avi    CAGGCCACAAATGCCCGAGATGCTTTAGCAAAGCACATCTATGCAAAGCTCTTTAACTGG 1980
           Q  A  T  N  A  R  D  A  L  A  K  H  I  Y  A  K  L  F  N  W  660

XM_00651  ATTGTTGACCACGTCAATCAGGCTCTCCATTCTGCTGTCAAGCAGCACTCTTTCATCGGC 1302
M5-Avi    ATTGTTGACCACGTCAATCAGGCTCTCCATTCTGCTGTCAAGCAGCACTCTTTCATCGGC 2040
           I  V  D  H  V  N  Q  A  L  H  S  A  V  K  Q  H  S  F  I  G  680

XM_00651  GTGCTGGACATCTATGGATTTGAAACATTTGAAATAAATAGTTTTGAACAGTTCTGCATA 1362
M5-Avi    GTGCTGGACATCTATGGATTTGAAACATTTGAAATAAATAGTTTTGAACAGTTCTGCATA 2100
           V  L  D  I  Y  G  F  E  T  F  E  I  N  S  F  E  Q  F  C  I  700

XM_00651  AATTATGCAAATGAAAAACTACAACAACAATTCAACATGCATGTCTTCAAATTGGAACAG 1422
M5-Avi    AATTATGCAAATGAAAAACTACAACAACAATTCAACATGCATGTCTTCAAATTGGAACAG 2160
           N  Y  A  N  E  K  L  Q  Q  Q  F  N  M  H  V  F  K  L  E  Q  720

XM_00651  GAGGAATATATGAAGGAACAGATTCCATGGACACTTATAGATTTCTATGATAATCAGCCT 1482
M5-Avi    GAGGAATATATGAAGGAACAGATTCCATGGACACTTATAGATTTCTATGATAATCAGCCT 2220
           E  E  Y  M  K  E  Q  I  P  W  T  L  I  D  F  Y  D  N  Q  P  740

XM_00651  TGTATCAATCTTATAGAATCTAAACTGGGAATTCTCGATTTGCTGGATGAGGAATGTAAG 1542
M5-Avi    TGTATCAATCTTATAGAATCTAAACTGGGAATTCTCGATTTGCTGGATGAGGAATGTAAG 2280
           C  I  N  L  I  E  S  K  L  G  I  L  D  L  L  D  E  E  C  K  760

XM_00651  ATGCCTAAAGGCACAGATGACACATGGGCCCAAAAACTGTACAACACACATTTGAACAAA 1602
M5-Avi    ATGCCTAAAGGCACAGATGACACATGGGCCCAAAAACTGTACAACACACATTTGAACAAA 2340
           M  P  K  G  T  D  D  T  W  A  Q  K  L  Y  N  T  H  L  N  K  780

XM_00651  TGTGCCCTCTTTGAGAAGCCCCGCATGTCAAACAAAGCTTTCATCATCAAACATTTTGCT 1662
M5-Avi    TGTGCCCTCTTTGAGAAGCCCCGCATGTCAAACAAAGCTTTCATCATCAAACATTTTGCT 2400
           C  A  L  F  E  K  P  R  M  S  N  K  A  F  I  I  K  H  F  A  800

XM_00651  GACAAAGTGGAGTACCAGTGTGAAGGTTTTCTTGAAAAGAATAAAGATACTGTTTTTGAA 1722
M5-Avi    GACAAAGTGGAGTACCAGTGTGAAGGTTTTCTTGAAAAGAATAAAGATACTGTTTTTGAA 2460
           D  K  V  E  Y  Q  C  E  G  F  L  E  K  N  K  D  T  V  F  E  820

XM_00651  GAACAAATTAAAGTCCTTAAGTCAAGCAAGTTTAAGATGCTACCAGAGCTATTTCAAGAT 1782
M5-Avi    GAACAAATTAAAGTCCTTAAGTCAAGCAAGTTTAAGATGCTACCAGAGCTATTTCAAGAT 2520
           E  Q  I  K  V  L  K  S  S  K  F  K  M  L  P  E  L  F  Q  D  840

XM_00651  GATGAGAAGGCCATCAGTCCCACCTCTGCCACCTCCTCAGGGCGCACTCCTCTCACTCGA 1842
M5-Avi    GATGAGAAGGCCATCAGTCCCACCTCTGCCACCTCCTCAGGGCGCACTCCTCTCACTCGA 2580
           D  E  K  A  I  S  P  T  S  A  T  S  S  G  R  T  P  L  T  R  860
```

```
XM_00651  GTTCCTGTAAAGCCCACCAAGGGCCGACCTGGCCAGACTGCCAAAGAGCACAAGAAGACA 1902
M5-Avi    GTTCCTGTAAAGCCCACCAAGGGCCGACCTGGCCAGACTGCCAAAGAGCACAAGAAGACA 2640
           V  P  V  K  P  T  K  G  R  P  G  Q  T  A  K  E  H  K  K  T  880

XM_00651  GTGGGACATCAGTTTCGAAACTCCCTTCACCTGCTTATGGAAACCCTTAATGCCACTACT 1962
M5-Avi    GTGGGACATCAGTTTCGAAACTCCCTTCACCTGCTTATGGAAACCCTTAATGCCACTACT 2700
           V  G  H  Q  F  R  N  S  L  H  L  L  M  E  T  L  N  A  T  T  900

XM_00651  CCTCACTATGTACGCTGTATTAAGCCTAATGATTTCAAGTTTCCATTCACATTTGATGAG 2022
M5-Avi    CCTCACTATGTACGCTGTATTAAGCCTAATGATTTCAAGTTTCCATTCACATTTGATGAG 2760
           P  H  Y  V  R  C  I  K  P  N  D  F  K  F  P  F  T  F  D  E  920

XM_00651  AAGAGGGCAGTGCAGCAGCTAAGAGCATGTGGTGTCCTGGAGACCATCCGGATCAGCGCA 2082
M5-Avi    AAGAGGGCAGTGCAGCAGCTAAGAGCATGTGGTGTCCTGGAGACCATCCGGATCAGCGCA 2820
           K  R  A  V  Q  Q  L  R  A  C  G  V  L  E  T  I  R  I  S  A  940

XM_00651  GCAGGGTTTCCCTCACGGTGGACTTACCAAGAGTTTTTCAGCCGGTACCGGGTCCTAATG 2142
M5-Avi    GCAGGGTTTCCCTCACGGTGGACTTACCAAGAGTTTTTCAGCCGGTACCGGGTCCTAATG 2880
           A  G  F  P  S  R  W  T  Y  Q  E  F  F  S  R  Y  R  V  L  M  960

XM_00651  AAGCAAAAAGATGTGCTGGGAGATAGAAAGCAAACGTGCAAGAATGTATTAGAGAAACTA 2202
M5-Avi    AAGCAAAAAGATGTGCTGGGAGATAGAAAGCAAACGTGCAAGAATGTATTAGAGAAACTA 2940
           K  Q  K  D  V  L  G  D  R  K  Q  T  C  K  N  V  L  E  K  L  980

XM_00651  ATATTGGACAAGGATAAATACCAGTTTGGTAAGACAAAGATCTTTTTCCGTGCTGGTCAA 2262
M5-Avi    ATATTGGACAAGGATAAATACCAGTTTGGTAAGACAAAGATCTTTTTCCGTGCTGGTCAA 3000
           I  L  D  K  D  K  Y  Q  F  G  K  T  K  I  F  F  R  A  G  Q  1000

XM_00651  GTGGCCTATCTTGAAAAATTGAGGGCTGACAAACTTCGGGCTGCCTGCATCCGGATCCAG 2322
M5-Avi    GTGGCCTATCTTGAAAAATTGAGGGCTGACAAACTTCGGGCTGCCTGCATCCGGATCCAG 3060
           V  A  Y  L  E  K  L  R  A  D  K  L  R  A  A  C  I  R  I  Q  1020

XM_00651  AAGACCATTCGTGGGTGGCTTCTAAGGAAGAGATACCTGTGTATGCAGAGGGCAGCCATC 2382
M5-Avi    AAGACCATTCGTGGGTGGCTTCTAAGGAAGAGATACCTGTGTATGCAGAGGGCAGCCATC 3120
           K  T  I  R  G  W  L  L  R  K  R  Y  L  C  M  Q  R  A  A  I  1040

XM_00651  ACAGTGCAGCGATACGTGCGGGGCTATCAGGCTCGATGCTATGCTAAGTTTCTGCGCAGA 2442
M5-Avi    ACAGTGCAGCGATACGTGCGGGGCTATCAGGCTCGATGCTATGCTAAGTTTCTGCGCAGA 3180
           T  V  Q  R  Y  V  R  G  Y  Q  A  R  C  Y  A  K  F  L  R  R  1060

XM_00651  ACCAAGGCAGCAACCACCATTCAAAAGTACTGGCGCATGTATGTGGTCCGCAGGAGGTAC 2502
M5-Avi    ACCAAGGCAGCAACCACCATTCAAAAGTACTGGCGCATGTATGTGGTCCGCAGGAGGTAC 3240
           T  K  A  A  T  T  I  Q  K  Y  W  R  M  Y  V  V  R  R  R  Y  1080

XM_00651  AAGATTAGACGAGCTGCCACGATTGTTATTCAGTCTTACTTGAGAGGCTACTTGACAAGA 2562
M5-Avi    AAGATTAGACGAGCTGCCACGATTGTTATTCAGTCTTACTTGAGAGGCTACTTGACAAGA 3300
           K  I  R  R  A  A  T  I  V  I  Q  S  Y  L  R  G  Y  L  T  R  1100

XM_00651  AATAGGTATCGCAAGATACTCCGTGAATACAAAGCAGTCATCATTCAGAAACGTGTCCGT 2622
M5-Avi    AATAGGTATCGCAAGATACTCCGTGAATACAAAGCAGTCATCATTCAGAAACGTGTCCGT 3360
           N  R  Y  R  K  I  L  R  E  Y  K  A  V  I  I  Q  K  R  V  R  1120

XM_00651  GGCTGGCTGGCCCGTACACATTATAAGAGGACCATGAAAGCCATCGTCTACCTTCAGTGC 2682
M5-Avi    GGCTGGCTGGCCCGTACACATTATAAGAGGACCATGAAAGCCATCGTCTACCTTCAGTGC 3420
           G  W  L  A  R  T  H  Y  K  R  T  M  K  A  I  V  Y  L  Q  C  1140

XM_00651  TGCTTCCGGCGGATGATGGCCAAGCGTGAGCTGAAGAAACTCAAAATTGAGGCTCGCTCT 2742
M5-Avi    TGCTTCCGGCGGATGATGGCCAAGCGTGAGCTGAAGAAACTCAAAATTGAGGCTCGCTCT 3480
           C  F  R  R  M  M  A  K  R  E  L  K  K  L  K  I  E  A  R  S  1160
```

```
XM_00651   GTGGAACGCTACAAGAAGCTCCATATTGGCATGGAGAACAAGATTATGCAGCTGCAGCGC 2802
M5-Avi     GTGGAACGCTACAAGAAGCTCCATATTGGCATGGAGAACAAGATTATGCAGCTGCAGCGC 3540
             V  E  R  Y  K  K  L  H  I  G  M  E  N  K  I  M  Q  L  Q  R  1180

XM_00651   AAAGTGGATGAGCAGAATAAAGACTACAAATGCCTCATGGAGAAACTGACCAATCTGGAA 2862
M5-Avi     AAAGTGGATGAGCAGAATAAAGACTACAAATGCCTCATGGAGAAACTGACCAATCTGGAA 3600
             K  V  D  E  Q  N  K  D  Y  K  C  L  M  E  K  L  T  N  L  E  1200

XM_00651   GGAGTATACAACTCTGAGACTGAAAAACTACGAAATGATGTAGAACGTCTTCAGCTAAGT 2922
M5-Avi     GGAGTATACAACTCTGAGACTGAAAAACTACGAAATGATGTAGAACGTCTTCAGCTAAGT 3660
             G  V  Y  N  S  E  T  E  K  L  R  N  D  V  E  R  L  Q  L  S  1220

XM_00651   GAAGAGGAAGCTAAGGTTGCCACTGGGCGGGTCCTTAGTCTGCAGGAAGAAATTGCAAAA 2982
M5-Avi     GAAGAGGAAGCTAAGGTTGCCACTGGGCGGGTCCTTAGTCTGCAGGAAGAAATTGCAAAA 3720
             E  E  E  A  K  V  A  T  G  R  V  L  S  L  Q  E  E  I  A  K  1240

XM_00651   CTCCGAAAAGACCTGGAACAAACTCGATCAGAGAAAAAGTCTATTGAAGAAAGAGCAGAT 3042
M5-Avi     CTCCGAAAAGACCTGGAACAAACTCGATCAGAGAAAAAGTCTATTGAAGAAAGAGCAGAT 3780
             L  R  K  D  L  E  Q  T  R  S  E  K  K  S  I  E  E  R  A  D  1260

XM_00651   AAATACAAACAAGAAACTGACCAGCTGGTGTCAAACTTGAAGGAAGAAAATACTTTGCTG 3102
M5-Avi     AAATACAAACAAGAAACTGACCAGCTGGTGTCAAACTTGAAGGAAGAAAATACTTTGCTG 3840
             K  Y  K  Q  E  T  D  Q  L  V  S  N  L  K  E  E  N  T  L  L  1280

XM_00651   AAGCAGGAAAAGGAGACCCTCAACCACCGCATTGTGGAGCAGGCGAAGGAGATGACAGAA 3162
M5-Avi     AAGCAGGAAAAGGAGACCCTCAACCACCGCATTGTGGAGCAGGCGAAGGAGATGACAGAA 3900
             K  Q  E  K  E  T  L  N  H  R  I  V  E  Q  A  K  E  M  T  E  1300

XM_00651   ACTATGGAGAGGAAGTTAGTAGAAGAGACAAAACAACTGGAGCTTGACCTGAATGATGAG 3222
M5-Avi     ACTATGGAGAGGAAGTTAGTAGAAGAGACAAAACAACTGGAGCTTGACCTGAATGATGAG 3960
             T  M  E  R  K  L  V  E  E  T  K  Q  L  E  L  D  L  N  D  E  1320

XM_00651   AGGCTGAGGTATCAGAACCTTCTGAATGAGTTCAGTCGCCTGGAGGAGCGCTATGATGAC 3282
M5-Avi     AGGCTGAGGTATCAGAACCTTCTGAATGAGTTCAGTCGCCTGGAGGAGCGCTATGATGAC 4020
             R  L  R  Y  Q  N  L  L  N  E  F  S  R  L  E  E  R  Y  D  D  1340

XM_00651   CTCAAGGAAGAGATGACCCTGATGCTGAATGTGCCTAAGCCAGGACACAAGAGAACAGAC 3342
M5-Avi     CTCAAGGAAGAGATGACCCTGATGCTGAATGTGCCTAAGCCAGGACACAAGAGAACAGAC 4080
             L  K  E  E  M  T  L  M  L  N  V  P  K  P  G  H  K  R  T  D  1360

XM_00651   TCTACCCACAGCAGTAATGAGTCTGAATACACCTTCAGCTCTGAGTTTGCAGAAACTGAA 3402
M5-Avi     TCTACCCACAGCAGTAATGAGTCTGAATACACCTTCAGCTCTGAGTTTGCAGAAACTGAA 4140
             S  T  H  S  S  N  E  S  E  Y  T  F  S  S  E  F  A  E  T  E  1380

XM_00651   GACATTGCACCAAGAACAGAGGAGCCAATTGAGAAGAAGGTGCCTCTGGATATGTCACTA 3462
M5-Avi     GACATTGCACCAAGAACAGAGGAGCCAATTGAGAAGAAGGTGCCTCTGGATATGTCACTA 4200
             D  I  A  P  R  T  E  E  P  I  E  K  K  V  P  L  D  M  S  L  1400

XM_00651   TTCCTTAAGCTCCAGAAGCGTGTCACAGAGCTGGAACAGGAGAAGCAGCTGATGCAGGAT 3522
M5-Avi     TTCCTTAAGCTCCAGAAGCGTGTCACAGAGCTGGAACAGGAGAAGCAGCTGATGCAGGAT 4260
             F  L  K  L  Q  K  R  V  T  E  L  E  Q  E  K  Q  L  M  Q  D  1420

XM_00651   GAGCTGGACCGCAAGGAGGAGCAGGTGTTCCGCAGCAAGGCAAAGGAAGAAGAAAGGCCA 3582
M5-Avi     GAGCTGGACCGCAAGGAGGAGCAGGTGTTCCGCAGCAAGGCAAAGGAAGAAGAAAGGCCA 4320
             E  L  D  R  K  E  E  Q  V  F  R  S  K  A  K  E  E  E  R  P  1440

XM_00651   CAGATAAGAGGAGCTGAACTAGAGTATGAGTCTCTCAAGCGTCAAGAACTGGAGTCAGAA 3642
M5-Avi     CAGATAAGAGGAGCTGAACTAGAGTATGAGTCTCTCAAGCGTCAAGAACTGGAGTCAGAA 4380
             Q  I  R  G  A  E  L  E  Y  E  S  L  K  R  Q  E  L  E  S  E  1460
```

```
XM_00651   AACAAAAAACTGAAAAACGAGCTGAATGAGTTGCGCAAAGCCCTCAGTGAGAAAAGTGCC 3702
M5-Avi     AACAAAAAACTGAAAAACGAGCTGAATGAGTTGCGCAAAGCCCTCAGTGAGAAAAGTGCC 4440
            N  K  K  L  K  N  E  L  N  E  L  R  K  A  L  S  E  K  S  A  1480

XM_00651   CCAGAAGTGACTGCGCCAGGTGCGCCTGCTTACCGAGTCCTCATGGAACAGCTGACCTCC 3762
M5-Avi     CCAGAAGTGACTGCGCCAGGTGCGCCTGCTTACCGAGTCCTCATGGAACAGCTGACCTCC 4500
            P  E  V  T  A  P  G  A  P  A  Y  R  V  L  M  E  Q  L  T  S  1500

XM_00651   GTGAGCGAGGAGCTCGACGTGCGCAAGGAGGAAGTCCTCATCTTGAGGTCGCAGCTGGTG 3822
M5-Avi     GTGAGCGAGGAGCTCGACGTGCGCAAGGAGGAAGTCCTCATCTTGAGGTCGCAGCTGGTG 4560
            V  S  E  E  L  D  V  R  K  E  E  V  L  I  L  R  S  Q  L  V  1520

XM_00651   AGCCAAAAAGAAGCCATCCAACCCAAGGATGACAAGAATACAATGACAGATTCCACAATT 3882
M5-Avi     AGCCAAAAAGAAGCCATCCAACCCAAGGATGACAAGAATACAATGACAGATTCCACAATT 4620
            S  Q  K  E  A  I  Q  P  K  D  D  K  N  T  M  T  D  S  T  I  1540

XM_00651   CTTTTAGAAGATGTACAGAAAATGAAAGACAAAGGTGAAATAGCACAAGCATATATTGGT 3942
M5-Avi     CTTTTAGAAGATGTACAGAAAATGAAAGACAAAGGTGAAATAGCACAAGCATATATTGGT 4680
            L  L  E  D  V  Q  K  M  K  D  K  G  E  I  A  Q  A  Y  I  G  1560

XM_00651   TTGAAAGAAACAAACAGGCTCTTAGAATCCCAGCTACAGTCACAGAAAAGAAGCCATGAG 4002
M5-Avi     TTGAAAGAAACAAACAGGCTCTTAGAATCCCAGCTACAGTCACAGAAAAGAAGCCATGAG 4740
            L  K  E  T  N  R  L  L  E  S  Q  L  Q  S  Q  K  R  S  H  E  1580

XM_00651   AATGAGGCTGAGGCCCTCCGTGGGGAGATCCAGAGCCTAAAGGAAGAAAACAACCGGCAA 4062
M5-Avi     AATGAGGCTGAGGCCCTCCGTGGGGAGATCCAGAGCCTAAAGGAAGAAAACAACCGGCAA 4800
            N  E  A  E  A  L  R  G  E  I  Q  S  L  K  E  E  N  N  R  Q  1600

XM_00651   CAGCAGCTGCTGGCCCAGAACCTGCAGCTGCCCCCTGAGGCCCGCATTGAGGCCAGCCTG 4122
M5-Avi     CAGCAGCTGCTGGCCCAGAACCTGCAGCTGCCCCCTGAGGCCCGCATTGAGGCCAGCCTG 4860
            Q  Q  L  L  A  Q  N  L  Q  L  P  P  E  A  R  I  E  A  S  L  1620

XM_00651   CAGCATGAGATCACCCGGCTGACCAATGAAAACCTGGATCTGATGGAACAACTTGAAAAG 4182
M5-Avi     CAGCATGAGATCACCCGGCTGACCAATGAAAACCTGGATCTGATGGAACAACTTGAAAAG 4920
            Q  H  E  I  T  R  L  T  N  E  N  L  D  L  M  E  Q  L  E  K  1640

XM_00651   CAGGATAAAACTGTCCGGAAACTGAAGAAACAACTGAAAGTCTTTGCCAAAAAAATTGGT 4242
M5-Avi     CAGGATAAAACTGTCCGGAAACTGAAGAAACAACTGAAAGTCTTTGCCAAAAAAATTGGT 4980
            Q  D  K  T  V  R  K  L  K  K  Q  L  K  V  F  A  K  K  I  G  1660

XM_00651   GAACTAGAAGTGGGGCAGATGGAGAACATATCTCCAGGACAGATCATCGATGAGCCTATC 4302
M5-Avi     GAACTAGAAGTGGGGCAGATGGAGAACATATCTCCAGGACAGATCATCGATGAGCCTATC 5040
            E  L  E  V  G  Q  M  E  N  I  S  P  G  Q  I  I  D  E  P  I  1680

XM_00651   CGGCCAGTCAACATTCCC----------------------------------------- 4320
M5-Avi     CGGCCAGTCAACATTCCCGGCCTGAATGATATTTTTGAAGCGCAGAAAATTGAATGGCAT 5100
            R  P  V  N  I  P  G  L  N  D  I  F  E  A  Q  K  I  E  W  H  1700

XM_00651   ------------------------------------------------------------
M5-Avi     GAAAGGCCTACGTCGACGAGCTCACTAGTCGCGGCCGCAGACTACAAGGACGACGATGAT 5160
           E  R  P  T  S  T  S  S  L  V  A  A  A  D  Y  K  D  D  D  D  1720

XM_00651   ------
M5-Avi     AAGTAG 5166
           K  X   1721
```

S3. Amino acid sequence of Myosin-5-cc construct

Sequence alignment was performed using the ClustalW webserver (Larkin et al., 2007). First line shows the DNA sequence of the brain isoform of mouse myosin-5a (NCBI Reference Sequence: XM_006510832.3). Second line shows the DNA sequence of the Myosin-5-cc construct. Third line shows the amino acid sequence corresponding to the Myosin-5-cc construct. Colouring of the amino acid sequence represents the distinct domains and motifs of the protein according to the legend. Numbers at the end of the lines represent the number of nucleic acids or amino acids up to that point in the sequence.

Legend:

GFP
Restriction sites: BssH II, EcoR I and Stu I
Mouse myosin-5a brain isoform with the whole coiled-coil domain, with additional 175 amino acid coiled-coil
Avi-tag
Restriction sites: Stu I, Sal I, Sst I, Spe I and Not I
Flag tag

```
XM_00651  ------------------------------------------------------------
M5-cc     ATGGTGAGCAAGGGCGAGGAGCTGTTCACCGGGGTGGTGCCCATCCTGGTCGAGCTGGAC 60
           M  V  S  K  G  E  E  L  F  T  G  V  V  P  I  L  V  E  L  D  20

XM_00651  ------------------------------------------------------------
M5-cc     GGCGACGTAAACGGCCACAAGTTCAGCGTGTCCGGCGAGGGCGAGGGCGATGCCACCTAC 120
           G  D  V  N  G  H  K  F  S  V  S  G  E  G  E  G  D  A  T  Y  40

XM_00651  ------------------------------------------------------------
M5-cc     GGCAAGCTGACCCTGAAGTTCATCTGCACCACCGGCAAGCTGCCCGTGCCCTGGCCCACC 180
           G  K  L  T  L  K  F  I  C  T  T  G  K  L  P  V  P  W  P  T  60

XM_00651  ------------------------------------------------------------
M5-cc     CTCGTGACCACCCTGACCTACGGCGTGCAGTGCTTCAGCCGCTACCCCGACCACATGAAG 240
           L  V  T  T  L  T  Y  G  V  Q  C  F  S  R  Y  P  D  H  M  K  80

XM_00651  ------------------------------------------------------------
M5-cc     CAGCACGACTTCTTCAAGTCCGCCATGCCCGAAGGCTACGTCCAGGAGCGCACCATCTTC 300
           Q  H  D  F  F  K  S  A  M  P  E  G  Y  V  Q  E  R  T  I  F  100

XM_00651  ------------------------------------------------------------
M5-cc     TTCAAGGACGACGGCAACTACAAGACCCGCGCCGAGGTGAAGTTCGAGGGCGACACCCTG 360
           F  K  D  D  G  N  Y  K  T  R  A  E  V  K  F  E  G  D  T  L  120

XM_00651  ------------------------------------------------------------
M5-cc     GTGAACCGCATCGAGCTGAAGGGCATCGACTTCAAGGAGGACGGCAACATCCTGGGGCAC 420
           V  N  R  I  E  L  K  G  I  D  F  K  E  D  G  N  I  L  G  H  140

XM_00651  ------------------------------------------------------------
M5-cc     AAGCTGGAGTACAACTACAACAGCCACAACGTCTATATCATGGCCGACAAGCAGAAGAAC 480
           K  L  E  Y  N  Y  N  S  H  N  V  Y  I  M  A  D  K  Q  K  N  160
```

```
XM_00651  ------------------------------------------------------------
M5-cc     GGCATCAAGGTGAACTTCAAGATCCGCCACAACATCGAGGACGGCAGCGTGCAGCTCGCC 540
          G  I  K  V  N  F  K  I  R  H  N  I  E  D  G  S  V  Q  L  A  180

XM_00651  ------------------------------------------------------------
M5-cc     GACCACTACCAGCAGAACACCCCCATCGGCGACGGCCCCGTGCTGCTGCCCGACAACCAC 600
          D  H  Y  Q  Q  N  T  P  I  G  D  G  P  V  L  L  P  D  N  H  200

XM_00651  ------------------------------------------------------------
M5-cc     TACCTGAGCACCCAGTCCGCCCTGAGCAAAGACCCCAACGAGAAGCGCGATCACATGGTC 660
          Y  L  S  T  Q  S  A  L  S  K  D  P  N  E  K  R  D  H  M  V  220

XM_00651  ------------------------------------------------------------
M5-cc     CTGCTGGAGTTCGTGACCGCCGCCGGGATCACTCTCGGCATGGACGAGCTGTACAAGGCG 720
          L  L  E  F  V  T  A  A  G  I  T  L  G  M  D  E  L  Y  K  A  240

XM_00651  ------------------ATGGCCGCGTCCGAGCTCTACACCAAGTTTGCCAGGGTTTGG  42
M5-cc     CGCGGAATTCAAAGGCCTATGGCCGCGTCCGAGCTCTACACCAAGTTTGCCAGGGTTTGG 780
          R  G  I  Q  R  P  M  A  A  S  E  L  Y  T  K  F  A  R  V  W  260

XM_00651  ATCCCTGATCCTGAGGAAGTGTGGAAATCGGCAGAGTTGCTCAAGGATTATAAGCCTGGA 102
M5-cc     ATCCCTGATCCTGAGGAAGTGTGGAAATCGGCAGAGTTGCTCAAGGATTATAAGCCTGGA 840
           I  P  D  P  E  E  V  W  K  S  A  E  L  L  K  D  Y  K  P  G  280

XM_00651  GATAAAGTGCTCCTGCTTCACCTCGAGGAAGGGAAGGATTTGGAATACCGTCTAGACCCA 162
M5-cc     GATAAAGTGCTCCTGCTTCACCTCGAGGAAGGGAAGGATTTGGAATACCGTCTAGACCCA 900
           D  K  V  L  L  L  H  L  E  E  G  K  D  L  E  Y  R  L  D  P  300

XM_00651  AAGACCGGTGAGCTCCCTCACTTACGGAACCCTGACATACTTGTTGGAGAAAATGACCTC 222
M5-cc     AAGACCGGTGAGCTCCCTCACTTACGGAACCCTGACATACTTGTTGGAGAAAATGACCTC 960
           K  T  G  E  L  P  H  L  R  N  P  D  I  L  V  G  E  N  D  L  320

XM_00651  ACAGCCCTCAGCTACCTTCACGAGCCCGCTGTGCTACATAATCTCCGAGTTCGCTTCATC 282
M5-cc     ACAGCCCTCAGCTACCTTCACGAGCCCGCTGTGCTACATAATCTCCGAGTTCGCTTCATC 1020
           T  A  L  S  Y  L  H  E  P  A  V  L  H  N  L  R  V  R  F  I  340

XM_00651  GATTCCAAACTTATTTATACGTATTGTGGAATAGTTCTGGTAGCTATAAATCCCTATGAG 342
M5-cc     GATTCCAAACTTATTTATACGTATTGTGGAATAGTTCTGGTAGCTATAAATCCCTATGAG 1080
           D  S  K  L  I  Y  T  Y  C  G  I  V  L  V  A  I  N  P  Y  E  360

XM_00651  CAGCTGCCTATTTATGGAGAAGATATTATTAATGCCTACAGTGGCCAGAACATGGGTGAC 402
M5-cc     CAGCTGCCTATTTATGGAGAAGATATTATTAATGCCTACAGTGGCCAGAACATGGGTGAC 1140
           Q  L  P  I  Y  G  E  D  I  I  N  A  Y  S  G  Q  N  M  G  D  380

XM_00651  ATGGATCCTCACATCTTCGCAGTAGCTGAAGAGGCTTACAAGCAAATGGCAAGGGATGAA 462
M5-cc     ATGGATCCTCACATCTTCGCAGTAGCTGAAGAGGCTTACAAGCAAATGGCAAGGGATGAA 1200
           M  D  P  H  I  F  A  V  A  E  E  A  Y  K  Q  M  A  R  D  E  400

XM_00651  CGAAATCAGTCCATCATTGTAAGTGGAGAGTCAGGCGCAGGGAAGACGGTCTCTGCTAAG 522
M5-cc     CGAAATCAGTCCATCATTGTAAGTGGAGAGTCAGGCGCAGGGAAGACGGTCTCTGCTAAG 1260
           R  N  Q  S  I  I  V  S  G  E  S  G  A  G  K  T  V  S  A  K  420

XM_00651  TATGCCATGCGGTACTTCGCAACTGTAAGTGGCTCTGCCAGTGAGGCCAATGTTGAGGAA 582
M5-cc     TATGCCATGCGGTACTTCGCAACTGTAAGTGGCTCTGCCAGTGAGGCCAATGTTGAGGAA 1320
           Y  A  M  R  Y  F  A  T  V  S  G  S  A  S  E  A  N  V  E  E  440

XM_00651  AAGGTCTTGGCCTCCAACCCCATCATGGAGTCAATTGGAAATGCCAAAACAACCAGGAAT 642
M5-cc     AAGGTCTTGGCCTCCAACCCCATCATGGAGTCAATTGGAAATGCCAAAACAACCAGGAAT 1380
           K  V  L  A  S  N  P  I  M  E  S  I  G  N  A  K  T  T  R  N  460
```

```
XM_00651  GATAATAGCAGCCGGTTTGGAAAATATATTGAAATTGGTTTTGACAAGAGGTACAGAATC 702
M5-cc     GATAATAGCAGCCGGTTTGGAAAATATATTGAAATTGGTTTTGACAAGAGGTACAGAATC 1440
           D  N  S  S  R  F  G  K  Y  I  E  I  G  F  D  K  R  Y  R  I  480

XM_00651  ATCGGTGCCAATATGAGAACTTACCTTTTAGAGAAATCCAGAGTGGTGTTCCAGGCAGAA 762
M5-cc     ATCGGTGCCAATATGAGAACTTACCTTTTAGAGAAATCCAGAGTGGTGTTCCAGGCAGAA 1500
           I  G  A  N  M  R  T  Y  L  L  E  K  S  R  V  V  F  Q  A  E  500

XM_00651  GAGGAGAGAAACTACCATATCTTCTATCAGCTCTGTGCTTCGGCAAAGTTACCTGAGTTT 822
M5-cc     GAGGAGAGAAACTACCATATCTTCTATCAGCTCTGTGCTTCGGCAAAGTTACCTGAGTTT 1560
           E  E  R  N  Y  H  I  F  Y  Q  L  C  A  S  A  K  L  P  E  F  520

XM_00651  AAAATGCTGCGGTTAGGAAATGCAGATAGTTTTCATTACACGAAGCAAGGAGGCAGCCCT 882
M5-cc     AAAATGCTGCGGTTAGGAAATGCAGATAGTTTTCATTACACGAAGCAAGGAGGCAGCCCT 1620
           K  M  L  R  L  G  N  A  D  S  F  H  Y  T  K  Q  G  G  S  P  540

XM_00651  ATGATAGAAGGAGTAGATGATGCGAAGGAGATGGCGCACACCAGGCAGGCCTGCACTCTG 942
M5-cc     ATGATAGAAGGAGTAGATGATGCGAAGGAGATGGCGCACACCAGGCAGGCCTGCACTCTG 1680
           M  I  E  G  V  D  D  A  K  E  M  A  H  T  R  Q  A  C  T  L  560

XM_00651  CTGGGAATTAGTGAATCTTACCAAATGGGAATTTTTCGAATACTTGCTGGCATTCTTCAC 1002
M5-cc     CTGGGAATTAGTGAATCTTACCAAATGGGAATTTTTCGAATACTTGCTGGCATTCTTCAC 1740
           L  G  I  S  E  S  Y  Q  M  G  I  F  R  I  L  A  G  I  L  H  580

XM_00651  TTAGGCAATGTTGGATTTGCATCTCGGGATTCAGACAGCTGCACAATACCTCCCAAGCAC 1062
M5-cc     TTAGGCAATGTTGGATTTGCATCTCGGGATTCAGACAGCTGCACAATACCTCCCAAGCAC 1800
           L  G  N  V  G  F  A  S  R  D  S  D  S  C  T  I  P  P  K  H  600

XM_00651  GAACCTCTTACCATCTTCTGTGACCTTATGGGTGTGGATTATGAAGAGATGTGTCACTGG 1122
M5-cc     GAACCTCTTACCATCTTCTGTGACCTTATGGGTGTGGATTATGAAGAGATGTGTCACTGG 1860
           E  P  L  T  I  F  C  D  L  M  G  V  D  Y  E  E  M  C  H  W  620

XM_00651  CTCTGCCACCGAAAGCTGGCTACTGCCACAGAGACATACATCAAGCCCATCTCCAAGCTG 1182
M5-cc     CTCTGCCACCGAAAGCTGGCTACTGCCACAGAGACATACATCAAGCCCATCTCCAAGCTG 1920
           L  C  H  R  K  L  A  T  A  T  E  T  Y  I  K  P  I  S  K  L  640

XM_00651  CAGGCCACAAATGCCCGAGATGCTTTAGCAAAGCACATCTATGCAAAGCTCTTTAACTGG 1242
M5-cc     CAGGCCACAAATGCCCGAGATGCTTTAGCAAAGCACATCTATGCAAAGCTCTTTAACTGG 1980
           Q  A  T  N  A  R  D  A  L  A  K  H  I  Y  A  K  L  F  N  W  660

XM_00651  ATTGTTGACCACGTCAATCAGGCTCTCCATTCTGCTGTCAAGCAGCACTCTTTCATCGGC 1302
M5-cc     ATTGTTGACCACGTCAATCAGGCTCTCCATTCTGCTGTCAAGCAGCACTCTTTCATCGGC 2040
           I  V  D  H  V  N  Q  A  L  H  S  A  V  K  Q  H  S  F  I  G  680

XM_00651  GTGCTGGACATCTATGGATTTGAAACATTTGAAATAAATAGTTTTGAACAGTTCTGCATA 1362
M5-cc     GTGCTGGACATCTATGGATTTGAAACATTTGAAATAAATAGTTTTGAACAGTTCTGCATA 2100
           V  L  D  I  Y  G  F  E  T  F  E  I  N  S  F  E  Q  F  C  I  700

XM_00651  AATTATGCAAATGAAAAACTACAACAACAATTCAACATGCATGTCTTCAAATTGGAACAG 1422
M5-cc     AATTATGCAAATGAAAAACTACAACAACAATTCAACATGCATGTCTTCAAATTGGAACAG 2160
           N  Y  A  N  E  K  L  Q  Q  Q  F  N  M  H  V  F  K  L  E  Q  720

XM_00651  GAGGAATATATGAAGGAACAGATTCCATGGACACTTATAGATTTCTATGATAATCAGCCT 1482
M5-cc     GAGGAATATATGAAGGAACAGATTCCATGGACACTTATAGATTTCTATGATAATCAGCCT 2220
           E  E  Y  M  K  E  Q  I  P  W  T  L  I  D  F  Y  D  N  Q  P  740

XM_00651  TGTATCAATCTTATAGAATCTAAACTGGGAATTCTCGATTTGCTGGATGAGGAATGTAAG 1542
M5-cc     TGTATCAATCTTATAGAATCTAAACTGGGAATTCTCGATTTGCTGGATGAGGAATGTAAG 2280
           C  I  N  L  I  E  S  K  L  G  I  L  D  L  L  D  E  E  C  K  760
```

```
XM_00651  ATGCCTAAAGGCACAGATGACACATGGGCCCAAAAACTGTACAACACACATTTGAACAAA 1602
M5-cc     ATGCCTAAAGGCACAGATGACACATGGGCCCAAAAACTGTACAACACACATTTGAACAAA 2340
           M  P  K  G  T  D  D  T  W  A  Q  K  L  Y  N  T  H  L  N  K  780

XM_00651  TGTGCCCTCTTTGAGAAGCCCCGCATGTCAAACAAAGCTTTCATCATCAAACATTTTGCT 1662
M5-cc     TGTGCCCTCTTTGAGAAGCCCCGCATGTCAAACAAAGCTTTCATCATCAAACATTTTGCT 2400
           C  A  L  F  E  K  P  R  M  S  N  K  A  F  I  I  K  H  F  A  800

XM_00651  GACAAAGTGGAGTACCAGTGTGAAGGTTTTCTTGAAAAGAATAAAGATACTGTTTTTGAA 1722
M5-cc     GACAAAGTGGAGTACCAGTGTGAAGGTTTTCTTGAAAAGAATAAAGATACTGTTTTTGAA 2460
           D  K  V  E  Y  Q  C  E  G  F  L  E  K  N  K  D  T  V  F  E  820

XM_00651  GAACAAATTAAAGTCCTTAAGTCAAGCAAGTTTAAGATGCTACCAGAGCTATTTCAAGAT 1782
M5-cc     GAACAAATTAAAGTCCTTAAGTCAAGCAAGTTTAAGATGCTACCAGAGCTATTTCAAGAT 2520
           E  Q  I  K  V  L  K  S  S  K  F  K  M  L  P  E  L  F  Q  D  840

XM_00651  GATGAGAAGGCCATCAGTCCCACCTCTGCCACCTCCTCAGGGCGCACTCCTCTCACTCGA 1842
M5-cc     GATGAGAAGGCCATCAGTCCCACCTCTGCCACCTCCTCAGGGCGCACTCCTCTCACTCGA 2580
           D  E  K  A  I  S  P  T  S  A  T  S  S  G  R  T  P  L  T  R  860

XM_00651  GTTCCTGTAAAGCCCACCAAGGGCCGACCTGGCCAGACTGCCAAAGAGCACAAGAAGACA 1902
M5-cc     GTTCCTGTAAAGCCCACCAAGGGCCGACCTGGCCAGACTGCCAAAGAGCACAAGAAGACA 2640
           V  P  V  K  P  T  K  G  R  P  G  Q  T  A  K  E  H  K  K  T  880

XM_00651  GTGGGACATCAGTTTCGAAACTCCCTTCACCTGCTTATGGAAACCCTTAATGCCACTACT 1962
M5-cc     GTGGGACATCAGTTTCGAAACTCCCTTCACCTGCTTATGGAAACCCTTAATGCCACTACT 2700
           V  G  H  Q  F  R  N  S  L  H  L  L  M  E  T  L  N  A  T  T  900

XM_00651  CCTCACTATGTACGCTGTATTAAGCCTAATGATTTCAAGTTTCCATTCACATTTGATGAG 2022
M5-cc     CCTCACTATGTACGCTGTATTAAGCCTAATGATTTCAAGTTTCCATTCACATTTGATGAG 2760
           P  H  Y  V  R  C  I  K  P  N  D  F  K  F  P  F  T  F  D  E  920

XM_00651  AAGAGGGCAGTGCAGCAGCTAAGAGCATGTGGTGTCCTGGAGACCATCCGGATCAGCGCA 2082
M5-cc     AAGAGGGCAGTGCAGCAGCTAAGAGCATGTGGTGTCCTGGAGACCATCCGGATCAGCGCA 2820
           K  R  A  V  Q  Q  L  R  A  C  G  V  L  E  T  I  R  I  S  A  940

XM_00651  GCAGGGTTTCCCTCACGGTGGACTTACCAAGAGTTTTTCAGCCGGTACCGGGTCCTAATG 2142
M5-cc     GCAGGGTTTCCCTCACGGTGGACTTACCAAGAGTTTTTCAGCCGGTACCGGGTCCTAATG 2880
           A  G  F  P  S  R  W  T  Y  Q  E  F  F  S  R  Y  R  V  L  M  960

XM_00651  AAGCAAAAAGATGTGCTGGGAGATAGAAAGCAAACGTGCAAGAATGTATTAGAGAAACTA 2202
M5-cc     AAGCAAAAAGATGTGCTGGGAGATAGAAAGCAAACGTGCAAGAATGTATTAGAGAAACTA 2940
           K  Q  K  D  V  L  G  D  R  K  Q  T  C  K  N  V  L  E  K  L  980

XM_00651  ATATTGGACAAGGATAAATACCAGTTTGGTAAGACAAAGATCTTTTTCCGTGCTGGTCAA 2262
M5-cc     ATATTGGACAAGGATAAATACCAGTTTGGTAAGACAAAGATCTTTTTCCGTGCTGGTCAA 3000
           I  L  D  K  D  K  Y  Q  F  G  K  T  K  I  F  F  R  A  G  Q  1000

XM_00651  GTGGCCTATCTTGAAAAATTGAGGGCTGACAAACTTCGGGCTGCCTGCATCCGGATCCAG 2322
M5-cc     GTGGCCTATCTTGAAAAATTGAGGGCTGACAAACTTCGGGCTGCCTGCATCCGGATCCAG 3060
           V  A  Y  L  E  K  L  R  A  D  K  L  R  A  A  C  I  R  I  Q  1020

XM_00651  AAGACCATTCGTGGGTGGCTTCTAAGGAAGAGATACCTGTGTATGCAGAGGGCAGCCATC 2382
M5-cc     AAGACCATTCGTGGGTGGCTTCTAAGGAAGAGATACCTGTGTATGCAGAGGGCAGCCATC 3120
           K  T  I  R  G  W  L  L  R  K  R  Y  L  C  M  Q  R  A  A  I  1040

XM_00651  ACAGTGCAGCGATACGTGCGGGGCTATCAGGCTCGATGCTATGCTAAGTTTCTGCGCAGA 2442
M5-cc     ACAGTGCAGCGATACGTGCGGGGCTATCAGGCTCGATGCTATGCTAAGTTTCTGCGCAGA 3180
           T  V  Q  R  Y  V  R  G  Y  Q  A  R  C  Y  A  K  F  L  R  R  1060
```

```
XM_00651  ACCAAGGCAGCAACCACCATTCAAAAGTACTGGCGCATGTATGTGGTCCGCAGGAGGTAC 2502
M5-cc     ACCAAGGCAGCAACCACCATTCAAAAGTACTGGCGCATGTATGTGGTCCGCAGGAGGTAC 3240
           T  K  A  A  T  T  I  Q  K  Y  W  R  M  Y  V  V  R  R  R  Y  1080

XM_00651  AAGATTAGACGAGCTGCCACGATTGTTATTCAGTCTTACTTGAGAGGCTACTTGACAAGA 2562
M5-cc     AAGATTAGACGAGCTGCCACGATTGTTATTCAGTCTTACTTGAGAGGCTACTTGACAAGA 3300
           K  I  R  R  A  A  T  I  V  I  Q  S  Y  L  R  G  Y  L  T  R  1100

XM_00651  AATAGGTATCGCAAGATACTCCGTGAATACAAAGCAGTCATCATTCAGAAACGTGTCCGT 2622
M5-cc     AATAGGTATCGCAAGATACTCCGTGAATACAAAGCAGTCATCATTCAGAAACGTGTCCGT 3360
           N  R  Y  R  K  I  L  R  E  Y  K  A  V  I  I  Q  K  R  V  R  1120

XM_00651  GGCTGGCTGGCCCGTACACATTATAAGAGGACCATGAAAGCCATCGTCTACCTTCAGTGC 2682
M5-cc     GGCTGGCTGGCCCGTACACATTATAAGAGGACCATGAAAGCCATCGTCTACCTTCAGTGC 3420
           G  W  L  A  R  T  H  Y  K  R  T  M  K  A  I  V  Y  L  Q  C  1140

XM_00651  TGCTTCCGGCGGATGATGGCCAAGCGTGAGCTGAAGAAACTCAAAATTGAGGCTCGCTCT 2742
M5-cc     TGCTTCCGGCGGATGATGGCCAAGCGTGAGCTGAAGAAACTCAAAATTGAGGCTCGCTCT 3480
           C  F  R  R  M  M  A  K  R  E  L  K  K  L  K  I  E  A  R  S  1160

XM_00651  GTGGAACGCTACAAGAAGCTCCATATTGGCATGGAGAACAAGATTATGCAGCTGCAGCGC 2802
M5-cc     GTGGAACGCTACAAGAAGCTCCATATTGGCATGGAGAACAAGATTATGCAGCTGCAGCGC 3540
           V  E  R  Y  K  K  L  H  I  G  M  E  N  K  I  M  Q  L  Q  R  1180

XM_00651  AAAGTGGATGAGCAGAATAAAGACTACAAATGCCTCATGGAGAAACTGACCAATCTGGAA 2862
M5-cc     AAAGTGGATGAGCAGAATAAAGACTACAAATGCCTCATGGAGAAACTGACCAATCTGGAA 3600
           K  V  D  E  Q  N  K  D  Y  K  C  L  M  E  K  L  T  N  L  E  1200

XM_00651  GGAGTATACAACTCTGAGACTGAAAAACTACGAAATGATGTAGAACGTCTTCAGCTAAGT 2922
M5-cc     GGAGTATACAACTCTGAGACTGAAAAACTACGAAATGATGTAGAACGTCTTCAGCTAAGT 3660
           G  V  Y  N  S  E  T  E  K  L  R  N  D  V  E  R  L  Q  L  S  1220

XM_00651  GAAGAGGAAGCTAAGGTTGCCACTGGGCGGGTCCTTAGTCTGCAGGAAGAAATTGCAAAA 2982
M5-cc     GAAGAGGAAGCTAAGGTTGCCACTGGGCGGGTCCTTAGTCTGCAGGAAGAAATTGCAAAA 3720
           E  E  E  A  K  V  A  T  G  R  V  L  S  L  Q  E  E  I  A  K  1240

XM_00651  CTCCGAAAAGACCTGGAACAAACTCGATCAGAGAAAAAGTCTATTGAAGAAAGAGCAGAT 3042
M5-cc     CTCCGAAAAGACCTGGAACAAACTCGATCAGAGAAAAAGTCTATTGAAGAAAGAGCAGAT 3780
           L  R  K  D  L  E  Q  T  R  S  E  K  K  S  I  E  E  R  A  D  1260

XM_00651  AAATACAAACAAGAAACTGACCAGCTGGTGTCAAACTTGAAGGAAGAAAATACTTTGCTG 3102
M5-cc     AAATACAAACAAGAAACTGACCAGCTGGTGTCAAACTTGAAGGAAGAAAATACTTTGCTG 3840
           K  Y  K  Q  E  T  D  Q  L  V  S  N  L  K  E  E  N  T  L  L  1280

XM_00651  AAGCAGGAAAAGGAGACCCTCAACCACCGCATTGTGGAGCAGGCGAAGGAGATGACAGAA 3162
M5-cc     AAGCAGGAAAAGGAGACCCTCAACCACCGCATTGTGGAGCAGGCGAAGGAGATGACAGAA 3900
           K  Q  E  K  E  T  L  N  H  R  I  V  E  Q  A  K  E  M  T  E  1300

XM_00651  ACTATGGAGAGGAAGTTAGTAGAAGAGACAAAACAACTGGAGCTTGACCTGAATGATGAG 3222
M5-cc     ACTATGGAGAGGAAGTTAGTAGAAGAGACAAAACAACTGGAGCTTGACCTGAATGATGAG 3960
           T  M  E  R  K  L  V  E  E  T  K  Q  L  E  L  D  L  N  D  E  1320

XM_00651  AGGCTGAGGTATCAGAACCTTCTGAATGAGTTCAGTCGCCTGGAGGAGCGC--------- 3273
M5-cc     AGGCTGAGGTATCAGAACCTTCTGAATGAGTTCAGTCGCCTGGAGGAGCGCCGCTACAAG 4020
           R  L  R  Y  Q  N  L  L  N  E  F  S  R  L  E  E  R  R  Y  K  1340

XM_00651  ------------------------------------------------------------
M5-cc     AAGCTCCATATTGGCATGGAGAACAAGATTATGCAGCTGCAGCGCAAAGTGGATGAGCAG 4080
           K  L  H  I  G  M  E  N  K  I  M  Q  L  Q  R  K  V  D  E  Q  1360
```

```
XM_00651  ------------------------------------------------------------
M5-cc     AATAAAGACTACAAATGCCTCATGGAGAAACTGACCAATCTGGAAGGAGTATACAACTCT 4140
          N  K  D  Y  K  C  L  M  E  K  L  T  N  L  E  G  V  Y  N  S  1380

XM_00651  ------------------------------------------------------------
M5-cc     GAGACTGAAAAACTACGAAATGATGTAGAACGTCTTCAGCTAAGTGAAGAGGAAGCTAAG 4200
          E  T  E  K  L  R  N  D  V  E  R  L  Q  L  S  E  E  E  A  K  1400

XM_00651  ------------------------------------------------------------
M5-cc     GTTGCCACTGGGCGGGTCCTTAGTCTGCAGGAAGAAATTGCAAAACTCCGAAAAGACCTG 4260
          V  A  T  G  R  V  L  S  L  Q  E  E  I  A  K  L  R  K  D  L  1420

XM_00651  ------------------------------------------------------------
M5-cc     GAACAAACTCGATCAGAGAAAAAGTCTATTGAAGAAAGAGCAGATAAATACAAACAAGAA 4320
          E  Q  T  R  S  E  K  K  S  I  E  E  R  A  D  K  Y  K  Q  E  1440

XM_00651  ------------------------------------------------------------
M5-cc     ACTGACCAGCTGGTGTCAAACTTGAAGGAAGAAAATACTTTGCTGAAGCAGGAAAAGGAG 4380
          T  D  Q  L  V  S  N  L  K  E  E  N  T  L  L  K  Q  E  K  E  1460

XM_00651  ------------------------------------------------------------
M5-cc     ACCCTCAACCACCGCATTGTGGAGCAGGCGAAGGAGATGACAGAAACTATGGAGAGGAAG 4440
          T  L  N  H  R  I  V  E  Q  A  K  E  M  T  E  T  M  E  R  K  1480

XM_00651  ------------------------------------------------------------
M5-cc     TTAGTAGAAGAGACAAAACAACTGGAGCTTGACCTGAATGATGAGAGGCTGAGGTATCAG 4500
          L  V  E  E  T  K  Q  L  E  L  D  L  N  D  E  R  L  R  Y  Q  1500

XM_00651  ------------------------------------TATGATGACCTCAAGGAAGAGATG 3297
M5-cc     AACCTTCTGAATGAGTTCAGTCGCCTGGAGGAGCGCTATGATGACCTCAAGGAAGAGATG 4560
          N  L  L  N  E  F  S  R  L  E  E  R  Y  D  D  L  K  E  E  M  1520

XM_00651  ACCCTGATGCTGAATGTGCCTAAGCCAGGACACAAGAGAACAGACTCTACCCACAGCAGT 3357
M5-cc     ACCCTGATGCTGAATGTGCCTAAGCCAGGACACAAGAGAACAGACTCTACCCACAGCAGT 4620
          T  L  M  L  N  V  P  K  P  G  H  K  R  T  D  S  T  H  S  S  1540

XM_00651  AATGAGTCTGAATACACCTTCAGCTCTGAGTTTGCAGAAACTGAAGACATTGCACCAAGA 3417
M5-cc     AATGAGTCTGAATACACCTTCAGCTCTGAGTTTGCAGAAACTGAAGACATTGCACCAAGA 4680
          N  E  S  E  Y  T  F  S  S  E  F  A  E  T  E  D  I  A  P  R  1560

XM_00651  ACAGAGGAGCCAATTGAGAAGAAGGTGCCTCTGGATATGTCACTATTCCTTAAGCTCCAG 3477
M5-cc     ACAGAGGAGCCAATTGAGAAGAAGGTGCCTCTGGATATGTCACTATTCCTTAAGCTCCAG 4740
          T  E  E  P  I  E  K  K  V  P  L  D  M  S  L  F  L  K  L  Q  1580

XM_00651  AAGCGTGTCACAGAGCTGGAACAGGAGAAGCAGCTGATGCAGGATGAGCTGGACCGCAAG 3537
M5-cc     AAGCGTGTCACAGAGCTGGAACAGGAGAAGCAGCTGATGCAGGATGAGCTGGACCGCAAG 4800
          K  R  V  T  E  L  E  Q  E  K  Q  L  M  Q  D  E  L  D  R  K  1600

XM_00651  GAGGAGCAGGTGTTCCGCAGCAAGGCAAAGGAAGAAGAAAGGCCACAGATAAGAGGAGCT 3597
M5-cc     GAGGAGCAGGTGTTCCGCAGCAAGGCAAAGGAAGAAGAAAGGCCACAGATAAGAGGAGCT 4860
          E  E  Q  V  F  R  S  K  A  K  E  E  E  R  P  Q  I  R  G  A  1620

XM_00651  GAACTAGAGTATGAGTCTCTCAAGCGTCAAGAACTGGAGTCAGAAAACAAAAAACTGAAA 3657
M5-cc     GAACTAGAGTATGAGTCTCTCAAGCGTCAAGAACTGGAGTCAGAAAACAAAAAACTGAAA 4920
          E  L  E  Y  E  S  L  K  R  Q  E  L  E  S  E  N  K  K  L  K  1640

XM_00651  AACGAGCTGAATGAGTTGCGCAAAGCCCTCAGTGAGAAAAGTGCCCCAGAAGTGACTGCG 3717
M5-cc     AACGAGCTGAATGAGTTGCGCAAAGCCCTCAGTGAGAAAAGTGCCCCAGAAGTGACTGCG 4980
          N  E  L  N  E  L  R  K  A  L  S  E  K  S  A  P  E  V  T  A  1660
```

```
XM_00651   CCAGGTGCGCCTGCTTACCGAGTCCTCATGGAACAGCTGACCTCCGTGAGCGAGGAGCTC 3777
M5-cc      CCAGGTGCGCCTGCTTACCGAGTCCTCATGGAACAGCTGACCTCCGTGAGCGAGGAGCTC 5040
            P  G  A  P  A  Y  R  V  L  M  E  Q  L  T  S  V  S  E  E  L  1680

XM_00651   GACGTGCGCAAGGAGGAAGTCCTCATCTTGAGGTCGCAGCTGGTGAGCCAAAAAGAAGCC 3837
M5-cc      GACGTGCGCAAGGAGGAAGTCCTCATCTTGAGGTCGCAGCTGGTGAGCCAAAAAGAAGCC 5100
            D  V  R  K  E  E  V  L  I  L  R  S  Q  L  V  S  Q  K  E  A  1700

XM_00651   ATCCAACCCAAGGATGACAAGAATACAATGACAGATTCCACAATTCTTTTAGAAGATGTA 3897
M5-cc      ATCCAACCCAAGGATGACAAGAATACAATGACAGATTCCACAATTCTTTTAGAAGATGTA 5160
            I  Q  P  K  D  D  K  N  T  M  T  D  S  T  I  L  L  E  D  V  1720

XM_00651   CAGAAAATGAAAGACAAAGGTGAAATAGCACAAGCATATATTGGTTTGAAAGAAACAAAC 3957
M5-cc      CAGAAAATGAAAGACAAAGGTGAAATAGCACAAGCATATATTGGTTTGAAAGAAACAAAC 5220
            Q  K  M  K  D  K  G  E  I  A  Q  A  Y  I  G  L  K  E  T  N  1740

XM_00651   AGGCTCTTAGAATCCCAGCTACAGTCACAGAAAAGAAGCCATGAGAATGAGGCTGAGGCC 4017
M5-cc      AGGCTCTTAGAATCCCAGCTACAGTCACAGAAAAGAAGCCATGAGAATGAGGCTGAGGCC 5280
            R  L  L  E  S  Q  L  Q  S  Q  K  R  S  H  E  N  E  A  E  A  1760

XM_00651   CTCCGTGGGGAGATCCAGAGCCTAAAGGAAGAAAACAACCGGCAACAGCAGCTGCTGGCC 4077
M5-cc      CTCCGTGGGGAGATCCAGAGCCTAAAGGAAGAAAACAACCGGCAACAGCAGCTGCTGGCC 5340
            L  R  G  E  I  Q  S  L  K  E  E  N  N  R  Q  Q  Q  L  L  A  1780

XM_00651   CAGAACCTGCAGCTGCCCCCTGAGGCCCGCATTGAGGCCAGCCTGCAGCATGAGATCACC 4137
M5-cc      CAGAACCTGCAGCTGCCCCCTGAGGCCCGCATTGAGGCCAGCCTGCAGCATGAGATCACC 5400
            Q  N  L  Q  L  P  P  E  A  R  I  E  A  S  L  Q  H  E  I  T  1800

XM_00651   CGGCTGACCAATGAAAACCTGGATCTGATGGAACAACTTGAAAAGCAGGATAAAACTGTC 4197
M5-cc      CGGCTGACCAATGAAAACCTGGATCTGATGGAACAACTTGAAAAGCAGGATAAAACTGTC 5460
            R  L  T  N  E  N  L  D  L  M  E  Q  L  E  K  Q  D  K  T  V  1820

XM_00651   CGGAAACTGAAGAAACAACTGAAAGTCTTTGCCAAAAAAATTGGTGAACTAGAAGTGGGG 4257
M5-cc      CGGAAACTGAAGAAACAACTGAAAGTCTTTGCCAAAAAAATTGGTGAACTAGAAGTGGGG 5520
            R  K  L  K  K  Q  L  K  V  F  A  K  K  I  G  E  L  E  V  G  1840

XM_00651   CAGATGGAGAACATATCTCCAGGACAGATCATCGATGAGCCTATCCGGCCAGTCAACATT 4317
M5-cc      CAGATGGAGAACATATCTCCAGGACAGATCATCGATGAGCCTATCCGGCCAGTCAACATT 5580
            Q  M  E  N  I  S  P  G  Q  I  I  D  E  P  I  R  P  V  N  I  1860

XM_00651   CCC------------------------------------------------------- 4320
M5-cc      CCCGGCCTGAATGATATTTTTGAAGCGCAGAAAATTGAATGGCATGAAAGGCCTACGTCG 5640
            P  G  L  N  D  I  F  E  A  Q  K  I  E  W  H  E  R  P  T  S  1880

XM_00651   ---------------------------------------------------
M5-cc      ACGAGCTCACTAGTCGCGGCCGCAGACTACAAGGACGACGATGATAAGTAG 5691
            T  S  S  L  V  A  A  A  D  Y  K  D  D  D  D  K  X  1896
```

S4. Amino acid sequence of Myosin-5-Ad construct

Amino acid sequence is shown with colouring that represents the distinct domains and motifs of the protein according to the legend. Numbers at the end of the lines represent the number of amino acids up to that point in the sequence.

Legend:

Avi-tag
Mouse myosin-5a brain isoform HMM with 175 aa of coiled-coil
175 aa of the coiled-coil from HMM again
Sal I site
350 aa coiled-coil motif interrupted by loops
Sal I site
GFP
Precision protease site
Nhe I site
Adhiron14
Nhe I site
Flag tag

```
M G L N D I F E A Q K I E W H E M A A S E L Y T K F A R     28
V W I P D P E E V W K S A E L L K D Y K P G D K V L L L     56
H L E E G K D L E Y R L D P K T G E L P H L R N P D I L     84
V G E N D L T A L S Y L H E P A V L H N L R V R F I D S    112
K L I Y T Y C G I V L V A I N P Y E Q L P I Y G E D I I    140
N A Y S G Q N M G D M D P H I F A V A E E A Y K Q M A R    168
D E R N Q S I I V S G E S G A G K T V S A K Y A M R Y F    196
A T V S G S A S E A N V E E K V L A S N P I M E S I G N    224
A K T T R N D N S S R F G K Y I E I G F D K R Y R I I G    252
A N M R T Y L L E K S R V V F Q A E E E R N Y H I F Y Q    280
L C A S A K L P E F K M L R L G N A D S F H Y T K Q G G    308
S P M I E G V D D A K E M A H T R Q A C T L L G I S E S    336
Y Q M G I F R I L A G I L H L G N V G F A S R D S D S C    364
T I P P K H E P L T I F C D L M G V D Y E E M C H W L C    392
H R K L A T A T E T Y I K P I S K L Q A T N A R D A L A    420
K H I Y A K L F N W I V D H V N Q A L H S A V K Q H S F    448
I G V L D I Y G F E T F E I N S F E Q F C I N Y A N E K    476
L Q Q Q F N M H V F K L E Q E E Y M K E Q I P W T L I D    504
F Y D N Q P C I N L I E S K L G I L D L L D E E C K M P    532
K G T D D T W A Q K L Y N T H L N K C A L F E K P R M S    560
N K A F I I K H F A D K V E Y Q C E G F L E K N K D T V    588
F E E Q I K V L K S S K F K M L P E L F Q D D E K A I S    616
P T S A T S S G R T P L T R V P V K P T K G R P G Q T A    644
K E H K K T V G H Q F R N S L H L L M E T L N A T T P H    672
Y V R C I K P N D F K F P F T F D E K R A V Q Q L R A C    700
G V L E T I R I S A A G F P S R W T Y Q E F F S R Y R V    728
L M K Q K D V L G D R K Q T C K N V L E K L I L D K D K    756
Y Q F G K T K I F F R A G Q V A Y L E K L R A D K L R A    784
A C I R I Q K T I R G W L L R K R Y L C M Q R A A I T V    812
Q R Y V R G Y Q A R C Y A K F L R R T K A A T T I Q K Y    840
W R M Y V V R R R Y K I R R A A T I V I Q S Y L R G Y L    868
```

T R N R Y R K I L R E Y K A V I I Q K R V R G W L A R T 896
H Y K R T M K A I V Y L Q C C F R R M M A K R E L K K L 924
K I E A R S V E R Y K K L H I G M E N K I M Q L Q R K V 952
D E Q N K D Y K C L M E K L T N L E G V Y N S E T E K L 980
R N D V E R L Q L S E E E A K V A T G R V L S L Q E E I 1008
A K L R K D L E Q T R S E K K S I E E R A D K Y K Q E T 1036
D Q L V S N L K E E N T L L K Q E K E T L N H R I V E Q 1064
A K E M T E T M E R K L V E E T K Q L E L D L N D E R L 1092
R Y Q N L L N E F S R L E E R R Y K K L H I G M E N K I 1120
M Q L Q R K V D E Q N K D Y K C L M E K L T N L E G V Y 1148
N S E T E K L R N D V E R L Q L S E E E A K V A T G R V 1176
L S L Q E E I A K L R K D L E Q T R S E K K S I E E R A 1204
D K Y K Q E T D Q L V S N L K E E N T L L K Q E K E T L 1232
N H R I V E Q A K E M T E T M E R K L V E E T K Q L E L 1260
D L N D E R L R Y Q N L L N E F S R L E E R V D Y D D L 1288
K E E M T L M L N V P K P G H K R T D S T H S S N E S E 1316
Y T F S S E F A E T E D I A P R T E E P I E K K V P L D 1344
M S L F L K L Q K R V T E L E Q E K Q L M Q D E L D R K 1372
E E Q V F R S K A K E E E R P Q I R G A E L E Y E S L K 1400
R Q E L E S E N K K L K N E L N E L R K A L S E K S A P 1428
E V T A P G A P A Y R V L M E Q L T S V S E E L D V R K 1456
E E V L I L R S Q L V S Q K E A I Q P K D D K N T M T D 1484
S T I L L E D V Q K M K D K G E I A Q A Y I G L K E T N 1512
R L L E S Q L Q S Q K R S H E N E A E A L R G E I Q S L 1540
K E E N N R Q Q Q L L A Q N L Q L P P E A R I E A S L Q 1568
H E I T R L T N E N L D L M E Q L E K Q D K T V R K L K 1596
K Q L K V F A K K I G E L E V G Q M E N I S P G Q I I D 1624
E P I R P V N I P V D M V S K G E E L F T G V V P I L V 1652
E L D G D V N G H K F S V S G E G E G D A T Y G K L T L 1680
K F I C T T G K L P V P W P T L V T T L T Y G V Q C F S 1708
R Y P D H M K Q H D F F K S A M P E G Y V Q E R T I F F 1736
K D D G N Y K T R A E V K F E G D T L V N R I E L K G I 1764
D F K E D G N I L G H K L E Y N Y N S H N V Y I M A D K 1792
Q K N G I K V N F K I R H N I E D G S V Q L A D H Y Q Q 1820
N T P I G D G P V L L P D N H Y L S T Q S A L S K D P N 1848
E K R D H M V L L E F V T A A G I T L G M D E L Y K S L 1876
E V L F Q G P A S M A S N S L E I E E L A R F A V D E H 1904
N K K E N A L L E F V R V V K A K E Q S D T P H W W W T 1932
T M Y Y L T L E A K D G G K K K L Y E A K V W V K E S P 1960
V H P K R L N F K D L Q E F K P V G D A A A A A S D Y K 1988
D D D D K 1993

References

Aizawa, H., Sameshima, M. and Yahara, I. 1997. A green fluorescent protein-actin fusion protein dominantly inhibits cytokinesis, cell spreading, and locomotion in Dictyostelium. *Cell Struct Func*. **22**(3),pp.335–45.

Ali, M.Y., Krementsova, E.B., Kennedy, G.G., Mahaffy, R., Pollard, T.D., Trybus, K.M. and Warshaw, D.M. 2007. Myosin Va maneuvers through actin intersections and diffuses along microtubules. *Proc Natl Acad Sci U S A*. **104**(11),pp.4332–4336.

Ali, M.Y., Uemura, S., Adachi, K., Itoh, H., Kinosita, K. and Ishiwata, S. 2002. Myosin V is a left-handed spiral motor on the right-handed actin helix. *Nat Struct Biol*. **9**(6),pp.464–7.

Allen, P.G. and Janmey, P.A. 1994. Gelsolin displaces phalloidin from actin filaments. A new fluorescence method shows that both Ca2+ and Mg2+ affect the rate at which gelsolin severs F-actin. *J Biol Chem*. **269**(52),pp.32916–23.

Altschul, S.F., Madden, T.L., Schäffer, A.A., Zhang, J., Zhang, Z., Miller, W. and Lipman, D.J. 1997. Gapped BLAST and PSI-BLAST: a new generation of protein database search programs. *Nucleic Acids Res*. **25**(17),pp.3389–402.

Andrecka, J., Ortega Arroyo, J., Takagi, Y., de Wit, G., Fineberg, A., MacKinnon, L., Young, G., Sellers, J.R. and Kukura, P. 2015. Structural dynamics of myosin 5 during processive motion revealed by interferometric scattering microscopy. *eLife*. **4**,p.e05413.

Ao, X. and Lehrer, S.S. 1995. Phalloidin unzips nebulin from thin filaments in skeletal myofibrils. *J Cell Sci*. **108**(11),pp.3397–403.

Arden, S.D., Puri, C., Au, J.S., Kendrick-Jones, J. and Buss, F. 2007. Myosin VI is required for targeted membrane transport during cytokinesis. *Mol Biol Cell*. **18**(12),pp.4750–4761.

Baboolal, T.G., Sakamoto, T., Forgacs, E., White, H.D., Jackson, S.M., Takagi, Y., Farrow, R.E., Molloy, J.E., Knight, P.J., Sellers, J.R. and Peckham, M. 2009. The SAH domain extends the functional length of the myosin lever. *Proc Natl Acad Sci U S A*. **106**(52),pp.22193–22198.

Baker, J.E., Krementsova, E.B., Kennedy, G.G., Armstrong, A., Trybus, K.M. and Warshaw, D.M. 2004. Myosin V processivity: multiple kinetic pathways for head-to-head coordination. *Proc Natl Acad Sci U S A*. **101**(15),pp.5542–5546.

Bao, J., Huck, D., Gunther, L.K., Sellers, J.R. and Sakamoto, T. 2013. Actin structure-dependent stepping of myosin 5a and 10 during processive movement. *PloS One*. **8**(9),p.e74936.

Barden, J.A., Miki, M., Hambly, B.D. and Dos Remedios, C.G. 1987. Localization of the phalloidin and nucleotide-binding sites on actin. *Eur J Biochem*. **162**(3),pp.583–8.

Barral, J.M., Hutagalung, A.H., Brinker, A., Hartl, F.U. and Epstein, H.F. 2002. Role of the myosin assembly protein UNC-45 as a molecular chaperone for myosin. *Science*. **295**(5555),pp.669–71.

Bausch, A.R., Moller, W. and Sackmann, E. 1999. Measurement of local viscoelasticity and forces in living cells by magnetic tweezers. *Biophys J*. **76**(1),pp.573–579.

Beckett, D., Kovaleva, E. and Schatz, P.J. 1999. A minimal peptide substrate in biotin holoenzyme synthetase-catalyzed biotinylation. *Protein Sci*. **8**(4),pp.921–9.

Beeg, J., Klumpp, S., Dimova, R., Gracià, R.S., Unger, E. and Lipowsky, R. 2008. Transport of Beads by Several Kinesin Motors. *Biophys J*. **94**(2),pp.532–541.

Belin, B.J., Goins, L.M. and Mullins, R.D. 2014. Comparative analysis of tools for live cell imaging of actin network architecture. *Bioarchitecture*. **4**(6),pp.189–202.

Belyantseva, I.A., Boger, E.T. and Friedman, T.B. 2003. Myosin XVa localizes to the tips of inner ear sensory cell stereocilia and is essential for staircase formation of the hair bundle. *Proc Natl Acad Sci U S A*. **100**(24),pp.13958–13963.

Benesh, A.E., Nambiar, R., McConnell, R.E., Mao, S., Tabb, D.L. and Tyska, M.J. 2010. Differential localization and dynamics of class I myosins in the enterocyte microvillus. *Mol Biol Cell*. **21**(6),pp.970–978.

Bird, J.E., Takagi, Y., Billington, N., Strub, M.P., Sellers, J.R. and Friedman, T.B. 2014. Chaperone-enhanced purification of unconventional myosin 15, a molecular motor specialized for stereocilia protein trafficking. *Proc Natl Acad Sci U S A*. **111**(34),pp.12390–12395.

Blanchoin, L. and Pollard, T.D. 2002. Hydrolysis of ATP by polymerized actin depends on the bound divalent cation but not profilin. *Biochemistry*. **41**(2),pp.597–602.

Bloemink, M.J. and Geeves, M.A. 2011. Shaking the myosin family tree: biochemical kinetics defines four types of myosin motor. *Semin Cell Dev Biol*. **22**(9),pp.961–967.

Bookwalter, C.S., Kelsen, A., Leung, J.M., Ward, G.E. and Trybus, K.M. 2014. A Toxoplasma gondii class XIV myosin, expressed in Sf9 cells with a parasite co-chaperone, requires two light chains for fast motility. *J Biol Chem*. **289**(44),pp.30832–41.

Burgess, S.A., Walker, M.L., Thirumurugan, K., Trinick, J. and Knight, P.J. 2004. Use of negative stain and single-particle image processing to explore dynamic properties of flexible macromolecules. *J Struct Biol*. **147**(3),pp.247–58.

Burgess, S., Walker, M., Wang, F., Sellers, J.R., White, H.D., Knight, P.J. and Trinick, J. 2002. The prepower stroke conformation of myosin V. *J Cell Biol*. **159**(6),pp.983–991.

Burkel, B.M., von Dassow, G. and Bement, W.M. 2007. Versatile fluorescent probes for actin filaments based on the actin-binding domain of utrophin. *Cell Motil Cytoskeleton*. **64**(11),pp.822–32.

Canetta, E., Duperray, A., Leyrat, A. and Verdier, C. 2005. Measuring cell viscoelastic properties using a force-spectrometer: influence of protein-cytoplasm interactions. *Biorheology*. **42**(5),pp.321–33.

Chen, Q., Nag, S. and Pollard, T.D. 2012. Formins filter modified actin subunits during processive elongation. *J Struct Biol*. **177**(1),pp.32–9.

Cheney, R.E., O'Shea, M.K., Heuser, J.E., Coelho, M. V, Wolenski, J.S., Espreafico, E.M., Forscher, P., Larson, R.E. and Mooseker, M.S. 1993. Brain myosin-V is a two-headed unconventional myosin with motor activity. *Cell*. **75**(1),pp.13–23.

Chothia, C., Levitt, M. and Richardson, D. 1981. Helix to helix packing in proteins. *J Mol Biol*. **145**(1),pp.215–50.

Le Clainche, C. and Carlier, M.-F. 2008. Regulation of actin assembly associated with protrusion and adhesion in cell migration. *Physiol Rev*. **88**(2),pp.489–513.

Clemen, A.E., Vilfan, M., Jaud, J., Zhang, J., Barmann, M. and Rief, M. 2005. Force-dependent stepping kinetics of myosin-V. *Biophys J*. **88**(6),pp.4402–4410.

Cline, J., Braman, J.C. and Hogrefe, H.H. 1996. PCR fidelity of pfu DNA polymerase and other thermostable DNA polymerases. *Nucleic Acids Res*. **24**(18),pp.3546–3551.

Conway, L., Wood, D., Tüzel, E. and Ross, J.L. 2012. Motor transport of self-assembled cargos in crowded environments. *Proc Natl Acad Sci U S A*. **109**(51),pp.20814–20819.

Cooper, J.A. 1987. Effects of cytochalasin and phalloidin on actin. *J Cell Biol*. **105**(4),pp.1473–8.

Cormack, B.P., Valdivia, R.H. and Falkow, S. 1996. FACS-optimized mutants of the green fluorescent protein (GFP). *Gene*. **173**(1),pp.33–38.

Coureux, P.-D., Sweeney, H.L. and Houdusse, A. 2004. Three myosin V structures delineate essential features of chemo-mechanical transduction. *EMBO J*. **23**(23),pp.4527–37.

Coureux, P.-D., Wells, A.L., Ménétrey, J., Yengo, C.M., Morris, C.A., Sweeney, H.L. and Houdusse, A. 2003. A structural state of the myosin V motor without bound nucleotide. *Nature*. **425**(6956),pp.419–23.

Cox, D., Berg, J.S., Cammer, M., Chinegwundoh, J.O., Dale, B.M., Cheney, R.E. and Greenberg, S. 2002. Myosin X is a downstream effector of PI(3)K during phagocytosis. *Nat Cell Biol*. **4**(7),pp.469–477.

Devi, V.S., Binz, H.K., Stumpp, M.T., Plückthun, A., Bosshard, H.R. and Jelesarov, I. 2004. Folding of a designed simple ankyrin repeat protein. *Protein Sci*. **13**(11),pp.2864–70.

Diensthuber, R.P., Müller, M., Heissler, S.M., Taft, M.H., Chizhov, I. and Manstein, D.J. 2011. Phalloidin perturbs the interaction of human non-muscle myosin isoforms 2A and 2C1 with F-actin. *FEBS Lett*. **585**(5),pp.767–71.

Dominguez, R. 2004. Actin-binding proteins – a unifying hypothesis. *Trends Biochem Sci*. **29**(11),pp.572–578.

Eakin, R.E., Snell, E.E. and Williams, R.J. 1940. A Constituent of Raw Egg White Capable of Inactivating Biotin in Vitro. *J Biol Chem*. **136**,pp.801–802.

von der Ecken, J., Heissler, S.M., Pathan-Chhatbar, S., Manstein, D.J. and Raunser, S. 2016. Cryo-EM structure of a human cytoplasmic actomyosin complex at near-atomic resolution. *Nature*. **534**(7609),pp.724–8.

Elzinga, M., Collins, J.H., Kuehl, W.M. and Adelstein, R.S. 1973. Complete amino-acid sequence of actin of rabbit skeletal muscle. *Proc Natl Acad Sci U S A*. **70**(9),pp.2687–91.

Espindola, F.S., Suter, D.M., Partata, L.B., Cao, T., Wolenski, J.S., Cheney, R.E., King, S.M. and Mooseker, M.S. 2000. The light chain composition of chicken brain myosin-Va: calmodulin, myosin-II essential light chains, and 8-kDa dynein light chain/PIN. *Cell Motil Cytoskeleton*. **47**(4),pp.269–281.

Espreafico, E.M., Cheney, R.E., Matteoli, M., Nascimento, A.A., De Camilli, P. V, Larson, R.E. and Mooseker, M.S. 1992. Primary structure and cellular localization of chicken brain myosin-V (p190), an unconventional myosin with calmodulin light chains. *J Cell Biol*. **119**(6),pp.1541–57.

Estes, J.E., Selden, L.A. and Gershman, L.C. 1981. Mechanism of action of phalloidin on the polymerization of muscle actin. *Biochemistry*. **20**(4),pp.708–12.

Ferron, F., Rebowski, G., Lee, S.H. and Dominguez, R. 2007. Structural basis for the recruitment of profilin-actin complexes during filament elongation by Ena/VASP. *EMBO J*. **26**(21),pp.4597–606.

Forgacs, E., Cartwright, S., Sakamoto, T., Sellers, J.R., Corrie, J.E., Webb, M.R. and White, H.D. 2008. Kinetics of ADP dissociation from the trail and lead heads of actomyosin V following the power stroke. *J Biol Chem*. **283**(2),pp.766–773.

Fujii, T., Iwane, A.H., Yanagida, T. and Namba, K. 2010. Direct visualization of secondary structures of F-actin by electron cryomicroscopy. *Nature*. **467**(7316),pp.724–8.

Galkin, V.E., Orlova, A., Salmazo, A., Djinovic-Carugo, K. and Egelman, E.H. 2010. Opening of tandem calponin homology domains regulates their affinity for F-actin. *Nat Struct Mol Biol*. **17**(5),pp.614–6.

Galkin, V.E., Orlova, A., VanLoock, M.S., Rybakova, I.N., Ervasti, J.M. and Egelman, E.H. 2002. The utrophin actin-binding domain binds F-actin in two different modes: implications for the spectrin superfamily of proteins. *J Cell Biol*. **157**(2),pp.243–51.

Van Gele, M., Dynoodt, P. and Lambert, J. 2009. Griscelli syndrome: a model system to study vesicular trafficking. *Pigment Cell Melanoma Res*. **22**(3),pp.268–282.

Goychuk, I., Kharchenko, V.O. and Metzler, R. 2014. Molecular motors pulling cargos in the viscoelastic cytosol: how power strokes beat subdiffusion. *Phys Chem Chem Phys*. **16**(31),pp.16524–35.

Green, N.M. 1963. Avidin. 1. The use of (14-C)biotin for kinetic studies and for assay. *Biochem J*. **89**,pp.585–91.

Guilford, W.H., Dupuis, D.E., Kennedy, G., Wu, J., Patlak, J.B. and Warshaw, D.M. 1997. Smooth muscle and skeletal muscle myosins produce similar unitary forces and displacements in the laser trap. *Biophys J*. **72**(3),pp.1006–1021.

Gunning, P.W., Ghoshdastider, U., Whitaker, S., Popp, D. and Robinson, R.C. 2015. The evolution of compositionally and functionally distinct actin filaments. *J Cell Sci*. **128**(11),pp.2009–19.

György, P., Melville, D.B., Burk, D. and DU Vigneaud, V. 1940. The Possible Identity of Vitamin H with Biotin and Coenzyme R. *Science*. **91**(2358),pp.243–5.

Hammer 3rd, J.A. and Sellers, J.R. 2012. Walking to work: roles for class V myosins as cargo transporters. *Nat Rev Mol Cell Biol*. **13**(1),pp.13–26.

Hartman, M.A. and Spudich, J.A. 2012. The myosin superfamily at a glance. *J Cell Sci*. **125**(Pt 7),pp.1627–1632.

Hasson, T. 2003. Myosin VI: two distinct roles in endocytosis. *J Cell Sci*. **116**(Pt 17),pp.3453–3461.

Hasson, T., Gillespie, P.G., Garcia, J.A., MacDonald, R.B., Zhao, Y., Yee, A.G., Mooseker, M.S. and Corey, D.P. 1997. Unconventional myosins in inner-ear sensory epithelia. *J Cell Biol*. **137**(6),pp.1287–1307.

Heintzelman, M.B., Hasson, T. and Mooseker, M.S. 1994. Multiple unconventional myosin domains of the intestinal brush border cytoskeleton. *J Cell Sci*. **107**(Pt 12),pp.3535–3543.

Herman, I.M. 1993. Actin isoforms. *Curr Opin Cell Biol*. **5**(1),pp.48–55.

Hertzog, M. and Carlier, M.F. 2005. Functional characterization of proteins regulating actin assembly. *Curr Protoc Cell Biol*. **Chapter 13**(Unit 13.6).

Hiller, Y., Gershoni, J.M., Bayer, E.A. and Wilchek, M. 1987. Biotin binding to avidin. Oligosaccharide side chain not required for ligand association. *Biochem J*. **248**(1),pp.167–71.

Hodges, A.R., Krementsova, E.B. and Trybus, K.M. 2007. Engineering the processive run length of Myosin V. *J Biol Chem*. **282**(37),pp.27192–7.

Hodi, Z., Nemeth, A.L., Radnai, L., Hetenyi, C., Schlett, K., Bodor, A., Perczel, A. and Nyitray, L. 2006. Alternatively spliced exon B of myosin Va is essential for binding the tail-associated light chain shared by dynein. *Biochemistry*. **45**(41),pp.12582–12595.

Hopkins, R. and Esposito, D. 2009. A rapid method for titrating baculovirus stocks using the Sf-9 Easy Titer cell line. *Biotechniques*. **47**(3),pp.785–788.

Houk Jr., T.W. and Ue, K. 1974. The measurement of actin concentration in solution: a comparison of methods. *Anal Biochem*. **62**(1),pp.66–74.

Huxley, H.E. 1963. Electron microscope studies on the structure of natural and synthetic protein filaments from striated muscle. *J Mol Biol*. **7**,pp.281–308.

Iwaki, M., Iwane, A.H., Ikezaki, K. and Yanagida, T. 2015. Local heat activation of single myosins based on optical trapping of gold nanoparticles. *Nano Lett*. **15**(4),pp.2456–61.

Jacobs, D.T., Weigert, R., Grode, K.D., Donaldson, J.G. and Cheney, R.E. 2009. Myosin Vc is a molecular motor that functions in secretory granule trafficking. *Mol Biol Cell*. **20**(21),pp.4471–4488.

Johnson, H.W. and Schell, M.J. 2009. Neuronal IP3 3-kinase is an F-actin-bundling protein: role in dendritic targeting and regulation of spine morphology. *Mol Biol Cell*. **20**(24),pp.5166–80.

Johnston, G.C., Prendergast, J.A. and Singer, R.A. 1991. The Saccharomyces cerevisiae MYO2 gene encodes an essential myosin for vectorial transport of vesicles. *J Cell Biol*. **113**(3),pp.539–51.

Kabsch, W., Mannherz, H.G., Suck, D., Pai, E.F. and Holmes, K.C. 1990. Atomic structure of the actin:DNase I complex. *Nature*. **347**(6288),pp.37–44.

Kang, H., Bradley, M.J., Elam, W.A. and De La Cruz, E.M. 2013. Regulation of Actin by Ion-Linked Equilibria. *Biophys J*. **105**(12),pp.2621–2628.

King, R., Tiede, C., Simmons, K., Fishwick, C., Tomlinson, D. and Ajjan, R. 2015. Inhibition of complement C3 and fibrinogen interaction: a potential novel therapeutic target to reduce cardiovascular disease in diabetes. *Lancet*. **385**,p.S57.

King, S.M., Barbarese, E., Dillman, J.F., Patel-King, R.S., Carson, J.H. and Pfister, K.K. 1996. Brain cytoplasmic and flagellar outer arm dyneins share a highly conserved Mr 8,000 light chain. *J Biol Chem*. **271**(32),pp.19358–66.

Knight, P.J., Thirumurugan, K., Xu, Y., Wang, F., Kalverda, A.P., Stafford, W.F., Sellers, J.R. and Peckham, M. 2005. The predicted coiled-coil domain of myosin 10 forms a novel elongated domain that lengthens the head. *J Biol Chem*. **280**(41),pp.34702–8.

Kovar, D.R., Harris, E.S., Mahaffy, R., Higgs, H.N. and Pollard, T.D. 2006. Control of the assembly of ATP- and ADP-actin by formins and profilin. *Cell*. **124**(2),pp.423–35.

Kreis, T.E., Geiger, B. and Schlessinger, J. 1982. Mobility of microinjected rhodamine actin within living chicken gizzard cells determined by fluorescence photobleaching recovery. *Cell*. **29**(3),pp.835–45.

Krementsov, D.N., Krementsova, E.B. and Trybus, K.M. 2004. Myosin V: regulation by calcium, calmodulin, and the tail domain. *J Cell Biol*. **164**(6),pp.877–886.

Kremer, H., van Wijk, E., Marker, T., Wolfrum, U. and Roepman, R. 2006. Usher syndrome: molecular links of pathogenesis, proteins and pathways. *Hum Mol Genet*. **15**(Spec No 2),pp.R262-70.

Kyle, H.F., Wickson, K.F., Stott, J., Burslem, G.M., Breeze, A.L., Tiede, C., Tomlinson, D.C., Warriner, S.L., Nelson, A., Wilson, A.J. and Edwards, T.A. 2015. Exploration of the HIF-1α/p300 interface using peptide and Adhiron phage display technologies. *Mol Biosyst*. **11**(10),pp.2738–49.

De La Cruz, E.M. and Ostap, E.M. 2004. Relating biochemistry and function in the myosin superfamily. *Curr Opin Cell Biol*. **16**(1),pp.61–67.

De La Cruz, E.M., Wells, A.L., Rosenfeld, S.S., Ostap, E.M. and Sweeney, H.L. 1999. The kinetic mechanism of myosin V. *Proc Natl Acad Sci U S A*. **96**(24),pp.13726–13731.

Larkin, M.A., Blackshields, G., Brown, N.P., Chenna, R., McGettigan, P.A., McWilliam, H., Valentin, F., Wallace, I.M., Wilm, A., Lopez, R., Thompson, J.D., Gibson, T.J. and Higgins, D.G. 2007. Clustal W and Clustal X version 2.0. *Bioinformatics*. **23**(21),pp.2947–8.

Larson, R.E., Pitta, D.E. and Ferro, J.A. 1988. A novel 190 kDa calmodulin-binding protein associated with brain actomyosin. *Braz J Med Biol Res*. **21**(2),pp.213–7.

Lemieux, M.G., Janzen, D., Hwang, R., Roldan, J., Jarchum, I. and Knecht, D.A. 2014. Visualization of the actin cytoskeleton: different F-actin-binding probes tell different stories. *Cytoskeleton*. **71**(3),pp.157–69.

Li, X.-D., Ikebe, R. and Ikebe, M. 2005. Activation of myosin Va function by melanophilin, a specific docking partner of myosin Va. *J Biol Chem*. **280**(18),pp.17815–22.

Liu, J., Taylor, D.W., Krementsova, E.B., Trybus, K.M. and Taylor, K.A. 2006. Three-dimensional structure of the myosin V inhibited state by cryoelectron tomography. *Nature*. **442**(7099),pp.208–11.

Liu, L., Srikakulam, R. and Winkelmann, D.A. 2008. Unc45 activates Hsp90-dependent folding of the myosin motor domain. *J Biol Chem*. **283**(19),pp.13185–93.

Liu, X., Shu, S., Yu, S., Lee, D.-Y., Piszczek, G., Gucek, M., Wang, G. and Korn, E.D. 2014. Biochemical and biological properties of cortexillin III, a component of Dictyostelium DGAP1-cortexillin complexes. *Mol Biol Cell*. **25**(13),pp.2026–38.

Livnah, O., Bayert, E.A., Wilchekt, M. and Sussman, J.L. 1993. Three-dimensional structures of avidin and the avidin- biotin complex. *Biochemistry*. **90**(11),pp.5076–5080.

Lorenz, M., Popp, D. and Holmes, K.C. 1993. Refinement of the F-actin model against X-ray fiber diffraction data by the use of a directed mutation algorithm. *J Mol Biol*. **234**(3),pp.826–836.

Lowey, S. and Cohen, C. 1962. Studies on the structure of myosin. *J Mol Biol*. **4**,pp.293–308.

Luby-Phelps, K. 2013. The physical chemistry of cytoplasm and its influence on cell function: an update. *Mol Biol Cell*. **24**(17),pp.2593–6.

Lupas, A., Van Dyke, M. and Stock, J. 1991. Predicting coiled coils from protein sequences. *Science*. **252**(5009),pp.1162–1164.

Lymn, R.W. and Taylor, E.W. 1971. Mechanism of adenosine triphosphate hydrolysis by actomyosin. *Biochemistry*. **10**(25),pp.4617–24.

Main, E.R.G., Xiong, Y., Cocco, M.J., D'Andrea, L. and Regan, L. 2003. Design of Stable α-Helical Arrays from an Idealized TPR Motif. *Structure*. **11**(5),pp.497–508.

Marttila, A.T., Laitinen, O.H., Airenne, K.J., Kulik, T., Bayer, E.A., Wilchek, M. and Kulomaa, M.S. 2000. Recombinant NeutraLite Avidin: a non-glycosylated, acidic mutant of chicken avidin that exhibits high affinity for biotin and low non-specific binding properties. *FEBS Lett*. **467**(1),pp.31–36.

McConnell, R.E. and Tyska, M.J. 2010. Leveraging the membrane - cytoskeleton interface with myosin-1. *Trends Cell Biol*. **20**(7),pp.418–426.

Mehta, A.D., Rock, R.S., Rief, M., Spudich, J.A., Mooseker, M.S. and Cheney, R.E. 1999. Myosin-V is a processive actin-based motor. *Nature*. **400**(6744),pp.590–3.

Mercer, J.A., Seperack, P.K., Strobel, M.C., Copeland, N.G. and Jenkins, N.A. 1991. Novel myosin heavy chain encoded by murine dilute coat colour locus. *Nature*. **349**(6311),pp.709–13.

El Mezgueldi, M., Tang, N., Rosenfeld, S.S. and Ostap, E.M. 2002. The kinetic mechanism of Myo1e (human myosin-IC). *J Biol Chem*. **277**(24),pp.21514–21521.

Miller, K.E. and Sheetz, M.P. 2000. Characterization of myosin V binding to brain vesicles. *J Biol Chem*. **275**(4),pp.2598–606.

Monaco, A.P., Neve, R.L., Colletti-Feener, C., Bertelson, C.J., Kurnit, D.M. and Kunkel, L.M. 1986. Isolation of candidate cDNAs for portions of the Duchenne muscular dystrophy gene. *Nature*. **323**(6089),pp.646–50.

Munsie, L.N., Caron, N., Desmond, C.R. and Truant, R. 2009. Lifeact cannot visualize some forms of stress-induced twisted F-actin. *Nat Methods*. **6**(5),p.317.

Nagy, A., Piszczek, G. and Sellers, J.R. 2009. Extensibility of the extended tail domain of processive and nonprocessive myosin V molecules. *Biophys J*. **97**(12),pp.3123–3131.

Nagy, A., Takagi, Y., Billington, N., Sun, S.A., Hong, D.K., Homsher, E., Wang, A. and Sellers, J.R. 2013. Kinetic characterization of nonmuscle myosin IIb at the single molecule level. *J Biol Chem*. **288**(1),pp.709–722.

Naisbitt, S., Valtschanoff, J., Allison, D.W., Sala, C., Kim, E., Craig, A.M., Weinberg, R.J. and Sheng, M. 2000. Interaction of the postsynaptic density-95/guanylate kinase domain-associated protein complex with a light chain of myosin-V and dynein. *J Neurosci*. **20**(12),pp.4524–4534.

Navarro, C., Puthalakath, H., Adams, J.M., Strasser, A. and Lehmann, R. 2004. Egalitarian binds dynein light chain to establish oocyte polarity and maintain oocyte fate. *Nat Cell Biol*. **6**(5),pp.427–435.

Nelson, S.R., Ali, M.Y., Trybus, K.M. and Warshaw, D.M. 2009. Random Walk of Processive, Quantum Dot-Labeled Myosin Va Molecules within the Actin Cortex of COS-7 Cells. *Biophys J*. **97**(2),pp.509–518.

Nguyen, H. and Higuchi, H. 2005. Motility of myosin V regulated by the dissociation of single calmodulin. *Nat Struct Mol Biol*. **12**(2),pp.127–32.

Nishida, E., Iida, K., Yonezawa, N., Koyasu, S., Yahara, I. and Sakai, H. 1987. Cofilin is a component of intranuclear and cytoplasmic actin rods induced in cultured cells. *Proc Natl Acad Sci U S A*. **84**(15),pp.5262–6.

Nyitrai, M. and Geeves, M.A. 2004. Adenosine diphosphate and strain sensitivity in myosin motors. *Philos Trans R Soc Lond B Biol Sci*. **359**(1452),pp.1867–1877.

Odronitz, F. and Kollmar, M. 2007. Drawing the tree of eukaryotic life based on the analysis of 2,269 manually annotated myosins from 328 species. *Genome Biol*. **8**(9),p.R196.

Oke, O.A., Burgess, S.A., Forgacs, E., Knight, P.J., Sakamoto, T., Sellers, J.R., White, H. and Trinick, J. 2010. Influence of lever structure on myosin 5a walking. *Proc Natl Acad Sci U S A*. **107**(6),pp.2509–2514.

Ortega Arroyo, J., Andrecka, J., Spillane, K.M., Billington, N., Takagi, Y., Sellers, J.R. and Kukura, P. 2014. Label-Free, All-Optical Detection, Imaging, and Tracking of a Single Protein. *Nano Lett*. **14**(4),pp.2065–2070.

Otterbein, L.R., Graceffa, P. and Dominguez, R. 2001. The crystal structure of uncomplexed actin in the ADP state. *Science*. **293**(5530),pp.708–11.

Pardee, J.D. and Spudich, J.A. 1982. Purification of muscle actin. *Methods Enzymol*. **85**(Pt B),pp.164–181.

Park, E., Graziano, B.R., Zheng, W., Garabedian, M., Goode, B.L. and Eck, M.J. 2015. Structure of a Bud6/Actin Complex Reveals a Novel WH2-like Actin Monomer Recruitment Motif. *Structure*. **23**(8),pp.1492–9.

Peckham, M. 2011. Coiled coils and SAH domains in cytoskeletal molecular motors. *Biochem Soc Trans*. **39**(5),pp.1142–1148.

Pelham, R.J. and Chang, F. 2002. Actin dynamics in the contractile ring during cytokinesis in fission yeast. *Nature*. **419**(6902),pp.82–86.

Pollard, T.D. 2010. A guide to simple and informative binding assays. *Mol Biol Cell*. **21**(23),pp.4061–7.

Pollard, T.D. 2016. Actin and Actin-Binding Proteins. *Cold Spring Harb Perspect Biol*. **8**(8).

Pollard, T.D. and Korn, E.D. 1973. Acanthamoeba myosin. I. Isolation from Acanthamoeba castellanii of an enzyme similar to muscle myosin. *J Biol Chem*. **248**(13),pp.4682–90.

Price, M.G., Landsverk, M.L., Barral, J.M. and Epstein, H.F. 2002. Two mammalian UNC-45 isoforms are related to distinct cytoskeletal and muscle-specific functions. *J Cell Sci*. **115**(Pt 21),pp.4013–23.

Quintero, O.A., DiVito, M.M., Adikes, R.C., Kortan, M.B., Case, L.B., Lier, A.J., Panaretos, N.S., Slater, S.Q., Rengarajan, M., Feliu, M. and Cheney, R.E. 2009. Human Myo19 is a novel myosin that associates with mitochondria. *Curr Biol*. **19**(23),pp.2008–2013.

Raposo, G., Cordonnier, M.N., Tenza, D., Menichi, B., Durrbach, A., Louvard, D. and Coudrier, E. 1999. Association of myosin I alpha with endosomes and lysosomes in mammalian cells. *Mol Biol Cell*. **10**(5),pp.1477–1494.

Rayment, I., Rypniewski, W.R., Schmidt-Bäse, K., Smith, R., Tomchick, D.R., Benning, M.M., Winkelmann, D.A., Wesenberg, G. and Holden, H.M. 1993. Three-dimensional structure of myosin subfragment-1: a molecular motor. *Science*. **261**(5117),pp.50–8.

Reed and Muench, H. 1938. A Simple Method of Estimating Fifty per Cent Endpoints. *Am J Hyg*. **27**(3),pp.493–497.

Riedl, J., Crevenna, A.H., Kessenbrock, K., Yu, J.H., Neukirchen, D., Bista, M., Bradke, F., Jenne, D., Holak, T.A., Werb, Z., Sixt, M. and Wedlich-Soldner, R. 2008. Lifeact: a versatile marker to visualize F-actin. *Nat Methods*. **5**(7),pp.605–7.

Root, D.D., Yadavalli, V.K., Forbes, J.G. and Wang, K. 2006. Coiled-coil nanomechanics and uncoiling and unfolding of the superhelix and alpha-helices of myosin. *Biophys J*. **90**(8),pp.2852–2866.

Rosenfeld, S.S. and Sweeney, H.L. 2004. A model of myosin V processivity. *J Biol Chem*. **279**(38),pp.40100–11.

Rybakova, I.N. and Ervasti, J.M. 2005. Identification of spectrin-like repeats required for high affinity utrophin-actin interaction. *J Biol Chem*. **280**(24),pp.23018–23.

Sakamoto, T., Wang, F., Schmitz, S., Xu, Y., Xu, Q., Molloy, J.E., Veigel, C. and Sellers, J.R. 2003. Neck length and processivity of myosin V. *J Biol Chem*. **278**(31),pp.29201–29207.

Sakamoto, T., Webb, M.R., Forgacs, E., White, H.D. and Sellers, J.R. 2008. Direct observation of the mechanochemical coupling in myosin Va during processive movement. *Nature*. **455**(7209),pp.128–132.

Sakamoto, T., Yildez, A., Selvin, P.R. and Sellers, J.R. 2005. Step-size is determined by neck length in myosin V. *Biochemistry*. **44**(49),pp.16203–16210.

Sambrook, J., Fritsch, E.F. and Maniatis, T. 1989. *Molecular Cloning: A Laboratory Manual*.

Schell, M.J., Erneux, C. and Irvine, R.F. 2001. Inositol 1,4,5-trisphosphate 3-kinase A associates with F-actin and dendritic spines via its N terminus. *J Biol Chem*. **276**(40),pp.37537–46.

Schilstra, M.J. and Martin, S.R. 2006. An elastically tethered viscous load imposes a regular gait on the motion of myosin-V. Simulation of the effect of transient force relaxation on a stochastic process. *J R Soc Interface*. **3**(6),pp.153–165.

Schneider, M.E., Dose, A.C., Salles, F.T., Chang, W., Erickson, F.L., Burnside, B. and Kachar, B. 2006. A new compartment at stereocilia tips defined by spatial and temporal patterns of myosin IIIa expression. *J Neurosci*. **26**(40),pp.10243–10252.

Schwaiger, I., Sattler, C., Hostetter, D.R. and Rief, M. 2002. The myosin coiled-coil is a truly elastic protein structure. *Nat Methods*. **1**(4),pp.232–5.

Sckolnick, M., Krementsova, E.B., Warshaw, D.M. and Trybus, K.M. 2013. More than just a cargo adapter, melanophilin prolongs and slows processive runs of myosin Va. *J Biol Chem*. **288**(41),pp.29313–22.

Sellers, J.R. and Veigel, C. 2006. Walking with myosin V. *Curr Opin Cell Biol*. **18**(1),pp.68–73.

Seperack, P.K., Mercer, J.A., Strobel, M.C., Copeland, N.G. and Jenkins, N.A. 1995. Retroviral sequences located within an intron of the dilute gene alter dilute expression in a tissue-specific manner. *EMBO J*. **14**(10),pp.2326–2332.

Sept, D. and McCammon, J.A. 2001. Thermodynamics and kinetics of actin filament nucleation. *Biophys J*. **81**(2),pp.667–74.

Sharkey, D.J., Scalice, E.R., Christy Jr., K.G., Atwood, S.M. and Daiss, J.L. 1994. Antibodies as thermolabile switches: high temperature triggering for the polymerase chain reaction. *Biotechnology*. **12**(5),pp.506–509.

Shen, M., Zhang, N., Zheng, S., Zhang, W.-B., Zhang, H.-M., Lu, Z., Su, Q.P., Sun, Y., Ye, K. and Li, X.-D. 2016. Calmodulin in complex with the first IQ motif of myosin-5a functions as an intact calcium sensor. *Proc Natl Acad Sci U S A*.

Shepard, K.A., Gerber, A.P., Jambhekar, A., Takizawa, P.A., Brown, P.O., Herschlag, D., DeRisi, J.L. and Vale, R.D. 2003. Widespread cytoplasmic mRNA transport in yeast: identification of 22 bud-localized transcripts using DNA microarray analysis. *Proc Natl Acad Sci U S A*. **100**(20),pp.11429–34.

Sousa, A.D. and Cheney, R.E. 2005. Myosin-X: a molecular motor at the cell's fingertips. *Trends Cell Biol*. **15**(10),pp.533–9.

Sparkes, I.A. 2010. Motoring around the plant cell: insights from plant myosins. *Biochem Soc Trans*. **38**(3),pp.833–838.

Spink, B.J., Sivaramakrishnan, S., Lipfert, J., Doniach, S. and Spudich, J.A. 2008. Long single alpha-helical tail domains bridge the gap between structure and function of myosin VI. *Nat Struct Mol Biol*. **15**(6),pp.591–7.

Spracklen, A.J., Fagan, T.N., Lovander, K.E. and Tootle, T.L. 2014. The pros and cons of common actin labeling tools for visualizing actin dynamics during Drosophila oogenesis. *Dev Biol*. **393**(2),pp.209–26.

Spudich, J.A. and Watt, S. 1971. The regulation of rabbit skeletal muscle contraction. I. Biochemical studies of the interaction of the tropomyosin-troponin complex with actin and the proteolytic fragments of myosin. *J Biol Chem*. **246**(15),pp.4866–4871.

Srikakulam, R., Liu, L. and Winkelmann, D.A. 2008. Unc45b forms a cytosolic complex with Hsp90 and targets the unfolded myosin motor domain. *PloS One*. **3**(5),p.e2137.

Steinmetz, M.O., Stoffler, D., Müller, S.A., Jahn, W., Wolpensinger, B., Goldie, K.N., Engel, A., Faulstich, H. and Aebi, U. 1998. Evaluating atomic models of F-actin with an undecagold-tagged phalloidin derivative. *J Mol Biol*. **276**(1),pp.1–6.

Sun, Y., Schroeder, H.W., Beausang, J.F., Homma, K., Ikebe, M. and Goldman, Y.E. 2007. Myosin VI walks 'wiggly' on actin with large and variable tilting. *Mol Cell*. **28**(6),pp.954–64.

Syamaladevi, D.P., Spudich, J.A. and Sowdhamini, R. 2012. Structural and functional insights on the Myosin superfamily. *Bioinform Biol Insights*. **6**,pp.11–21.

Szent-Györgyi, A.G., Szentkiralyi, E.M. and Kendrick-Jonas, J. 1973. The light chains of scallop myosin as regulatory subunits. *J Mol Biol*. **74**(2),pp.179–203.

Tabb, J.S., Molyneaux, B.J., Cohen, D.L., Kuznetsov, S.A. and Langford, G.M. 1998. Transport of ER vesicles on actin filaments in neurons by myosin V. *J Cell Sci*. **111**(Pt 21),pp.3221–3234.

Taggart, C., Cervantes-Laurean, D., Kim, G., McElvaney, N.G., Wehr, N., Moss, J. and Levine, R.L. 2000. Oxidation of either methionine 351 or methionine 358 in alpha 1-antitrypsin causes loss of anti-neutrophil elastase activity. *J Biol Chem*. **275**(35),pp.27258–65.

Thirumurugan, K., Sakamoto, T., Hammer 3rd, J.A., Sellers, J.R. and Knight, P.J. 2006. The cargo-binding domain regulates structure and activity of myosin 5. *Nature*. **442**(7099),pp.212–215.

Thompson, R.F. and Langford, G.M. 2002. Myosin superfamily evolutionary history. *Anat Rec*. **268**(3),pp.276–289.

Tiede, C., Tang, A.A., Deacon, S.E., Mandal, U., Nettleship, J.E., Owen, R.L., George, S.E., Harrison, D.J., Owens, R.J., Tomlinson, D.C. and McPherson, M.J. 2014. Adhiron: a stable and versatile peptide display scaffold for molecular recognition applications. *Protein Eng Des Sel*. **27**(5),pp.145–155.

Tinevez, J.Y., Perry, N., Schindelin, J., Hoopes, G.M., Reynolds, G.D., Laplantine, E., Bednarek, S.Y., Shorte, S.L., Eliceiri, K.W. 2016. TrackMate: An open and extensible platform for single-particle tracking. *Methods*. **16**,pp.S1046

Toepfer, C. and Sellers, J.R. 2014. Use of fluorescent techniques to study the in vitro movement of myosins. *EXS*. **105**,pp.193–210.

Trybus, K.M. 2013. Intracellular Transport: The Causes for Pauses. *Curr Biol*. **23**(14),pp.R623–R625.

Trybus, K.M. 2008. Myosin V from head to tail. *Cell Mol Life Sci*. **65**(9),pp.1378–1389.

Tuxworth, R.I., Weber, I., Wessels, D., Addicks, G.C., Soll, D.R., Gerisch, G. and Titus, M.A. 2001. A role for myosin VII in dynamic cell adhesion. *Curr Biol*. **11**(5),pp.318–329.

Uemura, S., Higuchi, H., Olivares, A.O., De La Cruz, E.M. and Ishiwata, S. 2004. Mechanochemical coupling of two substeps in a single myosin V motor. *Nat Struct Mol Biol*. **11**(9),pp.877–83.

Vale, R.D. 2003. Myosin V motor proteins: marching stepwise towards a mechanism. *J Cell Biol*. **163**(3),pp.445–450.

Veigel, C. and Schmidt, C.F. 2011. Moving into the cell: single-molecule studies of molecular motors in complex environments. *Nat Rev Mol Cell Biol*. **12**(3),pp.163–176.

Veigel, C., Schmitz, S., Wang, F. and Sellers, J.R. 2005. Load-dependent kinetics of myosin-V can explain its high processivity. *Nat Cell Biol*. **7**(9),pp.861–869.

Veigel, C., Wang, F., Bartoo, M.L., Sellers, J.R. and Molloy, J.E. 2002. The gated gait of the processive molecular motor, myosin V. *Nat Cell Biol*. **4**(1),pp.59–65.

Vicente-Manzanares, M., Ma, X., Adelstein, R.S. and Horwitz, A.R. 2009. Non-muscle myosin II takes centre stage in cell adhesion and migration. *Nat Rev Mol Cell Biol*. **10**(11),pp.778–790.

Wagner, W., Brenowitz, S.D. and Hammer, J.A. 2011. Myosin-Va transports the endoplasmic reticulum into the dendritic spines of Purkinje neurons. *Nat Cell Biol*. **13**(1),pp.40–8.

Wagner, W., Fodor, E., Ginsburg, A. and Hammer 3rd, J.A. 2006. The binding of DYNLL2 to myosin Va requires alternatively spliced exon B and stabilizes a portion of the myosin's coiled-coil domain. *Biochemistry*. **45**(38),pp.11564–11577.

Walker, M.L., Burgess, S.A., Sellers, J.R., Wang, F., Hammer 3rd, J.A., Trinick, J. and Knight, P.J. 2000. Two-headed binding of a processive myosin to F-actin. *Nature*. **405**(6788),pp.804–807.

Walsh, R., Rutland, C., Thomas, R. and Loughna, S. 2010. Cardiomyopathy: a systematic review of disease-causing mutations in myosin heavy chain 7 and their phenotypic manifestations. *Cardiology*. **115**(1),pp.49–60.

Wang, F., Chen, L., Arcucci, O., Harvey, E. V, Bowers, B., Xu, Y., Hammer 3rd, J.A. and Sellers, J.R. 2000. Effect of ADP and ionic strength on the kinetic and motile properties of recombinant mouse myosin V. *J Biol Chem*. **275**(6),pp.4329–4335.

Wang, F., Harvey, E. V, Conti, M.A., Wei, D. and Sellers, J.R. 2000. A conserved negatively charged amino acid modulates function in human nonmuscle myosin IIA. *Biochemistry*. **39**(18),pp.5555–5560.

Wang, F., Thirumurugan, K., Stafford, W.F., Hammer 3rd, J.A., Knight, P.J. and Sellers, J.R. 2004. Regulated conformation of myosin V. *J Biol Chem*. **279**(4),pp.2333–2336.

Wang, Z., Edwards, J.G., Riley, N., Provance Jr., D.W., Karcher, R., Li, X.D., Davison, I.G., Ikebe, M., Mercer, J.A., Kauer, J.A. and Ehlers, M.D. 2008. Myosin Vb mobilizes recycling endosomes and AMPA receptors for postsynaptic plasticity. *Cell*. **135**(3),pp.535–548.

Wang, Z. and Pesacreta, T.C. 2004. A subclass of myosin XI is associated with mitochondria, plastids, and the molecular chaperone subunit TCP-1alpha in maize. *Cell Motil Cytoskeleton*. **57**(4),pp.218–232.

Warshaw, D.M., Desrosiers, J.M., Work, S.S. and Trybus, K.M. 1990. Smooth muscle myosin cross-bridge interactions modulate actin filament sliding velocity in vitro. *J Cell Biol*. **111**(2),pp.453–63.

Warshaw, D.M., Kennedy, G.G., Work, S.S., Krementsova, E.B., Beck, S. and Trybus, K.M. 2005. Differential labeling of myosin V heads with quantum dots allows direct visualization of hand-over-hand processivity. *Biophys J*. **88**(5),pp.L30-2.

Wayment, J.R. and Harris, J.M. 2009. Biotin-avidin binding kinetics measured by single-molecule imaging. *Anal Chem*. **81**(1),pp.336–42.

Weeds, A.G. and Taylor, R.S. 1975. Separation of subfragment-1 isoenzymes from rabbit skeletal muscle myosin. *Nature*. **257**(5521),pp.54–6.

Wehland, J., Osborn, M. and Weber, K. 1977. Phalloidin-induced actin polymerization in the cytoplasm of cultured cells interferes with cell locomotion and growth. *Proc Natl Acad Sci U S A*. **74**(12),pp.5613–7.

Wieland, T. and Faulstich, H. 1978. Amatoxins, phallotoxins, phallolysin, and antamanide: the biologically active components of poisonous Amanita mushrooms. *CRC Crit Rev Biochem*. **5**(3),pp.185–260.

Wilkins, M.R., Gasteiger, E., Bairoch, A., Sanchez, J.C., Williams, K.L., Appel, R.D. and Hochstrasser, D.F. 1999. Protein identification and analysis tools in the ExPASy server. *Methods Mol Biol*. **112**,pp.531–552.

Woolner, S. and Bement, W.M. 2009. Unconventional myosins acting unconventionally. *Trends Cell Biol*. **19**(6),pp.245–252.

Wrigley, N.G. 1968. The lattice spacing of crystalline catalase as an internal standard of length in electron microscopy. *J Ultrastruct Res*. **24**(5–6),pp.454–464.

Wu, X., Bowers, B., Rao, K., Wei, Q. and Hammer JA 1998. Visualization of melanosome dynamics within wild-type and dilute melanocytes suggests a paradigm for myosin V function In vivo. *J Cell Biol*. **143**(7),pp.1899–918.

Wu, X., Sakamoto, T., Zhang, F., Sellers, J.R. and Hammer 3rd, J.A. 2006. In vitro reconstitution of a transport complex containing Rab27a, melanophilin and myosin Va. *FEBS Lett*. **580**(25),pp.5863–5868.

Wu, X., Wang, F., Rao, K., Sellers, J.R. and Hammer, J.A. 2002. Rab27a is an essential component of melanosome receptor for myosin Va. *Mol Biol Cell*. **13**(5),pp.1735–49.

Wu, X.S., Rao, K., Zhang, H., Wang, F., Sellers, J.R., Matesic, L.E., Copeland, N.G., Jenkins, N.A. and Hammer 3rd, J.A. 2002. Identification of an organelle receptor for myosin-Va. *Nat Cell Biol*. **4**(4),pp.271–278.

Wulf, E., Deboben, A., Bautz, F.A., Faulstich, H. and Wieland, T. 1979. Fluorescent phallotoxin, a tool for the visualization of cellular actin. *Proc Natl Acad Sci U S A*. **76**(9),pp.4498–502.

Yang, Y., Baboolal, T.G., Siththanandan, V., Chen, M., Walker, M.L., Knight, P.J., Peckham, M. and Sellers, J.R. 2009. A FERM domain autoregulates Drosophila myosin 7a activity. *Proc Natl Acad Sci U S A*. **106**(11),pp.4189–4194.

Yildiz, A., Forkey, J.N., McKinney, S.A., Ha, T., Goldman, Y.E. and Selvin, P.R. 2003. Myosin V walks hand-over-hand: single fluorophore imaging with 1.5-nm localization. *Science*. **300**(5628),pp.2061–5.

Zajac, A.L., Goldman, Y.E., Holzbaur, E.L. and Ostap, E.M. 2013. Local Cytoskeletal and Organelle Interactions Impact Molecular-Motor-Driven Early Endosomal Trafficking. *Curr Biol*. **23**(13),pp.1173–1180.

Zimmermann, D., Santos, A., Kovar, D.R. and Rock, R.S. 2015. Actin Age Orchestrates Myosin-5 and Myosin-6 Run Lengths. *Curr Biol*. **25**(15),pp.2057–2062.